City Research Online

City St George's, University of London

Citation: Gillespie-Gallery, H. (2015). Spatial and temporal aspects of visual performance in relation to light level and normal aging. (Unpublished Doctoral thesis, City University London)

This is the accepted version of the paper.

This version of the publication may differ from the final published version. To cite this item please consult the publisher's version.

Permanent repository link: https://openaccess.city.ac.uk/id/eprint/13520/

Copyright and Reuse: Copyright and Moral Rights remain with the author(s) and/or copyright holders. Copies of full items can be used for personal research or study, educational, or not-for-profit purposes without prior permission or charge, unless otherwise indicated, provided that the authors, title and full bibliographic details are credited, a hyperlink and/or URL is given for the original metadata page and the content is not changed in any way. For full details of reuse please refer to City Research Online policy.

City Research Online: http://openaccess.city.ac.uk/ publications@citystgeorges.ac.uk

Spatial and temporal aspects of visual performance in relation to light level and normal aging

Hanna Gillespie-Gallery

Doctor of Philosophy

Division of Optometry and Visual Science

July 2015

CITY UNIVERSITY LONDON
EST 1894

CityLibrary
Your space
Your resources
Your library

THE FOLLOWING PARTS OF THIS THESIS HAVE BEEN REDACTED FOR COPYRIGHT REASONS:

p36, Fig 6
p37, Fig 7
p52, Fig 14
p55, Fig 15
p57, Fig 16A
p167, Fig 45

Our lives at times seem a study in contrast... love hate, birth death, right wrong... everything seen in absolutes of black white. Too often we are not aware that it is the shades of grey that add depth meaning to the starkness of those extremes.

Ansel Adams

Contents

Contents 3

List of tables 10

List of figures 11

Acknowledgements 21

Declaration 22

Abstract 23

Abbreviations and symbols 24

1. The visual system 25

1.1. The structure of the human eye 26

1.2. The cornea and sclera 27

1.3. The pupil 27

1.4. The lens 28

1.5. The retina 28

1.5.1. Anatomy of the retina 28

1.5.2. The macula and fovea 30

1.5.3. Photoreceptors 31

1.5.4. Post-receptoral retinal pathways 34

1.6. Post-retinal visual processing 36

1.6.1. The lateral geniculate nucleus (LGN) 36

1.6.2. Visual cortex 38

1.7. The aging human visual system 40

1.7.1. Light scatter and absorption in the eye; the role of aging 41

1.7.2. Pupil miosis 44

1.7.3. Ocular aberrations 45

1.7.4. Presbyopia 47

1.7.5. Aging of the retina 48

1.7.6. Cellular aging in central visual pathways 50

1.7.7. Age related macular degeneration 52

1.8. Spatial, temporal and chromatic visual perception 54

1.8.1. Spatial vision 54

1.8.2. Temporal vision 60

1.8.3. Colour vision 64

1.9. Aims and objectives 68

2. Spatial contrast thresholds in photopic and mesopic conditions; separating normal aging from disease 69

2.1. Loss of spatial vision in aging and retinal disease 69

2.1.1. Contrast vision and aging 69

2.1.2. Loss of contrast sensitivity in retinal disease 73

2.1.3. Vision at low luminance levels in aging 76

2.1.4. Vision at low luminances in AMD 80

2.2. Changes to binocular summation in aging 85

2.2.1. Binocular summation beyond probability summation 85

2.2.2. Aging and binocular summation 88

2.2.3. Binocular summation variation with eccentricity 90

2.2.4. Binocular summation at low light levels 90

2.3. Aims and objectives of the contrast and luminance study 91

2.4. Methods 93

2.4.1. Participants 93

2.4.2. Contrast sensitivity assessment 93

2.4.3. Estimates of lens optical density 97

2.4.4. Pupil measurements 97

2.4.5. Estimating retinal illuminance 98

2.4.6. Calculating HR_{index} for contrast sensitivity 98

2.4.7. Identifying participants with significantly elevated contrast thresholds . 99

2.4.8. Calculating binocular summation ratio (BSR) and interocular percentage increase (IPI) 100

2.4.9. Statistical analysis 101

2.5. Results 102

2.5.1. Identification of outliers 102

2.5.2. Pupil size and age 103

2.5.3. Contrast vision and the HR_{index} 104

2.5.3. Binocular summation of contrast vision 113

2.6. Discussion 116

2.6.1. The HR_{index} at the fovea and parafovea 116

2.6.2. Binocular summation of contrast signals 118

2.7. Conclusions 119

3. Aging of temporal contrast sensitivity in the retina at mesopic and photopic luminances; separating normal aging from disease 121

3.1. Temporal contrast sensitivity changes in aging and disease 121

3.1.1 Temporal contrast sensitivity changes in normal aging 122

3.1.2 Temporal contrast sensitivity changes and retinal disease 124

3.1.3. Mechanisms for reduced temporal contrast sensitivity 127

3.2. Rod-cone interactions in flicker 129

3.3. Binocular summation of modulation flicker 130

3.4. Aims and objectives of the flicker and luminance study 131

3.5. Methods 132

3.5.1. Participants 132

3.5.2. Rapid Flicker Assessment (RFA) 132

3.5.3. Pupil measurements and retinal illuminance 135

3.5.4. Modulation sensitivity as a function of retinal illuminance 136

3.5.5. Calculating the HR_{index} for flicker sensitivity 136

3.5.6. Identifying participants with significantly elevated thresholds 137

3.5.7. Calculating binocular summation ratio (BSR) and Interocular Percentage Increase (IPI) 138

3.5.8. Statistical analysis 139

3.6. Results 140

3.6.1. Included and excluded participants 140
3.6.2. HR_{index} for monocular flicker thresholds 141
3.6.3. Comparison of HR_{index} for contrast and flicker 152
3.6.4. Binocular flicker thresholds and summation 154
3.7. Discussion 157
3.7.1. Flicker sensitivity declines non-linearly with age 157
3.7.2. Binocular summation of flicker 159
3.8. Conclusions 161
4. The effect of scotopic/photopic ratio on visual acuity 163
4.1. Night illumination for drivers and pedestrians 164
4.2. Rod pathways 166
4.2.1. Multiple rod pathways in the retina 166
4.2.2. Rod-cone signal interactions at the retina and cortex 169
4.3. Rod-cone interactions in spatial vision and detection 172
4.4. The effect of scotopic/photopic ratio on vision 174
4.4.1. The effects of S/P ratio on visual performance 175
4.4.2. Effect of S/P ratio on pupil size 177
4.5. Aims and objectives of the study 178
4.6. Methods 180
4.6.1. Participants 180
4.6.2. Visual acuity assessment 180

4.6.3. Illumination system 182

4.6.4. Calculation of S/P ratios 183

4.6.5. Pupil measurement and retinal illuminance 187

4.6.6. Function fitted to visual acuity and retinal illuminance 187

4.7. Results 188

4.7.1. Illuminance and S/P on contrast thresholds and pupil size 188

4.7.2. Pupil variations with S/P ratio 191

4.7.3. Contrast thresholds independent of pupil size 193

4.8. Discussion: Effect of S/P ratio in mesopic vision 198

4.8.1. The effect of S/P ratio in naturalistic viewing 198

4.8.2. The effect of S/P on visual acuity 198

4.8.2. The effect of S/P on pupil size 200

4.8.4. Recommendations for street lighting 201

4.9. Conclusions 202

5. General discussion 203

5.1. Aging of monocular spatial and temporal vision at photopic and mesopic light levels 203

5.2. Aging of binocular spatial and temporal vision 206

5.3. Scotopic/photopic ratios to optimise mesopic spatial vision 207

5.5. Further work 208

6. Conclusions 211

Appendix 1: Stability of accommodation at photopic and mesopic light levels 213

References 214

List of tables

Table 1. Description of visual acuity and refraction of participants in decade bins. 103

Table 2. Description of ANCOVAs describing the effects of age, foveal location and normalised interocular thresholds difference on binocular summation. 115

Table 3. Description of visual acuity and refraction of participants in decade bins. 141

Table 4. (x, y) co-ordinates of chromaticities employed for each S/P ratio..... 184

Table 5. Foveal acuity thresholds for S/P ratios 0.5 – 5.5 at retinal illuminances of 1.5 to -1.5 log trolands. The bold results show peak increases in the acuity thresholds. The highlighted values show the best acuity for that light level. Note that the poor acuity at the fovea at the lowest light level suggests that the stimulus size increases to stimulate rods outside the rod free zone. 199

Table 6. Peripheral acuity thresholds for S/P ratios 0.5 – 5.5 at retinal illuminances of 1.5 to -1.5 log trolands. The highlighted values show the best acuity for that retinal illuminance. 199

List of figures

Figure 1. The structures of the human eye (Kolb, 2007). 26

Figure 2. 3D section of the retina (Kolb et al., 2005) 29

Figure 3. Cone and rod photoreceptors (Burns & Lamb, 2004) 31

Figure 4. A The distribution of rods and cones in the human retina (Purves et al., 2001). B the distribution of the three types of cone in the retina (Sharpe, Stockman, Jägle, & Nathans, 1999). 33

Figure 5. Responses of a ON-centre retinal ganglion cell (Goldstein, 2009) 35

Figure 6. Colour and luminance channels (Barbur) 36

Figure 7. Pathways from the retina to the visual cortex. http://what-when-how.com/neuroscience/visual-system-sensory-system-part-3/ 37

Figure 8. Connections between the LGN and primary visual cortex (Thomson, 2010) 38

Figure 9. Centre-surround cell inputs to a simple cell in primary visual cortex http://www.scielo.br/scielo.php?script=sci_arttext&pid=S0104-65001997000200002) 39

Figure 10. Transmittance of the lens (Boettner & Wolter, 1962) 43

Figure 11. Changes in pupil diameter with age (Winn, Whitaker, Elliott, & Phillips, 1994) 44

Figure 12. Demonstration of presbyopia (http://seikoeyewear.com/eye-information/about-the-eyes/presbyopia) 47

Figure 13. Filled points and solid line show the maximal change in lens power for 27 human lenses (Glasser & Campbell, 1998). In addition these authors have plotted maximum and minimum amplitudes of accommodation from Duane (1912). 48

Figure 14. Comparison of normal retina with retina affected by wet AMD (http://www.vision-and-eye-health.com/macular-degeneration-types.html)..... 52

Figure 15. Photopic, mesopic and scotopic contrast sensitivity function, http://www.telescope-optics.net/aberrations_extended.htm..... 55

Figure 16. A Pelli-Robson chart http://www.psych.nyu.edu/pelli/pellirobson/. **B** Vision Contrast Test System. Spatial frequency varies vertically and contrast varies horizontally http://www.pacificu.edu/optometry/ce/courses/16554/agingeyepg2.cfm. **C** Functional Contrast Sensitivity test. Participants indicate the direction of the gap in the Landolt C which varies in contrast while size remains constant (Chisholm, Evans, Harlow, & Barbur, 2003a). 57

Figure 17. Modulation and luminance-pedestal flicker (Hogg & Chakravarthy, 2006)..... 60

Figure 18. A Modulation sensitivity throughout the retina. **B** CFF throughout the retina. Modified from Tyler (1987) 62

Figure 19. TCSF at various retinal illuminances (Kelly, 1961), from http://webvision.med.utah.edu/book/part-viii-gabac-receptors/temporal-resolution/ 63

Figure 20. Plot of the Stockman and Sharpe (2000) 2° cone fundamentals, normalised for sensitivity..... 64

Figure 21. **A** CIE 1931 Chromaticity diagram from Ripamonti, Woo, Crowther, and Stockman (2009). The wavelengths of light are plotted around the edge and the central line is the Planckian locus which is the colour of an incandescent black body as it changes temperature. D93, D65 and D50 indicate the chromaticity of CIE standard illuminants that represent natural light found in different parts of the world, for which D65 is an indication of daylight in Western Europe. **B** shows MacAdam ellipses plotted in CIE 1931 (x, y) chromaticity diagram. From http://www.ecse.rpi.edu/~schubert/Light-Emitting-Diodes-dot-org/chap17/F17-05%20MacAdam%20ellipses.jpg 67

Figure 22. Scotopic and photopic luminous efficiency functions, from www.cvrl.org 76

Figure 23. Screenshots from the functional Contrast Sensitivity Test. **A** the fixation cross with no stimulus presented. **B** an example of a high contrast foveal (0°) stimulus with the gap orientated towards the top right. **C** example of a low contrast foveal stimulus with the gap orientate towards the top left. **D** example of a low contrast parafoveal stimulus (+4°). The fixation cross remains on the screen during parafoveal presentations to ensure the participant fixates on the centre of the monitor. **E** example of a low contrast parafoveal stimulus located at -4° eccentricity. 96

Figure 24. Age distribution of included participants (n=74). 102

Figure 25. The decrease in pupil diameter and age from the current study. A linear fit finds that, pupil diameter = -0.0468*age + 7.5806, $R^2 = 0.41$. Data are the average pupil size for a monitor luminance of 34 cd/m^2. 104

Figure 26. Log contrast thresholds for participants at the range of light levels. For the foveal data each participant contributes two points for each screen luminance,

one from each eye. For the parafoveal data, each participant contributes four points for each luminance level, from ±4° in each eye. For plotting purposes, results were not averaged across eyes due to differences in the measured retinal illuminance between the eyes on each trial. Fit to foveal data: log contrast threshold = -0.4244*log E + 2.3123. Fit to parafoveal data: log contrast threshold = -0.3461*log E + 2.2444. 105

Figure 27. Contrast thresholds for participants at the range of light levels. For the foveal data each participant contributes two points for each screen luminance, one from each eye. For the parafoveal data, each participant contributes four points for each luminance level, from ±4° in each eye. For plotting purposes, results were not averaged across eyes due to differences in the measured retinal illuminance between the eyes on each trial Fit to foveal data: contrast threshold = $283.2*(e^{-1.036 * \log E}) + 3.86$. Fit to parafoveal data: contrast threshold = $213.3*(e^{-1.028 * \log E}) + 10.41$. 106

Figure 28. HR_{index} as a function of age. Panels **A** and **C** show the HR_{index} for the fovea and parafoveal respectively. Dashed lines show the 95% limits. Panels **B** and **D** show the probability density distributions of the value of errors from the regression line. 108

Figure 29. Examples of log contrast thresholds and the corresponding HR_{index} values at the fovea and parafovea for a younger (age 22) and older (age 69) participant. The younger participant has a smaller area under the curve than the group data, resulting in a positive HR_{index}. However the older participant has a greater area under the curve than the group data at the parafovea resulting in a negative and/or lower HR_{index}. 109

Figure 30. Examples of contrast thresholds and the corresponding HR_{index} values at the fovea and parafovea for a younger (age 22) and older (age 69) participant, re-plotted from **Figure 29.** 110

Figure 31. Foveal and parafoveal contrast thresholds at 900, 25 and 5 td. Upper panels show thresholds on a linear scale and lower thresholds on a log scale. Fit to foveal contrast thresholds on a linear scale, at 5 td, y = 0.7316x + 81.873, R^2 = 0.0857; at 25 td, y = 0.535x + 28.01, R^2 = 0.1343; at 900 td, y = 0.2700x + 4.7049, R^2 = 0.1556. Parafoveal contrast thresholds on a linear scale, at 5 td, y = 0.6422x + 84.848, R^2 = 0.0904; at 25 td, y = 0.5701x + 32.922, R^2 = 0.1876; at 900 td, y = 0.3659x + 5.9982, R^2 = 0.3077. Fit to foveal contrast thresholds on a log scale, at 5 td, y = 0.0029x + 1.906, R^2 =0.0910, 25 td, y = 0.0047x + 1.467, R^2 = 0.1533, 900 td, y = 0.0074x + 0.8226, R^2 = 0.2159. Fit to parafoveal contrast thresholds on a log scale, at 5 td, y = 0.0028x + 1.912, R^2 = 0.1243, 25 td, y = 0.0046x + 1.536, R^2 = 0.2295, 900 td, y = 0.0073x + 0.983, R^2 = 0.3651. 112

Figure 32. BSR values below 1 (the BSR inhibition threshold) indicate binocular inhibition. **A** binocular summation ratio for normal, binocular participants (n=71). Binocular summation was calculated as the best monocular contrast threshold divided by the binocular contrast threshold at retinal illuminances between 900 td and 2 td. The solid line shows the linear fit to the foveal data (-0.0049*age + 1.5296, r^2=0.048, p=0.067) and the dashed line the fit to parafoveal data (-0.0051*age +1.656, r^2=0.069, p<0.05). **B** a linear fit to both foveal and parafoveal points as the ANCOVA revealed no effects of eccentricity (-0.0035*IPI + 1.5013, r^2 = 0.08, p<0.01). **C** IPI has no relationship with age at the fovea (r^2=0.004, p=0.23) or parafovea (r^2=0.000, p=0.94). 115

Figure 33. The impulse response function at various retinal illuminances. At higher illuminances, the function is triphasic and rapid, however it is biphasic and sluggish at lower light levels..... 127

Figure 34. Examples of the flicker stimuli employed in this study. The top row shows the fixation and foveal stimulus. The bottom row shows examples of the four peripheral stimuli..... 133

Figure 35. Age distribution of 80 participants in the study. 140

Figure 36. Flicker thresholds for with retinal illuminance for included participants. For the foveal data each participant contributes two points for each screen luminance, one from each eye. For the parafoveal data, each participant contributes eight points for each luminance level, from each eye. Fit to foveal data: flicker threshold = $336*E^{-0.5492} + 1.108E-06$. Fit to parafoveal data: flicker threshold = $328*E^{-0.5351} + 5.696E-06$..... 142

Figure 37. Log flicker thresholds for with retinal illuminance for included participants. For the foveal data each participant contributes two points for each screen luminance, one from each eye. For the parafoveal data, each participant contributes eight points for each luminance level, from each eye. Fit to foveal data: flicker threshold = -0.5896*log E +2.5095. Fit to parafoveal data: flicker threshold = -0.4997*log E + 2.4137..... 143

Figure 38. HR_{index} as a function of age, fitted with a 2nd order polynomial quantile regression. Black lines show 50th percentile (i.e. HR_{index}), and dashed lines the 5th and 95th percentile. Equation for the HR_{index}, indicated by the 50th percentile, is shown above each graph. **A** HR_{index} values for the fovea. $5\text{th percentile fovea} = -0.0002 \times \text{Age}2 + 0.128 \times \text{Age} - 1.8511.$ $95\text{th percentile fovea} = -0.0006 \times \text{Age}2 + 0.042 \times \text{Age} - 0.1266.$ **B** HR_{index} values for the parafovea.

$5\text{th percentile parafovea} = -0.0015 \times \text{Age}2 + 0.113 \times \text{Age} - 2.2384.$

$95\text{th percentile parafovea} = -0.0002 \times \text{Age}2 + 0.014 \times \text{Age} + 0.2439.$..... 144

Figure 39. Examples of log modulation thresholds and the corresponding HR_{index} values for two normal participants, aged 21 and 74. The 21 year old has a smaller area than the group curve in both the fovea and the parafovea, resulting in a positive HR_{index}, whereas the 74 year old has a larger area under the curve at both eccentricities, resulting in a negative HR_{index}. 146

Figure 40. Examples of modulation thresholds and the corresponding HR_{index} values for two normal participants, aged 21 and 74. The 21 year old has a smaller area than the group curve in both the fovea and the parafovea, resulting in a positive HR_{index}, whereas the 74 year old has a larger area under the curve at both eccentricities, resulting in a negative HR_{index}. 147

Figure 41. Foveal and parafoveal contrast thresholds at 900, 400, 100, 50 and 25 td. First page shows contrast thresholds on a linear scale. 2nd order quantile fits are shown, with the solid line representing the 50th percentile, and dashed lines representing the 5th and 95th percentile. The second page shows contrast thresholds on a log scale. Points were derived from curves fitted to each individual's data and averaged across eyes at the fovea and eccentricities and eyes at the parafovea. 151

Figure 42. Bland-Altman plot of the mean of contrast and flicker HR_{index} index values and difference between these values. The middle line shows the mean difference value of 0.22. The other lines indicate the limits of agreement at difference values of 1.06 and -0.62..... 153

Figure 43. Modulation thresholds as a function of retinal illuminance for all participants for the worst eye, best eye and binocular viewing. For foveal modulation thresholds, each participant contributes five points for each of the three

curves as a result of measuring modulation thresholds at five light levels for each of the viewing conditions (viewed by worst eye, best eye and viewed binocularly). The fits to the group data are the following, where E is retinal illuminance: Worst eye foveal threshold = 390.3 * $E^{-0.5772}$ + 2.479E-05; Best eye foveal threshold = 368.5 * $E^{-0.6027}$ + 3.116E-05; Binocular foveal threshold = 387.8 * $E^{-0.683}$ + 6.533E-07. For parafoveal modulation thresholds, data points represent the average of four eccentricities as a result of four different parafoveal locations tested in each eye. The fits to the group data are the following: Worst eye parafoveal threshold = 390.1 * $E^{-0.5685}$ + 0.735; Best eye parafoveal threshold = 394.8 * $E^{-0.6144}$ + 1.604; Binocular parafoveal threshold = 347.5 * $E^{-0.689}$ + 0.1555. 154

Figure 44. Data are shown for participants at the fovea (solid circles) and parafovea (unfilled squares) **A** BSR does not change substantially with age at the fovea or parafovea, and **B** shows that IPI does not change systematically with age either. Furthermore, **C** shows that there is no substantive relationship between BSR and IPI. 156

Figure 45. Illustration of the two rod pathways through retinal circuitry (Sharpe & Stockman, 1999). 167

Figure 46. Experimental setup showing the display area, chin rest and one of two illumination systems 181

Figure 47. The spectral power distribution of each of the four primaries in the illumination system. 183

Figure 48. Constant S/P ratios in CIE space for a constant photopic luminance (CIE, 1931). **A** For a three primary system, S/P ratios fall along a line in CIE space. The three coloured points indicate the three primaries. **B** For a four primary system, S/P ratios lie in areas in CIE space, indicated by the blue lines. These areas form

quadrangles for lower S/P ratios (0.5 – 2.5) and subsequently form triangles (3.5 - 5.5). Green lines indicate the mid-points of the quadrangle used to calculate the centre point of each area of constant S/P ratio, which is indicated by a red cross. **C** The centre points of areas of constant S/P fall along the red line for S/P ratios between 0.5 and 5.5. 185

Figure 49. Chromatic information of the S/P values chosen. **A** The S/P values in CIE space (1931) and estimated subjective appearance. **B** Spectral power distributions of the S/P ratios. 186

Figure 50. Foveal acuity thresholds (primary y-axis) and corresponding pupil diameters (secondary y-axis) for illuminances 1, 0.1, 0.01 and 0.001 cd/m^2. 189

Figure 51. Peripheral acuity thresholds (primary y-axis) and corresponding pupil diameters (secondary y-axis) for illuminances 1, 0.1, 0.01 and 0.001 cd/m^2. 189

Figure 52. Mean pupil dianeter at photopic luminances. Error bars indicate one SE. 191

Figure 53. The effect of S/P ratio on pupil diameter at each photopic luminance. Error bars indicate 1 SE. 192

Figure 54. Acuity thresholds in arc min for each S/P ratio and light level at the fovea and peripheral averaged over all participants. Curves fitted to the points took the form: $T = a \times E - b + c$, where T is the acuity threshold, E is retinal illuminance and a, b and c are free parameters..... 194

Figure 55. Effect of S/P ratio on acuity thresholds at specific retinal illuminances. Error bars show 1 SE. 195

Figure 56. **A** Cone excitations at the S/P ratios used in the study. **B, C and D** Post-receptoral mechanisms at each S/P ratio selected. Note different scales for

each graph showing that in **B**, luminance is effectively stable, in **C** L/(L+M) also changes little but in **D** S/(L+M) changes substantially with S/P ratio. 196

Acknowledgements

I would like to sincerely thank my supervisor, John, for giving me the opportunity to conduct this work. Throughout, he has been patient in teaching me new skills, kind in discussions of my work, encouraged me to pursue my ideas, and has opened up many opportunities for the future, for which I will be forever grateful. I would also like to thank the post-doctoral researchers that I had the good fortune to work with and learn from. Evgenia, your diligence and productivity is something to aspire to. Gary, I appreciate the numerous hours spent poring over our results and for your patience in reviewing my code. Wei, your unique combination of attention to detail and easy-going attitude made working with you productive and enjoyable. Furthermore I would like to thank Alistair Harlow for providing technical support and practical solutions to issues encountered.

Additionally, I would like to thank those who sparked my interest in vision science and pursuing research. Dr Henning was the first person who taught me about perception and has always been generous with his time and advice over the years. Erin Babinsky noticed and developed my interest in research when we met at Oxford, and Miriam and Ahalya nurtured this when I worked with them as a research assistant at City, which was a very pleasant time. Your support has been more valuable than you could ever know.

This research would not have been possible without the hours of diligent observing by the participants, who kindly gave their time to take part in this research. I am particularly grateful for those who helped recruit more participants, you know who you are!

My time at City has been made deeply enjoyable by the many friends I have made and the experiences we have shared together. In particular, I want to thank Joe and Emily for good times we've had, in the UK and around the world – I hope we will keep adding locations to that list! I also want to thank Marisa, Eva, Irene, Yingxin, Priya and Emsal for discussions, drinks and advice. I am indebted to the efforts of James Perkins and Keith Simpson at City for their support during difficult times. Lucy and Sarah have been good friends and mentors, to discuss lab and health science with respectively.

My parents Marguerita and Alan, as well as my sister Muirin, have been persistently encouraging and supportive over the years of my education. I am grateful for the many hours they have spent listening to me talk about the ups and downs of research over the past three years, and for taking part in many of my experiments, often being one of the first participants before the procedure was fully streamlined.

Lastly, my thanks goes to Simon who has been the sounding board for ideas good and bad, the sympathetic ear, wonderful cook and importantly, the caring and long suffering partner. He has good-naturedly seen me through this thesis, the way he does with everything. No one could ask for more.

Declaration

I grant powers of discretion to the University Librarian to allow the thesis to be copied in whole or in part without further reference to me. This permission covers only single copies made for study purposes subject to normal conditions of acknowledgement.

Abstract

The research contained in this thesis describes three studies designed to investigate the ability of the observer to detect stimuli defined by changes in luminance in space and/or time in mesopic conditions, including contrast sensitivity, temporal flicker sensitivity and visual acuity.

The first two studies determined the effect of the aging of the retina on spatial and temporal contrast sensitivity at photopic and mesopic light levels. The literature states that older people experience losses of retinal neurons including rods, cones and ganglion cells. Furthermore, older people tend to have particular difficulties with vision at low light levels which can be attributed to greater loss of rods than cones, particularly at parafoveal eccentricities. Spatial and temporal contrast sensitivity was measured separately in two groups of participants, aged 20-73 (n=74) and 20-74 (n=80) years of age, respectively. Measures were taken to ensure that thresholds largely reflected age-related changes to the retina rather than the optics of the eye. Spectral content of the stimuli was restricted to the middle and long wavelength regions of the visual spectrum and the pupil was measured continuously so as to obtain participant-specific retinal illuminances for each condition. The HR_{index} was derived and calculated for each participant as a single number which summarized performance from photopic to mesopic light levels. As age increased both spatial and temporal contrast vision worsened and older participants showed particularly elevated thresholds at lower light levels when compared to younger participants. Spatial contrast thresholds show a steady linear decline with age, whereas temporal modulation thresholds were relatively stable up to 50 years of age and then demonstrated a rapid decline. These different trends of changes in performance with increasing age suggests that contrast and temporal HR_{index} may be measuring the aging of different retinal mechanisms. The normal limits of HR_{index} values were calculated which could be used in the future to detect abnormal performance.

A secondary aim of the first two studies was to determine if binocular summation of spatial and temporal contrast thresholds declined with age, while accounting for differences in retinal illuminance between monocular and binocular conditions. For spatial contrast vision, binocular summation declined significantly with age and 18% showed binocular inhibition. However, the binocular summation of flicker signals did not change significantly with age and only 1% of participants showed binocular inhibition. Interocular differences cannot explain our results.

The third study determined whether altering the scotopic/photopic luminous efficiency ratio could improve spatial acuity at mesopic light levels. This was achieved by altering the spectral power distribution of illuminating lights to increase the contribution of rods to vision at constant levels of photopic illumination. It was found that visual acuity at the fovea was improved by low levels of increased scotopic luminance, but peripheral acuity was improved by larger increases of scotopic luminance.

The three studies demonstrate that the detection of luminance defined stimuli can be compromised in a number of external conditions such as low light levels, as well as due to internal changes caused by aging to the optics of the eye, retina and/or the central visual system.

Abbreviations and symbols

°	Degrees	**P-cells**	Cells in the parvocellular pathway
µm	Micrometres	**R^2**	Square of the correlation coefficient
AMD	Age-related Macular Degeneration	**RF**	Receptive field
arc min	Minutes of arc	**RPE**	Retinal Pigment Epithelium
ARM	Age-Related Maculopathy	**s**	Seconds
BSR	Binocular summation ratio	**S cone**	Short wavelength sensitive cone
c/deg	Cycles per degree	**SD**	Standard Deviation
cd/m^2	Candelas per metre squared	**SE**	Standard Error
CFF	Critical flicker frequency	**SRCI**	Suppressive rod-cone interaction
CIE	Commission Internationale d'Eclairage	**SW**	Short wavelength
CNV	Choroidal neovascularisation	**TCSF**	Temporal contrast sensitivity function
CRT	Cathode Ray Tube	**td**	Trolands
CS	Contrast sensitivity	**V(λ)**	Photopic spectral responsivity function
CSF	Contrast sensitivity function (spatial)	**V'(λ)**	Scotopic spectral responsivity function
E	Retinal illuminance	**$V_{10}(\lambda)$**	Photopic spectral responsivity function for the 10° observer
FCS test	Functional contrast sensitivity test		
GA	Geographic atrophy		
HR_{index}	Health of the Retina Index		
Hz	Hertz		
IPI	Interocular percentage increase		
IPRGC	Intrinsically photosensitive retinal ganglion cells		
IRF	Impulse response function		
L cone	Long wavelength sensitive cone		
LogMAR	Logarithm of the Minimum Angle of resolution		
LW	Long wavelength		
m	Metres		
M	Mean		
M cone	Medium wavelength sensitive cone		
MAP	Macular Assessment Profile		
M-cells	Cells in the magnocellular pathway		
mm	Millimetre		
ms	Milliseconds		
MW	Medium wavelength		

1. The visual system

The aim of the studies carried out in this thesis were firstly to determine the limits that describe healthy aging in spatial contrast and flicker sensitivity under specified stimulus conditions over light levels that are frequently encountered in working environments (i.e., high mesopic to photopic range). Another aim was to determine whether mesopic spatial vision can be enhanced by biasing the spectral composition of the illuminant to favour the stimulation of rod photoreceptors.

The UK is facing an aging population problem (Office for National Statistics, 2009), which will increase the incidence of age related ocular disease. This in turn is likely to increase the number of people with visual impairment from an estimated 1.8 million in 2008 to nearly 4 million by 2050 (Access Economics, 2008). Visual impairment has wide ranging consequences on an individual's quality of life including an increased risk of depression (Branch et al., 1989 and Carabalese, Appollonio, Rozzini, Bianchetti, Frisoni et al., 1993), social isolation (Verstraten, Brinkmann, Stevens, & Schouten, 2005), and even increased incidence of falls and injury (Ivers, Cumming, & Mitchell, 2002).

The studies reported in this thesis were performed in order to determine limits of healthy, normal aging under specified stimulus conditions so that healthy aging changes could be separated from changes caused by early stages of retinal disease. The aim is to detect the earliest signs of disease, so as to increase the chances of successful treatment and hence prevent disease progression and subsequent loss of vision.

1.1. The structure of the human eye

The human eye is located in the orbit of the skull (**Figure 1**). The eye is a slightly asymmetrical sphere of approximately 24-25 mm in length and has three different layers starting from the outer surface and progressing to the inner surface. The external layer includes the cornea at the anterior of the eye, and the sclera surrounding the rest of the eye. The intermediate layer is divided into the anterior segment containing the iris, ciliary body and the lens, and the posterior segment containing the retina and choroid. The last layer is the internal layer, containing the retina, which is the first part of the visual sensory system. The eye contains three chambers of fluid; aqueous humor is contained within the interior chamber between the cornea and the iris, as well as in the posterior chamber which is between the iris, zonule fibers and the lens. Vitreous humor is found in the vitreous chamber which is between the lens and the retina (Kolb, 2007).

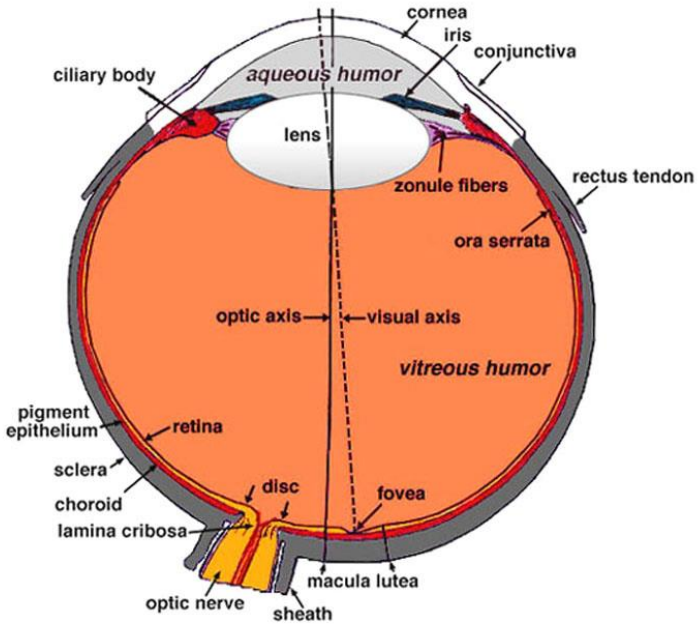

Figure 1. The structures of the human eye (Kolb, 2007).

1.2. The cornea and sclera

The cornea is a transparent structure at the most anterior region of the eye. The cornea is the first structure to refract light, and is responsible for two thirds of the refractive power of the eye which is required to focus a distant object into a sharp image on the retina. If the shape becomes irregular it results in a focusing defect known as astigmatism which causes a point source to be imaged as a line in two different image planes (Poon & Taylor, 1997). The cornea as a whole transmits light of 300 to 2500 nm, but has a maximum transmittance between 500 and 1300 nm (Boettner & Wolter, 1962).

The sclera is the continuation of the collagen fibres of the cornea towards the posterior of the eye, and is pierced throughout by blood vessels and nerves, the most substantial of which is the optic nerve. The primary function of the sclera is to provide a rigid and solid framework to the eye, allowing the formation of a retinal image.

1.3. The pupil

The iris is a pigmented disc with a central opening forming the pupil. The central layer of the iris, the stroma, contains blood vessels and two sheets of smooth muscle which control constriction and dilation of the iris, allowing changes in pupil size in response to a wide range of factors, but its primary function is to control the amount of light reaching the retina. It also narrows when accommodating for nearby objects and dilates for accommodation to more distant targets (Rogers, 2010).

1.4. The lens

The lens is a transparent body suspended by ligaments called zonule fibres which are attached to the ciliary body. Accommodation is caused by ciliary muscle action which contracts or relaxes the zonule fibres, changing the shape of the lens. Accommodation allows the formation of a sharp image on the retina (Kolb, 2007); when viewing a distant object the ciliary muscle relaxes resulting in increased tension in the zonules, flattening the lens, whereas to view a near object the ciliary muscles contract resulting in slack zonules and the lens returns to a thicker shape. In a young eye, the refractive power of the lens is only one third (approximately 13 dioptres) of the total power, as the cornea is responsible for the rest of the refractive power. It transmits wavelengths from around 350 to 1300 nm, a somewhat narrower range than the cornea (Boettner & Wolter, 1962).

1.5. The retina

1.5.1. Anatomy of the retina

The retina is the first part of the visual system that responds to light. It is formed embryonically from tissue that is connected to the brain by the optic nerve and therefore can be considered part of the brain (Rogers, 2010). The image is focused by the cornea and lens towards a central point along the visual axis, towards the macula, at the centre of which is the fovea. The optic nerve transmits neural signals from the retina to other regions of the brain and radiates major blood vessels to supply the retina with oxygen (Kolb, Fernandez, & Nelson, 2005).

There are a number of layers in the retina. Firstly the retinal pigment epithelium (RPE) layer next to the choroid contains a dark pigment which absorbs light to minimise back scatter within the eye. Together with Bruch's membrane, it forms a

blood/retinal barrier and transports nutrients from the blood to the photoreceptors, transports metabolites from retinal tissue to the blood and controls ion homeostasis (Strauss, 2005). There are three layers of nerve cell bodies (nuclear layers) and two layers of synapses (plexiform layers) in the main part of the retina as shown in **Figure 2**. The outer nuclear layer contains the cell bodies of rods and cones which are the light sensitive photoreceptor cells and the inner nuclear layer contains neurones called horizontal, bipolar and amacrine cells and the final ganglion cell layer contains the ganglion cells which transmit signals from the eye via the optic nerve. The outer plexiform layer contains connections between rods and cones, as well as vertically running bipolar cells and horizontally running horizontal cells. The inner plexiform layer connects the vertically running bipolar cells and lateral connections with amacrine cells, to the ganglion cells in their ganglion cell layer which transmit visual information via the optic nerve (Kolb et al., 2005).

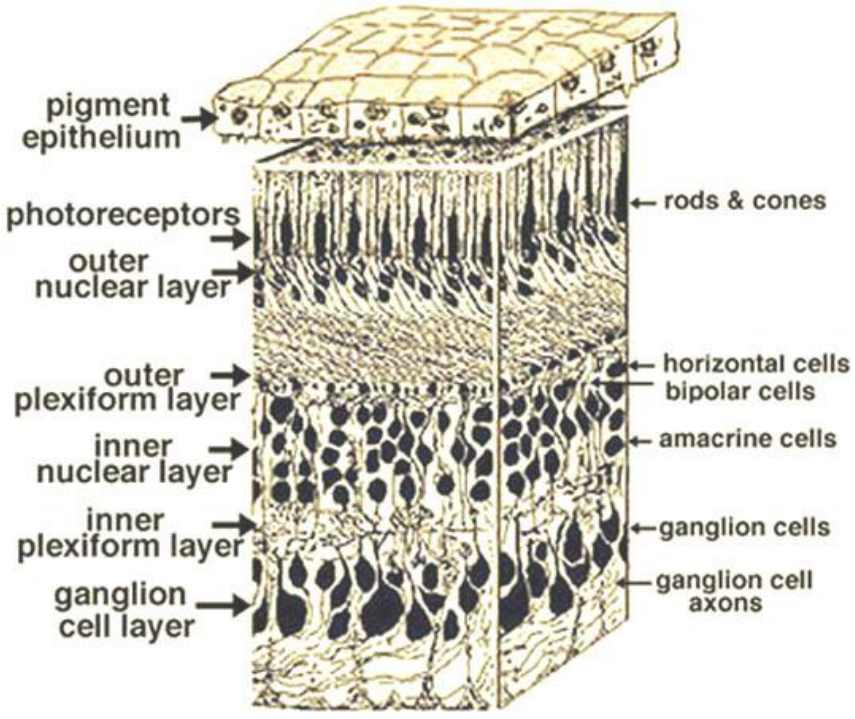

Figure 2. 3D section of the retina (Kolb et al., 2005)

1.5.2. The macula and fovea

The macula is the central part of the fundus and is approximately 6 mm which corresponds to 21° of visual angle. The macula is dark in appearance due to the presence of macular pigment which absorbs short wavelength light and reduces the effects of chromatic aberrations. The macula consists of three subsections; the first of which, the fovea, is the central part of the macula, 0.8 smm (2.75° of visual angle). It can be seen from **Figure 1**, that the fovea is not centred on the optic axis, but is offset by 4°. The fovea contains only cone photoreceptors and is surrounded by the parafovea which additionally contains rods and lies at 1-3mm from the fovea to 3.5° of visual angle. The parafovea is surrounded by the perifovea, which forms the last ring of the macula, up to 10° eccentricity. Rods outnumber cones by 9:1 in the macula and 20:1 in the whole eye. Maximum rod density lies in the parafovea, at 4-6mm from the fovea (Curcio, Sloan, Kalina, & Hendrickson, 1990).

1.5.3. Photoreceptors

The retina contains three kinds of photoreceptors, rods, cones and intrinsically photosensitive retinal ganglion cells (IPRGCs), however, for quality spatial and temporal vision, we rely on the signals from rods and cones. These photoreceptors convert light into electrical signals using a chemical cascade process known as phototransduction. Cones tend to be larger than rods and they differ in shape with cones showing a more pyramidal profile and rods appearing more cylindrical (**Figure 3**).

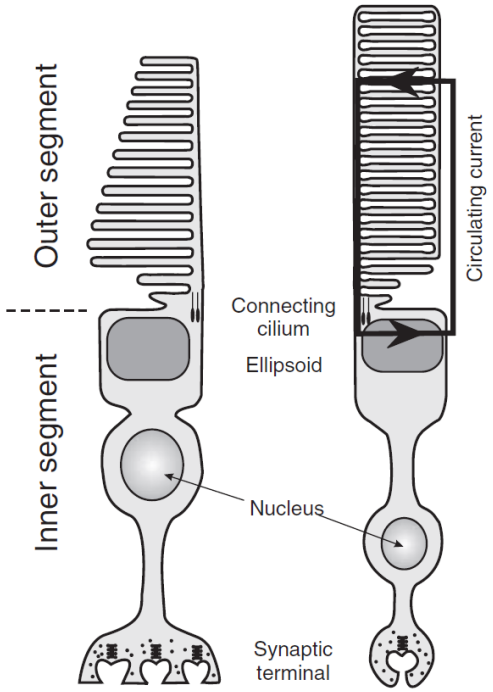

Figure 3. Cone and rod photoreceptors (Burns & Lamb, 2004)

The rods and cones each have an outer segment, an inner segment and synaptic ending. The outer segment contains a number of different light capturing proteins, broadly referred to as opsins. In cones the opsin is contained within the sac-like folds of the plasma membrane, whereas in rods opsin is contained in the intracellular organelles called discs which are discontinuous from the membrane of the receptor. The inner segment contains an area called the ellipsoid, providing a high density of mitochondria which function to supply adenosine triphosphate (ATP) to the outer segment, which is metabolically demanding. Other expected organelles are contained within the inner segment, such as the endoplasmic reticulum and Golgi apparatus (Burns & Lamb, 2004).

The process of phototransduction is activated by the absorption of a photon of light by a photopigment chromaphore, transforming it into an active state which activates a G protein transducin which subsequently activates the effector protein (a molecule that binds to another protein to regulate its activity), phosphodiesterase. Phosphodiesterase hydrolyses the messenger cyclic guanosine monophosphate (cGMP), decreasing its concentration within the photoreceptor, resulting in the closure of cGMP-gated ion channels which hyperpolarises the cell and generates an electrical response which is transmitted by the synaptic terminal (Burns & Lamb, 2004). It is worth noting that mammalian photoreceptors are activated by *hyperpolarisation* and other neurones tend to be activated by *depolarisation*.

The distribution of rods and cones varies across the retina as can be seen in **Figure 4**. Overall there are approximately 91 million rods in the human retina, whereas there are only roughly 4.5 million cones (Purves et al., 2001). At the fovea there are no rods and only cones within the central 1.25° (Curcio et al., 1990). The centre of the retina is dominated by middle wavelength (MW) and long wavelength (LW) cones, with relatively few short wavelength (SW) cones in the more peripheral retina (Sharpe, Stockman, Jägle, & Natans, 1999), making up only 7% of cones within the central retina (Curcio et al., 1991). Cones themselves vary in size across the retina, being smallest at the central fovea and increasing in size with increasing eccentricity (Curcio et al., 1990). As eccentricity from the fovea increases, the number of cones rapidly falls off and the number of rods increase to a peak density of approximately 20° (Osterberg, 1935). There are no photoreceptors at 10° nasally over the optic disk, forming the "blind spot".

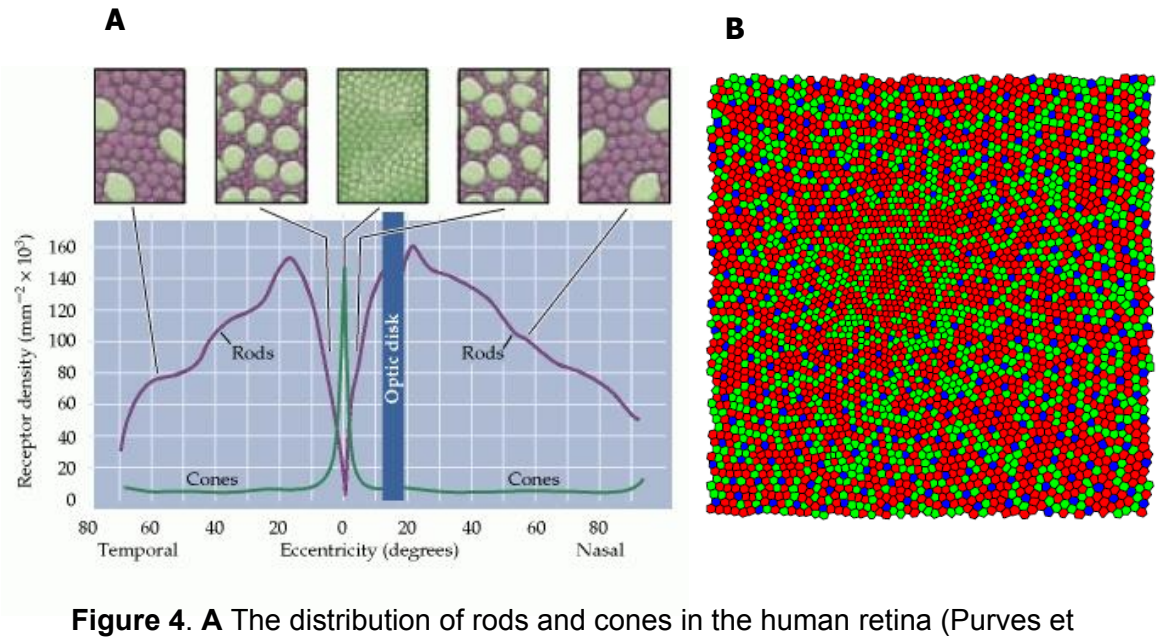

Figure 4. **A** The distribution of rods and cones in the human retina (Purves et al., 2001). **B** the distribution of the three types of cone in the retina (Sharpe, Stockman, Jägle, & Nathans, 1999).

Rods and cones have differential sensitivities to light level; rods are more sensitive to lower levels of light, whereas cones are less sensitive but contribute to a higher quality of spatial and temporal vision, as well as mediating colour vision under higher levels of illumination. At high levels of illumination (above ~ 3 cd/m^2) vision is dominated by cones, whereas below 0.0003 cd/m^2 only rods mediate vision. Rod mediated vision at low light levels is known as scotopic vision and cone mediated vision at higher light levels is known as photopic vision (Barbur & Stockman, 2010). At intermediate light levels, both rods and cones contribute to the visual response, which is known as mesopic vision. Rods and cones can interact in mesopic conditions, either directly via rod-cone gap junctions or more distally via other connections in the retina (Sharpe & Stockman, 1999).

1.5.4. Post-receptoral retinal pathways

Photoreceptors have three main pathways through the retina; Rod-cone gap junctions, the vertical pathways and the lateral pathways. The pathways involve connections between the photoreceptors, bipolar cells, horizontal cells, amacrine cells and ultimately they pass their signals on to ganglion cells. There are twenty kinds of retinal ganglion cells (Rodieck, 1998), however the main three types are midget, parasol and bistratified (Dacey & Lee, 1994; Kolb, Linberg, & Fisher, 1992; Polyak, 1941).

There are a number of neural pathways through the retina. Firstly, rods synapse onto cones using rod-cone gap junctions providing a direct pathway for interaction between these two types of photoreceptor. The second pathway is, known as the vertical pathway, where bipolar cells contact either rods or cones and pass signals on to retinal ganglion cells in the inner plexiform layer. The third pathway is the lateral pathway which has two levels using horizontal cells and amacrine cells to provide antagonistic lateral connections between both rods and cones to adjust the gain of photoreceptor output to generate spatial and chromatic opponency. This becomes the basis of ganglion receptive fields in which central areas of the receptive field are modulated by surrounding areas (Perlman, Kolb, & Nelson, 2005).

Retinal ganglion cell receptive fields commonly have a circular, centre-surround organisation meaning that the centre and surround react differently to light falling on these areas. ON-centre ganglion cells respond maximally when there is light in the centre of the receptive field and less light in the surround, whereas OFF-centre ganglion cells respond maximally to light at the surround and low levels in the centre. This means the receptive field responds best to spatially modulated patterns

of light rather than to uniform surfaces. **Figure 5** describes the responsive properties of a centre-surround ganglion cell with an ON centre and an OFF surround, which is made possible by lateral inhibition. The ganglion cell responds minimally when light stimulates the whole receptive field (d) or none of the field due to inhibitory lateral connections. The cell responds maximally when light falls over the whole of the ON centre and none of the OFF surround (b). A less optimal response is obtained if the light stimulates only some of the ON centre (a) or if it additionally falls partially on the OFF surround (c). This arrangement allows increased responses to luminance or chromatic contrast, as chromatic opponent retinal ganglion cells respond maximally to a particular range of wavelengths at the centre or surrounding areas. Receptive fields of ganglion cells overlap considerably in the retina so that each point may form part of many ON and OFF centre ganglion cells (Kandel, Schwartz, & Jessell, 2000).

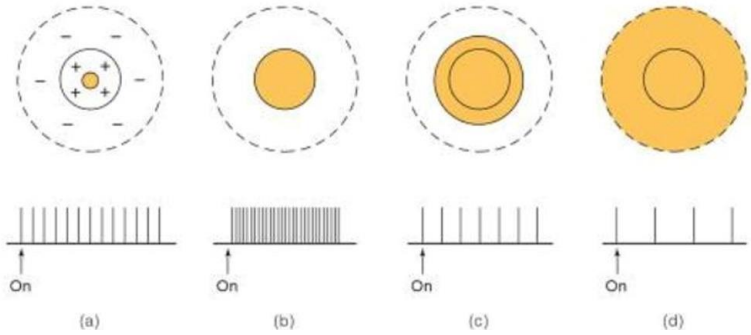

Figure 5. Responses of an ON-centre retinal ganglion cell (Goldstein, 2009)

Correspondingly, ON bipolar cells depolarise when the cone hyperpolarises in the presence of light. In contrast, OFF bipolar cells hyperpolarise in response to increments of light and depolarise in response to decrements in light. These bipolar cells then synapse separately with the corresponding ON or OFF ganglion cells. Only L and M cones are connected to both ON and OFF bipolars, S cones are only

connected to ON bipolars, but signals from all cone types can be connected to ON or OFF ganglion cells. It is clear from this stage that there are two relatively independent pathways for colour and luminance; rod signals and the sum of L and M cone signals are used for the scotopic and photopic luminance channels respectively, and the L-M and (L+M)-S signals contribute to the chromatic channels as shown in **Figure 6**.

Figure 6. Colour and luminance channels (Barbur)

1.6. Post-retinal visual processing

The axons of the retinal ganglion cells project to the optic disc and leave the eye via the optic nerve. They reach the optic chiasm when the nerves from the nasal visual field decussate whereas the temporal nerves remain on the ipsilateral side which allows the image from one side of the visual field to be transmitted to the contralateral cortical hemisphere. After this stage, the majority of nerves travel via the optic tract to the Lateral Geniculate Nucleus (LGN) in the thalamus which is the start of the major visual pathway to the cortex.

1.6.1. The lateral geniculate nucleus (LGN)

The LGN is a nucleus in the thalamus of the brain, located between the cerebral cortex and the midbrain. It is composed of two parts, located in each hemisphere

(**Figure 7**). M-cells from the retina project to the magnocellular layers of the LGN (layers 1 and 2), which are located ventrally, and the more numerous P-cells project to the parvocellular layers (layers 3-6) located more dorsally. The bistratified ganglion cells project to the koniocellular layers (Dacey & Lee, 1994) which are located between the interlaminar spaces of the principle magnocellular and parvocellular layers (Hendry & Yoshioka, 1994). There are similar numbers of cells in the magnocellular and interlaminar layers, however the koniocellular cells are very small and therefore difficult to study. Each layer receives input from one eye only; layers 1, 4 and 6 receive input from the contralateral eye whereas layers 2, 3 and 5 receive projections from the ipsilateral eye. The LGN also receives feedback from the primary cortex.

The M and P pathways have distinct response properties, specialised for the stimuli that they process. These differences can be described in five main ways (Hendry, Hsiao, & Brown, 2008). Firstly, the receptive field sizes of P-cells are much smaller than those for M-cells at the same retinal position. Secondly, the conduction speed of axons in M-cells tend to be faster than those for P-cells. Thirdly the responses of M-cells tends to be transient in comparison to the P-cells, which can produce sustained responses, particularly to chromatic stimuli. Fourthly, most P-cells are sensitive to wavelength differences whereas most M-cells are not. Finally M-cells are thought to be sensitive

Figure 7. Pathways from the retina to the visual cortex. http://what-when-how.com/neuroscience/visual-system-sensory-system-part-3/

to low luminance contrasts whereas P-cells are insensitive to small changes in luminance. These response properties are the basis for the P-cells chromatically selective responses, and the M-cells sensitivity to luminance contrast.

1.6.2. Visual cortex

Primary visual cortex is also known as V1, the striate cortex or Brodmann Area 17. As a result of hierarchical information flow, a number of more complex visual abilities emerge from the responses of neurones in primary visual cortex, including direction selectivity and binocular interactions as some neurones respond to stimulation from either eye.

Neurones from the various layers of the LGN project via the optic radiation to the primary visual cortex which itself has six layers (**Figure 8**). Inputs from the distinct areas of the LGN are initially kept separate in V1, with inputs from the magnocellular pathway terminating in sublayer 4Cα and lower layer 6 and parvocellular cells terminating in 4Cβ and lower layer 6 (Lund, Lund, Hendrickson, Bunt, & Fuchs, 1975). Both parvocellular and magnocellular neurones terminate in 4A whereas

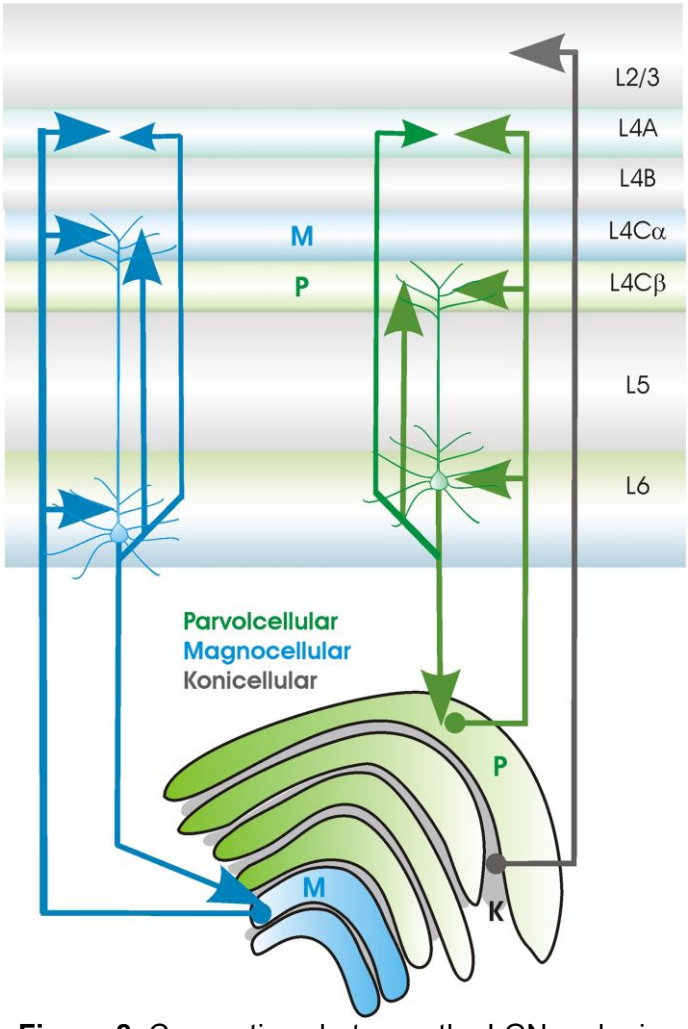

Figure 8. Connections between the LGN and primary visual cortex (Thomson, 2010)

koniocellular cells terminate in the "blob" regions of lower layer 3 (Livingstone & Hubel, 1984; Thomson, 2010).

The primary visual cortex has a functional architecture; cells are arranged in a systematic way so that neurones within a particular area respond to similar stimulus properties. For example, recording from neurones arranged in a column perpendicular to the surface of the cortex will reveal that different cells have similar orientation selectivity. Another property is that columns in primary visual cortex represent a particular region of the visual field and surrounding areas of the cortex represent the corresponding surrounding areas of the visual field, meaning that primary visual cortex is a retinotopic map of the visual field, however not all parts of the visual field are equally represented; the central visual field has a greater area of the cortex dedicated to it whereas there is less cortex dedicated to more peripheral areas of the visual field.

Functionally, achromatic contrast sensitivity is high in layers 4Cα and 4B (which receives input from 4Cα; Livingstone & Hubel, 1984). In addition to these areas, layer 6 contains direction selective cells (Hawken & Parker, 1990). Systematic connections between the LGN and visual cortex provide the required inputs for simple and complex cells found in the primary visual cortex of cats (Hubel & Wiesel, 1962). The simple cells had elongated OFF or ON surrounds, flanking an antagonistic centre which could be activated by the combined input of

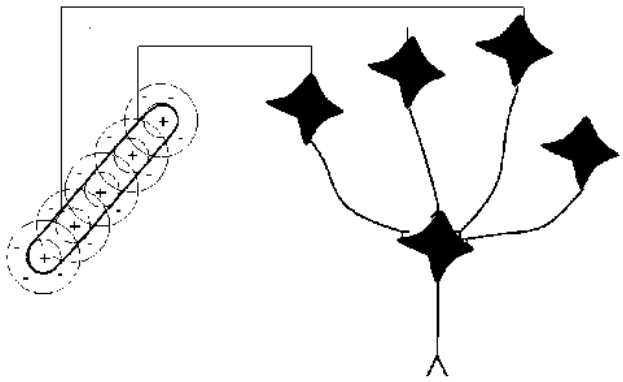

Figure 9. Centre-surround cell inputs to a simple cell in primary visual cortex http://www.scielo.br/scielo.php?script=sci_arttext&pid=S0104-65001997000200002)

centre-surround cells as shown in **Figure 9** and respond optimally to stimuli of a particular orientation. Complex cells responded optimally to a stimulus of a particular orientation but did not have ON or OFF regions within its receptive field or have an elongated receptive field itself. They speculated that simple cells projected to complex cells which would therefore respond selectively to an orientation presented anywhere within the receptive field.

From the visual cortex neural projections are sent to functionally distinct extrastriate areas to derive increasingly complex information from the visual input, often with reciprocal connections between the higher and lower areas in the hierarchy with shortcuts between. The staining of V2 with cytochrome oxidase reveals thick, thin and pale stripes. The thin stripes receive projections from the V1 blobs and underlying areas in layer 4B, whereas the thick and pale stripes receive input from the interblob areas (Sincich & Horton, 2005). Area MT/V5 is specialised for the detection of motion, containing neurones which respond selectively to motion in a particular direction (Allman & Kaas, 1971; Dubner & Zeki, 1971) with quite broad stimulus attributes. Streams have been suggested to be a higher order organising principle with the areas of temporal cortex forming the ventral stream which is broadly specialised for the recognition of objects and the areas of the parietal cortex forming the dorsal stream which is specialised for location and action (Ungerleider & Mishkin, 1982).

1.7. The aging human visual system

The aging of the visual system can be characterised as a number of changes to its components over time, affecting the optical structures of the eye as well as the receptors and other neurones. Even the functioning of the tear film can be affected including reduced tear volume and changes to the lipid viscosity with increasing age

(Mathers, Lane, & Zimmerman, 1996). In addition, the vitreous degenerates with increasing age (Oksala, 1978); there is an increase in liquid and decrease in gel volume (O'Malley, 1976) and an aggregation of fibres (Sebag & Balazs, 1985). One consequence of these changes to the vitreous is posterior vitreous detachment whereby the vitreous detaches from the retina (Sebag, 1987). Some have argued that the main cause of vision loss could be due to increased light scatter in the eye with increasing age (McLellan, Marcos, & Burns, 2001).

1.7.1. Light scatter and absorption in the eye; the role of aging

Light scatter is a result of light being captured by particles and instead of being able to travel in its original direction of propagation, it is released in another direction (Raman, 1978). Interocular light scatter is when the structures within the eye cause this light scatter. The cornea contributes to 30% of the total forward light scatter (Vos & Boogaard, 1963) and the ability of the cornea to transmit different wavelengths of light does not change with age (van den Berg & Tan, 1994). Scatter caused by the vitreous is not strongly wavelength dependent above 320 nm (Boettner, 1967; Maher, 1978; Ambach et al., 1994; van de Kraats & van Norren, 2007), and is not thought to increase significantly with age (Boettner, 1967; van de Kraats & van Norren, 2007).

In contrast, the optical density of the lens varies between individuals and increases with age, which results in reduced retinal illuminance and also increased interocular light scatter in the eye with age (Artal, Guirao, Berrio, Piers, & Norrby, 2003; Hennelly, Barbur, Edgar, & Woodward, 1998; Pokorny, Smith, & Lutze, 1987; Sample, Esterson, Weinreb, & Boynton, 1988). The lattice structure of the radial fibres at the periphery of the lens may cause small angle (under 8°) scatter, and the increase in scatter in the peripheral lens could be at least partially explained by

the finding that fibres continue to be laid down in the lens with increasing age (Simpson, 1953; Hemenger, 1988). However, more nuclear scatter may be caused by the deposits of macromolecules with different refractive indices from the surrounding lens tissue which increase with age (Spector, Li, & Sigelman, 1974).

These anatomical changes to the lens can cause different forms of visual discomfort. Firstly, forward scatter acts as a veiling luminance and reduces the contrast of the image formed on the retina (de Waard, IJspeert, van den Berg, & de Jong 1992). Absorption of light by age-related changes to the lens will reduce the amount of light that reaches the retina, but the effects may only cause significant impairment at low light levels (Elliott, Bullimore, Patla, & Whitaker, 1996). Scattered light increases with age (Weale, 1986) and may not be wavelength dependent (Wooten & Geri, 1987; Whitaker, Steen & Elliott, 1993).

Absorption of light by the lens is wavelength dependent, with shorter wavelengths being increasingly absorbed with age (**Figure 10**; Weale, 1987; Lerman, 1984; Cooper & Robson, 1969) causing reduced retinal illuminance. A cataract is when the lens has particularly high optical density which gives it a cloudy appearance, however there is no clear cut off point for when normal, age-related changes to the lens ends and a cataract begins (Owsley, Sekuler, & Siemsen, 1983), as it is often difficult to discriminate between biological changes that are due to old age and those that are due to disease (Ludwig & Smoke, 1980).

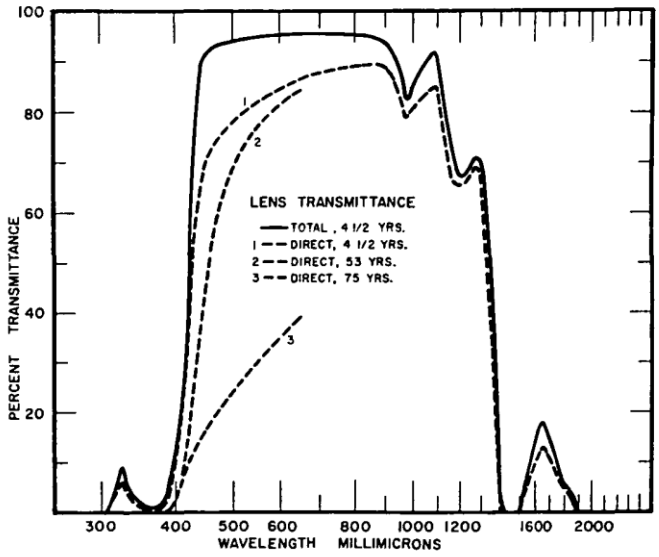

Figure 10. Transmittance of the lens (Boettner & Wolter, 1962)

Individual differences in iris pigment can also affect the forward light scatter in the eye. Previous studies have found that straylight is increased for individuals with blue/lighter rather than brown/darker iris pigmentation (Ijspeert, de Waard, van den Berg, & de Jong, 1990; Ginis, Perez, Bueno, Pennos, & Artal, 2013), and those with green iris pigmentation have intermediate levels of straylight (Coppens, Franssen, & van den Berg, 2006).

Light can also be reflected and scattered back from a number of structures within the eye. The light that is not absorbed by photoreceptors and the retinal pigment epithelium ends up back scattered within the eye ball. Although some reflections and back scatter are also produced by the cornea and the lens, most light scatter within the lens is forward scatter (Bettelheim & Ali, 1985). When structural changes become significant and are often described as cataracts, in addition to forwards and backwards scatter, much of the light is also absorbed in the lens. The amount is light that is absorbed and scattered also depends on the wavelength. It is estimated

that the retina contributes up to 40% of the enoptic scatter (Vos & Bouman, 1964; Vos, 2003) and the fundus contributes significantly to total stray light for wavelengths longer than 600 nm (Ginis et al., 2013).

1.7.2. Pupil miosis

It is well documented that pupil size decreases with increasing age (pupil miosis) as shown in **Figure 11**, due to the muscle atrophy of the controlling muscles. This trend holds over a range of different ambient illuminances (Winn, Whitaker, Elliott, & Phillips, 1994). By the age of 80, pupil size is effectively fixed (Loewenfeld, 1979, 1999).

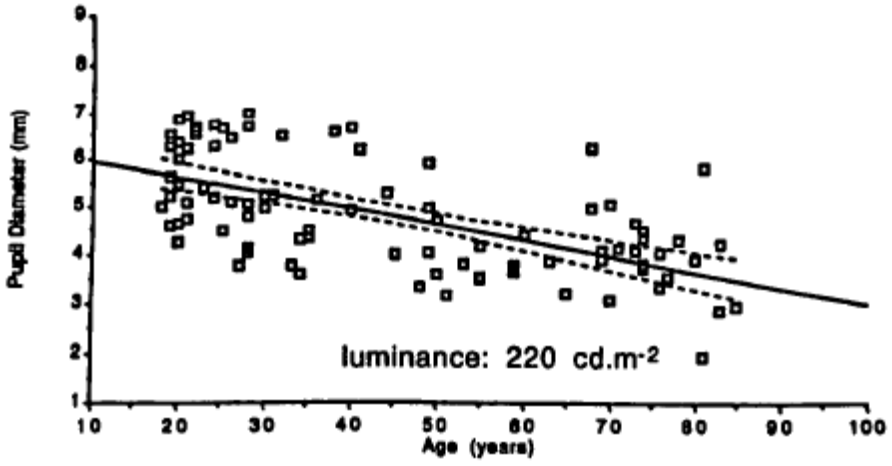

Figure 11. Changes in pupil diameter with age (Winn, Whitaker, Elliott, & Phillips, 1994)

Smaller pupils decrease retinal illuminance which can be defined as the luminous flux incident on the retina per unit solid angle of the object as seen at the eye and can be calculated by:

(1) $$T = L \times PA$$

Where L is the luminance of the stimulus in cd/m^2, PA is the pupil area in mm^2 to give T, the measure of retinal illuminance in Trolands. Weale (1963) estimated that the age related reduction in retinal illuminance is approximately 0.3 to 0.5 log units between the ages of 20 and 65 years. In support, **Figure 25** shows that from studies described in this thesis, between the years of 20 and 65 years retinal illuminance decreases by 0.42 log units due to reduced pupil size.

It is therefore important to calculate the retinal illuminance for each participant, because for a given screen luminance a younger person would have a higher retinal illuminance than an older person, and therefore may perform better on that basis alone. For example when viewing a display of 120 cd/m^2, for a group of sixteen 18-42 year olds, average pupil area was 9.05 mm^2 producing an average retinal illuminance of 1089 td, whereas the older group of twelve 65-86 year olds had an average pupil area of 6.57 mm^2 and corresponding retinal illuminance of 799 td (Mayer, Kim, Svingos, & Glucs, 1988).

1.7.3. Ocular aberrations

The eye is not a perfect optical system which reduces the quality of the image formed on the retina. Ocular aberrations occur when light originating from a particular object point does not converge only a single point when forming the image and can end up being distributed around the paraxial image point in different ways that are linked to spatial patterns associated with spherical aberration, coma, astigmatism, field curvature and distortion. Ocular aberrations increase with age (Artal, Ferro, Miranda, & Navarro, 1993; Guirao, Redondo, & Artal, 2000), including

coma, spherical aberrations and 3rd-7th order aberrations (McLellan et al., 2001) and thus contribute to increased visual difficulties with age.

Some authors have suggested that ocular aberrations are the main cause of vision loss with age (McLellan et al., 2001). However, the ratio of the modulation transfer function between younger and older participants peaks at intermediate frequencies, whereas loss of contrast sensitivity increases monotonically with spatial frequency (Artal et al., 1993), and thus could be due to a loss of sensitivity due to neural factors or reduced retinal illuminance. This topic is discussed further in section 2.1.1.

There are, however, some advantages of having a smaller pupil such as the increased depth of field (the depth in which objects are within an acceptable range of focus; Green, Powers, & Banks, 1980) as well as a reduction wave-front aberrations (Calver, Cox, & Elliott, 1999). For example, spherical aberrations are caused by peripheral rays of light being focused more tightly and thus bringing the focus of the image at shorter distances. However, a smaller pupil blocks peripheral rays resulting in reduced spherical aberrations. Spherical aberration and coma are also less effective at large pupil sizes than would be expected on the basis of geometric optics because of the directional sensitivity of cone photoreceptors, often described as the Stiles-Crawford effect (Stiles & Crawford, 1933). Under natural viewing conditions, the Stiles-Crawford effect and reduced pupil size in older subjects may balance out the increase in ocular aberrations. It has therefore been suggested that any increase in aberrations with age may not be as effective as one might expect on the basis of the expected, large pupil image degradation since the Stiles-Crawford effect reduces the effectiveness of peripheral rays and the pupil size also tends to decrease with age (Calver et al., 1999).

1.7.4. Presbyopia

Presbyopia is the progressive inability to accommodate to near objects due to a loss of flexibility in the lens and deterioration of the cilliary muscles. As shown in **Figure 12**, when someone who is younger with normal vision looks at nearby objects, the lens expands to bring the image into focus on the retina. However, when an individual with presbyopia attempts to focus on a nearby object, the lens cannot sufficiently expand and the image focal point lies behind the retina.

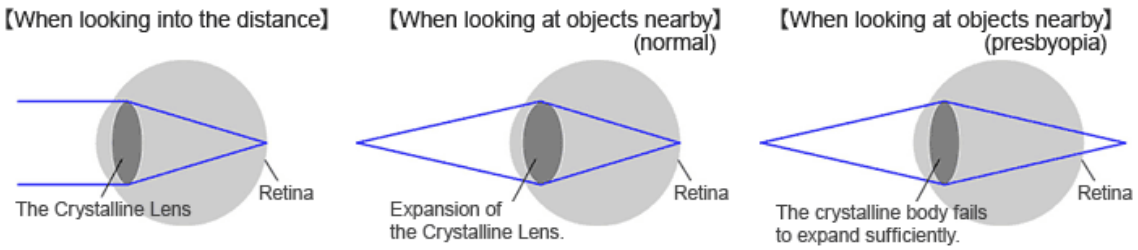

Figure 12. Demonstration of presbyopia (http://seikoeyewear.com/eye-information/about-the-eyes/presbyopia)

Figure 13 shows that the accommodative change of the lens decreases with age, and accommodative change reaches zero at approximately age 60 (Glasser & Campbell, 1998). Visual difficulties on focusing to objects of near and intermediate distances tend to be reported at around approximately 45 years of age, for which convex lenses can be prescribed with increasing power as presbyopia continues to progress, allowing an image to be formed on the retina (Shaw, Lee, & Stollery, 2013).

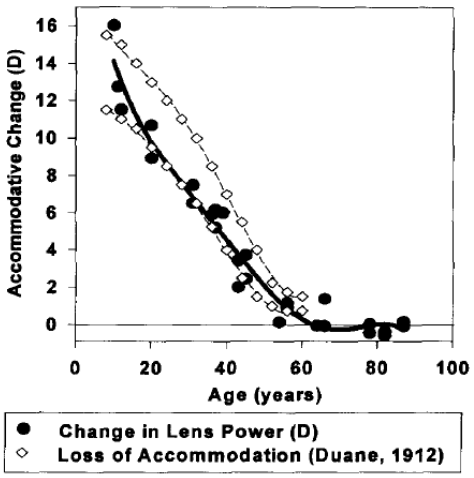

Figure 13. Filled points and solid line show the maximal change in lens power for 27 human lenses (Glasser & Campbell, 1998). In addition these authors have plotted maximum and minimum amplitudes of accommodation from Duane (1912).

1.7.5. Aging of the retina

Aging of the retina can manifest itself either in the loss of cells or reduction in the efficiency of the response of the neurones. In general, the number of cones at the fovea has been found to be stable with age (Curcio, Millican, Allen, & Kalina, 1993; Gao & Hollyfield, 1992), but there is a linear decrease of cones with age at more peripheral retina (Gao & Hollyfield, 1992). Rods display a different pattern of loss; greater numbers of rods die with age, showing a concentrated annulus of loss in the parafoveal region (3.5-10° from fixation) resulting in a reduction in the number of rods by 30% which equates to a loss of 2 rods per mm squared each day (Curcio et al., 1993). The rate of rod loss appears to be nonlinear and decreases faster between the 20s and 40s compared to between the 40s and 90s (Gao & Hollyfield, 1992). The space left by dead rods can be filled by rods with larger inner segments, making them 13.5% larger which results in similar rod coverage at all ages (Curcio et al., 1993). Older eyes have the greatest variability in the numbers of rods, cones, RPE cells and cells in the ganglion cell layer (Gao & Hollyfield, 1992). It is unclear

why rods are more susceptible to aging, but possible reasons could include sensitivity to light damage or to changes to the RPE which could be a causative mechanism for damage to the retina in age related macular degeneration (Curcio et al., 1993), however the RPE cells are lost at a linear rate, more similar to the loss of cones rather than the nonlinear loss of rods (Gao & Hollyfield, 1992). Another possible reason is that the delivery of oxygen becomes less efficient with age which could affect rods to a greater extent as they are more metabolically demanding than cones, particularly in the dark (Barbur & Connolly, 2011).

Retinal ganglion cells undergo a significant decrease in number with age, and again the rate of loss was greatest between the 20s and 40s, although the variability between people was found to be very high (Curcio & Drucker, 1993; Gao & Hollyfield, 1992). More recent studies have confirmed the loss of ganglion cells with age, however there is overall more loss at peripheral than central retina (Harman, Abrahams, Moore, & Hoskins, 2000).

Analogous findings of rod loss with aging have also been found in mice (Kolesnikov, Fan, Crouch, & Kefalov, 2010). Comparing rod physiology and function in adult mice (4 months old) and aged mice (2.5 years old), they found that aged mice had a 20% reduction in the number of rods, but unlike human rods, they were reduced in length and diameter resulting in a 40% overall reduction in the volume of the rod outer segment. This reduced number and size of the rods would result in reduced quantum catch and could at least partially explain a loss of sensitivity. In the same mice, they found a statistically significant 50% reduction in scotopic (at -4.45 log cd/m^2) visual acuity and contrast sensitivity in aged mice, whereas there were no significant differences in these measures in photopic conditions (1.85 log cd/m^2). Additionally, rod ERGs in aged mice had a reduced amplitude of a and b waves, and

sensitivity of aged rods determined from single cell recordings decreased 1.5 fold. Finally, they found that the level of cellular noise in the dark current (current when a rod is not stimulated) was increased in aged rods.

1.7.6. Cellular aging in central visual pathways

Similarly to the retina, aging in the higher visual pathways can manifest as a loss of cell numbers or decline in function of the cells that remain. In the LGN, a neuronal density decrease of 29% was found in magnocellular layers, and 41% in parvocellular layers in older compared to younger monkeys, however the decrease in the *number* of neurones was very small and was not statistically significant, whereas the LGN volume actually increased as a whole with age due to an increase in the size of neurones, blood vessels, volume of glia cells and neurophil (Ahmad & Spear, 1993). This has led to speculation that the size of cells increases over a lifetime or compensatory processes such as dendritic branching, increases in the number of synapses and/or decrease in the efficacy of synaptic transmission (Spear, 1993). In V1, decrease in cell density and loss of myelin sheath of axons has been reported but no loss of the overall numbers of nerve fibres (Peters, 2009).

Interestingly, loss of relay neurones in all layers of the LGN in animal models of glaucoma lags behind the degeneration of retinal ganglion cell axons in the optic nerve, and tends to be proportionate to the extent of optic nerve damage, although there are also some degenerative changes in areas driven by a non-glaucoma eye (Yücel, Zhang, Weinreb, Kaufman, & Gupta, 2003). Furthermore, some suggest there is no loss of ganglion cell bodies with age, but axons are selectively vulnerable to aging, manifesting as an observed decline in axon numbers in the optic nerve with the loss of approximately 4,000 axons per year (Jonas, Schmidt, Müller-Bergh, Schlötzer-Schrehardt, & Naumann, 1992; Mikelberg, Drance,

Schulzer, Yidegiligne, & Weis, 1989), representing a 0.5% annual loss (Calkins, 2013).

VEPs of older people tend to have a reduced amplitude and increased latency, especially for high spatial frequency stimuli (Bobak, Bodiswollner, Guillory, & Anderson, 1989). Faubert (2002) presents a theory of visual aging suggesting that less complex stimuli will not be majorly affected by aging of the visual pathways but if more complex visual stimuli are presented, or if multiple stimuli require processing by the same brain areas, the processing of the stimulus will be impaired by age-related changes to the brain. If all neural networks are affected equally by aging, a more complex visual task will recruit more networks and require more processing and thus the effects of aging will be more evident. For example, older participants recruit additional cortical areas for a specific task and there appeared to be less functional segregation in activation between the dorsal and ventral pathways (Grady & Rapoport, 1992). The authors suggest that in older people additional brain areas are recruited in addition to the primary one because the information is not processed efficiently. There are also suggestions that there is a reduction in inhibitory functions in the cortex, resulting in reduced centre surround suppression and increased cortical noise (Betts, Taylor, Sekuler, & Bennett, 2005).

1.7.7. Age related macular degeneration

Age-related Macular Degeneration (AMD) is the leading cause of blindness in developed countries, affecting 25 million people (Qiu & Leat, 2009). A cross-sectional sample of residents in Australia aged over 40 years found that 0.68% had AMD and 15.1% early age-related maculopathy (ARM). In addition, the bilaterality of ARM was strongly age related with a prevalence of 59% (VanNewkirk et al., 2000).

Figure 14 shows the difference between a normal retina and one with AMD. There are two types, "dry" AMD, and then some people progress to the "wet" (or exudative) form which results in more severe vision loss. Dry AMD accounts for the vast majority of cases and manifests as hyper or hypo-pigmentation of the RPE at the macula, an accumulation of drusen (extracellular deposits that vary in size, shape and location) and the death of rods and cones. Towards the end of the dry stage, macular degeneration of the RPE may occur (geographic atrophy; GA), resulting in increased death of the photoreceptors. GA has been defined as an area of 500+ micrometers of loss of RPE with colour and thickness changes relative to the surrounding retina and more prominent visualizations of the choroidal vessels (Sunness, et al., 2008). Geographic atrophy tends to spare the foveal centre until later in the disease at which point it causes

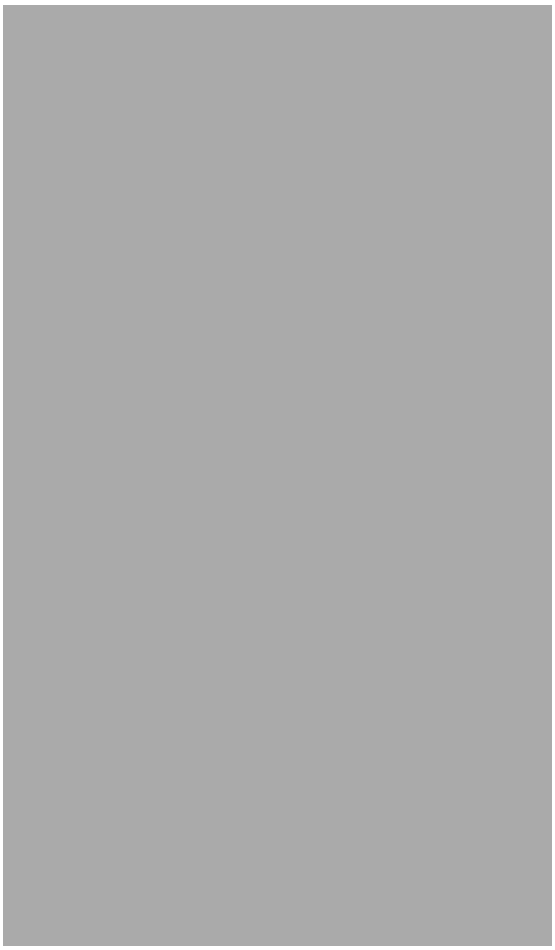

Figure 14. Comparison of normal retina with retina affected by wet AMD (http://www.vision-and-eye-health.com/macular-degeneration-types.html)

scotomas around the fovea (Sunness, et al., 1997). Wet AMD accounts for the rest of cases and is the reason for the large proportion of people registered as visually impaired. In wet AMD new blood vessels start to grow in the retina (choroidal neovascularisation; CNV) which leak blood and fluid resulting in more damage and later scarring of the macula.

There has been some difficulty identifying risk factors for who will acquire AMD and of those who have it, what the risk factors are for progressing from dry to wet AMD. Age and tobacco smoking tend to be the strongest and commonly found predictors of acquiring AMD (Eisner, Fleming, Klein, & Mauldin, 1987b; Smith et al., 2001; VanNewkirk et al., 2000), but having signs of AMD alone at early stages does not predict that AMD will develop. Early changes are found in 15% of the over 50s population, however only 1-2% develop severe vision loss and late stages of AMD (Smith et al., 2001; VanNewkirk et al., 2000). Factors such as drusen size, number, confluence and pigmentary changes have limited success at predicting the risk of progression and this has led to the suggestion that clinical signs of disease may not be the best predictors of progression, whereas tests of visual function could be (Luu et al., 2013).

AMD is not a homogenous disease, and people who are at a similar clinical stage may show a range of different symptoms. For example, Owsley et al. (2000) found many variations when investigating light and dark adapted visual sensitivity over 38 degrees of the visual field. Firstly, for dark adapted sensitivity, some patients had a concentrated area of severe sensitivity loss whereas others had more mild loss across their entire field. Secondly, some patients have normal sensitivities, others had reduced dark but not light sensitivities, some had both types of loss, and occasionally some patients had only light adapted loss.

1.8. Spatial, temporal and chromatic visual perception

The visual system extracts useful information from the visual input and computes the properties of the stimulus by the detection of change, such as the lateral inhibition in ganglion cell receptive fields. The three kinds of contrast in vision described here will be detection of changes in luminance over space (spatial vision), changes in the distribution of light over time (temporal vision) and finally chromatic changes in the spectral composition of light (Hendry et al., 2008).

1.8.1. Spatial vision

Spatial contrast can be broadly described as the fractional difference in luminance between two areas of the image detected either by the sum of L+M cones in photopic conditions or rods in scotopic conditions. Spatial form perception detects changes in luminance over space and can indicate the boundary between two objects or discriminate the object from the background (Norton, Corliss, & Bailey, 2002). Spatial acuity is defined as the finest spatial detail that can be detected, discriminated or resolved and it provides a benchmark of an individual's visual condition. Spatial frequency is the number of cycles per degree of visual angle and visual angle is a measure of the size of an object on the retina.

The Weber contrast of an object can be positive, i.e. brighter than the background, or negative, i.e. darker than the background. Weber contrast is defined by equation (2) where L is the luminance of the object and L_b is the luminance of the background

(2) $$Weber\ contrast = \frac{(L-L_b)}{(L_b)}$$

When a spatially periodic pattern such as a sinusoidal grating is employed, the grating contrast is often expressed as using the maximum and minimum luminances of the pattern, $(L_{max} – L_{min}) / (L_{max} + L_{min})$. The contrast sensitivity function (CSF) describes how the human visual system performs at a range of spatial frequencies. As shown in **Figure 15**, the contrast sensitivity function increases gradually and peaks at approximately 10 cycles per degree and rapidly drops off at higher spatial frequencies with the highest spatial frequencies that can be detected at around 30-60 c/deg. The high resolution limit is a result of the spacing between photoreceptors and the limit imposed by the optics of the eye. Underlying the visual systems CSF is each ganglion cell with its own CSF as a result of centre-surround organisation. For example an ON-centre cell would respond maximally to high luminance at the centre and low luminance in the surround, spatially matching the centre surround boundaries. At every retinal location there are ganglion cells with large and small receptive fields, allowing the detection of low and high spatial frequencies respectively. All spatial luminance patterns can be decomposed into sine wave gratings of particular spatial frequencies and contrasts (Ginsburg, 2003).

Figure 15. Photopic, mesopic and scotopic contrast sensitivity function, http://www.telescope-optics.net/aberrations_extended.htm

Contrast sensitivity depends on retinal illuminance. At mesopic levels (between 3 and 0.001 cd/m^2) visual function is mediated by both rods and cones providing reduced contrast sensitivity and acuity, but at scotopic levels (below 0.001 cd/m^2) visual function relies entirely on rods because the light level is below cone

thresholds (Barbur & Stockman, 2010). When rods are used for vision, sensitivity to high spatial frequencies is lost and the peak sensitivity drops to lower spatial frequencies due to the large numbers of rods which converge on ganglion cells resulting in larger receptive fields. This causes acuity differences at different light levels even though cones are more widely spaced than rods. Additionally the CSF shifts to lower spatial frequencies with increasing eccentricity due to there being fewer cones with increasing eccentricity.

There are a number of ways of measuring contrast sensitivity (**Figure 16**). A common method in clinical practice is the use of charts such as the Pelli-Robson chart for letters which are presented in sets of three, each triplet decreasing in negative contrast. The participant is instructed to identify as many letters as possible. Other charts utilise sinusoidal gratings which vary in both contrast and spatial frequency, whereby the participants identify the orientation of gratings. Psychophysical tests present the stimuli briefly and thus can measure visual performance at different eccentricities reliably, before the participant moves their head or eyes. The contrast of the stimulus will vary depending on the participant's responses to determine the individual's contrast sensitivity or contrast threshold. A wide range of stimuli can be used in psychophysical tests including alpha-numeric characters or gratings.

C

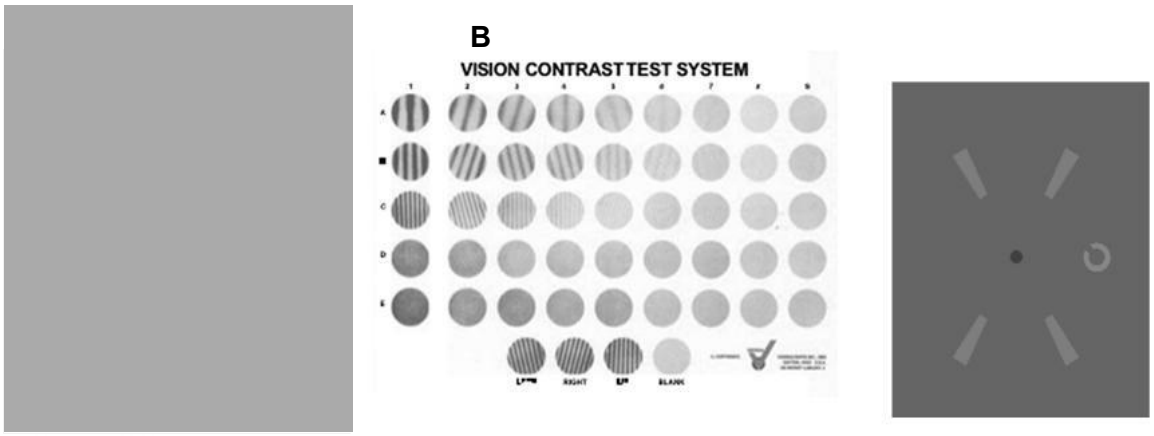

Figure 16. A Pelli-Robson chart http://www.psych.nyu.edu/pelli/pellirobson/. **B** Vision Contrast Test System. Spatial frequency varies vertically and contrast varies horizontally http://www.pacificu.edu/optometry/ce/courses/16554/agingeyepg2.cfm. **C** Functional Contrast Sensitivity test. Participants indicate the direction of the gap in the Landolt C which varies in contrast while size remains constant (Chisholm, Evans, Harlow, & Barbur, 2003a).

Decimal acuity, LogMAR (Minimum Angle of Resolution) or the Snellen Fractions is often used to determine visual performance, with a value of 1.0, 0.0 or 20/20 respectively are generally viewed to be normal or standard vision (Snellen & Landolt, 1984). However, if only 50% or 90% of the letters need to be read, acuity was found to be above 1.0 (decimal acuity) for all 100 observers aged 10-79 in one study, but acuity dropped below 1.0 between ages 57- 75 years if 100% of letters must be read (Frisén & Frisén, 1981). Other studies have found that participants aged 10 to 75+ also perform above the "standard acuity" (Elliott, Yang, & Whitaker, 1995). Therefore, depending on the criteria used, acuity of above 1.0 is quite normal and using this cut off point may not be very sensitive to age related changes. Furthermore, a large scale study (n = 900) to characterise various aspects of visual function and age including spatial vision measures, glare tests, visual fields, stereopsis, colour vision, temporal sensitivity and many others has found that each are affected differently by aging and non-standard measures could not always

be predicted by changes in clinically standard measures (Haegerstrom-Portnoy, 2005).

Therefore, the use of 20/20 visual acuity is unwarranted because it does not represent normal acuity as many perform better than this level and it is not representative of the visual functions of an individual. Furthermore, Frisén and Frisén (1979) have estimated that 20/20 acuity could be obtained by only having 45% of the normal number of foveal cones, suggesting that significant photoreceptor loss would have to occur before measures of visual acuity would be able to detect that there was disease. Additionally Brown and Lovie-Kitchin (1987) suggest that logMAR does not capture the full range of loss because a disease like ARM can affect extensive parts of the retina and logMAR may only test the fovea, therefore may not pick up a disease if it starts outside the fovea.

Contrast sensitivity may be more sensitive to disease related changes than acuity; Kleiner, Enger, Alexander, and Fine (1988) found that many patients with drusen had normal visual acuity but were impaired on measures of contrast sensitivity and Dimitrov et al. (2011) found that when comparing age and sex matched normal controls with people having early AMD, visual acuity only identified 7% of the patients as being abnormal, whereas other tests were much more sensitive because they identified a larger proportion of the early AMD group as being abnormal.

Visual acuity is also not a particularly good method for assessing the progression of retinal disease. For example, Sunness et al. (1997) tested people with various stages of AMD with visual acuity of at least 25/50 and found wide ranging visual impairment including dark adapted sensitivity and contrast sensitivity. When comparing eyes with only drusen to those with additional GA, that the GA group

had significantly worse visual acuity at reduced luminances, foveal dark adapted sensitivity and contrast sensitivity as high spatial frequencies, despite having similar conventional visual acuities (20/25 – 20/31). In addition, clinical signs of retinal disease may not be good predictors either. Eisner, Klein, Zilis, and Watkins (1992) found that slow foveal dark adaptation in combination with colour matching ability was a better predictor of developing sub retinal neovascularisation than drusen size, summed drusen/atrophic area or confluent drusen area. However, Eisner, Stoumbos, Klein, and Fleming (1991) found that certain clinical factors of eyes whose fellow eye had exudative AMD was correlated to reduced function. For example drusen area correlated with dark adaptation and absolute sensitivity. Declines in visual performance may instead be a better predictor of progression as changes in vision may preceed clinical signs of disease (Barbur & Konstantakopoulou, 2012; Owsley, 2011). There are also suggestions that clinical grading scales of disease do not adequately reflect visual function or predict risk of developing to the later stages of the disease (Luu et al., 2013). Furthermore, photopic VA does not correspond to performance on daily living tasks as Legge, Rubin, and Luebker (1987) found that an overall reduction in the CSF had a greater effect on reading performance than small depressions in spatial acuity. Therefore contrast sensitivity could be a better indicator of visual quality.

In conclusion, contrast sensitivity is likely to provide a better indication of changes to the retina as a result of aging and age-related diseases as it is more sensitive to retinal changes than visual acuity. It is possible that contrast sensitivity could be a better predictor of disease progression than visual acuity and clinical signs, however this is currently unknown.

1.8.2. Temporal vision

Temporal resolution acuity is the minimum temporal interval that can be resolved as flickering light by the visual system. Critical Flicker Frequency (CFF) is the frequency at which flickering is detected as flickering 50% of the time and steady/fused the other 50% of the time. This is measured as the minimum temporal interval between two flashes of light that the eye can detect as two flashes rather than one. The CFF is a measure of the temporal acuity and is analogous to spatial acuity in that it measures the upper limit of the visual system to detect alterations between light and dark with high contrast stimuli (Coletta, 2002). Another way of measuring the response of the visual system to transient stimuli is temporal contrast sensitivity (TCS), which is a measure of the change in modulation amplitude required for flicker detection. TC thresholds can be defined in the same way as spatial contrast thresholds but over time, as:

(3) $$Temporal\ Contrast = \frac{(L_{max} - L_{min})}{(L_{max} + L_{min})}$$

Flicker perception is commonly measured as a continuously alternating luminance profile over time which can be similar to a square-wave grating, meaning the luminance instantaneously goes from the maximum luminance (L_{max}) to the minimum luminance (L_{min}). Alternatively, using the same flicker frequency sine wave-like patterns in the luminance profile over time can be produced in which the luminance changes gradually from L_{max} to L_{min}. The

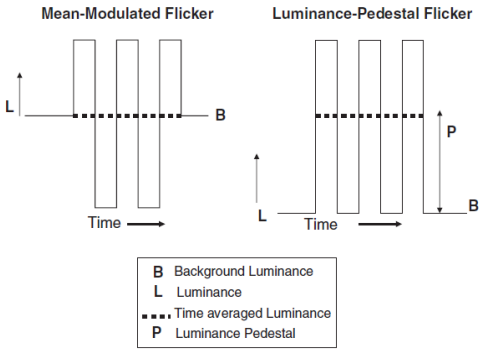

Figure 17. Modulation and luminance-pedestal flicker (Hogg & Chakravarthy, 2006).

period/cycle is the length of time for a complete cycle from L_{max} to L_{min}. The flicker rate/frequency is the number of cycles per second, measured in Hertz (Hz). A mean modulated flicker stimulus is one altered in luminance around a mean background level so that there is no change in the time averaged luminance from the background (**Figure 17**).

Temporal contrast sensitivity functions, also known as the de Lange function, have a similar shape to spatial contrast sensitivity functions. It is the envelope of various temporal frequency channels or filters which have overlapping response spectra, although there is no consensus on how many mechanisms the temporal contrast sensitivity function represents (Neelam, Nolan, Chakravarthy, & Beatty, 2009). At lower temporal frequencies, L and M cone modulation thresholds are mediated by chromatic pathways, but are modulated by the luminance pathways at higher temporal frequencies. For example, Sun, Pokorny, and Smith (2001) found lower thresholds for chromatic (L-M) stimuli than for luminance stimuli (L+M) at 2 Hz, but this was reversed at 10 Hz. They suggested that isolated cone sensitivities are processed by different post receptoral pathways at these different temporal frequencies. The opponent system (colour) is more sensitive to low flicker rates, utilising the parvocellular pathway and the non-opponent system (luminance) is more sensitive to high flicker rates, utilising the M pathway.

The temporal contrast sensitivity curve can be altered in shape by a number of different factors. One way of conceptualising the changes is as a change in sensitivity which would cause vertical shifts in the function, or of resolution which would cause horizontal changes in the function (Mayer et al., 1988).

The temporal responses of the visual system change with eccentricity; higher frequencies can be detected at the periphery rather than the fovea (**Figure 18**). The increase in the CFF with eccentricity is mainly at high luminances, and there is little change over the visual field at low luminances exception at the parafovea where an increase is seen at 3° (Tyler & Hamer, 1993).

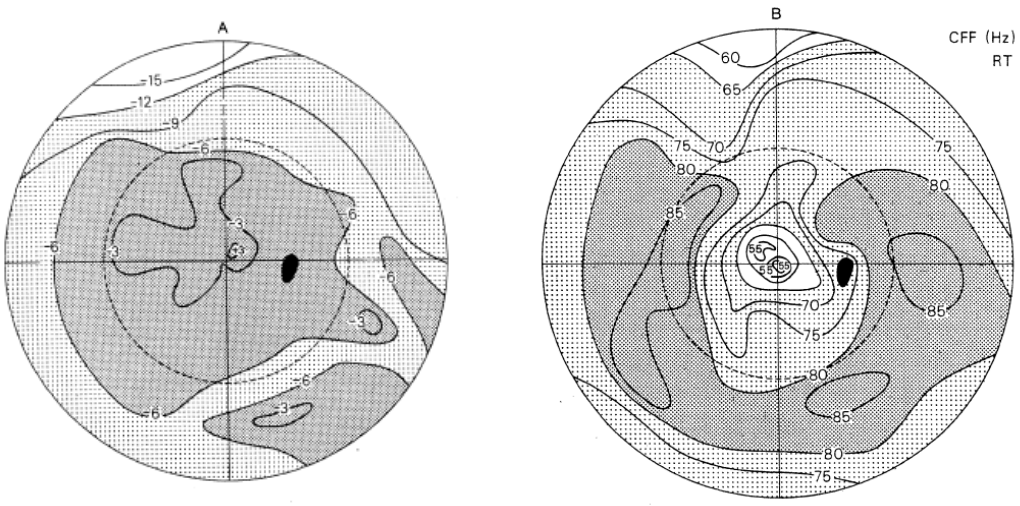

Figure 18. A Modulation sensitivity throughout the retina. **B** CFF throughout the retina. Modified from Tyler (1987).

Tyler (1987) describes the areas corresponding to particular CFFs across the visual field for a long-wavelength stimulus (660nm). Stimuli were scaled to stimulate a similar number of cones at each eccentricity in a flicker detection task. The CFF visual field profile is interesting because the CFF increases with eccentricity from the fovea despite cone photoreceptors declining in numbers and the lower and temporal visual field had higher CFFs. Eventually at the far periphery, CFF trails off, probably due to a decline in both photoreceptor and ganglion cell density. Shifts of the CFF to lower temporal frequencies, such as at the fovea reflect a change in the

time constant (slowing of impulse response) and could be due to variations in the outer segment sizes (Tyler, 1985)

Tyler (1987) measured the peak modulation sensitivity for 10 Hz flicker over the visual field in a similar way described above for CFF. These results vary significantly for the field results for CFF, primarily that the fovea has the greatest modulation sensitivity and also that modulation sensitivity declines more gradually with increasing eccentricity. Tyler suggests that this is because they have controlled for cone density, ganglion cell density may explain regional variations in modulation sensitivity. In support, Tyler (1985) found that when stimuli were size scaled according to the magnification of ganglion cells with increasing eccentricity, there was no loss of modulation sensitivity.

The Ferry-Porter law states that the CFF is directly proportional to the log of the stimulus luminance and so that as luminance increases, the CFF increases, meaning that we can see rapid flicker at high luminances but not at lower luminances. Similarly, Kelly (1961) plotted modulation thresholds for various luminances. The peak temporal contrast sensitivity is around 20 Hz at high luminances but shifts to 5 Hz at low luminances. Contrast sensitivity is poorer at low luminances at which people can only see low temporal frequencies of medium to high temporal contrasts (**Figure 19**).

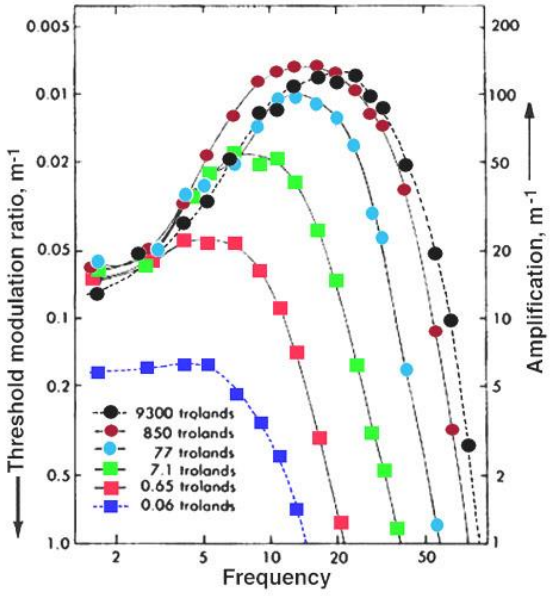

Figure 19. TCSF at various retinal illuminances (Kelly, 1961), from http://webvision.med.utah.edu/book/part-viii-gabac-receptors/temporal-resolution/

1.8.3. Colour vision

Humans with normal vision have one type of rod, with a peak spectral sensitivity at approximately 500nm and the three types of cone which have peak spectral sensitivities of short (442nm), medium (543nm) and long (570nm) wavelengths (Stockman & Sharpe, 2000), however as can be seen from **Figure 20**, each photoreceptor is sensitive over a range of wavelengths. The peak sensitivity refers to the wavelength of light which results in greatest absorbance of photons, and wavelengths of increasing and decreasing wavelength result in lower levels of absorbance, therefore the wavelength determines the probability of a particular cone type absorbing the photon.

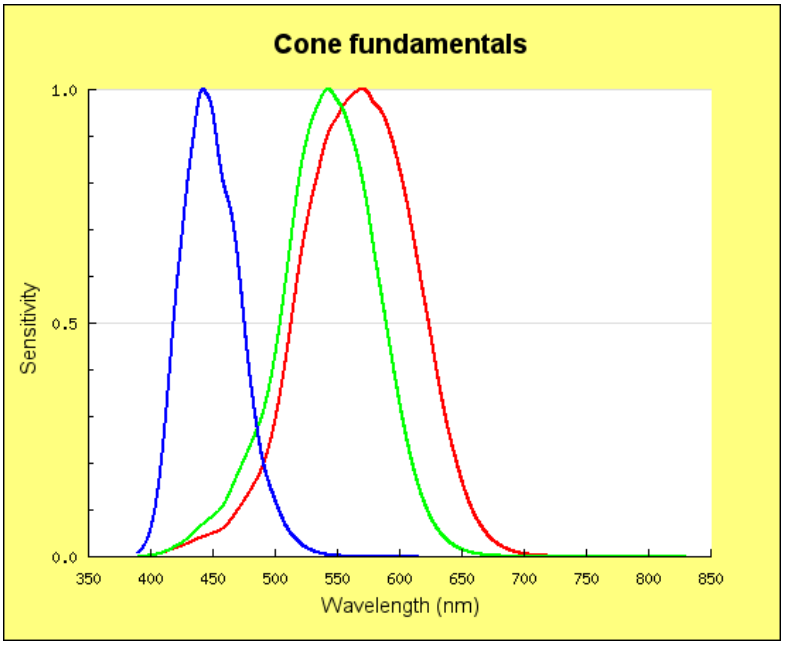

Figure 20. Plot of the Stockman and Sharpe (2000) 2° cone fundamentals, normalised for sensitivity.

Receptors themselves do not encode information about the wavelength of the photon absorbed, known as the Principle of Univariance (Rushton, 1972). Individually, photoreceptors are colour blind because their response depends on the number of photons it has absorbed which is affected by either the wavelength, intensity or both. Therefore the ability to distinguish between different wavelengths

relies on post receptoral processing. Normal human vision can be described as trichromatic due to the ability to match any perceived colour with a mixture of three primaries. As mentioned previously, in the opponent process theory (Hering, 1964) L and M signals are combined (L – M) in the Red-Green channel and these signals are combined with those from the S cones (L+M-S) in the Yellow-Blue channel. As the cones have overlapping spectral sensitivities, there are a vast number of combinations of excitation levels which leads to the ability to perceive a wide range of colours. However, the opponent process theory means that some colour combinations are not possible, such as a greenish red, or yellowish blue.

Numerous types of colour space have been devised in order to describe colours accurately. The first was created by the Commission Internationale de l'Eclairage (1931) and was called the CIE 1932 2° Standard Observer and was limited to the central 2° as cone types vary with eccentricity and thus different colour spaces would be required for different viewing angles. The system was based on the colour matching experiments using three primaries which are colours that cannot be created by any additive mixture of the other two primaries (Guild, 1932; Wright, 1929). In the experiments, a test wavelength had to be matched by a combination of the three primaries, and the value of each primary can be plotted against wavelength and resulting functions are denoted as $\bar{r}(\lambda)$, $\bar{g}(\lambda)$ and $\bar{b}(\lambda)$, where (λ) indicates the wavelength of light. One complication was that some test stimuli could only be matched by adding a primary to the test itself, resulting in negative values, therefore the CIE used modified functions $\bar{x}(\lambda)$, $\bar{y}(\lambda)$ and $\bar{z}(\lambda)$. Therefore, if given a colour with a spectral power distribution I(λ), one can obtain tristimulus values for that colour by multiplying the spectral distribution by each of the colour matching functions.

$$X = \int_{380}^{780} (\lambda)\, \bar{x}(\lambda) \mathrm{d}\lambda$$

$$Y = \int_{380}^{780} (\lambda)\, \bar{y}(\lambda) \mathrm{d}\lambda$$

$$Z = \int_{380}^{780} (\lambda)\, \bar{z}(\lambda) \mathrm{d}\lambda$$

Chromaticity diagrams plot colour matching data or cone spectral sensitivities in relative units. The CIE XYZ space is designed so that Y indicates brightness of a colour, and therefore the chromaticity can be isolated and specified by just two parameters, x and y, as the sum of x, y and z will always equal one. The CIE 1931 chromaticity diagram can be seen in **Figure 21**.

$$x = \frac{X}{X + Y + Z}$$

$$y = \frac{Y}{X + Y + Z}$$

$$z = \frac{Z}{X + Y + Z}$$

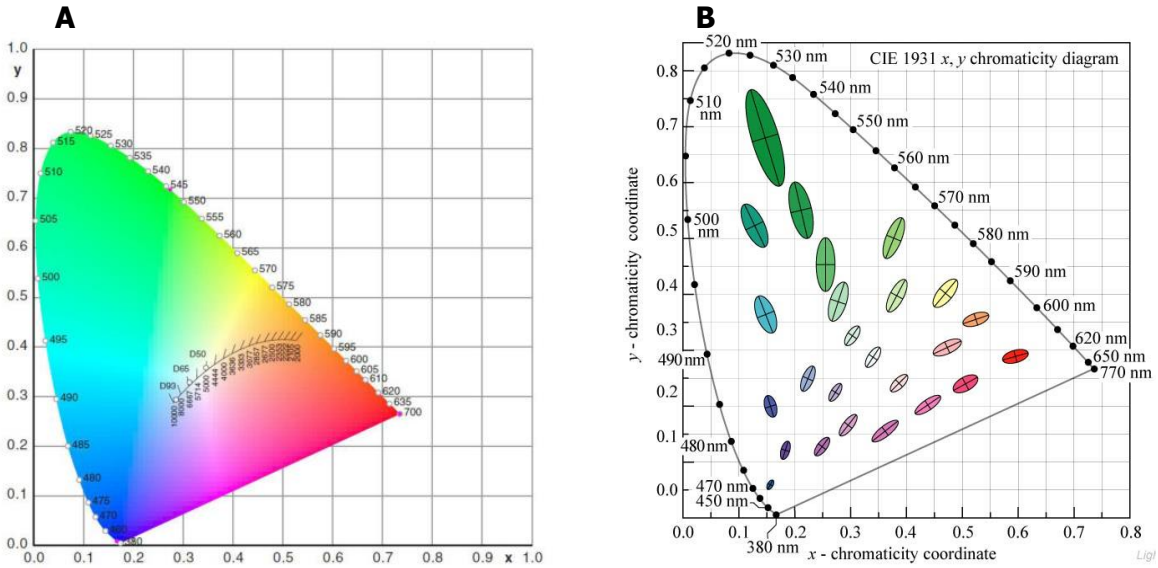

Figure 21. **A** CIE 1931 Chromaticity diagram from Ripamonti, Woo, Crowther, and Stockman (2009). The wavelengths of light are plotted around the edge and the central line is the Planckian locus which is the colour of an incandescent black body as it changes temperature. D93, D65 and D50 indicate the chromaticity of CIE standard illuminants that represent natural light found in different parts of the world, for which D65 is an indication of daylight in Western Europe. **B** shows MacAdam ellipses plotted in CIE 1931 (x, y) chromaticity diagram. From http://www.ecse.rpi.edu/~schubert/Light-Emitting-Diodes-dot-org/chap17/F17-05%20MacAdam%20ellipses.jpg

MacAdam ellipses are small regions of a constant luminance within the chromaticity diagram where changes in chromaticity do not produce discriminable colour differences. **Figure 21** B shows the CIE 1931 diagram with MacAdam ellipses which vary in size and shape across the CIE diagram. The variation in the size of the ellipses could be explained by the two dimensions; one where S cone signals varied, and one where MW and LW cones traded off against each other (Connolly & Hosking, 2009) and the ellipse size decreases with increasing background luminance (Jennings & Barbur, 2010).

1.9. Aims and objectives

This thesis investigates the effect of light level on spatial and temporal vision, and in particular the effect of aging on vision in photopic and mesopic conditions. This topic is important because the UK is facing an aging population (Office for National Statistics, 2009), which will increase the incidence of age related ocular disease. The studies were performed in order to determine the limits of normal aging so that performance could be separated from early stages of retinal disease. Specific studies investigated:

1. How aging affects spatial contrast thresholds in photopic and mesopic conditions
2. How aging affects temporal modulation thresholds in photopic and mesopic conditions
3. The effect of varying scotopic/photopic sensitivity ratios on spatial acuity

2. Spatial contrast thresholds in photopic and mesopic conditions; separating normal aging from disease

This section describes previous findings and outlines the methods developed to describe normal aging of early visual processing mechanisms in the retina, whilst controlling for optical factors. In addition, the same methods can be used to describe how age-related changes in visual performance are exacerbated in age-related disease. As people become older, various age-related physiological changes take place within the eye but are not disease related, such as pupil miosis and the loss of rods and cones, and each of these physiological changes can alter visual performance. The aim of this study is to quantify age-related changes in contrast vision as a result of changes to the retina, and to determine the limits that describe normal aging in order to screen for changes caused by disease.

2.1. Loss of spatial vision in aging and retinal disease

Large sample normative measures of the CSF shows a peak at 6 c/deg, with high variability at high spatial frequencies (Glass, 2007). There are a number of factors which can worsen contrast vision, and this section will describe the effects of age and related retinal diseases.

2.1.1. Contrast vision and aging

High contrast acuity is well maintained into old age (Elliott, Yang, & Whitaker, 1995), leading some researchers to suggest that measures of contrast vision may be more sensitive to age-related diseases (Kleiner et al., 1988). When measuring

changes to contrast vision due to aging, the cause may be optical due to light scatter reducing the contrast of the image on the retina or due to reduced retinal illuminance caused by pupil miosis. Another reason for reduced contrast sensitivity could be due to neural degeneration of photoreceptors in the retina with increasing age. Firstly evidence for the loss of contrast sensitivity with age will be described, followed by a discussion of the cause of this loss.

Low contrast tests of visual performance can reveal significant impairment with increasing age (Bühren, Terzi, Bach, Wesemann, & Kohnen, 2006; Brabyn, Schneck, Haegerstrom-Portnoy, & Lott, 2001; Haegerstrom-Portnoy, Schneck, & Brabyn, 1999; Rubin et al., 1997). Older people tend to have worse contrast sensitivity, with older adults (mean age 70) performing significantly worse on the Pelli Robson Chart for large letters than younger participants (mean age 27; Jackson, Owsley, Cordle, & Finley, 1998). Contrast sensitivity declines with each decade. The trend starts earlier and is more pronounced for higher spatial frequencies, with lower spatial frequencies less affected by age (Arundale, 1978; Derefeldt, Lennerstrand, & Lundh, 1979; Klein, Schieber, Abusamra, & Coyne, 1983; Owsley et al., 1983; Ross, Clarke, & Bron, 1985; Wright & Drasdo, 1985; Higgins, Jaffe, Caruso, & Demonasterio, 1988; Scialfa et al., 1988; Nameda, Kawara, & Ohzu, 1989; Elliott & Whitaker, 1992; Glass, 2007; Hohberger, Laemmer, Adler, Juenemann, & Horn, 2007).

Although there is much evidence for the selective loss of sensitivity to high spatial frequencies, some studies have reported losses for lower spatial frequencies. Owsley, Sekuler and Boldt (1981) found that younger observers (mean age 20.5) required less contrast than an older group (mean age 74.2) to detect and discriminate between faces, an activity that relies on low frequency information.

However, the older group may have been typical of older people in general, they were not all free from disease, as three had early macular degeneration. Additionally, Sekular, Hutman and Owsley (1980) found low spatial frequency losses in an older group compared to a younger group, but again not all older participants had good ocular heath and the older group was small. Owsley et al. (1983) states that it is important for studies to screen the ocular health of participants, correct them for the test distance and to have a sufficient number of older participants. By doing so, Owsley et al. (1983) found high frequency losses of contrast sensitivity for older participants. Therefore, there is more reliable evidence for age-related losses in contrast vision for higher spatial frequencies.

As discussed in section 1.7, a number of changes to the optical components of the eyes can occur with increasing age. Light scatter and ocular aberrations (Hemenger, 1988; McLellan et al., 2001) can reduce the contrast of the image on the retina, thus making the stimulus more difficult to discriminate. Pupil miosis, increased absorption of the lens and backscatter (Weale, 1987) reduces retinal illuminance which will reduce the contrast sensitivity of the retina.

Although these factors are thought to significantly impair contrast vision for older people, many researchers have suggested that this is not the only cause of vision loss, and there is also loss due to neural changes at the retina and/or higher visual system. Owsley et al. (1983) states that the loss of contrast vision in older people is not due to scattered light because forward scatter produces a veiling luminance, thus increasing the mean luminance and decreasing the contrast of all patterns of the retina. Therefore given that age-related deficits in contrast sensitivity seem to be specific to higher spatial frequencies, scattered light is unlikely to explain loss of sensitivity to higher spatial frequencies in older observers (Owsley et al., 1983).

Furthermore, higher order aberrations may not be able to explain the full loss of contrast vision in older people. When correcting higher order aberrations, the vision of younger and older participants improves to a similar extent when pupil miosis is controlled for yet still have worse sensitivity, and therefore higher order aberrations cannot entirely explain the reduction in spatial vision for older participants (Elliott et al., 2009). However other authors have suggested that because older subjects have smaller pupils, they experience marginally smaller wave-front aberrations under natural viewing conditions than do younger subjects and have no consequent reduction in modulation transfer function compared with younger subjects (Calver et al., 1999).

Reducing retinal illuminance by a factor of three in a group of younger subjects to approximate that in older subjects does reduce contrast sensitivity at higher frequencies, but not to the level of older subjects (Owsley et al., 1983). Simulating *both* reduced retinal illuminance and light scatter experienced by older people by using smaller pupils, a neutral density filter and a solution causing light scatter, in participants with a mean age of 28 years did not show significant changes to the CSF compared to natural viewing conditions, and furthermore the CSF did not change to resemble the CSF of older healthy participants with a mean age of 69 (Whitaker & Elliott, 1992; also see Elliott, Whitaker, & MacVeigh, 1990). Finally, using laser interference fringes to bypass the optics of the eye, a small difference in photopic contrast sensitivity was found between younger and older participants and the authors suggest there may be a greater effect of neural deficits at lower light levels (Burton, Owsley, & Sloan, 1993).

Therefore, there are a number of different optical factors that can reduce the contrast sensitivity of older people, however, they are not the only cause and age-

related changes to the retinal or higher visual pathways may also play a role in reduce contrast vision. One of the causes of the loss of spatial vision with age could be the loss of photoreceptors or other retinal neurones (Curcio et al., 1993; Gao & Hollyfield, 1992).

In summary, aging causes a loss of contrast sensitivity, particularly at high spatial frequencies. Furthermore, performance on low contrast vision tests has been found to predict subsequent acuity loss, better than measures of glare recovery, colour discrimination and stereopsis (Schneck, Haegerstrom-Portnoy, Lott, Brabyn, & Gildengorin, 2004). These findings suggest that contrast sensitivity is an effective measure of aging of the visual system. Losses of contrast sensitivity in older people are likely due to a combination of optical factors (increased scatter, higher order aberrations, increased lens absorption and pupil miosis) as well as neural degeneration.

2.1.2. Loss of contrast sensitivity in retinal disease

Many studies have found further contrast sensitivity losses in people with AMD or early signs in ARM, beyond that observed in normal aging. In addition to visual acuity being an insensitive measure of aging, it may not be a reliable indicator of retinal health. For example when comparing the ability of various tests to identify people with early AMD as having disease related retinal changes, the visual acuity test only identified 7% of the patients as being abnormal (Dimitrov et al., 2011).

In a study measuring contrast sensitivity with the Pelli Robson chart, a significant difference was found between the four groups (younger normal, older normal, early ARM and late ARM) on mean log CS for the eye with best visual acuity. However the individual group comparisons showed no difference between the older normals and

those with early ARM (Jackson, McGwin, Phillips, Klein, & Owsley, 2006). This suggests that the use of contrast sensitivity charts at high light levels may not be sufficiently sensitive to identify early ARM because clinical signs of retinal disease may manifest first before reduced CS. However, another study found using the same eye chart that participants with early AMD performed significantly worse than age matched normals. In spite of this, the scores may not be sensitive to progression of the disease as there was no further deterioration after one year (Feigl, Brown, Lovie-Kitchin, & Swann, 2005).

Other studies with charts have indicated that this method could be useful for identifying early stage disease because participants with drusen but normal visual acuity (20/20) read fewer letters on the Regan low contrast letter chart than age matched controls, and performance correlated with drusen severity (Kleiner et al., 1988). Furthermore, patients with GA performed worse than those with only drusen and no GA (Sunness et al., 1997).

The question of whether eye charts at high light levels can differentiate between people with the early stages of retinal disease and age matched normals remains unanswered. In addition these tests only assess central vision, which may not be where photoreceptors are lost at the earliest or greatest rate. Eye charts do not allow stringent control over the direction of gaze and therefore participants are not necessarily using central vision, but may use an area of the retina that produces the best vision (Brown & Lovie-Kitchin, 1987).

Other studies using psychophysical methods have found more consistent results regarding the role of AMD in contrast vision. Midena, Degli Angeli, Blarzino, Valenti, & Segato (1997) found in a sine-wave detection task that those with early AMD

(drusen with or without RPE alterations), contrast sensitivity was significantly worse than for age matched controls. As with aging, it is the high spatial frequencies that are affected most by AMD (Brown & Lovie-Kitchin, 1987; Sjöstrand, 1979; Sjöstrand & Frisén, 1977) and the peak of the CSF moves to a lower spatial frequency (Brown, Adams, Coletta, & Haegerstrom-Portnoy, 1986). There are greater differences between the performance of normals and those with drusen at high but not lower spatial frequencies (Kleiner et al., 1988).

The loss of contrast sensitivity in AMD tends to affect the central 5° more than other eccentricities, particularly at the higher spatial frequencies (Brown & Lovie-Kitchin, 1987). Hahn et al. (2009) investigated parafoveal letter recognition at contrasts 5-100% in normal aging and with patients who had risk factors for AMD (early signs of AMD or fellow eye with AMD). Letters were presented for 250 ms at 1, 2, 4, 6 and 8°, with stimuli size scaled for the loss of sensitivity with increasing eccentricity. In normal participants, an age related decline was found but could be seen at earlier ages for lower contrasts; a linear decline was found from 63 years for 100% contrast letters but from 51 years for 5% contrast letters. In addition, the differentiation between patients and controls was clearest at 5 and 10% contrast. Using these contrast values, 67% of eyes with a fellow eye with AMD and 67% of eyes with early signs of AMD were outside the 95% age corrected limits.

Contrast sensitivity may be a more sensitive measure to describe normal aging and age related diseases than high contrast visual acuity. Contrast vision tends to be lost in AMD in a similar way to normal aging but performance declines to a greater extent. Therefore one measure of contrast sensitivity could pick up normal age related changes, and anyone who falls outside the normal limits of a particular age

may have early stage disease, and those with even poorer performance are likely to have more advanced forms of the disease.

2.1.3. Vision at low luminance levels in aging

The previous sections suggested that the loss of contrast vision with age is at least partially a result of photoreceptor loss in the retina. However, because rods are lost at a greater rate than cones (Gao & Hollyfield, 1992; Curcio et al., 1993), contrast sensitivity at low light levels may be particularly sensitive to aging. This section will firstly review the evidence for a number of low luminance visual functions being particularly affected by aging, and then specifically review the effect of low luminance on the contrast vision of older people.

Figure 22 shows the scotopic and mesopic luminous efficiency functions. The scotopic function has a peak sensitivity at shorter wavelengths than the photopic function. There is no generally accepted efficiency function for mesopic vision as the way that rods and cones interact will depend no only on the luminance of the background but many other properties of each the stimulus and background.

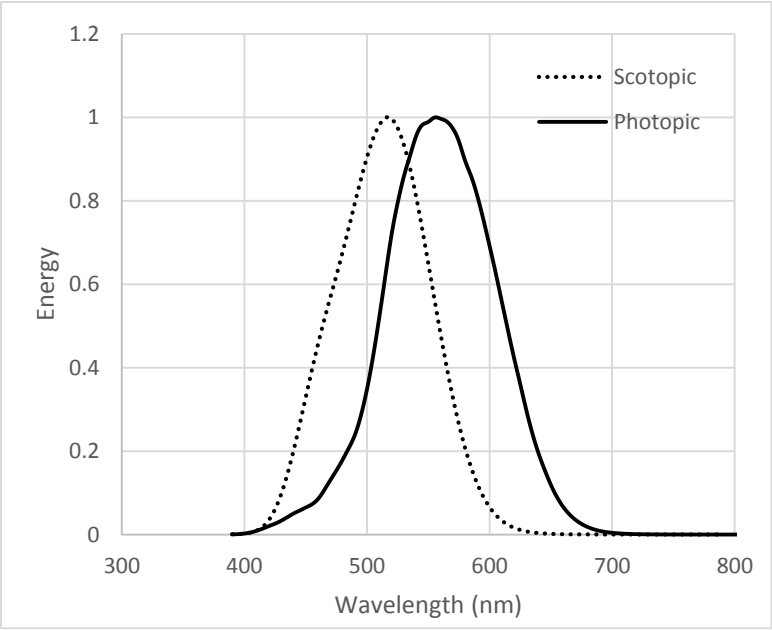

Figure 22. Scotopic and photopic luminous efficiency functions, from www.cvrl.org

Performance changes with light level in functional tests such as visual search and reaction time (Barbur & Connolly, 2011). Measuring visual function at lower light levels has been suggested to be more informative of the heath of the retina. For example, Jackson and Owsley (2000) found that that scotopic normal age related sensitivity losses were twice as high as photopic sensitivity losses.

2.1.2. (a) Reduced mesopic and scotopic absolute sensitivity in normal aging

Absolute sensitivity is a measure of the lowest stimulus intensity a person can detect. Older adults with good macular health have reduced, rod-mediated sensitivity for stimulus detection and the magnitude of this reduction in scotopic sensitivity is similar throughout the macula (Jackson et al., 1998). Even when corrected for lens density and pupils were dilated, scotopic sensitivity was worse than photopic in 80% of adults, and declines faster throughout adulthood, but both decline at a linear rate from the 20s to the 80s (Jackson & Owsley, 2000).

Interestingly the absolute scotopic sensitivity loss does not appear to vary with eccentricity (Jackson & Owsley, 2000; Jackson et al., 1998) so there was no larger decrease in scotopic sensitivity at the parafoveal region, where Curcio et al. (1993) found greatest rod loss. Because scotopic sensitivity declined gradually with age and did not vary with eccentricity, one may not be able to purely attribute this observation to the rod loss found by Curcio et al. (1993). The increased size of rods with age may mean that there are no gaps in the retinal mosaic and therefore the rod loss will not manifest as reduced absolute sensitivity, but instead as increased spatial summation which has been found with age in the parafovea at 6° in scotopic and photopic conditions in accordance with ganglion cell loss at these locations, and

accordingly, there was no association with age and increased summation at the fovea in photopic conditions where there is less ganglion cell loss (Malania et al., 2011; Schefrin, Bieber, McLean, & Werner, 1998). Therefore increased summation with age due to neural changes in the retina may not affect absolute sensitivity but may have another effect on visual performance with age, such as spatial sensitivity.

2.1.2. (b) Slower photoreceptor adaptation in normal aging

In older adults with good macular health, rod-mediated dark adaptation is significantly slower than in younger adults (Jackson, Owsley, & McGwin Jr, 1999). For example, dark adaptation functions of normal participants and recovery after a 98% bleach were 10 minutes longer in 70 year olds than for 20 year olds (Jackson & Owsley, 2000). Eisner, Fleming, Klein, and Mauldin (1987a) however did not find that dark adaptation rate increased with age but only included participants aged 60+ so the range may not have been large enough to detect a trend and pupil size was not controlled.

Dark adaptation and scotopic sensitivity were not found to be correlated, suggesting that these are separate mechanisms (Jackson & Owsley, 2000). Possible reasons for slowed dark adaptation in aging could be due to issues with gain control in the cortex due to post reception visual function change in aging or alternatively this is due to reduced speed of rhodopsin regeneration with age (Jackson et al., 2006).

Interestingly there have been some findings of abnormal cone adaptation in normal aging following a 96% bleach and using a 4° diameter spot (covering 2° from the fovea). The time constant of cone recovery was found to be significantly correlated with age between 20 and 83 years (Gaffney, Binns, & Margrain, 2012).

2.1.2. (c) Reduced mesopic and scotopic contrast sensitivity normal aging

Haughom and Strand (2013) established normal limits of contrast sensitivity in a relatively young sample, (17-54 years) at spatial frequencies 1.5-18.0 c/deg. There was no age effect, possibly due to the limited age range, but more people fell outside the normal limits at high spatial frequencies in the mesopic conditions (11%) than the photopic conditions (4.5%) suggesting that mesopic conditions may be more sensitive to the detection of abnormal vision performance. However, older people also perform worse at lower spatial frequencies (0.5 c/deg) in mesopic conditions but not at photopic levels (Zhang & Sturr, 1994). Scotopic contrast sensitivity measured at 6° of eccentricity has been found to decline with age for spatial frequencies below 1.2 c/deg, and in addition the high frequency cut off of the CSF also declines with age (Schefrin, Tregear, Harvey, & Werner, 1999).

Loss of contrast sensitivity, as measured using the Pelli Robson chart, declines approximately 10 years earlier (51-60 years) than photopic sensitivity (61-70 years), and mean photopic and mesopic performance increased significantly with age (Puell, Palomo, Sanchez-Ramos, & Villena, 2004). This mirrors the pattern of rod loss found in the aging retina whereby the loss of rods precedes the loss of cones (Curcio et al., 1993).

Therefore in normal aging, loss of spatial sensitivity follows patterns of rod loss because mesopic contrast sensitivity declines before photopic, but it is unclear if this is area specific, i.e. there is greater loss of spatial sensitivity in normal aging at the parafovea relative to other areas at the retina which contain rods. There is a loss of absolute sensitivity and abnormal adaptation in normal aging but this may not be due to photoreceptor loss as these changes are not limited to areas with rod loss and adaptation changes occur for both rods and cones.

2.1.4. Vision at low luminances in AMD

Many clinical disorders are more evident at low rather than higher light levels (Petzold & Plant, 2006). People with age related disease can have additional problems with visual function at low light levels compared to those aging normally. For example, Owsley, McGwin, Scilley and Kallies (2006) produced a Low Luminance Questionnaire to assess how those with ARM are particularly affected. In developing the questionnaire, they found that driving, mobility, emotional distress, extreme lighting conditions, peripheral vision and general lighting problems were all affected even at the early stages of ARM when visual acuity is unimpaired.

2.1.4. (a) Photoreceptor loss associated with AMD

Curcio, Owsley and Jackson (2000) review evidence that photoreceptor changes in AMD involve predominantly rods rather than cones. In eyes with non-exudative AMD, the parafoveal cones were still present though misshapen or enlarged, and rod loss exceeded cone loss at most foveal locations. Greatest rod loss was found at 1.5-10 degrees. In eyes with late, exudative AMD, photoreceptors contained within retinal scars and along their margins tended to be cones. Virtually all surviving photoreceptors were cones in the fovea which reverses the normal predominance of rods (Medeiros & Curcio, 2001). Additionally, Curcio, Medeiros and Millican (1996) noted that a patient with non-exudative AMD who had the most parafoveal loss in the study eye, actually had exudative AMD in the fellow eye, suggesting that parafoveal rod loss precedes the more severe form of AMD.

Relatively little cone loss has been found in the retinas affected by AMD. Zayit-Soundry, Duncan, Syed, Menghini, & Roorda (2013) investigated cone spacing in AMD with Adaptive Optics Scanning Laser Ophthalmoscopy (AOSLO). Four eyes had

GA and four eyes had drusen, and were compared to age-similar controls. Cone spacing was measured in areas over drusen and GA margins and regions without either. The cone mosaic continued to the edges of GA and overlay drusen. At these areas, almost all cone spacing was within normal limits, and continued to be so throughout the progression of GA over 12-21 months, and OCT scans showed progression of drusen during this time. However, there was reduced cone reflectivity in drusen areas and around GA areas, forming a "transition zone". The authors suggest this could be due to drusen disrupting the shape of the retina and hence the vertical alignment of the cones reducing reflectivity or compromise of photoreceptor structure. Photoreceptors overlying drusen also show decreased numbers of synaptic terminals (Johnson, Brown, Pulliam, Anderson, & Johnson 2005), shortening of photoreceptor inner and outer segments (Johnson et al., 2003), whereas bipolar, horizontal, amacrine and ganglion cells in these areas were unaffected (Johnson et al., 2003). Therefore, although there is less loss of cones, they may not be functioning entirely normally.

2.1.4. (b) Reduced absolute sensitivity in AMD

Both cone and rod mediated sensitivity is found to be reduced in AMD. Eisner et al. (1987b) found that the photopic absolute threshold was higher for fellow eyes of an eye with exudative AMD when compared to people with healthy eyes in a similar age group. Sunness et al. (1997) found that people with GA had worse foveal dark adapted sensitivity when compared to people with just drusen. However Eisner et al. (1992) found that absolute sensitivity did not effectively predict the development of exudative AMD. Jackson et al. (1998) found that the reduction in scotopic sensitivity in patients with AMD was not reliably associated with the three different gradings of ARM; 60% of adults in the study exhibited early signs of ARM (such as

small drusen) however even those with no drusen and a similar age had a similar reduction in sensitivity.

The rod mediated sensitivity tends to suffer more in AMD than cone mediated sensitivity. Owsley et al. (2000) measured the sensitivity of 38 degrees of the central visual field using an automated perimeter test in AMD patients (n=80) and normal participants (n=12) who all had pupils dilated and corrected for pre-retinal absorption of the lens. AMD patients had worse dark adapted sensitivity loss that was greater in magnitude than the light adapted sensitivity loss (6.7 dB and 2.2 dB of loss respectively). Interestingly a statistically significant effect of eccentricity was found for the dark but not light adapted condition; the dark adapted sensitivity was worst at 2-8°, but improved with increasing eccentricity. Therefore, sensitivity loss at the parafovea is found in accordance with rod loss in this area in AMD but not in normal aging.

2.1.4. (c) Slower photoreceptor adaptation in AMD

In early ARM, dark adaptation is much slower than age matched controls by approximately 15 minutes (Owsley, Jackson, White, Feist, & Edwards, 2001). For patients with AMD, following exposure to a bleaching stimulus, disturbances were found in the rod components of dark adaptation (time to rod-cone break, rod-slope and rod sensitivity) following exposure to a bleaching stimulus, but none were found for the cone mediated component of adaptation at 12° parafoveally (Owsley, McGwin, Jackson, Kallies, & Clark, 2007).

However some other studies have found abnormalities of cone adaptation in AMD. ARM participants showed larger thresholds for stimulus detection at all eccentricities between 0° and 40°, but the greatest difference with normals was at 5°. Similar

results were found for cone recovery following a bleach and time to rod-cone break for ARM at the parafovea, with the largest differences between the normal and ARM group at 12° (Gaffney, Binns, & Margrain, 2011). Abnormal cone time constants, in addition to delayed rod-cone break and prolonged rod constant have also been found in people with Bruch's membrane changes compared to a healthy age matched comparison group between 3 and 15° (Steinmetz, Haimovici, Jubb, Fitzke, & Bird, 1993).

Dark adaptation has been found to be a risk factor for AMD, as fellow eyes of an exudative AMD eye have slower recovery rates for dark adaptation compared to normals with healthy eyes in a similar age group (Eisner et al., 1987b). Slower recovery rates for dark adaptation are also associated with drusen confluence, predominant drusen size and largest drusen size (Eisner et al., 1991) and predicting subsequent visual acuity loss from geographic atrophy in AMD (Sunness et al., 2008). Additionally, slower dark adaptation, in combination with the colour match area was able to predict the development of exudative sub-retinal neovascularisation, comparable to most fundoscopic risk factors (Eisner et al., 1992).

2.1.4. (d) Reduced mesopic contrast sensitivity in AMD

Brown and Garner (1983) investigated the CSF of AMD patients at various light levels. At higher (0.72 cd/m^2) and low mesopic light levels (0.0072 cd/m^2) the peak spatial frequency of the patients was always below that of the normals, but it was similar at medium light levels (0.072 cd/m^2). The authors concluded that that most of the abnormalities in AMD are apparent at photopic light levels. However there are a number of problems with this study; the authors did not use a forced choice procedure, meaning that the study could be affected by response bias, and the

patients may have higher response criteria than the normals. In addition there was no control of pupil size, which varies between patients at different light levels.

2.1.4. (e) Other mesopic and scotopic findings for AMD

Rod-mediated ERGs tend to be abnormal in AMD (Feigl et al., 2005; Jackson et al., 2006), however cone responses are not significantly different from those of normal people (Feigl et al., 2005). This method may not be sensitive enough to differentiate between older people and early ARM and is not associated with clinical fundus characteristics, possibly because ERG measures the functioning of photoreceptors in the full visual field and dysfunction could be localised to the macula (Jackson et al., 2006).

2.1.4. (f) Psychophysical correlates of clinical symptoms of AMD

It is difficult to determine what aspects of AMD result in changes to visual function. Number of drusen correlates weakly with visual acuity, but not dark or light adapted sensitivity, although these last two measures were worse than in normals (Jackson et al., 1998; Owsley et al., 2000). Multiple disease mechanisms may cause different changes in visual function.

However, absolute sensitivity and dark adaptation were correlated with drusen confluence, predominant drusen size and drusen area in another study (Eisner et al., 1991). Furthermore, in patients with GA, worsening of acuity in decreased luminance conditions was significantly correlated with contrast sensitivity and foveal dark adapted sensitivity (Sunness et al., 1997).

Therefore there is no consensus on whether there is one measure which reliably detects retinal disease and perhaps a combination of factors would be more

appropriate, for example slow adaptation rates in combination with the colour matching area effect was able to predict the development of sub-retinal neovascularisation, but neither were effective predictors on their own (Eisner et al., 1992).

2.2. Changes to binocular summation in aging

Binocular summation is the enhancement of visual performance as a result of using two eyes rather than one. Binocular interactions can occur in four ways; Facilitation when output is greater than the sum of the inputs, summation (additive or linear) where output is the sum of the inputs, occlusion when output is less than the sum of the two inputs but greater than that of a single input, and finally inhibition when the output is less than or equal to response generated by a single output (Blake & Fox, 1973).

It is useful to distinguish between the type of interaction that will occur at the neural and behavioural level for the same event. For example, in some cells there may be binocular facilitation in terms of the firing rate, however this may only manifest as binocular summation at the behavioural level in terms of percentage correct or contrast threshold. In the brain, there are cells that respond to binocular summation in different ways, some cells sum inputs from both eyes linearly and others will only respond when both eyes are stimulated simultaneously (Hubel & Wiesel, 1962; Ohzawa & Freeman, 1986).

2.2.1. Binocular summation beyond probability summation

Based on the fact that with two eyes rather than one, we have two opportunities to detect the stimulus in accordance with signal detection theory (SDT), and performance would be the same if the two opportunities were successive, assuming

the detection probabilities of each eye were independent. Based on this, the Probability Summation Model estimated that detection of the stimulus is increased by 25% (factor of 1.25; Pirenne, 1943). If performance exceeds that predicted by probability summation then it can be concluded that there may be neural summation of the signal which enhances detection further than the additional opportunity provides, and it has been found that binocular performance is greater for simultaneous than successive presentations in detection tasks (Matin, 1962; Westendorf, Blake & Fox, 1972).

Numerous studies have found that binocular to monocular detection ratio was approximately $\sqrt{2}$ (1.41), for example Campbell and Green (1965b), however this factor can vary significantly. A review of studies published between 1965 and 2008 found that on average the mean summation ratio for contrast sensitivities reported in the literature for in-phase achromatic sinusoidal gratings was 1.52, with a range between 0.75 and 2.75 for normal observers (Baker, 2008). The level of binocular enhancement depends on the difficulty of the task; there is greater binocular enhancement for near threshold tasks, and least for suprathreshold tasks (Legge, 1984a; Meese, Georgeson & Baker, 2006), possibly because at high stimulus strengths, the signal saturates the response magnitude and binocular summation can provide no further enhancement (Meese et al., 2006).

Instead of assuming independence of the monocular signals until a decision is made, many models combine the monocular signals to form a binocular signal on which the observer's decision is made, accounting for the $\sqrt{2}$ better binocular over monocular performance in a number of different ways. Campbell and Green (1965b) suggest that monocular signals contain independent, uncorrelated noise so that when summed, the noise is summed too, resulting in a binocular signal to noise

ratio that is $\sqrt{2}$ times greater than the monocular signal to noise ratio, accounting for the $\sqrt{2}$ difference between binocular and monocular thresholds. However, problems include the implicit assumptions that the ratio of signal to noise (d') remains constant at all background levels, which is not the case (Legge, 1984a, 1984b) and that there is no noise from the non-viewing eye in monocular conditions which is unlikely. Legge (1984a, 1984b) suggests that binocular output is a result of compressive non linearity and the addition of central noise. This predicts a quadratic summation relationship between binocular and monocular thresholds which results from the fact that when two noisy signals are added the standard deviation increases by the square root of the number of signals, which for 2 eyes is $\sqrt{2}$. The increase of the contrast increment threshold is accounted for by the compressive transformation and the addition of noise. At low contrasts *input* noise limits performance. As the contrast rises, the variance contributed by central noise remains constant but the variance contributed by input noise is attenuated by compressive nonlinearity, meaning that central noise dominates so that the increment rises with background contrast, limiting suprathreshold discrimination.

Frisen and Lindblom (1988) proposed the hierarchic model after finding, like Legge (1984a), that the degree of binocular summation was related to the complexity of the task. There was most binocular summation for detection, exceeding that predicted by quadratic summation theory (Legge, 1984b) but less for acuity resolution and none for pattern recognition. Based on physiological evidence (Hubel & Wiesel, 1972) the authors suggest that as one moves up the visual system, there are less monocularly driven and more binocularly driven cells. A less complex task (e.g. light detection) uses primarily monocular driven cells as the eyes can be considered as two independent detectors, and would lead to a high degree of

summation as these signals converge on the binocular cells. However for a more complex task (e.g. resolution) there is less summation since a higher proportion of cells are binocularly driven at this higher processing level and the magnitude of summation would depend on the relative response of individual cells to binocular and monocular summation. If a task was completely driven by binocular cells, then no binocular summation would be seen, in the case of pattern recognition.

The distribution model (Anderson & Movshon, 1989) is more complex than models described so far and is a multiple mechanism and multiple channel model. The theory postulated multiple binocular channels that vary in their sensitivity to the two monocular inputs and sum signals they receive linearly which may help to explain the role of ocular dominance channels that have been overlooked by other models. They suggest that the noise in the channels is at least partially correlated because they did not find any evidence of probability summation across channels and they postulate that they share many common inputs.

2.2.2. Aging and binocular summation

Multiple studies have found departures from 1.4 binocular enhancement factor for older participants. Younger participants show greater binocular summation in contrast sensitivity both at low and medium spatial frequencies (Pardhan, 1996) or just high spatial frequencies (Gagnon & Kline, 2003). In an absolute detection task, the binocular enhancement dropped from 1.54 in the younger group to 1.27 in the older group (Pardhan, 1997).

Reduced binocular summation could be due to differences in sensitivity between the two eyes, for example, the eyes of older people may age at different rates (Cagenello, Arditi, & Halpern, 1993; Gilchrist & Pardhan, 1987; Pardhan, 1997) and

symmetry along the midline of the retinal volume decreases with age (Nesmith, Gupta, Strange, Schaal, & Schaal, 2014). Wood, Collins and Carkeet (1992) found that summation reduces with increasing interocular difference, especially for smaller stimulus sizes and if the difference between the sensitivity of the two eyes is particularly large inhibition may occur (Gilchrist & Pardhan, 1987). Pardhan (1996) found that the older participants had greater interocular differences and that binocular summation was dependent on the interocular difference. Furthermore, Pardhan (1997) found that there was a correlation between binocular summation ratio and the difference in monocular sensitivity, r=0.69. However, Gagnon and Kline (2003) did not find a significant correlation between interocular differences and binocular summation, so concluded that the reduced binocular summation in older participants in their study must be due to other reasons.

Another possible reason for lower levels of binocular summation in older participants could be a result of differences in cortical processing. Pardhan (1996) suggests that to determine if this is the case the contrast sensitivity of young and older people with the same interocular ratios should be compared, however the small sample size in this study did not allow her to complete this analysis. One explanation is that there is an increase in noise from each eye which may decrease the signal to noise ratio required to detect and discriminate between stimuli. As noise increases, binocular summation decreases (Pardhan & Rose, 1999). Another explanation is that there is an increase in the correlation of this noise between the eyes, making the discrimination between the signal and noise more difficult (Pardhan & Rose, 1999). This however is unlikely because neural degeneration in older participants is unlikely to be completely symmetrical between the eyes (Gagnon & Kline, 2003).

2.2.3. Binocular summation variation with eccentricity

One of the problems of many previous studies of binocular summation is that they do not consider the effect of stimulus eccentricity. There is evidence to suggest a binocular summation will vary across the visual field, however this is dependent on stimulus size. Wood et al. (1992) found that for a stimulus size of 0.108° (Goldmann Size I) binocular summation decreased with increasing eccentricity from the fovea to 75° along the horizontal meridian, however binocular summation remained constant for a stimulus of 0.431° (Goldmann Size III) and actually increased from the fovea to 7° for a 1.752° (Goldmann Size V) stimulus before decreasing. There was no effect of stimulus size at the fovea. The effect of size and eccentricity were statistically significant but there was no statistically significant interaction. Wood et al. suggest that their results could at least partially be explained by interocular differences increasing with eccentricity. Other studies have had mixed results, some also finding that summation declines with eccentricity (Pardhan, 1997), whereas others used both Goldman Sizes I and III and found no summation variation with eccentricity in any meridian (Whitaker & Pardhan, 1997).

2.2.4. Binocular summation at low light levels

At lower light levels binocular summation tends to be decreased, as found in a detection and letter recognition task (Home, 1978), but increased at lower light levels in a discrimination task. Similarly, Connolly (2010) measured foveal contrast sensitivity at the fovea using a detection procedure with sinusoidal Gabor patches at light levels 28, 2.8 and 0.28 cd/m^2 binocularly and in the dominant eye and found that binocular summation was greatest at the lowest light level at the highest spatial frequency. He suggests that because binocular summation has a greater effect at lower light levels this is because there is more monocular noise at lower

light levels, severely limiting monocular contrast sensitivity compared to higher light levels. This supports the idea that there is limiting noise in the ocular rather than central nervous system, so it is present in each eye and "cancelled" by binocular summation of the signal.

2.3. Aims and objectives of the contrast and luminance study

The review of the previous literature suggests that contrast performance is a sensitive measure of visual function in normal aging and disease, and suggests that conducting tests under low luminance conditions may be particularly sensitive, however few studies have combined spatial vision and luminance in this way. Psychophysical methods will allow us to test different areas of the retina, to determine whether there are differences in parafoveal functions in normal aging at low light levels, as this has been found for adaptation in AMD (Owsley et al., 2000) but not normal aging (Jackson & Owsley, 2000; Jackson et al., 1998). Therefore the use of a combination of sensitive measures could be particularly effective (Eisner et al., 1992). We have also investigated the role of interocular differences to determine whether this is the reason for reduced binocular summation in older people, or if there is a cause of these changes within the higher visual pathways. The methodology of the study goes to great lengths to measure changes in contrast sensitivity as a result of aging at the retina, controlling for age related changes in optical factors that may confound the findings, which were not always accounted for in previous studies. Therefore this study aims to:

- Determine the normal limits of contrast sensitivity and age over a range of retinal illuminances

- Determine whether parafoveal contrast sensitivity declines more rapidly with age than foveal contrast sensitivity
- Determine if there is a decline in binocular summation in normal aging when retinal illuminance is controlled and whether this is due to interocular differences or higher level, age-related changes.

2.4. Methods

2.4.1. Participants

94 participants (age range 20 to 73 years) were recruited by advertising the study within City University London. Tests were approved by the City University Research and Ethics Committee and the study adhered to the principles of the Declaration of Helsinki. Informed consent was obtained for all participants. The participants underwent an ophthalmic assessment by a qualified optometrist which included measurement of visual acuity, refraction for the test distance, binocular vision assessment, pupil reactions, slit lamp assessment of the anterior eye and indirect ophthalmascopy of the macula, optic nerve head and peripheral retina using a 90 D lens.

2.4.2. Contrast sensitivity assessment

The contrast vision of each participant was assessed using a 'Functional Contrast Sensitivity' (FCS) test (Chisholm, Evans, Harlow, & Barbur, 2003b). Test-retest data indicate that the contrast test had good reliability (coefficient of variation = 8.6% in three subjects for which thresholds were measured over a number of days; Kvansakul, 2004). Stimuli were presented on a high resolution NEC Multisync Diamondtron CRT monitor (model FR2141 SB, 19.5 in), using a 30 bit colour graphics card (ELSA, Model Gloria, SL, Germany) with 1280x1024 pixels, at a frame rate of 120 Hz. The monitor was calibrated automatically with a LMT 1009 luminance meter and bespoke software (LUMCAL, City Occupational Ltd, UK).

Screen shots of the FCS test are shown in **Figure 23**. Participants viewed the display from 2 m. The task was to discriminate the direction of the gap in a Landolt ring optotype, which occurred in one of four diagonal directions. Between

presentations, a fixation cross and four oblique guides were displayed to help maintain central fixation and accommodation. The spectral composition of the background had predominantly long-wavelength (LW) and middle-wavelength (MW) content (CIE x=0.43, y= 0.485) to minimise chromatic aberrations and variation in short wavelength (SW) absorption of light by the macular pigment and the crystalline lens (van de Kraats & van Norren, 2007). The stimulus was presented for 80ms at the specified contrast with 2σ Gaussian-weighted, rising and falling profiles (σ = 53ms). Stimuli were presented in one of three randomly interleaved locations, at +4°, 0° or -4° from fixation, along the horizontal meridian. A staircase procedure with 13 reversals, was employed, to vary the Weber Contrast of the stimulus using a two-down, one-up procedure reducing the chance response probability to 1/16 (Levine & Shefner, 1991). Interleaved staircases employed increments which decreased according to an exponential function (a method developed at City University). Starting contrast increments were 5% and ending contrast increments were 1% for the highest light level and 10% and 2%, respectively, for the lowest light level. Final contrast thresholds were the average of the last 8 reversals.

Size scaling of the stimulus was employed to account for the reduction in spatial resolution with increasing eccentricity. The gap size was 4 min arc at 0° (diameter 20 min arc) and 6 min arc at ±4° (diameter 30 arc min), corresponding to spatial frequencies of 7.5 and 5 c/deg, important in tasks on visual displays (Chisholm et al., 2003a) and are affected by aging, whereas lower spatial frequencies are mostly unaffected by aging (Ross et al., 1985). The fixed gap size was significantly larger than the acuity limit at high light levels to ensure it would not be below the acuity limit at low light levels, resulting in mid to high spatial frequencies being used to discriminate the location of the gap.

Participants were tested at background luminances, 34.00, 7.60, 3.20, 1.60 and 0.12 cd/m^2, to span the photopic and mesopic range. Spectrally calibrated neutral density filters were employed for background luminances below 3 cd/m^2. Preliminary experiments on observers aged 23 and 59 were carried out to ensure that participants in the main experiment would be able to effectively accommodate at mesopic light levels (Appendix 1).

Participants viewed the screen binocularly, followed by the right eye alone and then the left eye alone at each light level because this was believed to be most intuitive and comfortable for the participants, and order of tested eye has not be found to have significant effects on measures of visual function (Grimson, Schallhorn, & Kaupp, 2002). The eye not being tested was covered with an opaque, infrared transmitting filter which allowed the iris illumination needed for pupil measurements. The participants were tested at the brightest screen luminance first, followed by the next, lower screen luminance meaning that less time was required for adaptation between luminance levels than using a randomised procedure. A minimum of five minutes adaptation time was provided for the lowest luminance from the second lowest luminance and two minutes for other luminances.

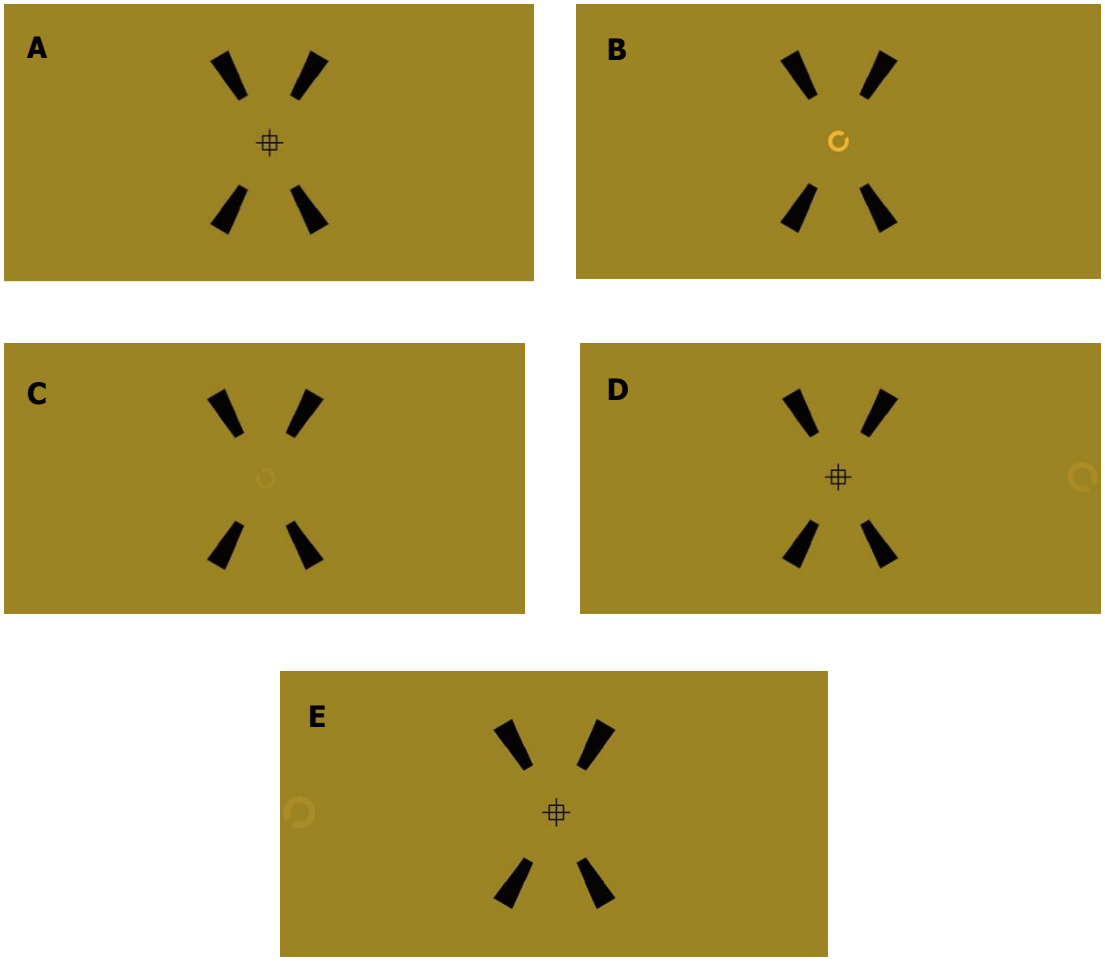

Figure 23. Screenshots from the functional Contrast Sensitivity Test. **A** the fixation cross with no stimulus presented. **B** an example of a high contrast foveal (0°) stimulus with the gap orientated towards the top right. **C** example of a low contrast foveal stimulus with the gap orientate towards the top left. **D** example of a low contrast parafoveal stimulus (+4°). The fixation cross remains on the screen during parafoveal presentations to ensure the participant fixates on the centre of the monitor. **E** example of a low contrast parafoveal stimulus located at -4° eccentricity.

2.4.3. Estimates of lens optical density

The SW absorption of the crystalline lens was measured with the Macular Assessment Profile (MAP) test (Barbur et al., 2010). Using an optical notch filter, the output of the three screen phosphors are separated into two components, the SW test beam and the LW reference beam. The SW test beam is strongly absorbed by the lens, whereas the reference beam is not significantly absorbed by the pre-receptoral filters. The two beams are modulated sinusoidally in counter phase at 17 Hz. The test stimulus is a sector annulus at 6.8° and 7.8°. The task of the subject is to cancel the perception of flicker by adjusting the luminance of the test beam using a modified staircase with variable step sizes until the perception of the flicker is cancelled. At the flicker-null point, the threshold is recorded. Both the lower and the higher flicker-null thresholds were measured at each eccentricity and the average was then recorded. Although the absolute lens density cannot be measured, the technique makes it possible to estimate the subject's lens optical density for short wavelength light with respect to the mean density measured in young observers; Therefore, a negative value for optical density means that the subject's lens absorption of blue light is less than the mean value for the young subject group. Therefore, the MAP test estimates lens optical density (OD) for SW light with respect to the mean density of young observers. The test was performed monocularly for each eye at a viewing distance of 0.7 m. The OD was measured to ensure that no participants had excessively high values of lens OD.

2.4.4. Pupil measurements

Pupil diameter was measured during the FCS test using the P_SCAN 100 system (Alexandridis, Leendertz, & Barbur, 1991; Barbur & Thomson, 1987) which employs infrared video imaging techniques with pulsed infrared illumination to measure the

centre co-ordinates of the pupil and to compute its size. Pupil measurements were taken monocularly while the participant performed the test and were averaged to produce a mean pupil size for each luminance; separate estimates were made for binocular and monocular viewing.

2.4.5. Estimating retinal illuminance

Retinal Illuminance (*E*) was measured in trolands (td) as $E = L \times P$, where L is the screen luminance in cd/m^2 and P is the pupil area in mm^2.

2.4.6. Calculating HR_{index} for contrast sensitivity

The group data provided an average measure of the change in threshold contrast sensitivity with retinal illuminance for five light levels. Change in the contrast discrimination thresholds as a function of retinal illuminance were fitted with equation (4):

(4) $$T = k \times e^{a \log_{10} E} + T_o$$

Where T is the measure of contrast threshold, E is the retinal illuminance, T_o is the asymptotic threshold, and k and a are constants. The best-fit parameters k, a and T_o were computed for the group of participants. The fitted curve for the group was used as a reference against which every participant was compared at each retinal location. The equation was then integrated to compute the area under the curve for thresholds at each of the three retinal locations in each eye producing six values for each participant (5).

(5) $$A = \int_2^{900} (T = k \times e^{a \log_{10} E} + T_o) d \log_{10} E =$$

$$\left[\frac{k}{a} \times e^{a \log_{10} E} + T_o \log_{10} E + C\right]_{2}^{900}$$

Then the equations above were used separately to compute participant-specific dependence on retinal illuminance and the corresponding HR_{index}. To improve stability of the nonlinear fitting algorithm, a sixth point was added to the dataset to correspond to 80% of the best threshold (predicted, best threshold at high retinal illuminance at 3000 td, corresponding to approximately 150 cd/m^2).

The HR_{index} was defined by equation (6), as the difference between the area under the participant's threshold curve (A_p) and the corresponding area computed for the normal group (A_{group}), from which outliers were excluded (see section 2.4.7 below).

(6) $$HR_{index} = 1 - \frac{A_p}{A_{group}}$$

A positive HR_{index} indicates performance better than the average normal participant. Correspondingly, a negative value indicates contrast discrimination that falls below that expected for the average normal participant.

For each participant, a HR_{index} at three retinal locations, one foveal and two parafoveal, was calculated for each eye. The same method was applied to the binocular measurements.

2.4.7. Identifying participants with significantly elevated contrast thresholds

Participants with detectable clinical signs of disease were excluded from the calculation of the HR_{index}. Participants were also excluded if they exhibited significant interocular differences bases on the Tukey method as early stage retinal

diseases tend to affect the eyes asymmetrically and/or start at the parafovea (Curcio et al., 1996; Medeiros & Curcio, 2001). To identify participants with substantial interocular differences in contrast thresholds ($IO_{difference}$) the following parameter was calculated:

(7) $$IO_{difference} = \frac{A_{LE} - A_{RE}}{Best\ area}$$

Where A_{LE} is the area under the curve for one eccentricity for the left eye, and A_{RE} is the area under the curve for the corresponding eccentricity in the right eye. Outliers for the HR_{index} were excluded based on Cook's D test.

2.4.8. Calculating binocular summation ratio (BSR) and interocular percentage increase (IPI)

BSRs were calculated as the ratio of the best eye's contrast threshold to the binocular contrast threshold.

(8) $$BSR = \frac{Best\ eye\ threshold}{Binocular\ threshold}$$

Interocular percentage increase (IPI) was calculated to investigate its influence on binocular summation. It was calculated as the absolute difference of the thresholds between the eyes as a ratio of the best eye threshold, where T_{LE} is the average left eye threshold and T_{RE} is the corresponding right eye threshold.

(9) $$IPI = \frac{|T_{LE} - T_{RE}|}{Best\ eye\ threshold}$$

2.4.9. Statistical analysis

The JMP statistical software was used to fit the non-linear function that describes the variation in the participant's threshold with retinal illuminance (SAS Institute Inc., Cary, North Carolina). MATLAB (The MathsWorks, Inc.) was used to estimate the probability density functions for the measured HR_{index} values and to compute the 95% limits. SPSS (IBM SPSS for Windows, Version 19.0, Armonk, NY) was used for statistical analysis on repeated measures ANCOVAs for the analysis of changes in BSR and IPI with age as a covariate and eccentricity an independent variable. Averaged data from two eyes was used for curve fitting and statistical analysis because there was no significant differences between the eyes ($F(1,82)=0.002$, $p=0.967$), variance between the eyes was similar because people with significant interocular differences were excluded, and the intra class correlation was close to one ($ICC(3,k)= 0.972$) based on Armstrong (2013). Therefore, in statistical analysis, each participant contributed one data point only for each condition, obtained by averaging results across eyes and eccentricities.

2.5. Results

2.5.1. Identification of outliers

A total of 94 subjects were recruited (age range 20 to 73 years). After the clinical exam, 12 participants (12.8%) were excluded due to presence or history of ocular disease or injury. Five (5.3%) participants had significant interocular differences in the area under the curve detected by the Tukey Method, and three (3.2%) were outliers for the regression of HR_{index} and age using Cook's D.

The HR_{index} was calculated for each remaining participant separately for each parafoveal and foveal location. **Figure 24** shows the age distribution of all participants (n=74 normals, mean age ± SD = 44.6 ± 15.6 years). **Table 1** describes the visual acuity of participants included in the study.

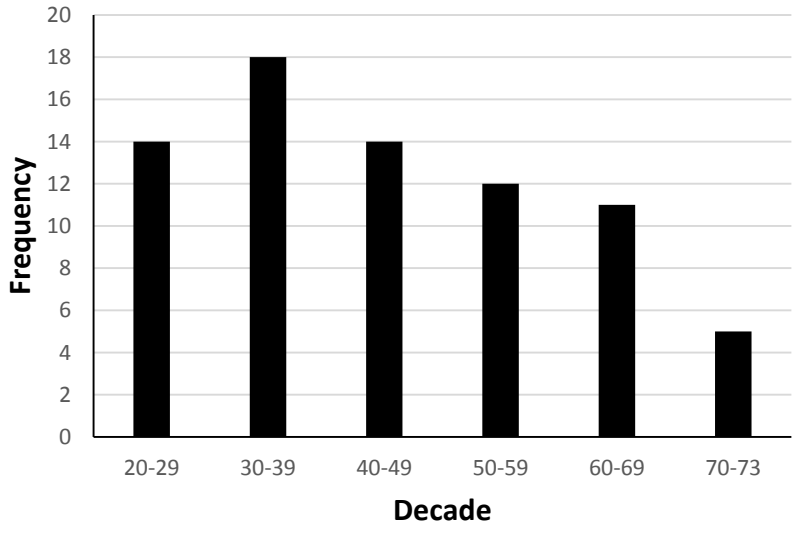

Figure 24. Age distribution of included participants (n=74).

Table 1. Description of visual acuity (logMAR) and refraction of participants in decade bins.

			Range		Mean refractive error used			Mean subjective refraction		
Age bin	Data available for	Mean VA	Min VA	Max VA	SPH	Cyl	Axis	SPH	Cyl	Axis
20-29	13	-0.07	-0.15	0.00	-1.46	-0.23	57.92	-1.17	-0.29	85.83
30-39	15	-0.06	-0.12	0.06	-2.79	-1.00	58.93	-0.25	0.00	0.00
40-49	14	-0.04	-0.20	0.05	-0.58	-0.50	88.33	-0.19	-0.75	132.50
50-59	11	-0.03	-0.20	0.06	2.05	-0.39	76.67	0.63	-0.34	55.00
60-69	11	0.01	-0.05	0.05	-2.73	-1.16	90.50	-2.53	-1.01	68.13
70-73	5	0.03	0.00	0.06	-1.18	-0.20	39.00	0.75	-0.31	52.50

2.5.2. Pupil size and age

Figure 25 shows that pupil diameter declines as a function of age. For 34 cd/m^2 and using the linear fit to the data, a 20 year old would expect to have a pupil diameter of 6.6 mm and a 75 year old of 4.1 mm. This would result in retinal illuminances of 3.07 and 2.65 log trolands respectively. This reduction in retinal illuminance of 0.42 log units is in agreement with Weale (1963).

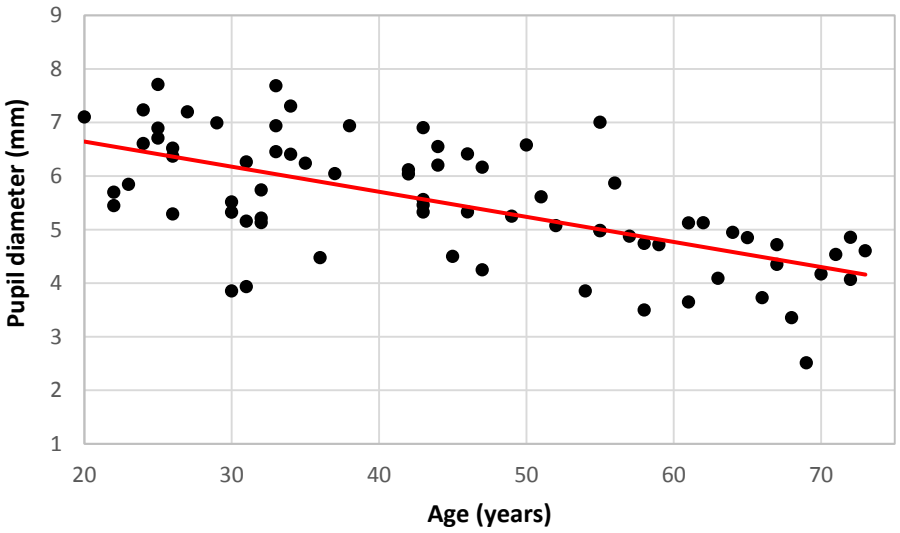

Figure 25. The decrease in pupil diameter and age from the current study. A linear fit finds that, pupil diameter = -0.0468*age + 7.5806, $R^2 = 0.41$. Data are the average pupil size for a monitor luminance of 34 cd/m^2.

2.5.3. Contrast vision and the HR_{index}

Contrast thresholds for the group as a whole increase with decreasing retinal illuminance for both fovea and parafoveal targets as shown below with contrast plotted in log units (**Figure 26**) and linear units (**Figure 27**).

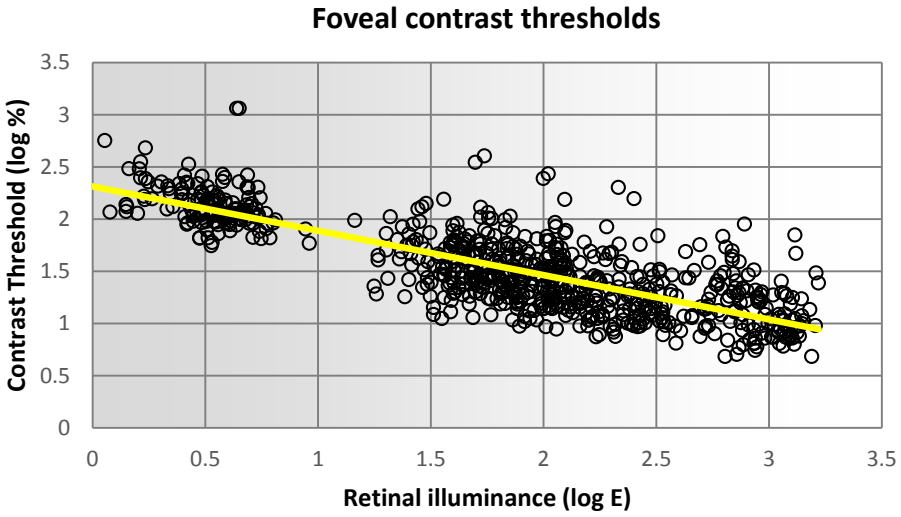

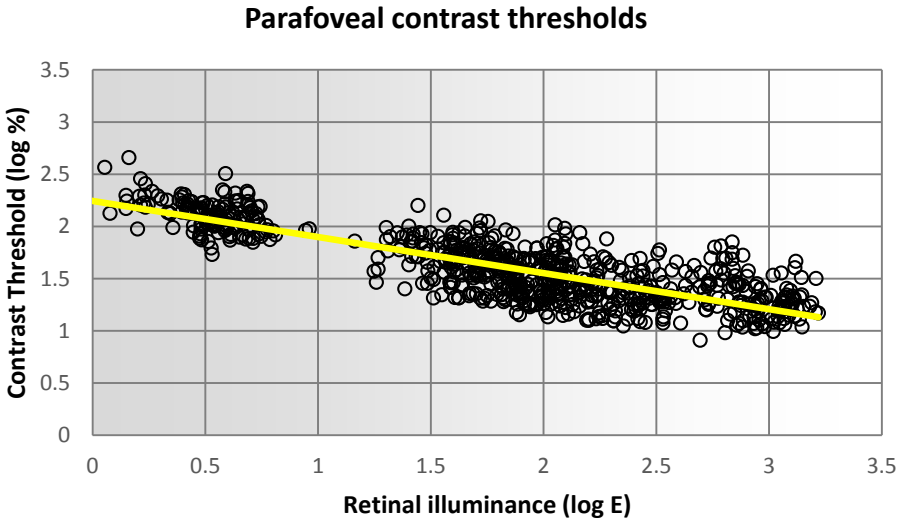

Figure 26. Log contrast thresholds for participants at the range of light levels. For the foveal data each participant contributes two points for each screen luminance, one from each eye. For the parafoveal data, each participant contributes four points for each luminance level, from ±4° in each eye. For plotting purposes, results were not averaged across eyes due to differences in the measured retinal illuminance between the eyes on each trial. Fit to foveal data: log contrast threshold = -0.4244*log E + 2.3123. Fit to parafoveal data: log contrast threshold = -0.3461*log E + 2.2444.

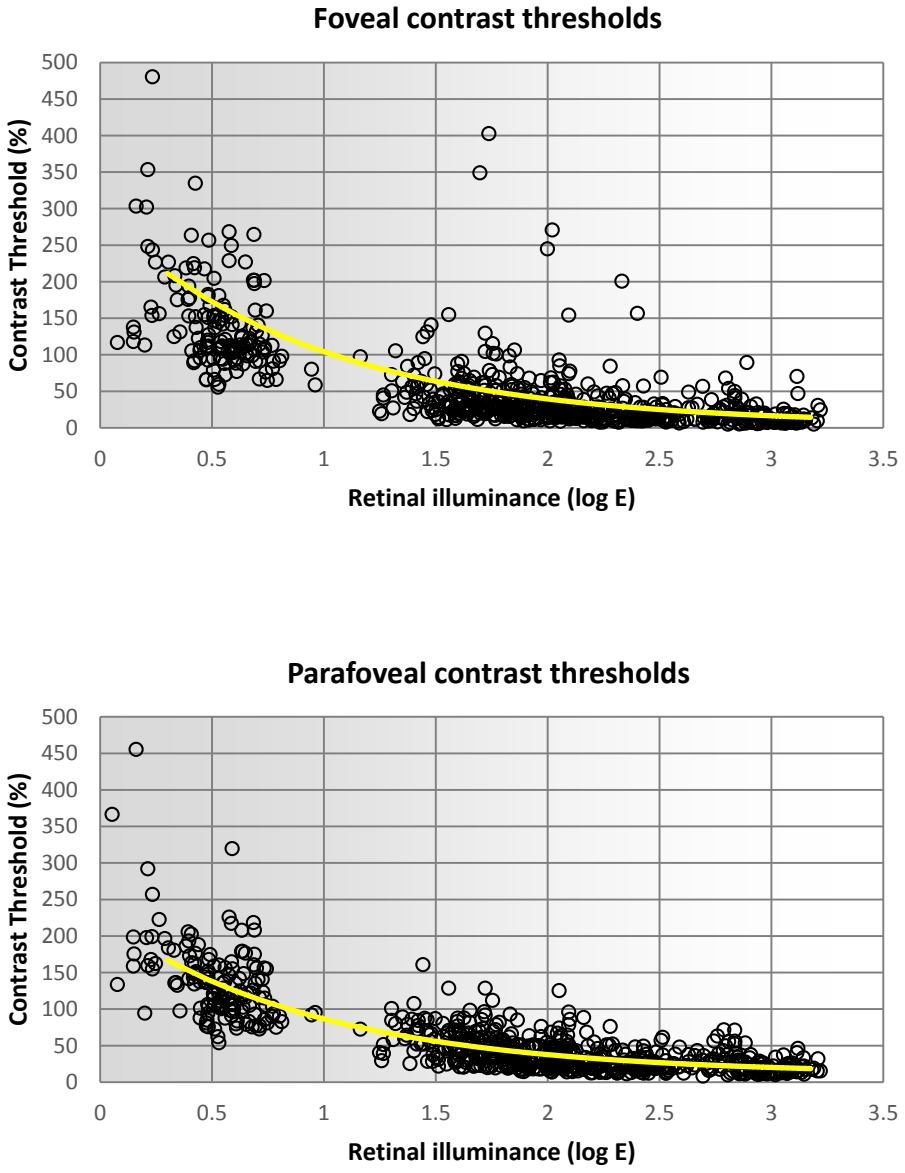

Figure 27. Contrast thresholds for participants at the range of light levels. For the foveal data each participant contributes two points for each screen luminance, one from each eye. For the parafoveal data, each participant contributes four points for each luminance level, from ±4° in each eye. For plotting purposes, results were not averaged across eyes due to differences in the measured retinal illuminance between the eyes on each trial Fit to foveal data: contrast threshold = $283.2*(e^{-1.036 * \log E}) + 3.86$. Fit to parafoveal data: contrast threshold = $213.3*(e^{-1.028 * \log E}) + 10.41$.

Figure 28 shows the HR_{index} as a function of age at the fovea and parafovea (R^2=0.11, p<0.001 and R^2=0.16, p<0.001, respectively), where no differences were found in the variance of older and younger participants at the fovea or parafovea (Levene's

statistic=1.068, p=0.305 and Levene's statistic=0.206, p=0.651, respectively). Therefore 95% limits were found for the data (dashed lines) which did not vary with age.

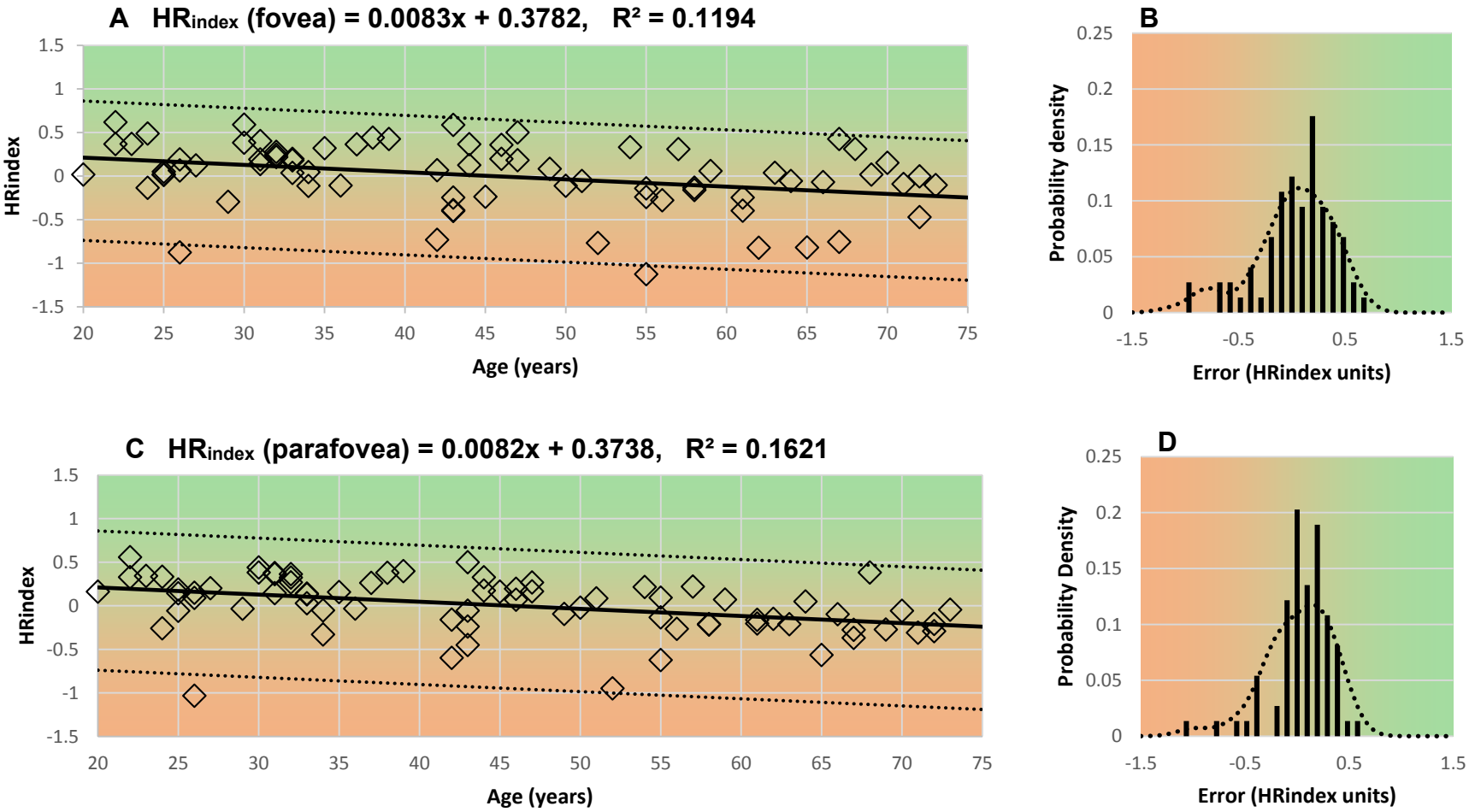

Figure 28. HR_{index} as a function of age. Panels **A** and **C** show the HR_{index} for the fovea and parafoveal respectively. Dashed lines show the 95% limits. Panels **B** and **D** show the probability density distributions of the value of errors from the regression line.

Contrast thresholds for typical young and older participants are shown in **Figure 29** for log contrast thresholds and **Figure 30** for contrast thresholds on a linear scale. Normal participants show a steady increase in contrast thresholds with decreasing retinal illuminance.

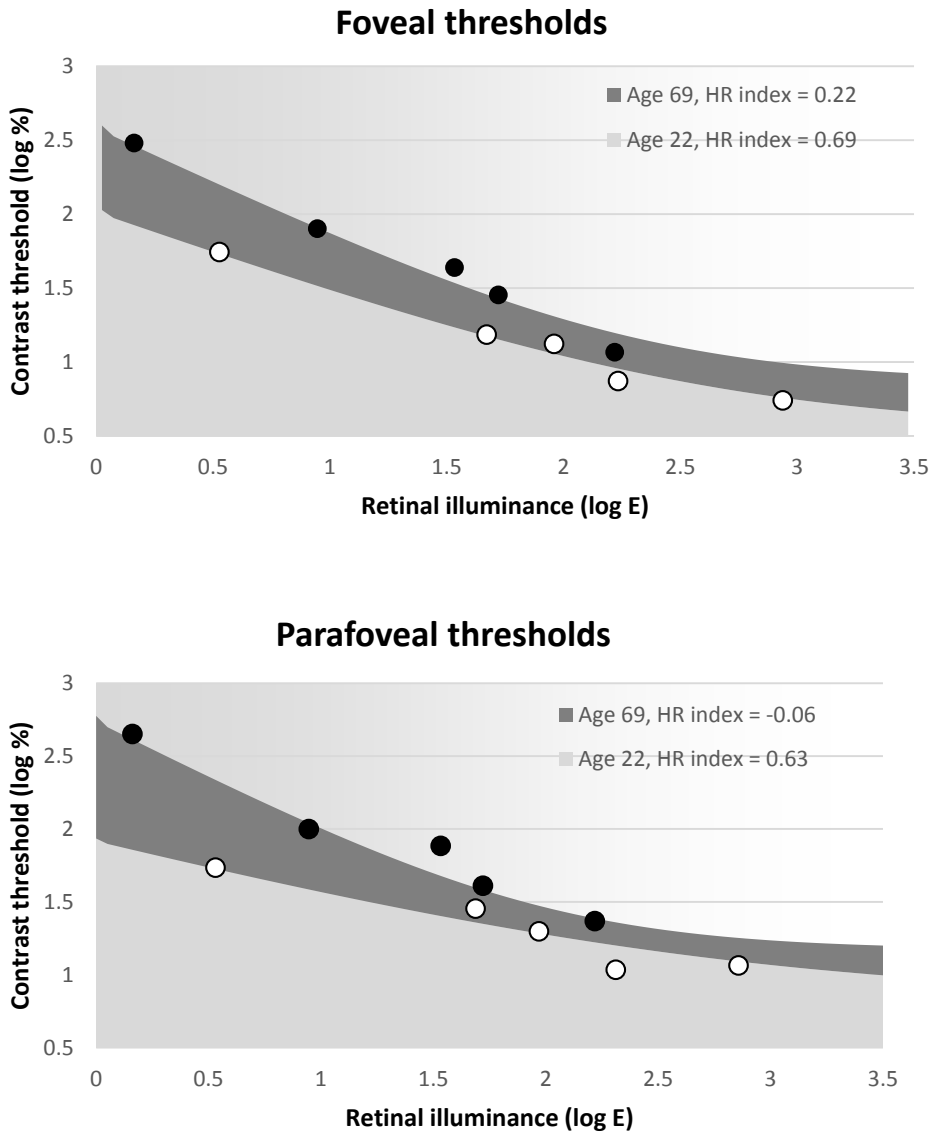

Figure 29. Examples of log contrast thresholds and the corresponding HR_{index} values at the fovea and parafovea for a younger (age 22) and older (age 69) participant. The younger participant has a smaller area under the curve than the group data, resulting in a positive HR_{index}. However the older participant has a greater area under the curve than the group data at the parafovea resulting in a negative and/or lower HR_{index}.

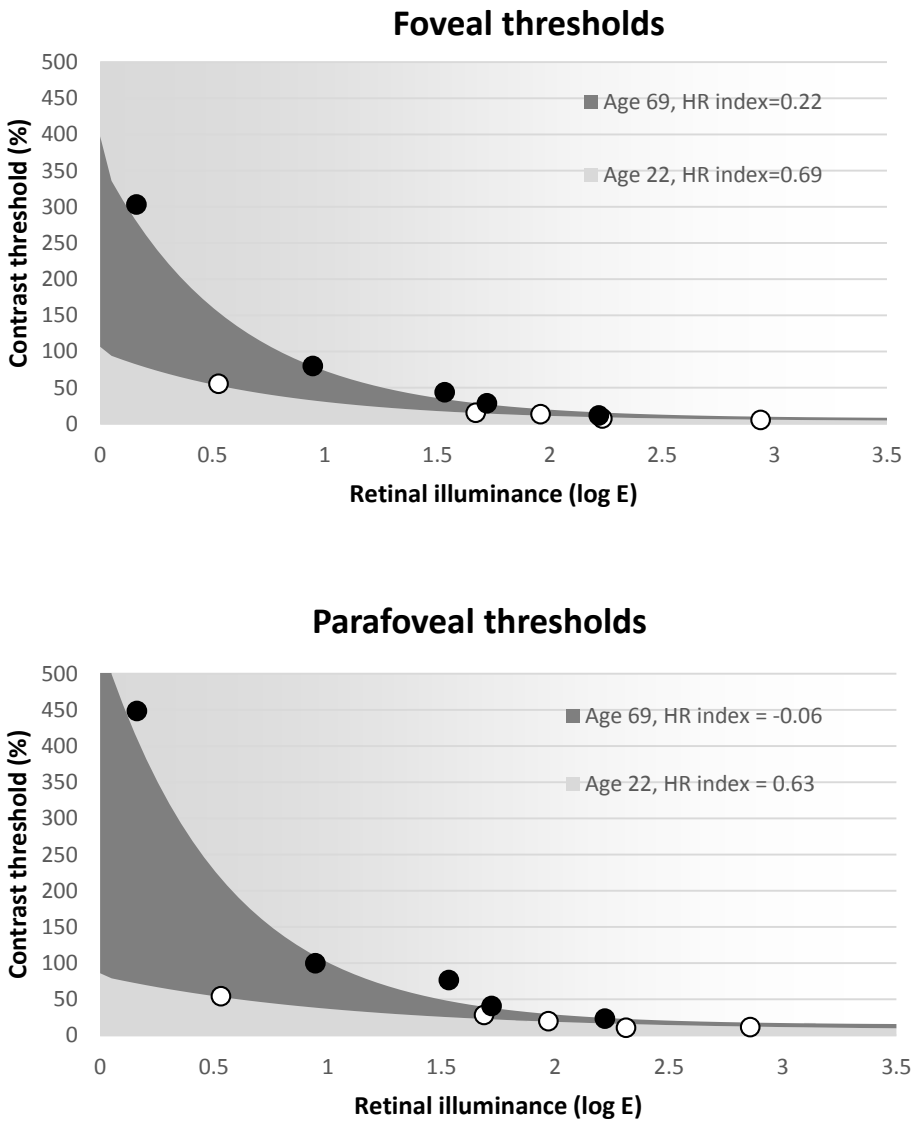

Figure 30. Examples of contrast thresholds and the corresponding HR_{index} values at the fovea and parafovea for a younger (age 22) and older (age 69) participant, re-plotted from **Figure 29.**

Figure 31 shows how contrast thresholds change at the fovea and parafovea for three retinal illuminance levels as a function of age. Upper panels show contrast thresholds on a linear scale and lower panels on a log scale, for comparison to other studies. Points were derived from curves fitted to each individual's data. A repeated measures ANCOVA with two factors, eccentricity (fovea and parafovea) and light level (900, 25, 5 td) with age as a covariate was performed on linear thresholds. Thresholds were best at the fovea ($F(1,73)=5.993$, $p<0.05$), at higher light levels ($F(2,146)=864.638$, $p<0.01$) and in younger participants ($F(1,72)=12.740$, $p<0.001$). More interestingly contrast thresholds increased more rapidly with age at lower light levels ($F(1,144)=3.276$, $p<0.05$), but no difference in the rate of decline in contrast thresholds with age was found with eccentricity.

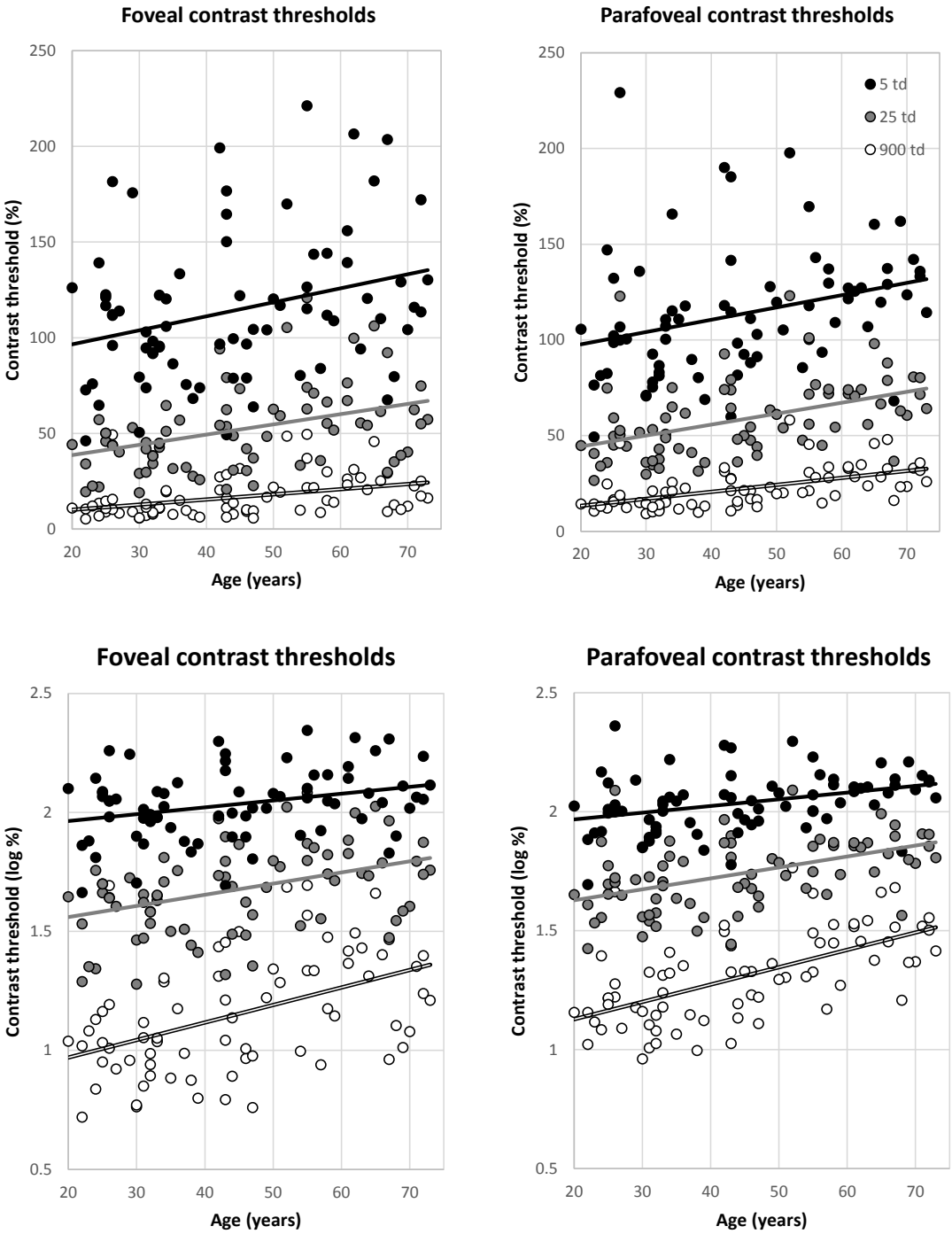

Figure 31. Foveal and parafoveal contrast thresholds at 900, 25 and 5 td. Upper panels show thresholds on a linear scale and lower thresholds on a log scale. Fit to foveal contrast thresholds on a linear scale, at 5 td, y = 0.7316x + 81.873, R^2 = 0.0857; at 25 td, y = 0.535x + 28.01, R^2 = 0.1343; at 900 td, y = 0.2700x + 4.7049, R^2 = 0.1556. Parafoveal contrast thresholds on a linear scale, at 5 td, y = 0.6422x + 84.848, R^2 = 0.0904; at 25 td, y = 0.5701x + 32.922, R^2 = 0.1876; at 900 td, y = 0.3659x + 5.9982, R^2 = 0.3077. Fit to foveal contrast thresholds on a log scale, at 5 td, y = 0.0029x + 1.906, R^2 =0.0910, 25 td, y = 0.0047x + 1.467, R^2 = 0.1533, 900 td, y = 0.0074x + 0.8226, R^2 = 0.2159. Fit to parafoveal contrast thresholds on a log scale, at 5 td, y = 0.0028x + 1.912, R^2 = 0.1243, 25 td, y = 0.0046x + 1.536, R^2 = 0.2295, 900 td, y = 0.0073x + 0.983, R^2 = 0.3651.

2.5.3. Binocular summation of contrast vision

71 of the 74 participants had binocular vision. BSRs were calculated at 1 td increments between 2-900 td and then averaged to produce one BSR value using the curve fitted to each participant's thresholds to account for differing retinal illuminance both between participants and in monocular and binocular conditions. The BSRs for contrast sensitivity are variable (mean 1.37, range 0.75-2.75; Baker, 2008) and all but one participant fell within this range. A repeated measures ANCOVA with eccentricity and age revealed that they both had a significant effect on binocular summation (**Table 2**), suggesting that BSRs are higher at the parafovea (M=1.43, SD=0.31) than the fovea (M=1.31, SD=0.35; $p<0.01$) and that overall BSRs decreases with age ($p<0.05$). The interaction between age and eccentricity was not significant. BSRs were significantly correlated with age at the parafovea ($r^2=0.069$, $p<0.05$) and were close to significance at the fovea ($r^2=0.048$, $p=0.067$; **Figure 32** A). Thirteen participants showed binocular inhibition (BSR <1) nine of whom were over the mean age of 44.6.

Increasing interocular differences can reduce binocular summation and cause inhibition. An independent measures ANCOVA with eccentricity and IPI (**Table 2**) revealed a main effect of IPI on binocular summation, but no effect of eccentricity or an interaction between these factors. Low values of IPI result in high levels of binocular summation and vice versa ($r^2=0.08$, $p<0.01$, **Figure 32** B). IPI has no relationship with age at the fovea ($p=0.59$) or parafovea ($p=0.94$) (**Figure 32** C).

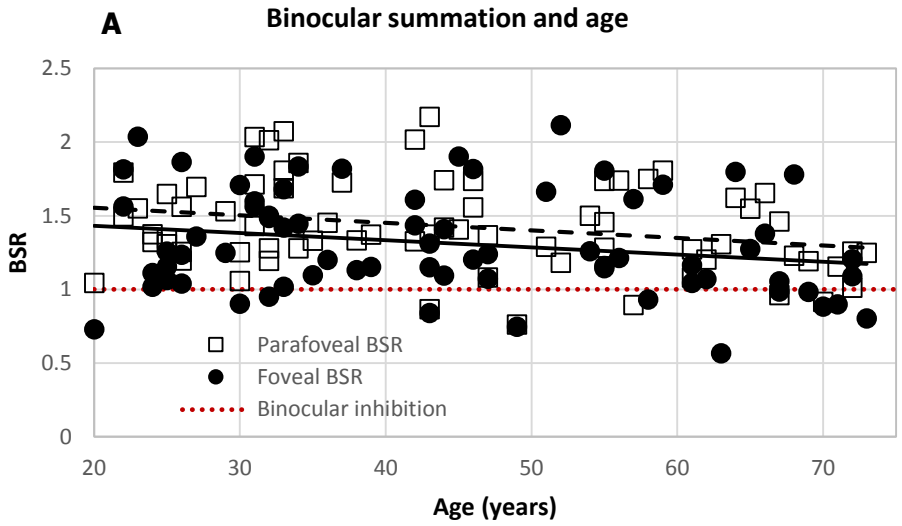
A
Binocular summation and age
BSR
Age (years)
Parafoveal BSR
Foveal BSR
Binocular inhibition

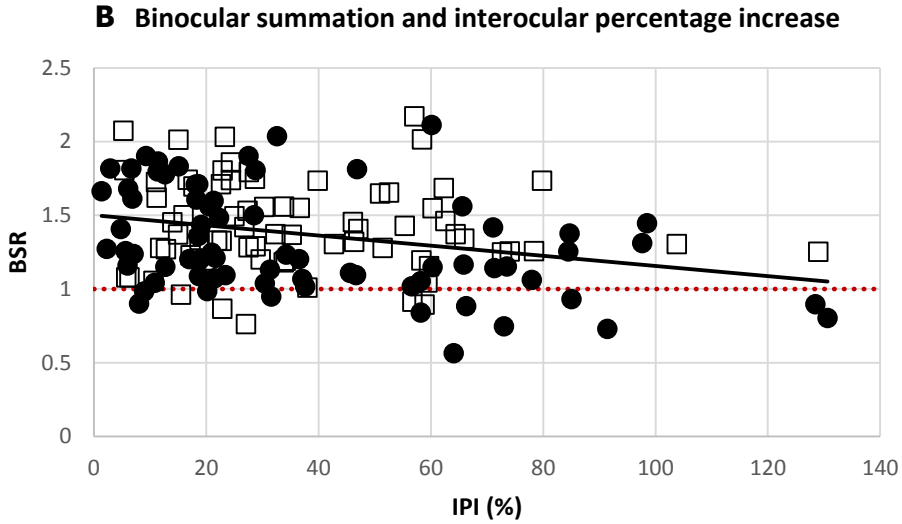
B Binocular summation and interocular percentage increase
BSR
IPI (%)

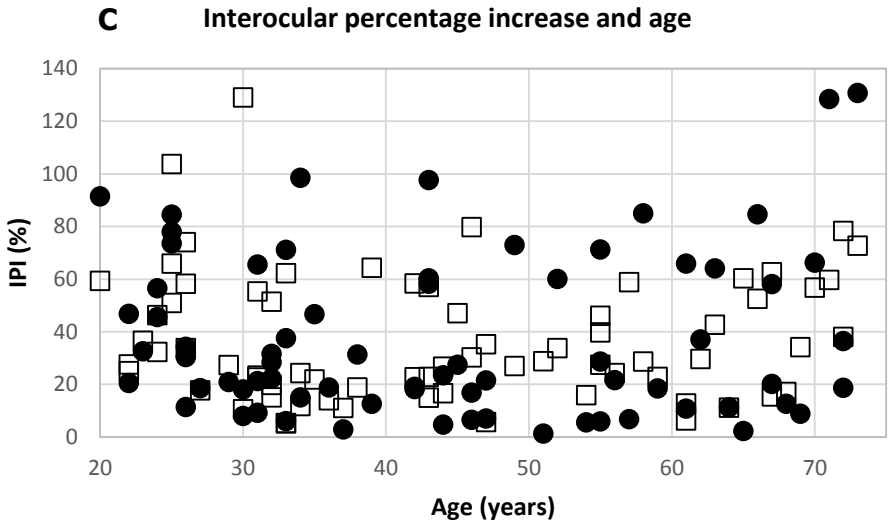
C
Interocular percentage increase and age
IPI (%)
Age (years)

Figure 32. BSR values below 1 (the BSR inhibition threshold) indicate binocular inhibition. **A** binocular summation ratio for normal, binocular participants (n=71). Binocular summation was calculated as the best monocular contrast threshold divided by the binocular contrast threshold at retinal illuminances between 900 td and 2 td. The solid line shows the linear fit to the foveal data (-0.0049*age + 1.5296, r^2=0.048, p=0.067) and the dashed line the fit to parafoveal data (-0.0051*age +1.656, r^2=0.069, p<0.05). **B** a linear fit to both foveal and parafoveal points as the ANCOVA revealed no effects of eccentricity (-0.0035*IPI + 1.5013, r^2 = 0.08, p<0.01). **C** IPI has no relationship with age at the fovea (r^2=0.004, p=0.23) or parafovea (r^2=0.000, p=0.94).

Table 2. Description of ANCOVAs describing the effects of age, foveal location and normalised interocular thresholds difference on binocular summation.

ANCOVA	F	p value
Age and Eccentricity		
Age (covariate)	6.064	p<0.05
Eccentricity (fovea and parafovea)	7.523	p<0.01
Age x Eccentricity	0.007	p=0.93
IPI and Eccentricity		
IPI (covariate)	9.458	p<0.01
Eccentricity (fovea and parafovea)	0.010	p=0.97
IPI x Eccentricity	2.519	p=0.12

2.6. Discussion

Although it may seem like we have excluded a large number of participants in the study, the proportions are comparable to other studies of aging and visual function. Haughom and Strand (2013) excluded 17.2% of participants due to disease or history of disease (as well as if the participant happened to be dilated), whereas we only excluded 12.8% on this basis. Barbur and Konstantakopoulou (2012) excluded 11.7% of participants for falling outside the normal limits of performance of a study of the HR_{index} for chromatic discrimination, whereas this study only excluded 8.5%. In total, Paramei and Oakley (2014) excluded 31.2% of participants for a number of reasons including history of ocular disease and poor performance on other tests. Therefore it was believed that the number of people excluded was comparable to other studies and was important to ensure that the 95% limits were based on a sample with clinically normal vision.

Contrast thresholds appeared to decline at a linear rate with age (**Figure 31**), which was obtained by fitting the data to estimated thresholds at particular retinal illuminances. When retinal illuminance is not accounted for in older observers, previous studies have found that performance over the lifespan is best fit with bilinear and/or exponential functions, or only show a decline from 50 years of age (Hahn et al., 2009, Haegerstrom-Portnoy et al., 1999).

2.6.1. The HR_{index} at the fovea and parafovea

The HR_{index} method provides a single number to simply represent contrast performance over a range of light levels, finding that contrast vision declines with age, consistent with large population studies of aging and contrast vision (Haegerstrom-Portnoy, Schneck & Brabyn, 1999; Rubin et al., 1997). The current approach, however attempts

to isolate the cause of the decline in contrast vision to retinal factors, independently of decreased retinal illuminance and increased optical density of the lens.

Foveal and parafoveal performance did not show differences in the rate of decline with age in the measure of the HR_{index} (**Figure 28**). This is consistent with earlier studies which also have not found greater functional declines at the parafovea compared to the fovea in normal aging (Jackson & Owsley, 2000; Jackson et al., 1998), but have in early AMD (Brown et al., 1986; Gaffney et al., 2011; Owsley et al., 2007; Steinmetz et al., 1993). This is despite the fact the parafovea exhibits a significant loss of rod photoreceptors with healthy aging, and particularly in patients diagnosed with AMD (Curcio et al., 1996; Curcio et al., 1993). Since older eyes have 13.5% larger rods, resulting in similar rod coverage (Curcio et al., 1993) and increased parafoveal spatial summation, (Malania et al., 2011; Schefrin et al., 1998) age-related functional loss at the macula may manifest as a loss of contrast or other spatial perception rather than absolute sensitivity. No difference in the rate of parafoveal and foveal decline was found using the HR_{index} which summarises performance at photopic and mesopic light levels, suggesting that to quantify the effects of aging research should focus on performance at lower light levels. However, even in **Figure 31**, for estimated thresholds at 5 td, there is no greater decline in thresholds with age between the fovea and parafovea. However, this figure shows that there is a greater decline in contrast thresholds with age at lower retinal illuminances on a linear scale.

Interocular differences can have functional consequences such as increasing the number of driving accidents (Ivers, Mitchell, & Cumming, 1999). In this study those with significant interocular differences were excluded; differences in contrast sensitivity between the eyes could be due to differences in optical aberrations, accommodation and absorbed light, however the use of Landolt ring gap sizes of four and six arc min

and the restriction of light to MW and LW are likely to minimise these effects. Selective structural changes in the retina or an imbalance in the cortical area dedicated to each eye may contribute more to the measured differences in contrast sensitivity between the eyes, suggesting that any deficits in HR_{index} might be related to photoreceptor/retinal or higher processing deficits.

The decline in contrast sensitivity with age shows a greater decrease than previously calculated for colour vision (Barbur & Konstantakopoulou, 2012). The assessment of more retinal locations, the extension into the lower mesopic range and the use of interocular differences as an additional filter may have made this assessment more sensitive.

2.6.2. Binocular summation of contrast signals

BSRs were calculated, for the first time accounting for retinal illuminance differences between participants and monocular and binocular conditions, as pupil size varies between monocular and binocular conditions (Boxer Wachler, 2003). BSR decreased with age in accordance with previous findings (Gagnon & Kline, 2003; Pardhan, 1996). In addition, thirteen out of seventy four participants showed binocular inhibition, a greater proportion than previously reported (Azen et al., 2002), despite the fact that our methods maximised BSR which is highest for stimuli at threshold (Cagenello et al., 1993; Home, 1978). These findings could be because BSR was averaged from 900-2td, whereas previous studies are conducted under photopic conditions whereas BSR is lower under low luminances in our study (2 td M =1.15, 900 td M = 1.31). These results suggest that when measuring visual function over a large range of light levels, a greater proportion of people may experience difficulties in binocular vision than previously reported.

The decrease in BSR in normal aging has often been attributed to increases in interocular differences with age (Cagenello et al., 1993; Haegerstrom-Portnoy et al., 1999; Pardhan, 1997). However, as the thresholds of the eyes increase, the interocular difference should also increase proportionately in accordance with Weber's Law. If one defines the interocular difference as the interocular percentage increase (IPI) in contrast thresholds, as described above, IPI has no relationship with age at the fovea or parafovea (**Figure 32** C). Therefore, any decrease in BSR with age must be explained by changes in higher visual pathways. In support of a central, neural aetiology, BSR declines at the same rate with age for both foveal and parafoveal locations. Possible explanations include increases in cortical noise or delayed signal timing with age (Wang, Zhou, Ma & Leventhal, 2005; Yang et al., 2008; Zhang et al., 2008).

BSR was higher at the parafovea compared to the fovea, contrary to previous findings (Pardhan, 1997; Wood et al., 1992). In this study a slightly larger target size was used at the parafovea compared to the fovea, which improves summation (Wood et al., 1992). Most studies of binocular summation use the same target size across the visual field; this results in a corresponding reduction in sensitivity as the receptive fields of retinal ganglion cells increase, acting as an additional extraneous factor. The stimuli in this study were size scaled to control for differences in sensitivity, possibly revealing a real increase in binocular summation when sensitivity changes are corrected for.

2.7. Conclusions

Independently of retinal illuminance, older people have difficulty with contrast vision due to neural changes in the retina and higher visual pathways as demonstrated by the increase in thresholds and reduced binocular summation respectively. Methods employed in this study have identified individuals with losses of spatial vision despite

minimizing the effects of pupil miosis by calculating retinal illuminance and light scatter by the use of MW and LW light, which have not been controlled in many other studies of contrast vision and aging. The contrast-based HR_{index} confirms previous findings on chromatic sensitivity and extends its applicability. BSRs revealed a number of older individuals showing binocular inhibition, raising questions about the quality of binocular vision in older people in a wider range of light levels than conventionally measured in eye clinics, in the absence of clinically recognizable deficits or disease.

3. Aging of temporal contrast sensitivity in the retina at mesopic and photopic luminances; separating normal aging from disease

This chapter outlines the method for the detection of normal aging from disease using rapid flicker sensitivity. The methods are similar to those in the previous chapter and focus on age related changes at the retina rather than changes that affect the optics of the eye, and to determine if, like for contrast vision, age related changes affect mesopic vision more than photopic vision. The main objective is, however, to establish normal, age-related, upper thresholds limits for rapid flicker sensitivity. The study and therefore the literature reviewed will focus less on CFF and more on temporal modulation sensitivity.

3.1. Temporal contrast sensitivity changes in aging and disease

Similarly to spatial contrast sensitivity, there is evidence for changes to temporal contrast sensitivity in normal aging and to a greater extent in retinal disease. Firstly the evidence for these changes will be outlined, followed by a review of the possible mechanisms of these changes. Unlike for spatial contrast vision, there are relatively few studies that investigate the effect of aging or disease on mesopic temporal contrast vision.

3.1.1 Temporal contrast sensitivity changes in normal aging

Unlike spatial contrast sensitivity, temporal contrast sensitivity is relatively insensitive to scatter and absorption of light as result of the increased optical density of the lens with age or refractive defocus (Kim & Mayer, 1994; Lachenmayr et al., 1994; Mayer et al., 1988; Tyler, 1989; Wright & Drasdo, 1985). Therefore, it could be argued to be a more reliable indicator of performance which reflects the state of the retina than spatial contrast vision.

Mayer and various colleagues conducted many studies of flicker in normal aging and disease. As part of the initial project, Mayer et al. (1988) defined the CSF for flicker under photopic conditions (120 cd/m^2) for a long wavelength foveal stimulus in a group of older (65-86) and younger (18-42) participants. When results are corrected for retinal illuminance, the CSF for flicker is similar in shape for the older and younger group, however the older group's CSF is shifted down showing worse sensitivity and also shifted slightly left, meaning that peak threshold was at slightly lower frequencies. The loss of sensitivity reached significance, meaning that the older group had significantly worse mean thresholds. Therefore these researchers suggest there is a general loss of sensitivity rather than a change in the overall temporal characteristics of the response system. In a more comprehensive investigation of 89 observers (aged 18-77) older participants showed worse losses at high temporal frequencies, but only tended to decline after 44 years of age (Kim & Mayer, 1994). A greater effect of aging at higher temporal frequencies at the fovea has also been found by other researchers (Casson, Johnson & Nelson-Quigg, 1993; Elliott et al., 1990; Tyler, 1989; Wright & Drasdo, 1985), although often all frequencies are affected, but to a lesser extent than higher frequencies (Casson et al., 1993; Culham & Kline, 2002; Kuyk & Wesson, 1991; Mayer et al., 1988).

Therefore, when correcting for retinal illuminance, Mayer and colleagues find that older people perform worse than younger participants, and some studies have found older people still perform worse when younger people when tested under reduced retinal illuminance (Elliott et al., 1990), suggesting that older people's poorer performance is due to neural rather than optical changes. However, Wright and Drasdo (1985) and Culham and Kline (2002) did not control for retinal illuminance for their participants, and found that the younger participants with lower retinal illuminance had flicker performance that was similar to older people and this did not suggest there were neural changes to the retina or visual pathways causing this change. However, Culham and Kline (2002) do suggest that the 0.5 neutral density filter they used may have been too large, and therefore just because retinal illuminance can be reduced to mirror the effect, does not mean that the loss of flicker sensitivity in older people is solely for this reason.

Like Kim and Mayer (1994), other studies have found a non-linear decline in temporal sensitivity. For example, a retrospective analysis of visual field data using standard programs on the Humphrey field analyser, for people age 10-89 (n=562), found that the best fitting function was a non-linear function to describe loss of sensitivity with age, more rapid loss at older ages, however they used white rather than LW light and there was no pupil control (Spry & Johnson, 2001).

The loss of flicker sensitivity with age may occur at different rates for different eccentricities. At eccentricities between 0 and 26°, older people perform worse than younger people for a LW flickering stimulus, but there were only significant differences found at the extremes of 0 and 26° (Zele, et al., 2008). Similarly, perimetry has found steeper decline in thresholds outside 10° than within 10° (Spry & Johnson, 2001), outside 20° with an increasing age difference with increasing eccentricity (Casson et

al., 1993), and there was a greater decline at superior rather than inferior hemifields (Casson et al., 1993; Spry & Johnson, 2001).

In summary, aging causes a general loss of temporal contrast sensitivity that may affect all temporal frequencies, but the loss of sensitivity is greatest at higher frequencies. Some researchers believe this is due to neural rather than optical age-related changes in the eye. The findings are not, however, always consistent and there is therefore no general consensus.

3.1.2 Temporal contrast sensitivity changes and retinal disease

There is much evidence for the loss of temporal contrast sensitivity in AMD, which has led to the statement that "…the functional status of an eye does not always correspond with the predicted hierarchy of risk of vision loss based on clinical fundus signs". This statement is based on the fact there was not always a reduction in flicker sensitivity when pigmentary disturbances or the presence of GA were seen in the fellow eye which changes the grading in clinical classifications of AMD (Luu et al., 2013).

People whose fellow eye had exudative AMD had worse temporal contrast sensitivity, particularly at 14 Hz where the difference between the AMD and age-matched normal group was significant. In addition, some participants had done the Pelli-Robson chart and the AMD risk group did significantly worse. This suggests that spatial and temporal contrast sensitivity could both be affected by AMD (Mayer, Spiegler, Ward, Glucs & Kim, 1992b).

The greatest differences between those with AMD and age matched normals are more evident for higher frequencies (Mayer et al., 1992b). Higher frequencies would

therefore be more appropriate to use when attempting to detect disease related changes.

Eccentricity has been found to be important in differentiating people with AMD from older age matched normals. For example people with ARM and diabetes were outside the 95% limits set by age matched normals but only within central 4° and not outside this eccentricity (Zele et al., 2008). Other researchers have found that those with early AMD perform worse in central 3° (Phipps, Dang, Vingrys, & Guymer, 2004).

Mayer and colleagues went further to investigate what aspects of flicker performance identified eyes at risk from AMD and could predict development of later stages of AMD. Loss of sensitivity to high frequency flicker (using a combination of 10 and 14 Hz) identified the largest number (78%) of eyes at risk from AMD, whose fellow eye already had exudative AMD, from healthy age matched eyes. This score was higher than what could be achieved using other properties of the TCSF function such as low frequency slope, high frequency slope, maximum sensitivity and peak frequency and parameters of the Stork and Falk/Swanson impulse response function (Mayer, Spiegler, Ward, Glucs, & Kim, 1992a). The same participants were studied to determine whether the tested eye went on to develop exudative AMD or stayed stable from previous performance. 5 and 10 Hz flicker identified 100% of those who developed exudative AMD from those who stayed stable as well as age matched normals, whereas fundus scores could only discriminate the exudative from the normal group (Mayer et al., 1994). Furthermore, people who go on to develop GA or CNV have worse flicker sensitivity compared to both a control group and an AMD group that did not progress (Luu et al., 2012). Clinical signs may not be as good as risk factors because taking the fellow eye with late AMD or pigmentary changes as risk factors alone failed to achieve high prediction rates (Luu et al., 2012).

Some research further suggests that fundus status may not be the best indicator of disease progression. Luu et al. (2013) graded 274 AMD patients on severity from 1-10 based on fundus photographs and in addition, participants detected the presence of a static or flickering stimulus which could be arranged at eccentricities 1°, 3°, 6° or 10° degrees from the fovea. For the 1° stimulus the participants from group 4 had worse flicker perimetry, but no further decline in performance was demonstrated until group 7. In the study's one year follow up (with n=129) those that had a stable grading showed no decline in flicker performance but those whose grading got worse showed a decrease in flicker performance. As flicker mirrors grading, but grading doesn't always mirror flicker, one may be justified to suggest that clinical classification of AMD based on visible changes to the fundus may not correspond to visual function and do not necessarily predict future risk. To illustrate this point, one participant had early signs of AMD at baseline and was followed up once every six months for 2 years, at the end of which GA had manifested at a particular location. In the time preceding the detection of GA, the same location showed increasingly poor flicker sensitivity, as did the surrounding area showing that flicker can pick up retinal changes that cannot be detected using current imaging techniques (Luu et al., 2012).

In summary, AMD can be distinguished from age-matched normals easily at higher temporal frequencies, as this is where the largest difference in performance is demonstrated. Furthermore, high temporal frequency flicker shows worse performance for eyes at risk of developing AMD or later stages of AMD, and may be able to detect retinal changes before they are apparent with current imaging techniques.

3.1.3. Mechanisms for reduced temporal contrast sensitivity

The current section considers the mechanisms and possible changes that can cause a loss of flicker sensitivity. Loss of photoreceptors in the retinal mosaic has obvious consequences for spatial sensitivity, but because cone sizes increase with age (Curcio et al., 1993), there should be similar levels of photon absorption over time meaning that reduced temporal contrast sensitivity with age may have a different aetiology. However some researchers have attributed the loss of temporal contrast sensitivity in aging and retinal disease to declines in the number of photoreceptors and / or other visual neurones (Mayer et al., 1988; Mayer et al., 1992b).

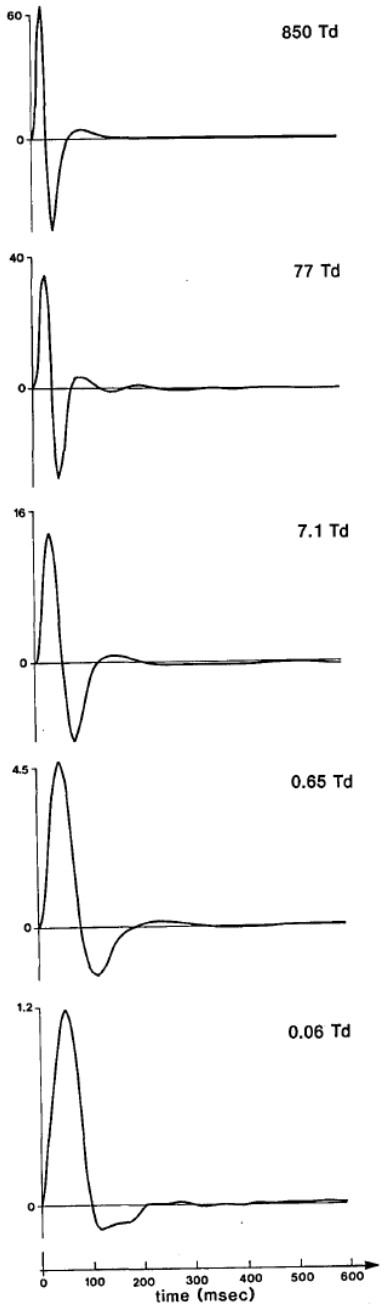

Figure 33. The impulse response function at various retinal illuminances. At higher illuminances, the function is triphasic and rapid, however it is biphasic and sluggish at lower light levels.

Other researchers have attributed changes in temporal contrast sensitivity to alterations in the dynamic responses of the visual system, as revealed by measuring / deriving the impulse response function (IRF, **Figure 33**). The IRF was reconstructed from large-field sinusoidal flicker sensitivity curve from Kelly (1961), is dependent on biological and neurophysiological properties of the visual system such as reaction and diffusion rates of photoproducts

within photoreceptors, and time constants of neural information flow, but the IRF may not be an explicit neural signal but describes the response of many temporal channels. As shown in **Figure 33**, the impulse response function is quick and triphasic at high retinal illuminances, but becomes biphasic and sluggish at lower retinal illuminances (Stork & Falk, 1987).

Aging and disease may affect the timing parameters of the IRF such as time to peak, duration of responses and timing of zero crossings (Tyler, 1989) which would increase the length of the visual systems response and therefore explain the loss of high temporal frequencies with increasing age. However, in a study of normal observers aged 16 to 86 years with controlled pupil size, no changes were found in the time to first peak or first zero crossing in observers over the age of 60, however the amplitude of the inhibitory response was reduced relative to the excitatory phase making IRFs and the speed of response reasonably stable up to 80 years of age (Shinomori & Werner, 2003). Other studies have also found age-related reductions in the amplitude of the response, but not timing of the response (Kim & Mayer, 1994), and with a greater effect outside 5° (Gerth, Sutter, & Werner, 2003). However, particular pathways such as the S-cone OFF pathway may show selective slowing with age, but not the S-cone ON pathway (Shinomori & Werner, 2012).Therefore, it seems that rather than the visual system as a whole slowing its response, the level of response may be sub-optimal, so that the visual system does not respond maximally to flickering stimuli or only particular pathways may show a slowing with increasing age.

One possible explanation for the reduced response could be changes to the photoreceptors, despite their increasing size, meaning they absorb fewer photons. Alternatively, older people may experience reduced blood flow in the retina, which is tightly coupled with neural activity (Neelam et al., 2009). Flickering stimuli cause

approximately a 30% increase in blood flow compared to static stimuli, and even more so in the perifoveal region (Kiryu, Asrani, Shahidi, Mori, & Zeimer, 1995). Furthermore, in AMD, the thickening of Bruch's membrane reduces the diffusion across the choroid and atrophy of the choriocapillaris (capillary network of the choroid; Arden, Sidman, Arap, & Schlingemann, 2005) meaning that the blood supply to photoreceptors for patients with AMD may not meet the metabolic needs of the patients and hence their reduced performance in the detection of flickering stimuli.

3.2. Rod-cone interactions in flicker

Many studies have investigated changes to flicker perception at low light levels, particularly as a way of investigating rod-cone interactions, however few studies have considered low light level flicker and aging. The best temporal contrast sensitivity occurs at approximately 1200 td, and declines as light level decreases (Kim & Mayer, 1994). However, due to the different temporal response properties of rods and cones, signal interactions can take place in the visual pathway to cause either constructive or destructive interference.

Flicker signals may enhance or cancel each other depending on the phase of the signal when they reach a particular neural locus (MacLeod, 1972; Sun et al., 2001). The temporal responses of rods and cones differ, with cones responding more rapidly to the onset of a stimulus than rods. This means that in mesopic conditions when both kinds of photoreceptor are responding to the same stimulus, the response of the rods are delayed relative to the cones. When presenting a 3° yellow disk located at 5° on the retina at mesopic levels, rod and cone signals were out of phase at 7.5 Hz and cancelled but were visible at scotopic and photopic levels when the rod and cone signals were isolated (MacLeod, 1972). In the study conducted in this chapter, the stimulus was 15 Hz, and in the same study at mesopic levels, rod and cone signals

constructively interfere (MacLeod, 1972), however at purely scotopic levels the two different rod pathways cancel at 15 Hz (Sharpe, Stockman, & MacLeod, 1989; Stockman & Sharpe, 2006).

Dark adapted rods suppress both L and M cone mediated flicker, but not chromatic flicker detection. This suggests that the magnocellular pathway is a possible site for rod-cone interaction (Cao, Zele, & Pokorny, 2006). Dark adapted rods can suppress cone mediated flicker in adjacent areas of the retina (Zele, Cao, & Pokorny, 2008) and furthermore, rod-cone interactions in flicker may only affect the "fast" pathways (via rod-cone gap junctions) rather than the "slow" pathway (via rod bipolar and amacrine cells) because raising cone excitation in the background of a display increases this rod threshold (Buck, 2004).

Rods have been found to reduce the amplitude and to delay the timing of cone mediated IRFs which reduce the temporal bandwidth of the system (Zele, et al., 2008). These effects may also act to reduce the latency differences between the rod and cone systems (Sun et al., 2001). One intriguing possibility following on from this finding is that reduced numbers of rods relative to cones may then have less of an influence on the IRFs of older people, resulting in greater latency differences between rods and cones, thus reducing further their sensitivity at mesopic light levels.

3.3. Binocular summation of modulation flicker

Relatively little research into the binocular summation of flicker has been conducted compared to binocular summation of spatial signals, and furthermore we are not aware of any investigations into the binocular summation of flicker signals in normal aging. The BSR may be of a similar magnitude for flicker of about 1.3 when the non-test eye

was occluded in the monocular condition, but interestingly BSR increased to 1.8 when the non-test eye was presented with a steady light field (Cavonius, 1979).

Interocular differences in flicker sensitivity work in a similar way to interocular differences in spatial sensitivity, in that delaying a 20 Hz flicker to one eye increases the modulation required in order to detect the stimulus, following a sine wave pattern (Cavonius, 1979). Phase lags from 0° (simultaneous) to 180° (counter-phase) result in decreasing BSR with increasing phase lag, but more so for slower temporal frequencies than higher (Levi, Pass, & Manny, 1982). It is possible that an acquired phase lag specific to one eye in older people could reduce sensitivity.

3.4. Aims and objectives of the flicker and luminance study

The literature suggests that higher frequency flicker is a sensitive measure of aging and risk of retinal disease, but it is unknown if age related changes of the retina affect flicker at lower light levels rather than higher, if parafoveal flicker will be more affected than foveal flicker due to loss of photoreceptors or other neurones and whether binocular summation of flicker changes with age in the same way it does for spatial vision.

In view of this knowledge this study aims to:

- Determine the normal limits of rapid flicker sensitivity in relation to age and retinal illuminance
- Determine whether parafoveal temporal rapid flicker sensitivity declines more rapidly than in the foveal region with increasing age.

- Determine if there is a decline in binocular summation with age when retinal illuminance is controlled and whether this is similar to that found for spatial vision

3.5. Methods

3.5.1. Participants

Participants were recruited by advertising the study at the City University Eye Clinic. All participants had undergone detailed ophthalmic assessment to determine whether they qualified as being clinically normal. The tests included measurement of visual acuity, refraction for test distance, binocular vision assessment, pupil reactions, slit-lamp assessment of the anterior eye and indirect ophthalmoscopy of the macular, optic nerve head and peripheral retina. The study was approved by the City University Research and Ethics Committee and it adhered to the principles of the Declaration of Helsinki. Informed consent was obtained for every participant.

3.5.2. Rapid Flicker Assessment (RFA)

It is of interest to produce a practical test that can be implemented within the time constraints imposed in a clinical setting. Investigation of the full range of temporal frequencies in normal aging may yield diminished returns and the time involved would rule out the use of such a test in routine clinical practice. Our aim was also to investigate a large number of participants in order to establish the effects of normal aging and this limits the duration of the tests that can be carried out. Based on the findings in the literature, it was decided to concentrate on the loss of rapid flicker sensitivity by selecting a fixed temporal frequency of 15 Hz.

The modulation sensitivity of each participant was assessed using the Flicker-*Plus* test which was modified to include measurement of pupil size. Stimuli were presented on a high resolution, 20" NEC Multisync Diamondtron CRT monitor (Model FR2141 SB, NEC, Tokyo, Japan), using a 10 bit graphics card (Elsa Gloria XL) with 1600 × 1200 resolution at a frame rate of 120 Hz. The monitor was calibrated automatically with an LMT 1009 luminance meter and bespoke software (LUMCAL; City Occupational Ltd., London, UK).

Examples of the stimuli used are shown in **Figure 34**. Participants viewed the display from 1.4 m. A fixation point and four oblique guides were displayed to maintain central fixation and to minimise accommodation fluctuations. The background was composed of only mid to long wavelength light (CIE x=0.413, y=0.507) in order to minimize variations in absorption of short wavelength light by the crystalline lens (van de Kraats & van Norren, 2007) and the macular pigment.

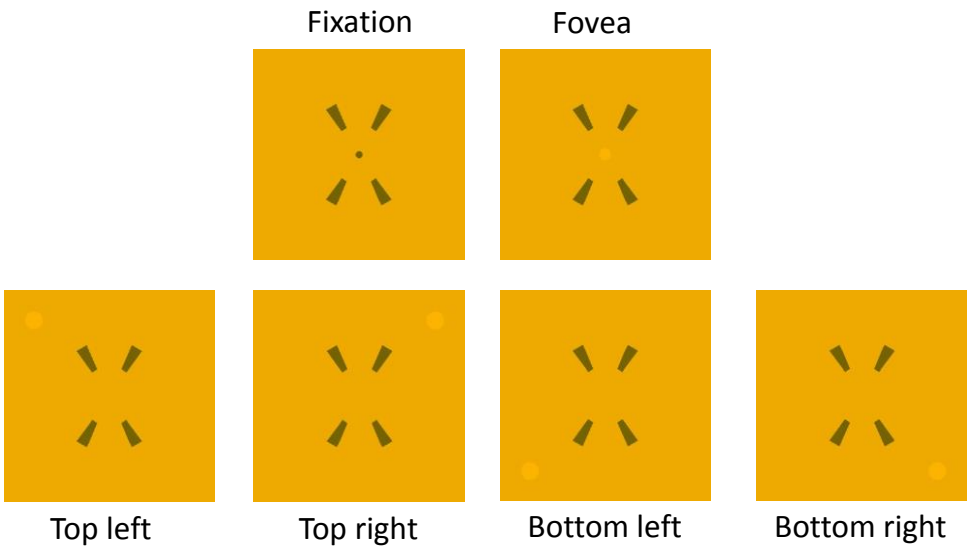

Figure 34. Examples of the flicker stimuli employed in this study. The top row shows the fixation and foveal stimulus. The bottom row shows examples of the four peripheral stimuli.

The psychophysical method of measuring flicker thresholds was based on a five alternative forced choice procedure designed around the five locations of the stimulus. The subject indicated the location of stimulus presentation by pressing one of five buttons arranged to simulate the geometry of the screen. A separate button was provided when the subject was totally unaware of any stimulus. When this button was pressed the program allocated the subject's response randomly to one of the five buttons. Five randomly interleaved staircases with variable step sizes were employed and these corresponded to the five stimulus locations: 0° eccentricity or one of four parafoveal locations, 4° away from fixation in the inferior nasal, superior nasal, inferior temporal or superior temporal visual field. A central guide was displayed 695 ms prior to the flicker stimulus to help the subject to maintain central fixation.

The stimulus diameter subtended 20 arc min at the fovea and 30 arc min at the parafoveal locations. Stimuli were presented for 334 ms at a temporal frequency of 15 Hz as this frequency has been shown to be sensitive to age related changes (Wright & Drasdo, 1985). The mean luminance of the flickering stimulus remained constant and equal to that of the uniform background. When flicker detection was absent, the participants were unaware of anything presented in the visual field. Each staircase employed 10 reversals using a two-down, one-up procedure which reduces change probability to 1/25 (Levine & Shefner, 1991). The step changes in the staircase procedure was moderated with the number of steps in accordance with an exponential function. The starting value was also variable and adjusted appropriately to reflect the loss of flicker sensitivity at lower luminances.

Participants were given a short practice session and then were tested at background luminances of: 0.6, 1.87, 3.75, 7.5 and 60 cd/m^2. The display subtended a visual angle of 15.5^o horizontally and 12.5^o vertically. A spectrally calibrated neutral density filter

was used to produce the lowest background luminance to ensure accurate reproduction of flicker modulation on the display. For each light level participants viewed the screen binocularly, followed by monocular presentations (RE or LE was alternated between participants). This provided comfortable, naturalistic viewing conditions at the start of each light level and reduced initial learning effects on the monocular conditions for this part of the study without introducing significant order effects (Grimson et al., 2002). The non-tested eye was covered with an opaque, infrared transmitting filter allowing iris illumination and pupil size measurements. Participants were tested on the lowest screen luminance first, after verification that they could clearly see the fixation stimulus, followed by the next, higher screen luminance meaning that less time was required for adaptation between luminance levels than using a randomized procedure in order to reduce participant fatigue. Since detection of rapid flicker relies mostly on M and L cone signals, the initial adaptation time was initially limited to five minutes before the first test commenced, and three minutes adaptation time was allowed for each subsequent, higher luminance.

3.5.3. Pupil measurements and retinal illuminance

Pupil diameter was measured continuously during the Flicker-*Plus* tests. An infrared light source was mounted below the camera to provide illumination of the eye. The pupil of the left eye was measured using the P_SCAN system (Alexandridis et al., 1991; Barbur & Thomson, 1987) and the pupil images were processed using MATLAB functions (The MathsWorks, Inc., Natick, MA). Thresholding and edge detection techniques were used to locate the pupil boundary, allowing the pupil diameter to be computed with a resolution better than 0.01mm. Pupil measurements were taken approximately 3 times per second. Measurements within one standard deviation of the

mean were averaged to produce a mean pupil size for each luminance and viewing condition.

Retinal Illuminance (E) was calculated in trolands (td) as $E = L \times P$, where L is the screen luminance in cd/m^2 and P is the pupil area in mm^2. Separate estimates of retinal illuminance were obtained for binocular and monocular viewing conditions because of expected differences in pupil size (Boxer Wachler, 2003).

3.5.4. Modulation sensitivity as a function of retinal illuminance

Modulation threshold data for each individual across different retinal illuminances were fitted with the empirical non-linear function, equation (10).

(10) $$T = a \times E^{-b} + c$$

Where T is the modulation threshold, a and b are constants, E is retinal illuminance and c is the asymptote threshold which represents the best performance, normally achieved at a high light level. To improve the stability of the non-linear fitting algorithm a pseudo-point was added at 8000 td which corresponded to 80% of the participant's best thresholds.

3.5.5. Calculating the HR_{index} for flicker sensitivity

The group data provided an average measure of the change in flicker modulation threshold with retinal illuminance. For each participant at each eccentricity, the area under the measured threshold versus retinal illuminance curve (A_p) was calculated between the limits of 900 and 25 td according to equation (11). The HR_{index} represents the difference between the area under the participant's threshold curve (A_p) and the corresponding median curve for the group (A_{group}), expressed as a fraction of the median curve (equation 3, repeated for clarity). For each participant, the HR_{index} was

calculated at the fovea and then separately at the parafovea, using a combination of all parafoveal points. This was done simply because no significant difference was found within this normal group between the areas under the curve at the four peripheral locations.

(11) $$\mathrm{A_p} = \int_{25}^{900}(a \times E^{-b} + c)dE = \left[\frac{a}{1-b} \times E^{(1-b)} + cE\right]_{25}^{900}$$

(3) $$\mathrm{HR_{index}} = 1 - \frac{\mathrm{A_p}}{\mathrm{A_{group}}}$$

3.5.6. Identifying participants with significantly elevated thresholds

The aim was to determine the mean and 95% confidence limits of the $\mathrm{HR_{index}}$ for a normal population so three measures were taken to exclude participants with significantly elevated threshold that may not reflect normal aging. Firstly, participants with clinical signs of disease were excluded.

The second filter excluded participants who could not detect flicker in the mesopic range. If a participant could not detect flicker of 100% modulation above 1.6 log td in the high mesopic range they were excluded. This was because they were subsequently unable to provide measurable thresholds below 1.6 log td and therefore their thresholds for the entire mesopic range would be unknown. See section 3.7 for a discussion of any effects this may have on the results and conclusions.

Finally, participants were excluded if they exhibited significant differences in modulation sensitivity between the two eyes at corresponding loci using the Tukey method. The justification for the introduction of this filter is based on empirical observations which suggest that in most cases, early stage retinal diseases tend to

affect the eyes differently. The formula described in equation (12) was used to identify participants with substantial interocular differences (IODs) in modulation sensitivity:

(12) $$IOD = \frac{|A_{LE} - A_{RE}|}{A_{Best\ eye}}$$

Where A_{LE} is the area under the curve for the particular eccentricity for the left eye and A_{RE} is the area under the curve for the corresponding eccentricity in the right eye. If a participant was excluded on this basis, all of his/her results were excluded.

3.5.7. Calculating binocular summation ratio (BSR) and Interocular Percentage Increase (IPI)

Using each participant's fitted curves, BSRs were calculated according to the formula in equation (8), for foveal and peripheral stimuli at 1 td increments between 25 and 900 td, providing a BSR at each retinal illuminance. BSR values were averaged over retinal illuminance to produce one value for BSR at each eccentricity for each participant.

(8) $$BSR = \frac{Best\ eye\ threshold}{Binocular\ threshold}$$

The best eye was determined as the eye with lowest thresholds. IPI was calculated to investigate its influence on binocular summation, as the absolute difference in the thresholds between the eyes as a ratio of the best eye threshold, where T_{LE} is the average left eye threshold, and T_{RE} is the corresponding right eye threshold (equation (9). This was also calculated at 1 td increments between 25 and 900 td, and was averaged over retinal illuminance to produce one value for IPI at each eccentricity for each participant.

(9) $$IPI = \frac{|T_{LE} - T_{RE}|}{Best\ eye\ threshold}$$

3.5.8. Statistical analysis

Customized software was used to fit the nonlinear function describing the variation of modulation thresholds with retinal illuminance, compute the 95% limits of value distributions and some statistical analysis (MATLAB, The MathsWorks, Inc., Natick, MA). SPSS (IBM SPSS for Windows, Version 21.0, Armonk, NY) was used for statistical analysis on repeated measures ANCOVAs for the analysis of changes in BSR and IPI with age as a covariate and eccentricity an independent variable. Averaged data from two eyes was used for curve fitting and statistical analysis because there was no significant differences between the eyes ($F(1,87)=0.862$, $p=0.356$), variance between the eyes was similar because people with significant interocular differences were excluded, and the intra class correlation was close to one ($ICC(3,k)= 0.961$) based on Armstrong (2013). Therefore, in statistical analysis, each participant contributed one data point only for each condition, obtained by averaging results across eyes and eccentricities.

3.6. Results

3.6.1. Included and excluded participants

102 participants were recruited to the study (aged 20-75 years). In total, 22 (21.6%) were excluded from the analysis: 13 (12.7%) presented with ocular conditions, 7 (6.9%) participants had significant interocular differences in the area under the curve detected by the Tukey Method and 2 (2.0%) could not achieve thresholds below 100% modulation at light levels above 1.6 log td. The HR_{index} was calculated based on the thresholds obtained for the remaining 80 participants (mean age = 46.0, SD = 17.0 years). **Figure 35** shows the age distribution of all 80 participants included in the study and **Table 3** shows the visual acuity and refraction for participants.

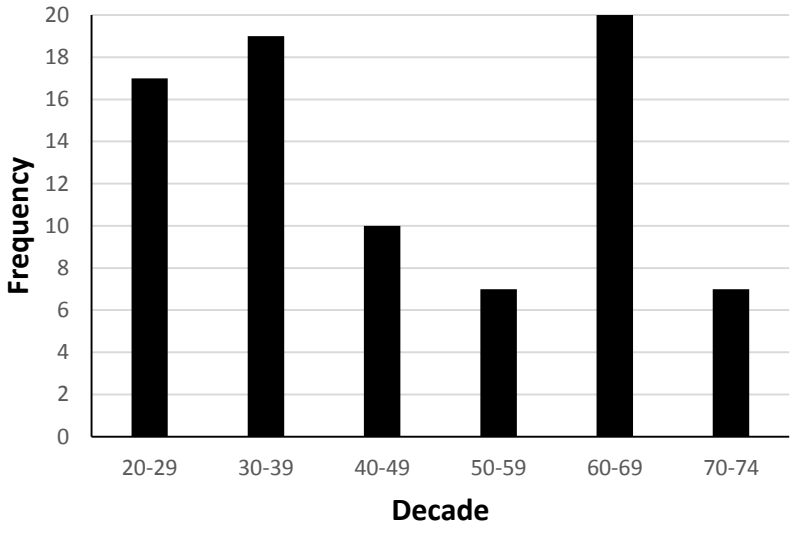

Figure 35. Age distribution of 80 participants in the study.

Table 3. Description of visual acuity (logMAR) and refraction of participants in decade bins.

			Range		Mean refractive error used			Mean subjective refraction		
Age bin	Data available for	Mean VA	Min VA	Max VA	SPH	Cyl	Axis	SPH	Cyl	Axis
20-29	9	-0.05	-0.12	0.00	-1.34	-0.13	22.50	-0.13	0.00	0.00
30-39	15	-0.09	-0.21	0.06	-0.92	-0.89	77.20	-1.40	-0.22	29.38
40-49	8	-0.13	-0.20	0.05	-2.32	-0.43	92.79	-2.30	-0.48	60.80
50-59	7	-0.02	-0.10	0.03	-0.95	-0.74	77.00	1.17	-0.31	58.33
60-69	17	-0.01	-0.15	0.09	-1.00	-0.63	63.25	-0.78	-0.75	68.06
70-74	7	0.06	0.00	0.20	-0.56	-0.46	66.67	-0.08	-0.48	60.50

3.6.2. HR_{index} for monocular flicker thresholds

Figure 36 shows flicker detection thresholds as a function of retinal illuminance at the fovea and parafovea using flicker thresholds, and log flicker thresholds in **Figure 37.** The foveal graph shows data for both eyes and similarly, results for all parafoveal eccentricities for each eye were plotted together because there were no significant differences between the eyes (see section 3.5.8). An unanticipated proportion of participants could not detect 100% modulation flicker, and it was reasoned that if participants could not do so above 1.6 log trolands they would be excluded on the basis that they could not detect maximum modulation flicker in photopic conditions.

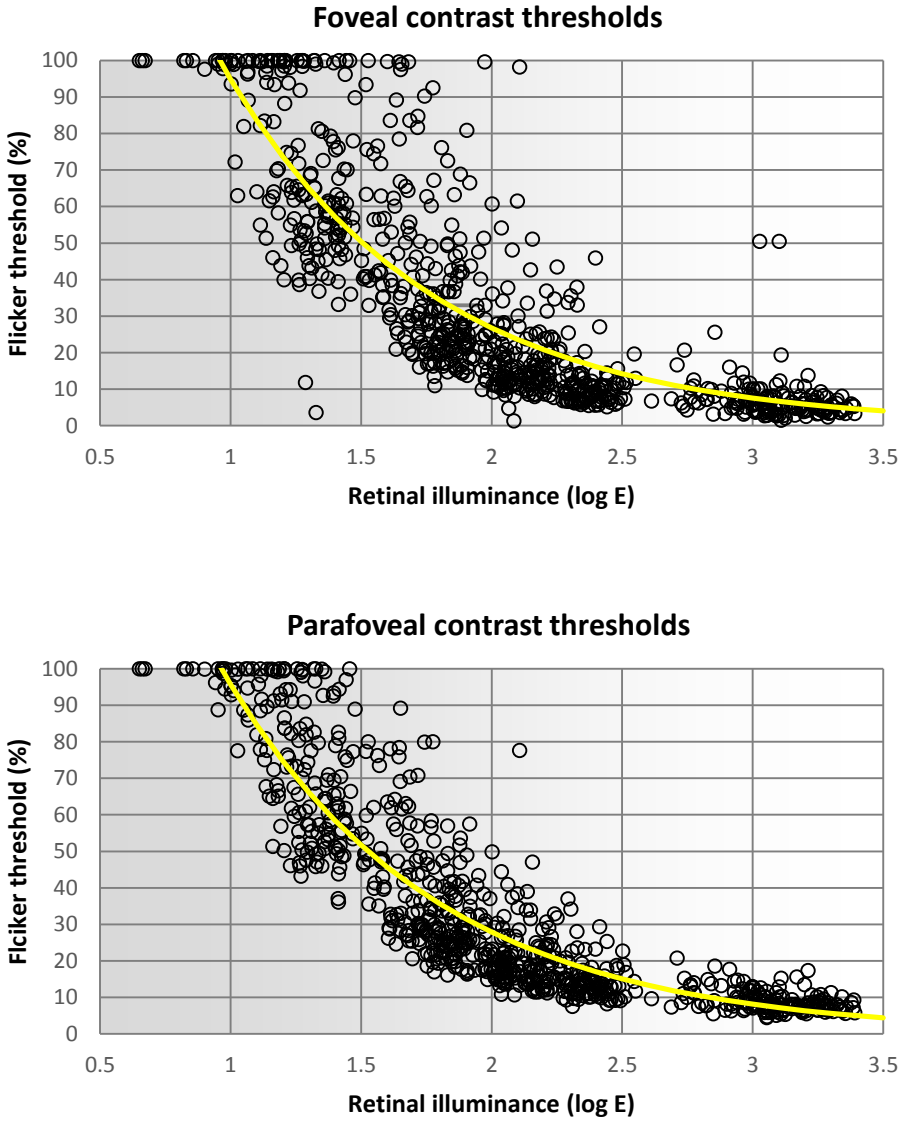

Figure 36. Flicker thresholds with retinal illuminance for included participants. For the foveal data each participant contributes two points for each screen luminance, one from each eye. For the parafoveal data, each participant contributes eight points for each luminance level, from each eye. Fit to foveal data: flicker threshold = $336*E^{-0.5492} + 1.108E-06$. Fit to parafoveal data: flicker threshold = $328*E^{-0.5351} + 5.696E-06$.

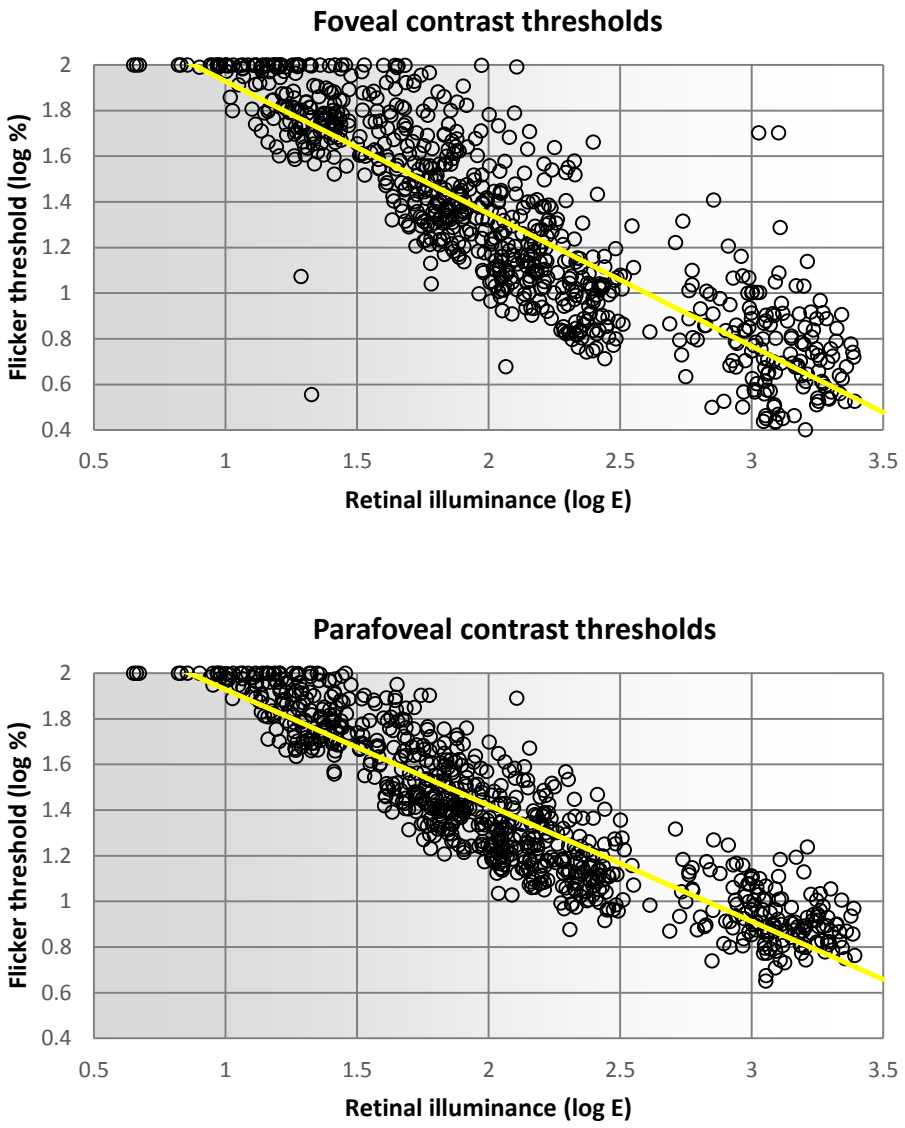

Figure 37. Log flicker thresholds with retinal illuminance for included participants. For the foveal data each participant contributes two points for each screen luminance, one from each eye. For the parafoveal data, each participant contributes eight points for each luminance level, from each eye. Fit to foveal data: flicker threshold = -0.5896*log E +2.5095. Fit to parafoveal data: flicker threshold = -0.4997*log E + 2.4137.

A $\mathbf{HR_{index}\ (fovea) = \left(-0.0006 \times Age^2\right) + \left(0.033 \times Age\right) - 0.1107}$

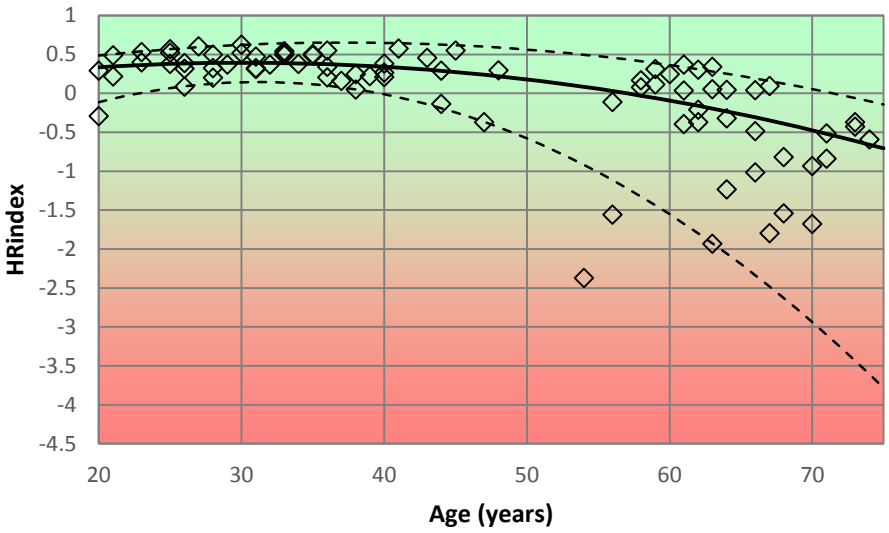

B $\mathbf{HR_{index}\ (parafovea) = \left(-0.0005 \times Age^2\right) + \left(0.031 \times Age\right) - 0.2369}$

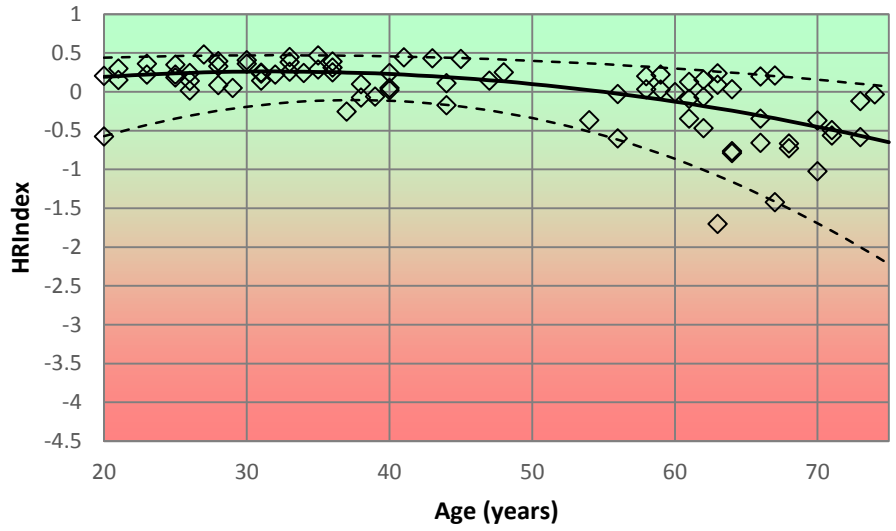

Figure 38. HR_{index} as a function of age, fitted with a 2nd order polynomial quantile regression. Black lines show 50th percentile (i.e. HR_{index}), and dashed lines the 5th and 95th percentile. Equation for the HR_{index}, indicated by the 50th percentile, is shown above each graph. **A** HR_{index} values for the fovea. $\text{5th percentile (fovea)} = (-0.0002 \times \text{Age}^2) + (0.128 \times \text{Age}) - 1.8511.$ $\text{95th percentile (fovea)} = (-0.0006 \times \text{Age}^2) + (0.042 \times \text{Age}) - 0.1266.$ **B** HR_{index} values for the parafovea. $\text{5th percentile (parafovea)} = (-0.0015 \times \text{Age}^2) + (0.113 \times \text{Age}) - 2.2384.$ $\text{95th percentile (parafovea)} = (-0.0002 \times \text{Age}^2) + (0.014 \times \text{Age}) + 0.2439.$

Figure 38 shows how the HR_{index} changes with age at the fovea and at the peripheral locations. The data show the 50th percentile (median) of the thresholds measured in the two eyes. In the case of peripheral thresholds, each data point shows the average of the 8 HR_{index} measurements taken in both eyes. The observed variability increased with age, at both the fovea (Levene's statistic = 7.349, $p < 0.001$) and parafovea (Levene's statistic = 8.460, $p < 0.001$). In order to fit the changing variability, a 2nd order polynomial quantile regression was performed (Koenker, 2006), with the 50th percentile forming the fit to the HR_{index} data with age, and the 5th and 95th percentiles forming the limits of normal performance around the fit. The HR_{index} changes in a similar way at the fovea and parafovea with age, however the limits of normal performance are wider at the fovea. This suggests that normal older people have greater variability in foveal rather than parafoveal performance. **Figure 39** and **Figure 40** show examples of normal data from a younger and older participant and their corresponding HR_{index} values.

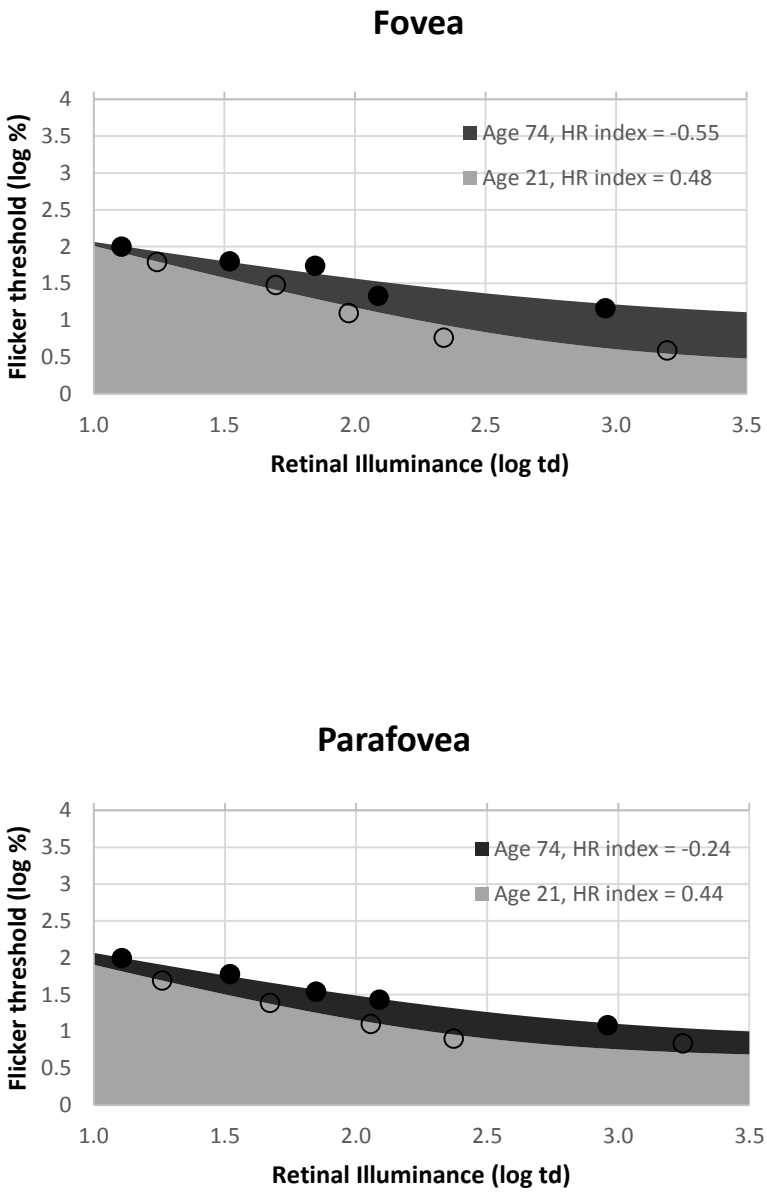

Figure 39. Examples of log modulation thresholds and the corresponding HR_{index} values for two normal participants, aged 21 and 74. The 21 year old has a smaller area than the group curve in both the fovea and the parafovea, resulting in a positive HR_{index}, whereas the 74 year old has a larger area under the curve at both eccentricities, resulting in a negative HR_{index}.

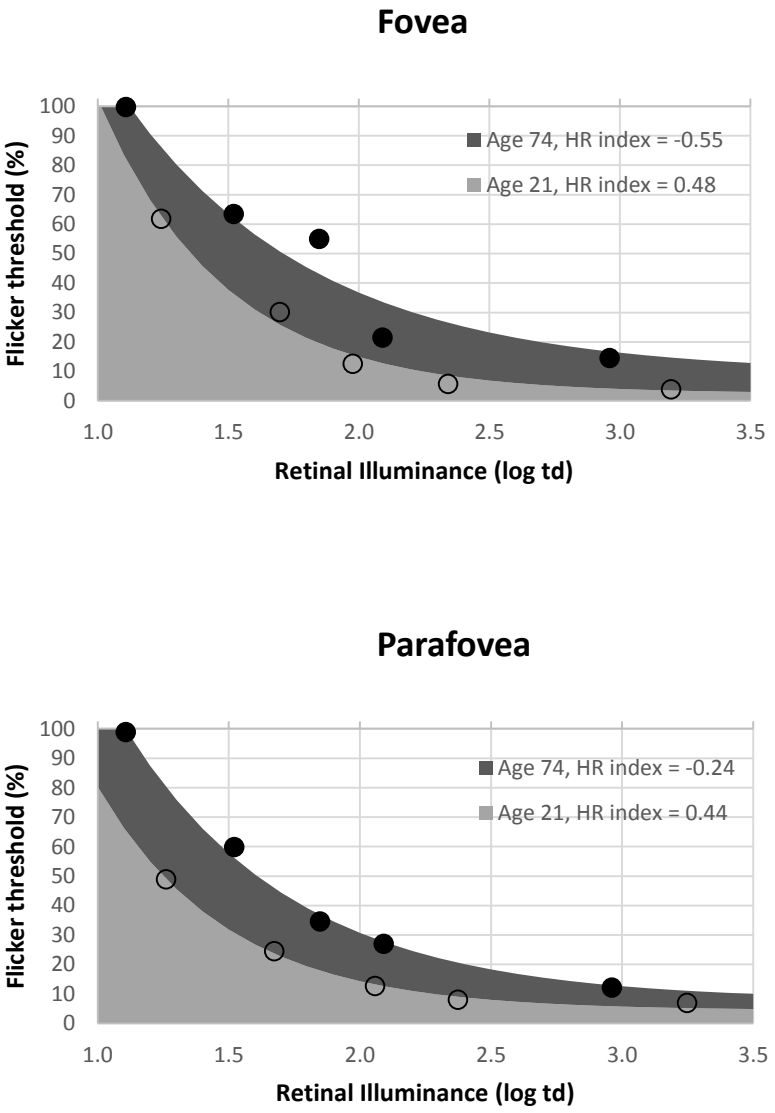

Figure 40. Examples of modulation thresholds and the corresponding HR_{index} values for two normal participants, aged 21 and 74. The 21 year old has a smaller area than the group curve in both the fovea and the parafovea, resulting in a positive HR_{index}, whereas the 74 year old has a larger area under the curve at both eccentricities, resulting in a negative HR_{index}.

Figure 41 shows how modulation thresholds change at the fovea and parafovea for five retinal illuminance levels as a function of age. Points were derived from curves fitted to each individual's data and averaged across eyes at the fovea and eccentricities and eyes at the parafovea. As light level declines, there is a steeper increase in modulation threshold with age, evident at both the fovea and parafovea to similar extents.

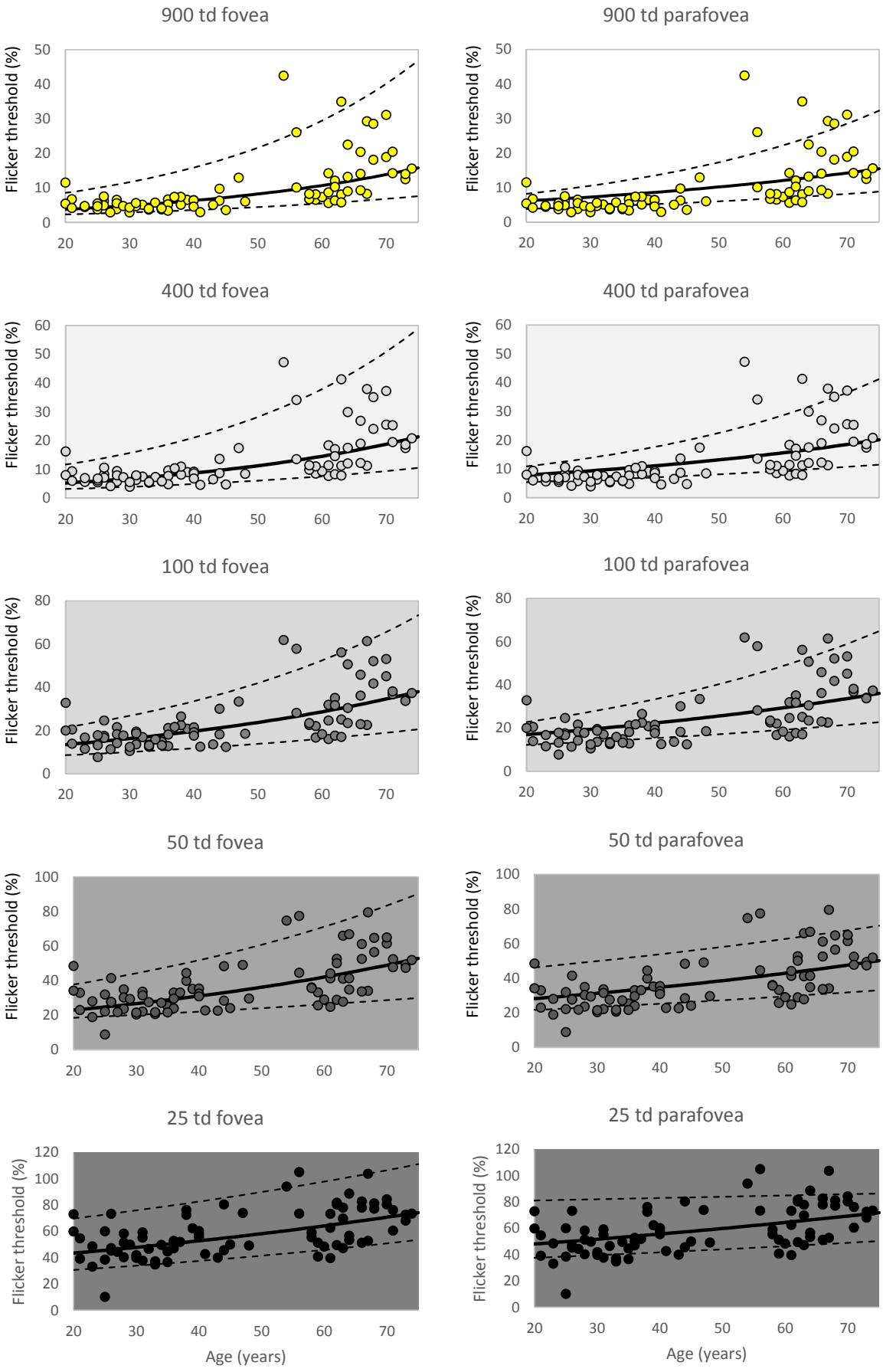
900 td fovea
900 td parafovea
400 td fovea
400 td parafovea
100 td fovea
100 td parafovea
50 td fovea
50 td parafovea
25 td fovea
25 td parafovea
Flicker threshold (%)
Age (years)

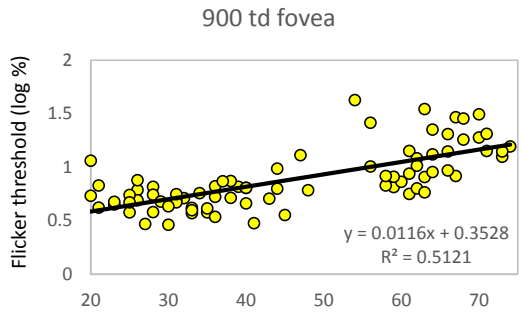
900 td fovea
Flicker threshold (log %)
y = 0.0116x + 0.3528
R² = 0.5121

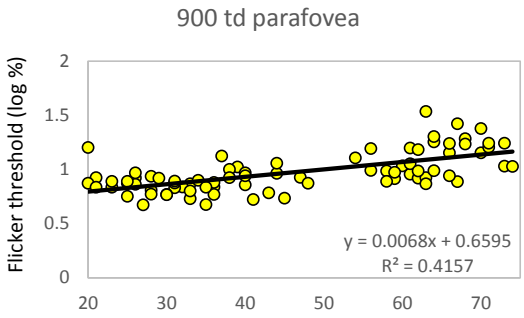
900 td parafovea
Flicker threshold (log %)
y = 0.0068x + 0.6595
R² = 0.4157

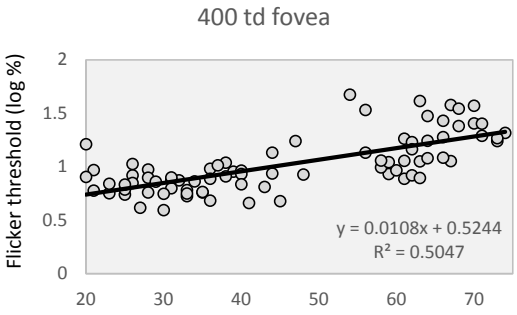
400 td fovea
Flicker threshold (log %)
y = 0.0108x + 0.5244
R² = 0.5047

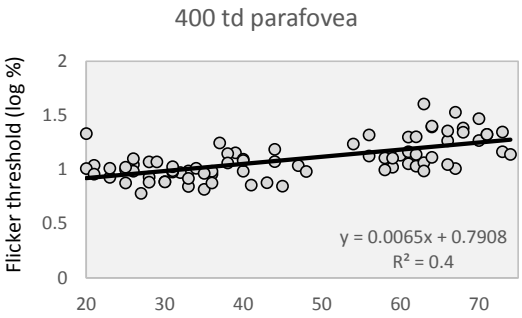
400 td parafovea
Flicker threshold (log %)
y = 0.0065x + 0.7908
R² = 0.4

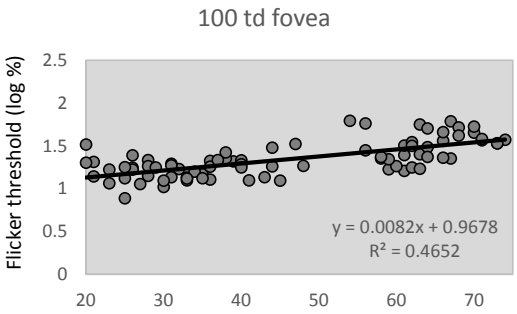
100 td fovea
Flicker threshold (log %)
y = 0.0082x + 0.9678
R² = 0.4652

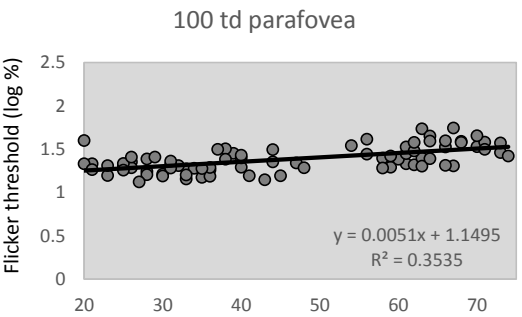
100 td parafovea
Flicker threshold (log %)
y = 0.0051x + 1.1495
R² = 0.3535

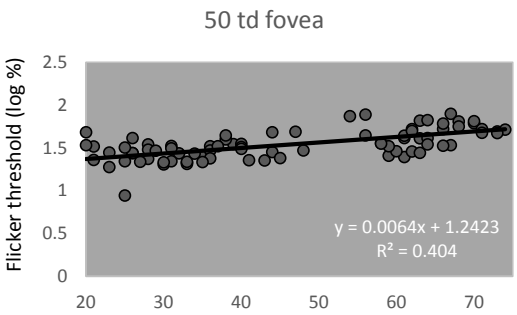
50 td fovea
Flicker threshold (log %)
y = 0.0064x + 1.2423
R² = 0.404

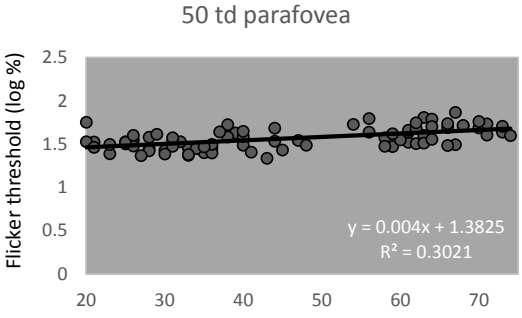
50 td parafovea
Flicker threshold (log %)
y = 0.004x + 1.3825
R² = 0.3021

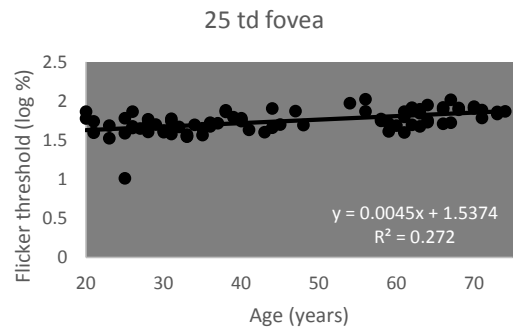
25 td fovea
Flicker threshold (log %)
y = 0.0045x + 1.5374
R² = 0.272
Age (years)

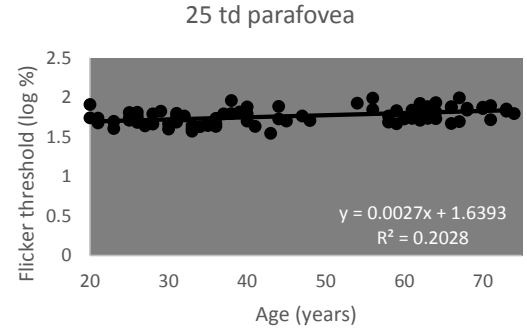
25 td parafovea
Flicker threshold (log %)
y = 0.0027x + 1.6393
R² = 0.2028
Age (years)

Figure 41. Foveal and parafoveal contrast thresholds at 900, 400, 100, 50 and 25 td. First page shows contrast thresholds on a linear scale. 2nd order quantile fits are shown, with the solid line representing the 50th percentile, and dashed lines representing the 5th and 95th percentile. The second page shows contrast thresholds on a log scale. Points were derived from curves fitted to each individual's data and averaged across eyes at the fovea and eccentricities and eyes at the parafovea.

3.6.3. Comparison of HR_{index} for contrast and flicker

Values for HR_{index} for contrast and flicker thresholds were available for a subset of participants (n=32; 13 participants aged 20-34, 9 participants aged 35-60 and 10 participants aged 60-75). Contrast and flicker HR_{index} values were compared, averaged across eccentricities. A one-sample t-test of the differences between the scores indicated that they were significantly different from zero ($t(31)=2.894$, $p<0.01$). A Bland-Altman plot of the differences between the two measures and mean of the HR_{index} (**Figure 42)** shows that although there are similar numbers of points above and below the mean, for low mean values of the HR_{index}, there are larger differences. This conclusion follows directly from the different fits to the HR_{index} data for contrast (a slow linear age decline) and for flicker data (a rapid decline after 50 years). Therefore if someone has a lower mean HR_{index}, indicating they are older, the difference between the two measures will be larger. To clearly demonstrate this, we can consider the top leftmost point; the participant aged 61, has a contrast HR_{index} of -0.04, and a flicker HR_{index} of -1.82. The mean HR_{index} value is low at -0.93, and the difference is large at 1.78. Given the current results, different trends of the contrast and flicker HR_{index} values with age and previous literature (Kim & Mayer, 1994; Spry & Johnson, 2001), we suggest that contrast and flicker tests are tapping into and reflect the performance of different visual mechanisms which may age independently and at different rates.

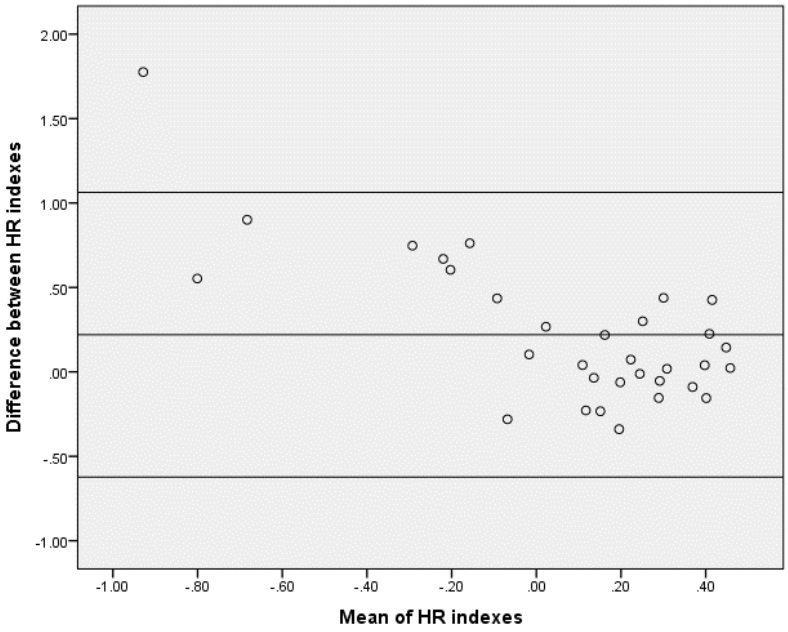

Figure 42. Bland-Altman plot of the mean of contrast and flicker HR_{index} index values and difference between these values. The middle line shows the mean difference value of 0.22. The other lines indicate the limits of agreement at difference values of 1.06 and -0.62.

3.6.4. Binocular flicker thresholds and summation

Figure 43 depicts the thresholds for participants but re-represented as the worst eye, best eye, and results from binocular viewing for foveal and parafoveal thresholds. The best fitting non-linear model is shown for each condition using equation (10).

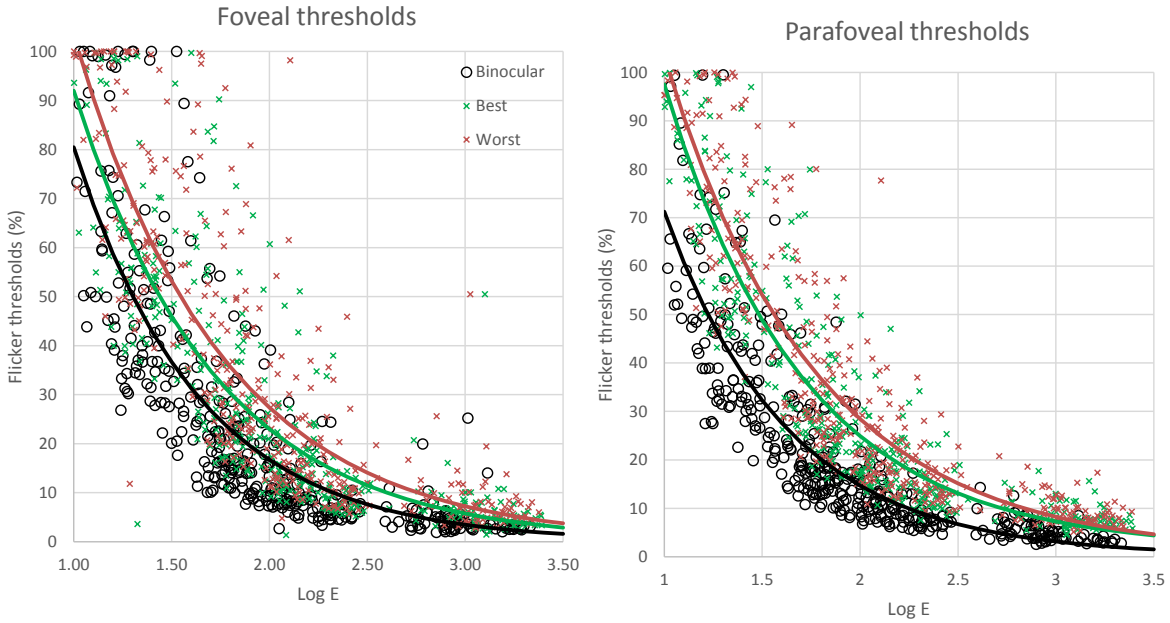

Figure 43. Modulation thresholds as a function of retinal illuminance for all participants for the worst eye, best eye, and binocular viewing. For foveal modulation thresholds, each participant contributes five points for each of the three curves as a result of measuring modulation thresholds at five light levels for each of the viewing conditions (viewed by worst eye, best eye and viewed binocularly). The fits to the group data are the following, where E is retinal illuminance: Worst eye foveal threshold = 390.3 * $E^{-0.5772}$ + 2.479E-05; Best eye foveal threshold = 368.5 * $E^{-0.6027}$ + 3.116E-05; Binocular foveal threshold = 387.8 * $E^{-0.683}$ + 6.533E-07. For parafoveal modulation thresholds, data points represent the average of four eccentricities as a result of four different parafoveal locations tested in each eye. The fits to the group data are the following: Worst eye parafoveal threshold = 390.1 * $E^{-0.5685}$ + 0.735; Best eye parafoveal threshold = 394.8 * $E^{-0.6144}$ + 1.604; Binocular parafoveal threshold = 347.5 * $E^{-0.689}$ + 0.1555.

Figure 44 A shows binocular summation of flicker thresholds as a function of age at the fovea and parafovea, and only one participant showed binocular inhibition (a BSR of under 1), who was aged 41. A repeated measures ANCOVA was conducted on BSR with age as a covariate and eccentricity as an independent variable. It was shown that BSR did not change with age ($F(1,78)=0.086$, $p=0.770$), and that the gradient of the function of BSR with age did not differ between the two eccentricities ($F(1,78)=0.473$, $p=0.494$). Overall, BSR was significantly higher at the parafovea ($M=1.82$, $SD=0.43$) compared to the fovea ($M=1.66$, $SD=0.43$; $F(1,79)=10.363$, $p<0.01$).

IPI was investigated to determine whether it could explain the lack of change in BSR with age. The results are shown in **Figure 44 B**. A repeated measures ANCOVA on IPI with age as a covariate and eccentricity as an independent variable found the IPI did not significantly increase with age ($F(1,78)=1.588$, $p=0.211$, and that IPI did not differ with eccentricity ($F(1,79)=1.200$, $p=0.277$). **Figure 44 C** shows that there is little relationship between the BSR and IPI for flicker.

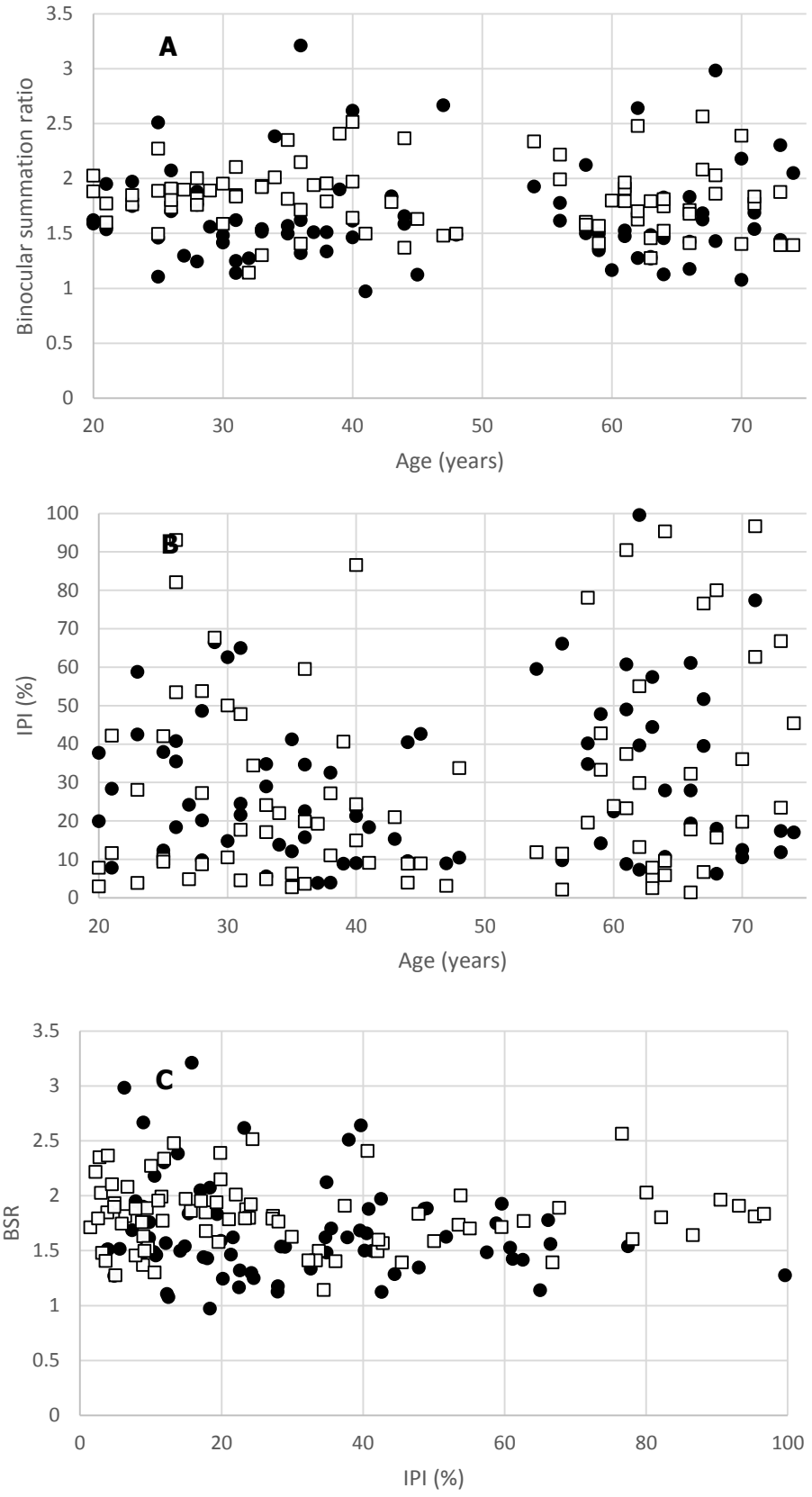

Figure 44. Data are shown for participants at the fovea (solid circles) and parafovea (unfilled squares) **A** BSR does not change substantially with age at the fovea or parafovea, and **B** shows that IPI does not change systematically with age either. Furthermore, **C** shows that there is no substantive relationship between BSR and IPI.

3.7. Discussion

3.7.1. Flicker sensitivity declines non-linearly with age

This study shows that rapid flicker sensitivity declines with age, in agreement with findings from other similar studies (Casson et al., 1993; Elliott et al., 1990; Kim & Mayer, 1994; Mayer et al., 1988; Royer & Gilmore, 1985; Tyler, 1989; Wright & Drasdo, 1985), and demonstrates that the decline in flicker sensitivity with age is greater at lower levels of retinal illuminance. The new approach developed here employs a number of filters designed to screen for normal aging by eliminating participants with large flicker thresholds that could be attributed to other factors. In addition, we minimize the effects of inter-subject variation in the absorption of short wavelength light by the lens and the macular pigment and produce individual measures of retinal illuminance to account for differences in pupil size. The participant's sensitivity to rapid flicker at the fovea and in the periphery and the way this changes with light level is captured by a single number, the HR_{index}.

This study supports the previously reported finding that the rate of the decline in rapid flicker sensitivity is nonlinear (**Figure 38**); the overall sensitivity as determined by the HR_{index} is relatively stable until approximately 50 years of age and subsequently the rate of decline increases with increasing age, similar to previous findings of rapid declines in flicker thresholds with age as percent modulation depth (Haegerstrom-Portnoy et al., 1999), and after 50 years when changes in retinal illuminance were accounted for (Kim & Mayer, 1994). Furthermore we have noted that over the age of 50 years the loss of flicker sensitivity prevents some subjects from detecting the 100% modulation flicker at photopic light levels and the distribution of HR_{index} values becomes increasingly asymmetric (**Figure 38**). Although participants were screened to be clinically normal, a future longitudinal

study would be needed to determine whether the participants with elevated photopic thresholds and those who are outside the HR_{index} limits were demonstrating pre-clinical retinal changes which cannot be detected by standard ophthalmological tests. This would allow further refinement of the normal limits, or if retinal disease did not manifest would demonstrate that the normal limits are reliable.

The current study demonstrates that the trend of non-linear age dependence remains for mesopic and photopic conditions (**Figure 41**) but appears to become increasingly linear at low retinal illuminances. **Figure 41** provides the limits of normal performance at a range of retinal light levels for direct clinical application. These results are somewhat different to the more linear declines for the aging of colour and contrast vision (Barbur & Konstantakopoulou, 2012; Gillespie-Gallery, Konstantakopoulou, Harlow, & Barbur, 2013), suggesting that different retinal or higher level mechanisms are involved in the processing of the two stimulus attributes and that this processing is affected differently in aging.

Interestingly, the rate of decline in modulation thresholds in normal aging is similar at the fovea and parafovea (**Figure 38**). When regional differences occur in flicker sensitivity across the retina, it can be indicative of disease progression, for example reduced sensitivity at a particular retinal location can occur prior to the onset of geographic atrophy at that same area (Luu et al., 2012). In the current study, variability between observers increased with age at both retinal locations and this finding is expected as older eyes have greater variability in the numbers of photoreceptors and retinal ganglion cells (Gao & Hollyfield, 1992), but performance was particularly variable for foveal thresholds.

Because the fovea and parafovea did not differ in the rate of decline over photopic and mesopic light levels, this could suggest that rapid flicker sensitivity as measured in this study reflects detection by mostly L and M cone signals and is not adversely affected by age related loss of rod photoreceptors (Curcio et al., 1993), unlike age-related changes in spatial vision (Gillespie-Gallery et al., 2013). Therefore, normal aging of flicker sensitivity should occur similarly at foveal and parafoveal eccentricities and light levels, and any regional differences could be indicative of early stage retinal disease.

Other studies have found a greater decline in modulation sensitivity outside the fovea when using a fixed stimulus size (Casson et al., 1993; Spry & Johnson, 2001; Zele et al., 2008), in contrast to our findings indicating that the loss of temporal sensitivity declines at similar rates in both the fovea and parafovea when the stimulus size was scaled for loss of spatial sensitivity. Since peripheral flicker thresholds depend strongly on stimulus size, it remains to be shown how stimulus size for peripheral measurements also affects the rate of decline with age and the dependence of flicker thresholds on retinal illuminance. Our results suggest that the loss of rapid flicker sensitivity with age is not due to a loss of rod photoreceptors, as these decline at different rates at the eccentricities investigated, but may be instead due to the well documented changes in retinal ganglion cells with increasing age (Curcio & Drucker, 1993; Gao & Hollyfield, 1992; Harman et al., 2000; Tyler, 1985). This loss of sensitivity could be attributed, at least in part, to a loss of ganglion cell axons in the optic nerve (Calkins, 2013; Jonas et al., 1992; Mikelberg et al., 1989).

3.7.2. Binocular summation of flicker

The temporally modulated stimuli used in this study were composed of MW and LW light, which are relatively unaffected by age-related increases in the optical density

of the lens. This means that the effect of aging can be attributed largely to retinal and/or more central visual systems (Kim & Mayer, 1994; Lachenmayr et al., 1994; Mayer et al., 1988; Tyler, 1989; Wright & Drasdo, 1985). The analysis calculated retinal illuminance separately under monocular and binocular conditions, which is important as pupil sizes vary between these conditions (Boxer Wachler, 2003).

Our findings suggest that binocular summation was stable with age. This result is of great interest since the stability of binocular summation for temporally modulated stimuli as a function of age is in stark contrast to the measured monocular thresholds which increase with age and is in contrast to previous findings for spatial stimuli which found that BSR does decline with age (Gagnon & Kline, 2003; Gillespie-Gallery et al., 2013; Pardhan, 1996; Pardhan, 1997). Furthermore, only one participant exhibited binocular inhibition for flickering stimuli, compared to the previously reported 13 out of 74 for stimuli defined by spatial contrast (section 2.5.3). To determine whether stable interocular differences with age could explain why BSR does not change with age, the IPI was determined for each participant and interestingly it did not change, thus IPI and BSR show similar age independence. Therefore, BSR may not decline with age because interocular differences are stable with age, however, BSR of contrast vision declined despite stable interocular differences. Therefore interocular differences could be only a partial explanation for the decline in binocular summation.

Interestingly, the level of binocular summation was generally higher for foveal than parafoveal stimuli. When stimulus size is scaled with increasing eccentricity to stimulate similar numbers of cones, the fovea has the greatest modulation sensitivity to high frequency flicker, which drops off very gradually with increasing eccentricity (Tyler, 1987). Therefore, slight differences in modulation sensitivity may

be due to differences in ganglion cell density between these locations (Tyler, 1987). Furthermore, the ganglion cell magnification factor at the retina is comparable to that at V1 (Perry & Cowey, 1985; Wässle, Grünert, Röhrenbeck, & Boycott, 1990) where binocular summation is first observed (Hubel & Wiesel, 1962). Therefore, we suggest that both better foveal monocular thresholds and foveal BSRs are a result of neural magnification of similar factors at the retina and central visual system respectively. To test this hypothesis with greater precision, BSR would need to be measured across the visual field.

3.8. Conclusions

Normal aging reveals relatively stable rapid flicker thresholds in central vision and this extends up to just under 50 years of age. Retinal illuminance affects sensitivity to rapid flicker at any age, and when the effect of retinal illuminance is accounted for, there is overall a more rapid decline in rapid flicker sensitivity above 50 years of age. Nevertheless, older subjects will, in general, have decreased retinal illuminance, often caused by pupil miosis and absorption of light by the increasing optical density of the lens. Rapid flicker sensitivity declines at a similar rate with increasing age, both at the fovea and the parafovea. One may therefore be able to describe the health of the retina in relation to flicker sensitivity by a single number, the HR_{index}, which captures the subject's sensitivity to flicker and its dependence on retinal illuminance. This index may turn out to be clinically important when assessing patients with glaucoma, diabetes and hypertension. Preliminary results suggest that in addition to the overall decrease in rapid flicker sensitivity in such patients, the loss is greater at lower light levels (Dowse, 2012). Although by no means definitive, the findings from this study suggest that the loss of flicker sensitivity with increased age is more likely to reflect the decrease in retinal

ganglion cell density or loss of axons, rather than the loss of photoreceptors, whereas changes in spatial vision with age and light level as reflected in functional contrast sensitivity tests are more likely to reflect the normal age-related changes in photoreceptors (Gillespie-Gallery et al., 2013).

Despite flicker thresholds declining with age the binocular summation of monocular inputs is preserved and remarkably stable, along with interocular differences. Furthermore, few people experience binocular inhibition of temporally modulated stimuli. It is of interest to determine the mechanisms which cause spatial, but not temporal binocular summation to decline with age, and if age related changes in visual processes that utilize both spatial and temporal signals, such as motion perception (Billino, Bremmer, & Gegenfurtner, 2008; Bogfjellmo, Bex, & Falkenberg, 2013; Habak & Faubert, 2000), are limited mostly by the age-related changes in the properties of spatial rather than temporal mechanisms.

4. The effect of scotopic/photopic ratio on visual acuity

This experiment examines how changes in the spectral content of the illuminant affects visual acuity in the mesopic range. The aim was to optimise visual acuity using different SPDs of light at given levels of surface illumination. Illuminating a surface rather than using a self-luminous monitor was chosen so that the experiment was more applicable to real-life situations such as pedestrian street lighting. Therefore a review of literature on street lighting, rod-cone interactions and visual performance as they relate to spatial vision is provided.

Visual acuity is the limit of the eye to resolve spatial detail. There are many factors that will affect spatial acuity, including aberrations and photoreceptor density (Smith, 1997) and, furthermore, illumination and location of the retina at which visual acuity is being assessed. Objects are imaged on the retina as a point spread function (PSF) as a result of distortions caused by the optics of the eye. The PSF means that when a point of light is imaged on the retina, the relative intensity of the point is distributed over the retina. Raleigh's Criterion states that if two objects are separated by the width of their point spread function then they can be resolved, but not if any closer. Cone spacing in central vision is another limiting criterion (Green, 1970), and a grating can be resolved if there is a row of unstimulated cones between a row of stimulated cones (Helmholtz, 1867, cited in Kalloniatis & Luu, 1995), a basic principle that can be applied to more complex stimuli. Using laser-generated interference patterns to bypass the optics of the eye to create sinusoidal gratings on the retina, Campbell and Green (1965a) found that up to 60 c/deg could be resolved, which is supported by cone spacing in the fovea being

approximately 2.5 μm (28 seconds of arc; Curcio et al., 1990). The acuity of the rod system cannot be determined by spacing alone due to the fact that their inputs are summed over a wide area. Of course, the optics of the eye limits acuity to below 60 c/deg as already discussed. Furthermore, acuity is limited by retinal illuminance, presentation time of the stimulus, area of the retina stimulated and eye movements (Kalloniatis & Luu, 1995).

Mesopic visual performance is difficult to quantify and predict for a number of reasons. Some of these include rod-cone interactions, mixed photoreceptor sensitivities, different rod and cone distributions with eccentricity as well as the different spectral, spatial and temporal properties of the rod and cone systems (Stockman & Sharpe, 2006). Several attempts have been made to model the mesopic luminance efficiency function using a weighted combination of the photopic and scotopic luminance efficiency functions, for example by using a non-linear formula relating V'(λ) and V_{10}(λ) (Palmer, 1968), considering the contributions of the three cone classes and rods (He, Bierman & Rea, 1998) or by utilising brightness rather than luminance functions (He et al., 1998; Ikeda & Shimozono, 1981). Stockman and Sharpe (2006) created a number of functions using a linear combination of V(λ) and V'(λ) with different phase delays in a flickering signal from 0 to 180° in 45° steps. A cancellation effect occurs when sensitivity of V(λ) and V'(λ) are equal and changes if mesopic sensitivity results from changes in the relative rod-cone sensitivities.

4.1. Night illumination for drivers and pedestrians

In the UK road lighting requirements are specified by the BS 13201-2:2003 and BS 5489-1:2003 lighting standards. These require residential streets to be illuminated with the S-series of lights. The level of pavement illuminance varies from country to

country; it is 2-15 lux in the UK, whereas it is 3-5 lux in Japan and Austria. The choice of light level has been suggested to be based on convention and politics rather than visual needs (Fotios, 2014).

Driving accidents occur more at night than day time; During 2012, 82% of fatal road accidents occurred between 22:00 and 06:00 (Keep & Rutherford, 2013). Poor vision could be a contributing factor, however alcohol and fatigue also likely to make a significant contribution in many cases. In support of the contribution of degraded vision, a number of studies have shown that drivers do not change their driving behaviour in low light level conditions, for example they do not tend to drive slower at night. Owens (2003) suggested that drivers do not substantially alter their driving behaviour at night because they retain "ambient" visual functions, utilising full field information from rod mediated peripheral vision, meaning that control of the vehicle's speed and direction is unimpaired. However, "focal" visual abilities are impaired to a much greater extent because of diminished abilities of cone-mediated central vision at low light levels. Thus, because "ambient" abilities are maintained, people are unaware that the quality of their vision has declined and base their behaviour on changes in ambient rather than focal vision, known as the selective degradation hypothesis. These authors also found that tunnel vision (disrupting ambient visual processing) impaired steering abilities but had no effect on acuity, and conversely that blur (disrupting focal visual processing) selectively impaired acuity but not steering. Interestingly, reduced retinal illuminance compromised both acuity and steering, but acuity was much more impaired (Owens & Tyrrell, 1999).

4.2. Rod pathways

4.2.1. Multiple rod pathways in the retina

There are different rod pathways; a fast and spatially accurate pathway and a slow pathway which is sluggish and less spatially accurate (Sharpe & Stockman, 1999). The different pathways are shown in **Figure 45**. The slow pathway is used for single photon events at very low light levels. It utilises ON rod bipolar, amacrine II cells and ON and OFF cone bipolars. In this pathway, rods synapse onto a single type of bipolar cell (ON) which depolarises following stimulation by light. ON bipolars contact amacrine II cells at a sign conserving glutamate synapse (neurotransmitter release results in hyperpolarisation of the post synaptic membrane). The slow pathway interacts with the cone circuitry in two ways; Exciting ON (depolarising) cone bipolar cells through electrical gap junctions and inhibiting OFF (hyperpolarising) cone bipolar cells through glycinergic synapses. Using these different pathways, signal separation is maintained in further circuitry: ON bipolars excite ON ganglion cells and OFF bipolars excite OFF ganglion cells. Therefore rods do not have any independent pathways to the retinal ganglion cells (Buck, 2004).

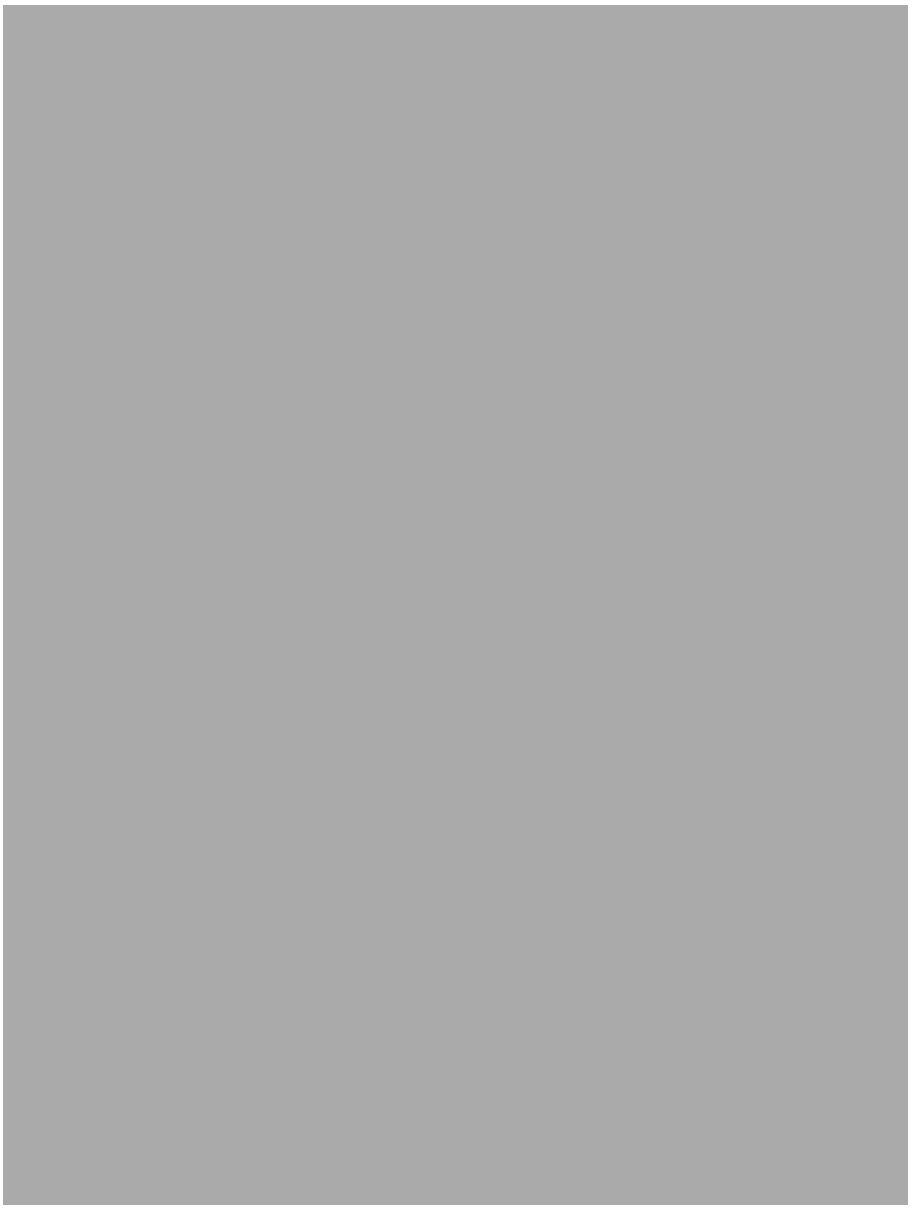

Figure 45. Illustration of the two rod pathways through retinal circuitry (Sharpe & Stockman, 1999).

The fast pathway is used for multiple photon events at higher light levels. It utilises rod-cone gap junctions and ON and OFF cone bipolars. Telodendria projecting from the cone pedicles make gap-junction contacts with rod spherules allowing electrical transmission. 3-5 occur on a single rod spherule, most originating at L- or M-cones. Rods therefore have access to ON and OFF cone bipolars and therefore to ON and OFF ganglion cells. Primate H1 cells (horizontal cells) receive input, possibly from rod-cone gap junctions and H1 dendrites (Verweij, Dacey, Peterson, & Buck, 1999). Interestingly, Ahnelt, Keri and Kolb (1990) found that pedicles of S-cones in humans have no, or very few, telodendria connecting to other cones, but they do contact rods. Significant differences were found between S-cones and other cones (M- and L- cones were not differentiated) in the numbers of contacts via telodendria with rods, with S-cones making fewer contacts with rods per cone. Cluster analysis suggested that L- and M-cones do not have different levels of direct rod contact via telodendria. Furthermore, rod signals can be detected in the vast majority of M- and L- cones, but were not seen in recorded S- cones (Hornstein, Verweij, Li, & Schnapf, 2005). One particularly confusing finding is that increases of rod stimulation in mesopic fields produce changes that are matched well by stimuli that increased M-cone excitation more than L-cone stimulation, suggesting a greater effect of rods on the M than L cone pathway (Cao, Pokorny, & Smith, 2005), but the origin of the "rod green bias" and the differential effect of rods on L- and M-cone pathways is currently unknown (Buck, 2014).

Psychophysical evidence of the two rod pathways have demonstrated that the slow pathway has a peak CFF at 15Hz at low light intensities and the fast pathway has a CFF of 28Hz at higher light levels, in contrast to the cone CFF of around 50 Hz (Blakemore & Rushton, 1965). In normals, as background intensity increases the CFF will disappear at around 15Hz, then reappear at a higher background

luminance (Sharpe et al., 1989). This is a result of destructive interference between the fast and slow rod signals as the slow one is delayed by approximately 33.3ms and at this time the signals are in opposite phase and cancel.

The following properties of rod-cone gap junctions make the fast pathways useful at mesopic levels but not scotopic levels (Buck, 2004; Schneeweis & Schnapf, 1995). Firstly, rod and cone responses combine on the cone or horizontal cell with the same direction of influence and each photoreceptor can adapt independently. Secondly, cones have transient responses whereas the responses from rods contribute in the short term to the initial peak and to prolonged after-responses (OFF responses). Finally, rod responses increase in speed and contribute more to the transient peak at higher light levels.

Rods have been found to differentially feed into three different retinal ganglion cell types; midget ganglion cells (projecting to parvocellular layers), parasol cells (projecting to magnocellular layers) and bistratified cells (projecting to koniocellular layers). There are findings of strong input to parasol cells (Virsu, Lee, & Creutzfeldt, 1987; Virsu & Lee, 1983; Wiesel & Hubel, 1966), however there is less consistent input to midget cells, with only a small proportion having rod input; most M-cone centre cells, whereas few L-cone centre cells showed rod input and when this occurred, the input was weak (Virsu et al., 1987; Virsu & Lee, 1983).

4.2.2. Rod-cone signal interactions at the retina and cortex

Interactions between rods and cones can be additive or inhibitory. For example, Buck and Knight (1994) found for detection, rod signals combine with either M- or L-cones in isolation, to improve detection. Rod and cone generated signals exhibit temporal differences as a result of signals arising from the photoreceptors

themselves as well as the differences between rod and cone post-receptoral pathways (Sharpe & Stockman, 1999; Stockman & Sharpe, 2006). Furthermore, the degree of rod-cone interactions will depend on whether particular rod and cone signals are transmitted to the cortex in parallel or in combined pathways. Summation is often incomplete because of the different temporal profiles/latencies of rods and cones which is why much research into rod-cone interactions has focused on their contribution to temporally modulated stimuli (Sun et al., 2001).

A number of studies have found that as rods dark adapt, they have an increasing effect on cone mediated flicker sensitivity; after approximately 5 minutes of dark adaptation, LW flicker of 25 Hz can be detected at low luminances, but less so after 10 minutes of dark adaptation, suggesting an inhibitory effect of rods (Alexander & Fishman, 1984; Coletta & Adams, 1984). For example, Coletta and Adams (1984) investigated rod-cone interactions in flicker detection (25 Hz) at the fovea and parafovea. Flicker detection of variable sizes of spot (10' arc at the fovea, 40' arc at 4°) were used for wavelengths favouring cones on a 7° background which was varied in luminance. Increasing the background radiance, improved the flicker detection of the test spot, which was attributed to rods as the sensitivity to various wavelengths of the background resembled the rod spectral sensitivity curve. Interestingly, rod interaction may be specific or greater for L cones than M cones, with higher wavelengths of flicker being affected by rods at lower luminances, although they suggest the signals travel through the luminance pathway. This occurred at both the fovea and parafovea supporting the idea that horizontal connections influence cone thresholds at the central fovea, where there are no rods present.

The effect has been called the "suppressive rod-cone interaction" (SRCI), and could be due to inhibitory influences by dark adapted/ing rods, but is reversed by light adaptation (Frumkes & Eysteinsson, 1988). The SRCI effect may be specific to L-cones, because it is absent in protanopes (no normal L-cone pigment) but is present in deuteranopes (lacking normal M cone-pigment; Coletta & Adams, 1985). However more recent studies have found that the CFF mediated by L- or M- cones is equally suppressed by a dark adapted rod surround, but not the CFF of S-cones (Cao et al., 2006; Shapiro, 2002).

The magnitude of interaction is dependent on background size, being greater on smaller backgrounds and smaller on larger backgrounds, but is not confined to small backgrounds (Buck & Makous, 1981). Interactions occur in the fovea from rods in the surrounding 2° (Coletta & Adams, 1984) and the magnitude of the interaction is greatest for test stimuli less than 3°, and this increases with test size and eccentricity (Alexander & Fishman, 1986). This suggests that rods and cones interact via lateral pathways such as amacrine cells.

Rods and cones do not have separate visual pathways to the brain but share pathways using joint inputs to retinal ganglion cells (Schneeweis & Schnapf, 1995). Rods have major input to the magnocellular pathway but less input to the parvocellular pathway (Wiesel & Hubel, 1966) and rod signals in koniocellular pathways have been found in some cases (Field et al., 2009). In support, Sun et al. (2001) found that when cones were mediated by the MC pathway (inferred by a higher temporal frequency, 10Hz) rods and cones (L + rods, or M + rods) showed almost linear summation, being affected by phase differences, however when cone thresholds were mediated by the PC pathway (at 2 Hz), rod and cone thresholds showed probability summation with little effect of phase. Similarly the luminance

pathway (L+M and rods) showed linear summation and the chromatic pathway (L-M) showed probability summation. As a result, providing higher rod contrast to a surround increases reaction times to a cone-mediated test field which stimulated the MC pathways (L+M+S) but there was a weaker effect on test fields that stimulated the PC pathway (L-M) or the KC pathway (Zele, Maynard, Joyce, & Cao, 2014).

In conclusion rod-cone interactions occur mainly in the magnocellular pathway for luminance defined stimuli. Although rod signals contribute to colour perception at longer presentation times (Zele, Maynard, & Feigl, 2013) they may not interact within the PC pathways (Sun et al., 2001).

4.3. Rod-cone interactions in spatial vision and detection

It is difficult to describe how the visual system behaves to spatial stimuli in the mesopic range because of the differing interactions between rods and cones which vary with eccentricity, stimulus properties and retinal illuminance. When participants judged Landolt rings at 7° as being higher or lower in contrast than another (effective contrast), stimulus photopic luminance contrast, scotopic luminance contrast, and chromatic contrast all contributed to effective contrast in the mesopic range. Furthermore, each factor's contributions were not independent and varied with background luminance. Chromatic signal strength had less of an effect with decreasing light level and did not have a purely additive relationship with either photopic or scotopic luminance contrast suggesting that at a suprathreshold level colour and luminance were not completely independent (Walkey et al., 2005).

Rods and cones can interact positively to resolve spatial patterns (Brown & Woodward, 1957; D'Zmura & Lennie, 1986). For example, D'Zmura and Lennie

(1986) found that by measuring CSFs at 10° in the retina, raising the light level within the mesopic range increases the contrast sensitivity of the rod system to an acuity around 6 c/deg. Over this range the cone system was less sensitive but had better acuity of around 15 c/deg. Their method was to modulate between two lights that are scotopic metamers which makes a light invisible to rods and not cones, and conversely to modulate between lights that are photopic (but not scotopic) metamers to make lights invisible to cones but not rods. Sub-threshold stimulation of the cone system may affect the rod system because threshold luminances of acuity gratings at retinal illuminances too low to be detected by the cone system do not always follow the scotopic spectral sensitivity (Brown & Woodward, 1957).

Dark adapted rods can facilitate cones to improve spatial acuity at higher mesopic levels but these effects are spatial frequency dependent with smaller effects on low spatial frequency targets and larger effects for high spatial frequency targets (Naarendorp, Denny, & Frumkes, 1988; Naarendorp & Frumkes, 1991). Naarendorp et al. (1988) investigated the effects of light and dark adapted rods on cone mediated spatial acuity (square wave grating, size 6°, with surround of 17° in diameter) in the parafovea (3°). It was found that by light adapting rods, spatial acuity for MW and LW gratings was optimised in dim condition at higher spatial frequencies; between 7 and 21 c/deg, acuity improved for 480 nm background levels between 0.01 and 1 cd/m^2. A background of 655 nm, which would have stimulated cones more, did not improve the visibility of a LW (red) 14 c/deg stimulus. Because of the effects on high spatial frequencies, the authors suggest that this is the result of rod action on cones. For dark adapting rods, observers were first presented with a bleach and the observer continuously adjusted the grating luminance to threshold throughout dark adaptation. They found a similar effect as the SRCI for temporal stimuli; for spatial frequencies 7-21 c/deg between

1 and 5 minutes, 512 nm and red gratings improved in threshold, however, between 6 and 10 minutes thresholds continue to increase. The effect is stronger with higher spatial frequencies and weaker for lower spatial frequencies.

Naarendorp and Frumkes (1991) investigated the influence of the early stages of both rod and cone adaptation on grating visibility presented at either the fovea or parafovea (5°) for a surround of either 0.3 td (only rods stimulated) or 316 td (to stimulate rods and cones). Participants were fully dark adapted for 30 minutes. Parafoveal thresholds for a square wave grating were improved by the use of the low level adapting field but made worse by the higher level adapting field initially, and then improved steadily, until it became better than baseline. Rod enhancement was similar in magnitude at the fovea and parafovea.

In conclusion, in the higher mesopic range rods and cones can interact in order to facilitate spatial vision (D'Zmura & Lennie, 1986; Naarendorp et al., 1988; Naarendorp & Frumkes, 1991), possibly specifically with L- and M- cones.

4.4. The effect of scotopic/photopic ratio on vision

Light sources that are widely available do not have a wide range of S/P ratios, presumably to keep the light achromatic in appearance. For example, low pressure sodium lamps have an S/P ratio of 0.23 whereas a Sun + Sky CIE D65 Illuminant has an S/P ratio of 2.47 (Berman, 1992). The effects of S/P on vision have been investigated in three main areas; spatial performance, pupil size and brightness perception. The majority of research has been carried out into spatial brightness, but the focus of the current chapter is whether visual performance at mesopic light levels can be improved by varying the S/P ratio. I will briefly discuss findings regarding spatial brightness perception which may echo the effects of S/P ratio on

visual performance, depending on what criteria participants use to make their judgements.

Spatial brightness can be defined as the ambient amount of light in a large field space (20° or more) rather than lighting a small field surface or judgement of a particular light source (Fotios, Atli, Cheal, Houser, & Logadottir, 2013). An extensive review found an effect of SPD on perception of brightness in 17 out of 19 studies. Some suggested those with higher CCT were perceived as brighter but not all, and there was no overwhelming direction to this effect. They suggest that photometry relying solely on V(λ) will not faithfully describe the perception of brightness (Fotios et al., 2013).

4.4.1. The effects of S/P ratio on visual performance

Berman (1992, 2000) has suggested that by biasing the spectral power distribution of light towards that to which rods are more sensitive, a reduction in light could be made without sacrificing visual performance.

A number of studies have found that using illuminants with higher S/P ratios improves visual performance. For example, lamps with a higher scotopic component in the surround lighting of the test area improved Landolt C discrimination in younger (Berman, Fein, Jewett, & Ashford, 1993) and older participants (Berman, Fein, Jewett, & Ashford, 1994). Furthermore, Navvab (2001, 2002) found that both letter acuity and word reading was improved under surround lighting at a higher S/P of 2.3 than 1.3, even though the former lamp had an illumination level that was 40% lower.

It is somewhat surprising that S/P ratio had such a significant effect on visual performance since these studies were conducted in photopic light levels. Not unexpectedly, a higher S/P ratio improves Landolt C discrimination by a greater degree at lower light levels than higher, and a greater effect is found for low contrasts of the target rather than higher (Berman et al., 1993), but improvements in acuity generally persist from low to high photopic light levels (Navvab, 2002).

However, a number of other studies have not managed to find an effect of S/P ratio on visual performance, making the findings reported previously somewhat controversial. For example neither Boyce, Akashi, Hunter and Bullough (2003) nor Veitch and McColl (1995) found an effect of lamp S/P ratio on the speed or accuracy of discriminating Landolt rings. No effect of S/P was found for contrast sensitivity or speed or accuracy in a numerical verification task (Vrabel, Bernecker, & Mistrick, 1998). Furthermore one study has found that the lowest S/P ratio resulted in best performance and the highest S/P ratio in worst performance, measured in number of Landolt Cs correctly identified, at both high and low contrasts (Fotios & Cheal, 2011).

One of the reasons these studies failed to find an effect of S/P ratio could be because they used very limited ranges of S/P ratios that only vary by 0.5-0.8, due to being limited to lamps that were commercially available (Boyce et al., 2003). Studies that found effects of S/P tend to use lamps that differ in S/P by 1 to 4. Another reason could be because changes in performance will only be observed in stimuli close to threshold (Boyce et al., 2003)

Therefore if a sufficient range of S/P ratios is implemented for a near-threshold task, higher S/P ratios can compensate for declines in task performance caused by

a reduction in illumination and in this way one could save energy by shifting lamp spectra to obtain greater scotopic stimulation (Berman et al., 1993). In support, when participants adjust lamps to a light level they are most comfortable with, lamps of higher S/P ratio were adjusted to lower luminances (Navvab, 2002). In the following section, the mechanisms by which higher S/P ratios improve visual performance will be discussed.

4.4.2. Effect of S/P ratio on pupil size

The main mechanism proposed to explain the improvement in spatial vision with higher S/P ratios is that it reduces pupil size. Although this reduces retinal illuminance, this could be outweighed by the contribution that smaller pupils make to a greater depth of field and reduced spherical aberrations.

A number of different studies have found that higher S/P ratios result in smaller pupil sizes over ranges from 10 to 500 cd/m^2 (Berman et al., 1993, 1994; Berman et al., 1987). Smaller pupil sizes as a result of higher S/P ratios have also been found in which no corresponding improvements in visual performance were obtained (Boyce et al., 2003). For example, at a constant photopic luminance of 63 cd/m^2, pupil size can be reduced by 43% by increasing the S/P from 0.24 to 4.31 (Berman et al., 1993). Furthermore, scotopic luminance accounts for 70% of the variance in pupil area, whereas photopic luminance only accounts for 47% of the variance (Berman et al., 1987). In order to predict pupil area (mm^2), pupil luminance (L_p) was derived as $L_P = P(S/P)^D$. D is 0.78 when the full field of view is illuminated by 10-300 cd/m^2 (Berman, Fein, Jewett, Saika, & Ashford, 1992). Pupil luminance can be a good predictor of pupil area over photopic light levels, but it is not known if it holds over mesopic light levels.

Berman et al. disregard any potential effects that the S/P or SPD may have on neural processing of spatial stimuli and attribute all improvements in performance of higher S/P ratios to the decrease in pupil size and its effect on the optics of image formation. However, rod-cone interactions may, at least partially, explain the improvements in visual performance. When the experiments of Berman et al. (1993) in a group of young participants were repeated in a group of older participants, they found that although the older participants showed less of a change in pupil size in response to higher S/P ratios, they showed similar improvements in performance (Berman et al., 1994). This suggests that higher S/P ratios may result in rod-cone, or other neural, interactions that improve visual performance. This is further supported by the finding the S/P ratio has a greater effect at lower light levels (Berman et al., 1993).

In conclusion, increasing the S/P of the illuminant may improve visual spatial performance if the range of S/P used is larger than 1, and a near-threshold task is used. It is however less clear whether the improvements reported are due to pupil size or neural factors, and whether this trend extends throughout the mesopic range.

4.5. Aims and objectives of the study

The literature suggests that visual performance can be improved under high mesopic levels by rods and cones interacting constructively (D'Zmura & Lennie, 1986; Naarendorp et al., 1988; Naarendorp & Frumkes, 1991) and that this interaction can be controlled by using appropriate S/P ratios (Berman et al., 1993, 1994; Navvab, 2001, 2002).

Therefore the aims of the current study are to determine:

- Whether S/P ratios at given photopic illuminance can improve visual acuity in the mesopic range. This was done so that the S/P ratio could be optimised for a specific photopic luminance, if street lighting was to be provided at that specific luminance.
- Whether any changes in visual performance are a result of neural factors (cone excitations or post-retinal processing) by equating retinal illuminance over different S/P ratios.
- If the pupil size at a particular illuminance can be varied by changes in S/P ratio.

4.6. Methods

4.6.1. Participants

Four emmetropic observers took part in the experiments, aged 25 to 35 years of age. Each had normal or corrected to normal spatial vision.

4.6.2. Visual acuity assessment

Acuity assessment was conducted in a full field display illuminated by two custom illumination units. Participants viewed the display from a distance of 1.7 m in a chin rest. The display field was neutral grey and subtended 75.6°. Stimuli were presented on an E-ink (Kindle) display subtending 3.03° and located in the centre of the field. A picture of the experimental set up is shown below in **Figure 46**.

Figure 46. Experimental setup showing the display area, chin rest, and one of two illumination systems

The experiment was based on a 4AFC design whereby participants discriminated the direction of the gap in a Landolt ring optotype at 100% contrast, which occurred in one of four diagonal directions. Between presentations, a fixation cross was displayed to help maintain fixation and accommodation. The Landolt ring increased or decreased in size according to previous responses, based on a staircase procedure. The stimulus was presented for 1000 ms, ± 250 ms. Two independent staircases were implemented simultaneously with 11 reversals to vary the size of the stimulus using a two-down, one-up procedure for which increments decreased according to an exponential function. Visual acuity was computed as the average of

the last six reversals for each staircase, and then the final acuity as the average of the two staircases.

Participants were tested at 0° and 12° eccentricity to test areas of the retina containing mostly cones and a combination of rods and cones respectively. Peripheral experiments were conducted by placing a fixation cross at 12° away from the E-ink display, as shown in **Figure 46**. Participants were tested at photopic illuminances of 1, 0.1, 0.01 and 0.001 cd/m^2 and participants were adapted for 5, 10, 20 and 30 minutes for each condition respectively. Spectrally calibrated neutral density filters were employed for background luminances below 0.1 cd/m^2. At each light level, acuity was measured for six S/P ratios, 0.5, 1.5, 2.5, 3.5, 4.5 and 5.5. Participants completed foveal measurements first, starting at the highest light level to the lowest. The order of presentation of each S/P ratio was randomised within a session of a particular light level. Peripheral measurements were carried out using the same procedure.

4.6.3. Illumination system

The illumination system consisted of two units each containing 6 LED light sources. Conventional light sources/display devices are composed of three primary lights, whereas the units for the current study were composed of four primary LED lights, for which the SPDs are shown in **Figure 47**. The spectral reflectance of the E-ink device was measured and the illumination system was spectrally calibrated. The photopic luminance of the E-ink device could therefore be computed for a number of specified S/P ratios. The output of the LED sources was calibrated by linearising their outputs.

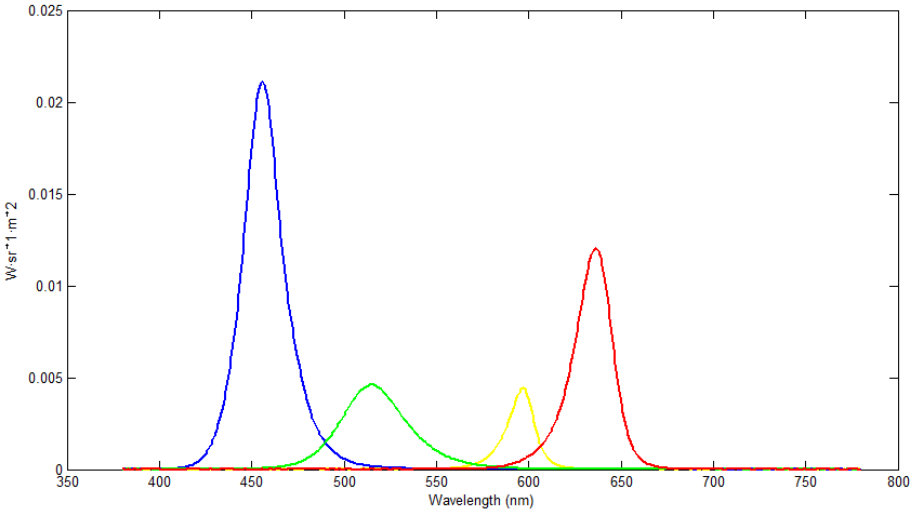

Figure 47. The spectral power distribution of each of the four primaries in the illumination system.

4.6.4. Calculation of S/P ratios

S/P ratio is the ratio of scotopic (V'(λ); CIE 1951) to photic sensitivity (V(λ)) (CIE 1931), which varies with wavelength. With a three primary system, different hues are created with a mixture of the three primary lights in different ratios. Using such a system one can obtain a set of lights that stimulate rods to the same extent (constant scotopic luminance) and another to stimulate cones to the same extent (constant photopic luminance). Each set of lights would lie on a plane in 3D space and the planes would intersect along a line which would produce values for constant scotopic and photopic luminance, whereas chromaticity would vary at various points along the line (Shapiro, Pokorny, & Smith, 1996). In CIE space, this method can be used to find lines that have different scotopic luminances for a constant photopic luminance, thus increasing the S/P ratio (**Figure 48 A**). Doubling the photopic luminance, doubles the scotopic luminance, thus the S/P ratio remains constant. However, using a four primary system, the combination of lights must be described in 4D space and lights that have constant photopic and scotopic luminance lie in an area in 4D space. Areas with constant S/P ratio can thus be

plotted (**Figure 48 B**). This means that there are areas in CIE space with constant S/P ratio, but with varying chromaticity. Conversely, as these areas overlap, there are points in CIE space where the chromaticity remains constant but the S/P ratio changes (not shown). This system allows for visual performance testing under a wide range of illumination conditions where chromaticity, photopic luminance, scotopic luminance and S/P ratio can each be varied independently to determine the optimal conditions for mesopic visual performance.

S/P ratios were calculated using the CIE 1931 2° observer. The midpoint of 5 S/P ratio areas were obtained and are detailed in **Table 4**. Their locations in CIE space and SPD are shown in **Figure 48**.

Table 4. (x, y) co-ordinates of chromaticities employed for each S/P ratio

S/P ratio	x	y
0.5	0.590	0.341
1.5	0.471	0.331
2.5	0.357	0.355
3.5	0.257	0.290
4.5	0.235	0.181
5.5	0.218	0.138

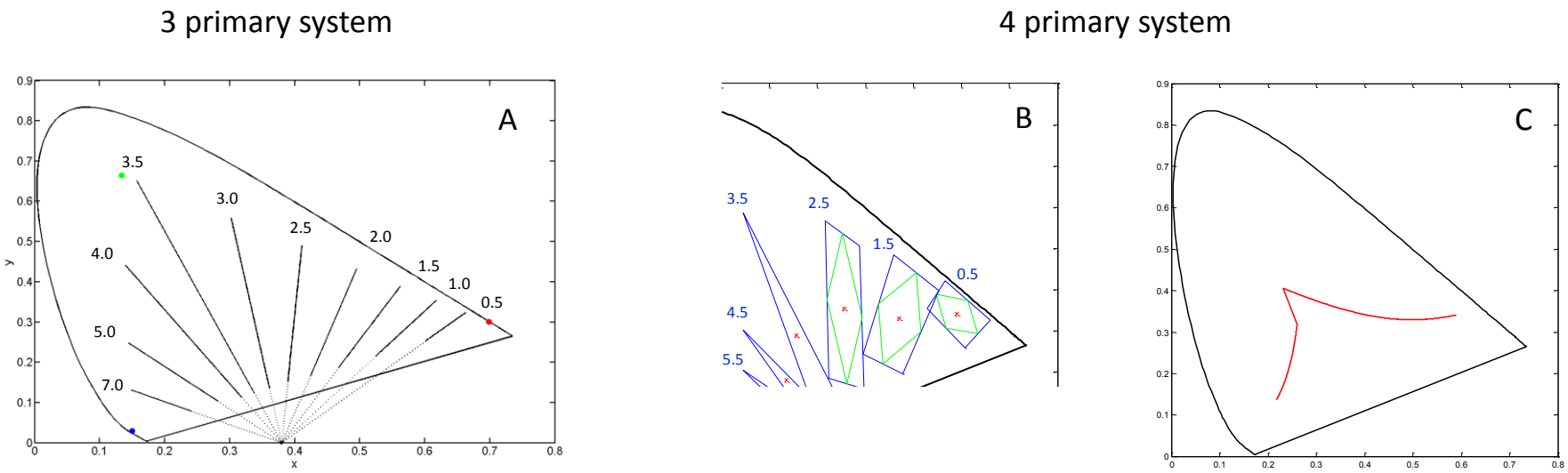

Figure 48. Constant S/P ratios in CIE space for a constant photopic luminance (CIE, 1931). **A** For a three primary system, S/P ratios fall along a line in CIE space. The three coloured points indicate the three primaries. **B** For a four primary system, S/P ratios lie in areas in CIE space, indicated by the blue lines. These areas form quadrangles for lower S/P ratios (0.5 – 2.5) and subsequently form triangles (3.5 - 5.5). Green lines indicate the mid-points of the quadrangle used to calculate the centre point of each area of constant S/P ratio, which is indicated by a red cross. **C** The centre points of areas of constant S/P fall along the red line for S/P ratios between 0.5 and 5.5.

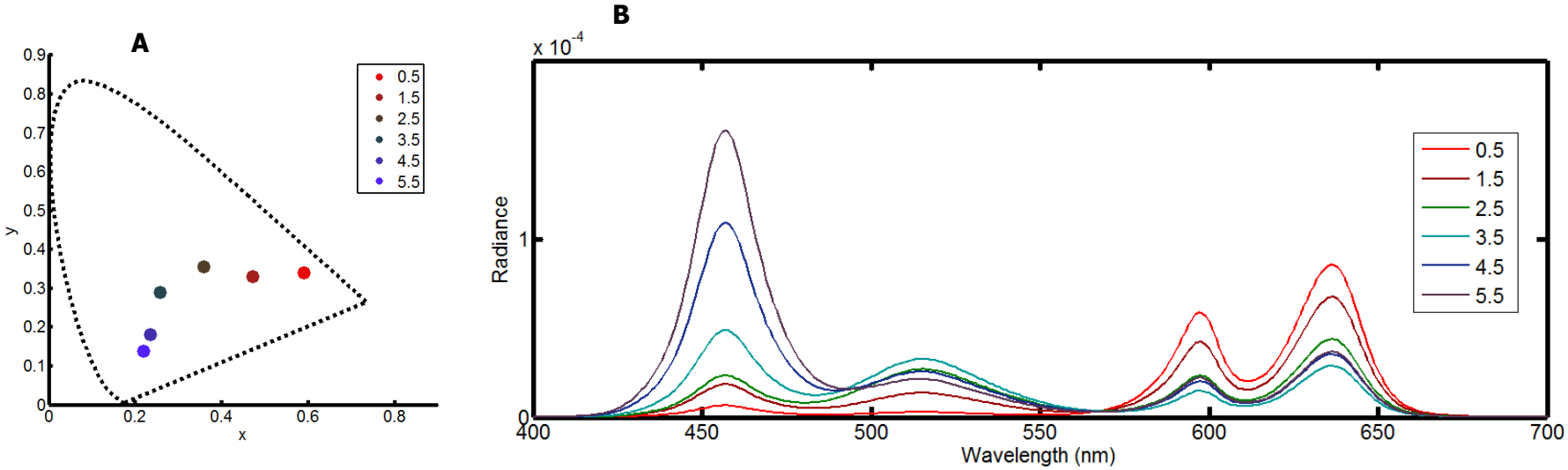

Figure 49. Chromatic information of the S/P values chosen. **A** The S/P values in CIE space (1931) and estimated subjective appearance. **B** Spectral power distributions of the S/P ratios.

4.6.5. Pupil measurement and retinal illuminance

Pupil diameter was measured continuously during the acuity test to calculate retinal illuminance as detailed in section 3.5.3. To ensure participants reliably fixated on the required part of the display, eye movements were tracked and stimuli were re-presented if fixation deviated by 1.5° or more along the horizontal meridian.

4.6.6. Function fitted to visual acuity and retinal illuminance

To evaluate the effect of S/P ratio on acuity independently of any effects on pupil size, a function was fitted to changes in acuity with light level for each S/P separately.

(13) $$T = a \times E^{-b} + c$$

Where T is acuity threshold, E is retinal illuminance, and a, b and c are free parameters.

4.7. Results

Contrast thresholds and pupil diameters were averaged over the four observers to produce average results and standard errors. The following sections present the results for these observers.

4.7.1. Illuminance and S/P on contrast thresholds and pupil size

This section presents measured visual acuity data at each of the illuminance level employed to determine how thresholds change when the photopic illuminance is constant and one varies the S/P ratio. This approach makes it possible to investigate the effect of S/P at a number of photopic illuminance levels under large field, naturalist viewing conditions.

Figure 50 shows foveal thresholds and pupil diameters averaged over the four observers. At the two highest illuminance levels, S/P ratio has very little effect on visual performance. This is to be expected as there are no rods and few S-cones at the central fovea and therefore biasing the SPD of the illuminant to higher S/Ps is unlikely to have a significant effect at constant photopic luminances. However, as the light level decreases to 0.01 cd/m^2, a lower S/P ratio improves visual acuity. Finally, at the lowest light level, acuity is substantially improved by a high S/P. It is unlikely that cones are functioning effectively at this level and therefore the size of the stimulus increases until it stimulates rods outside the foveal, rod-free zone. The estimated size of the rod free zone varies between 250 and 750 μm which is 51 to 156 arc min (Ahnelt, Kolb, & Pflug, 1987; Hendrickson & Yuodelis, 1984; Polyak, 1941; Yamada, 1969). Therefore a stimulus with a gap size of 10.4 – 31.2 arc min is estimated to fall outside the rod free zone. In **Figure 50**, all acuity values fall above 20 arc min, are therefore likely to stimulate both rods and cones.

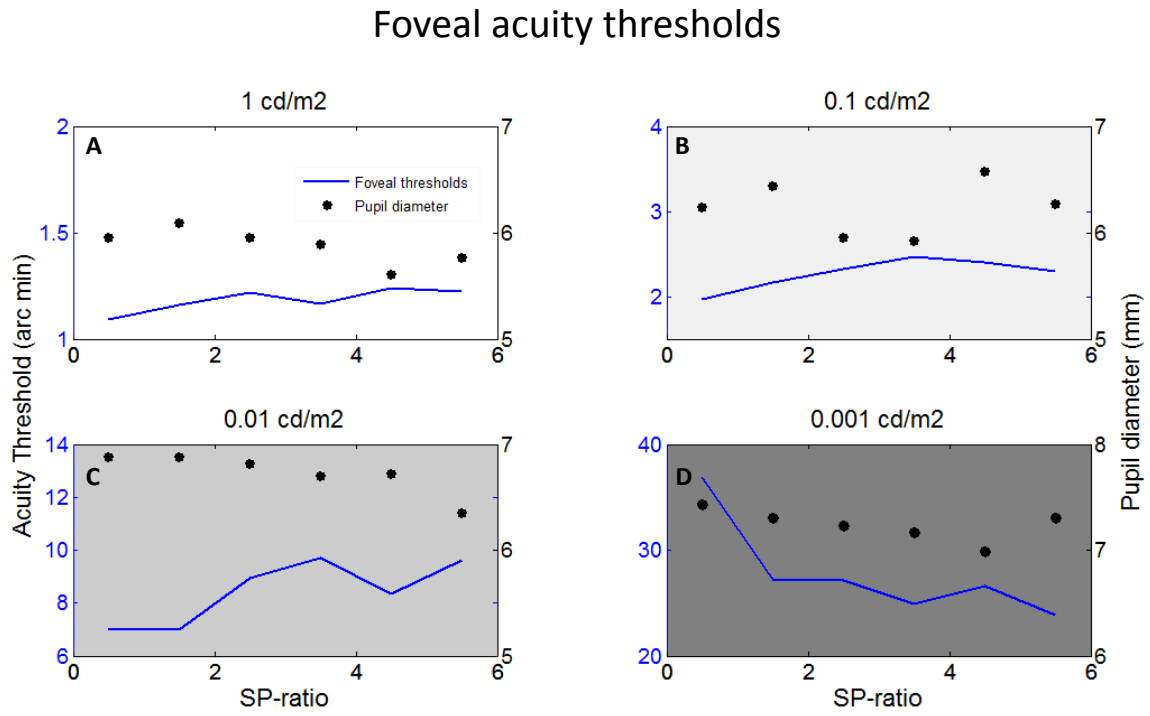

Figure 50. Foveal acuity thresholds (primary y-axis) and corresponding pupil diameters (secondary y-axis) for illuminances 1, 0.1, 0.01 and 0.001 cd/m^2.

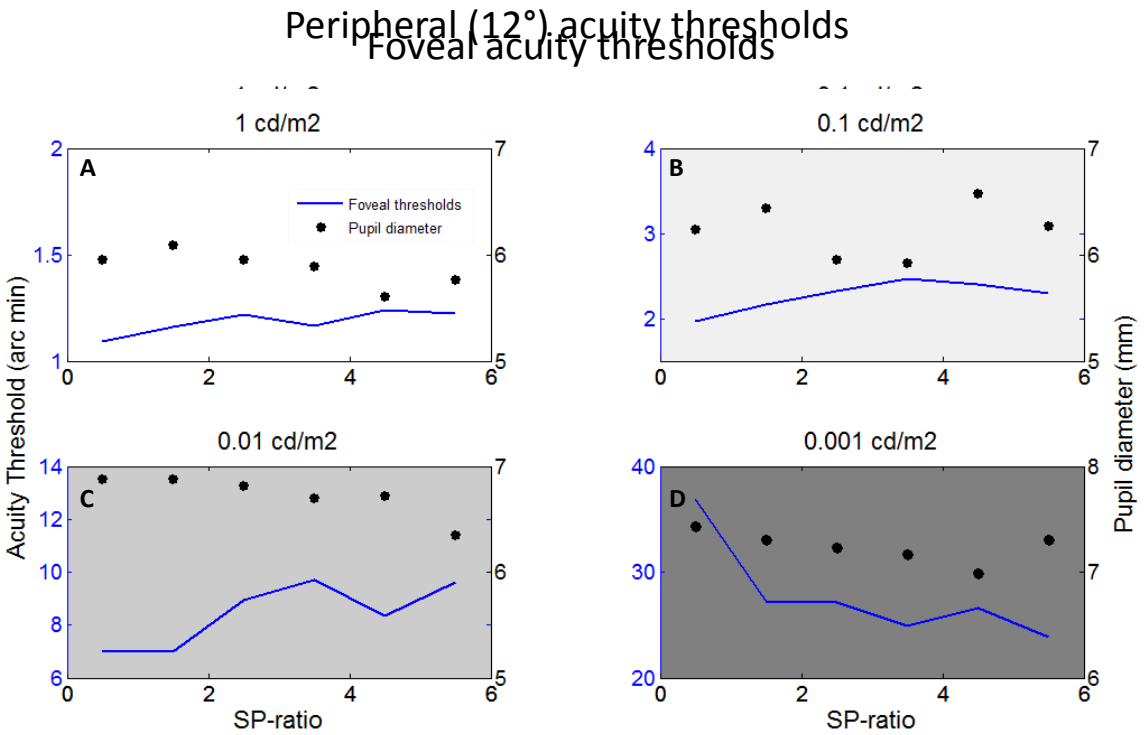

Figure 51. Peripheral acuity thresholds (primary y-axis) and corresponding pupil diameters (secondary y-axis) for illuminances 1, 0.1, 0.01 and 0.001 cd/m^2.

The peripheral acuity thresholds in **Figure 51** show little effect of S/P ratio at the highest light level, but at all lower light levels increasing the S/P ratio improves acuity substantially. It is worth noting that at the lowest light level, peripheral acuity (**Figure 51**) is better than foveal acuity (**Figure 50**). However once an S/P is increased beyond a value of 2, no significant improvements are made.

Pupil size is unlikely to change substantially depending on foveal or peripheral presentations and therefore the results for these two eccentricities will be considered together, in **Figure 50** and **Figure 51**. At the two lowest light levels, pupil size changes little, which could be due to reaching its maximum diameter at approximately 7 mm. However, by mainly considering the two highest light levels, it is apparent that a slight decrease in pupil size occurs with increasing S/P. According to Berman (1992), a decrease in pupil size may cause improved acuity. When considering the two highest light levels only, this pattern may hold in half the cases; at the fovea at 1 cd/m^2 and at the periphery at 0.1 cd/^{2}. However the size of the effect is small. Interestingly at the fovea at 0.1 cd/m^2 when pupil size reduces at mid S/P values, acuity gets worse, which is what one would expect based on the corresponding changes in retinal illuminance.

In summary, parafoveal thresholds can be improved by altering the SPD to favour rods at low light levels, and by a smaller factor of improvement at higher light levels. However to improve foveal vision, lower S/Ps are optimal. If an optimal S/P value were to be chosen to optimise both fovea and peripheral vision, an S/P of 2 may be most appropriate as this value will produce significant cone stimulation. Higher S/P values at the fovea produce few if any improvements.

4.7.2. Pupil variations with S/P ratio

The primary determinants of pupil variation were investigated. **Figure 52** shows that pupil size can be reasonably described as a function of photopic luminance by the ambient light source described in the methods, decreasing with increasing luminance. Pupil size was measured whist the participant was both fixating at the fovea and separately at the fixation cross at 12° eccentricity.

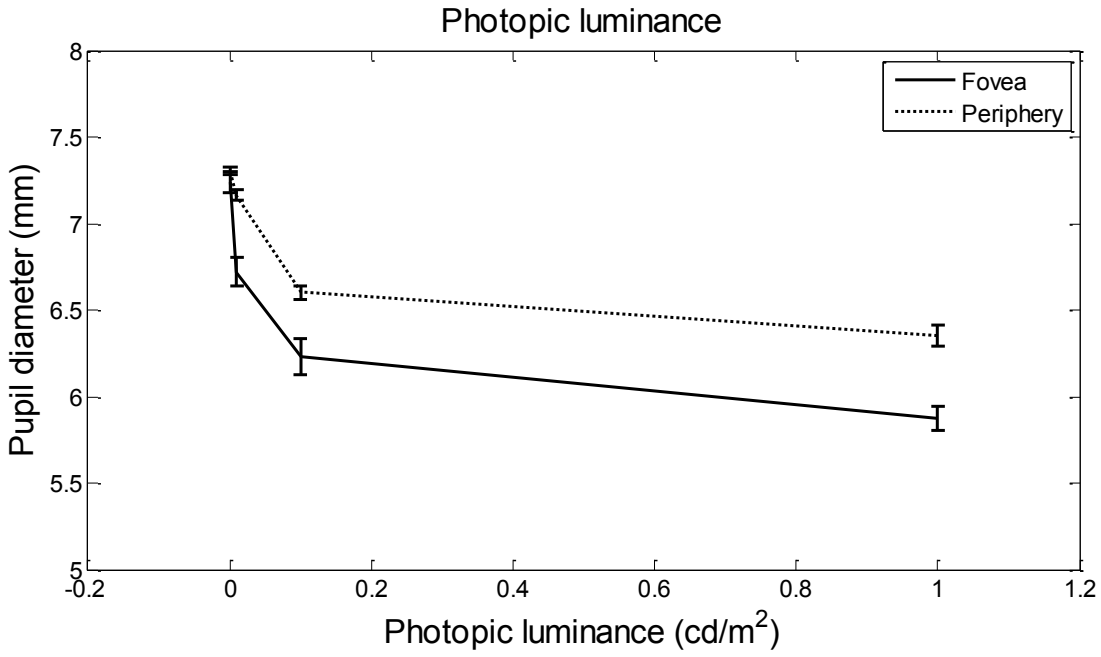

Figure 52. Mean pupil dianeter at photopic luminances. Error bars indicate one SE.

It is of interest to establish whether S/P ratio can have a secondary effect on pupil size. **Figure 53** shows the effect of S/P ratio on pupil diameter at each photopic luminance at the fovea and periphery. At the two highest light levels S/P ratio has a marginal effect on pupil diameter, causing it to slightly decrease. However at the lowest light levels there is no effect, possibly due to the pupil size being at its maximum diameter.

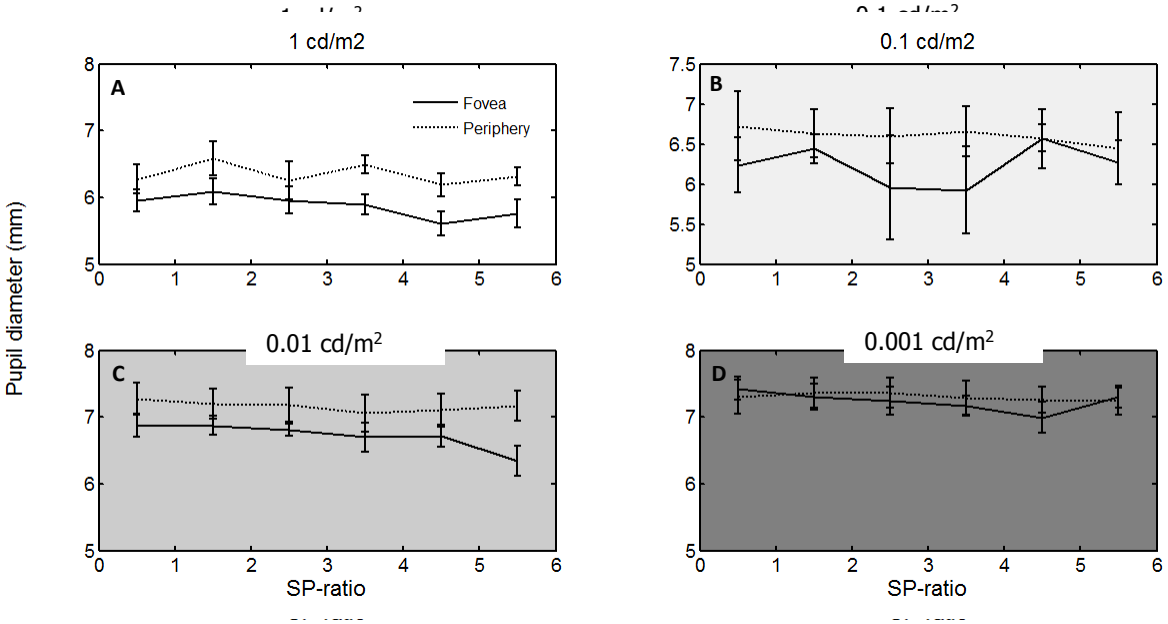

Figure 53. The effect of S/P ratio on pupil diameter at each photopic luminance. Error bars indicate 1 SE.

4.7.3. Contrast thresholds independent of pupil size

Figure 54 shows the variation in acuity thresholds with retinal illuminance at both the fovea and in the periphery. At both eccentricities, S/P ratio appears to have little effect until approximately -0.5 log trolands. Above -0.5 log trolands, foveal acuity is superior whereas below -0.5 log trolands, peripheral acuity is better. At the fovea and below this retinal illuminance, increasing the S/P ratio improves acuity substantially, but at the periphery, increasing S/P ratio provides few improvements beyond an S/P ratio of 2.5.

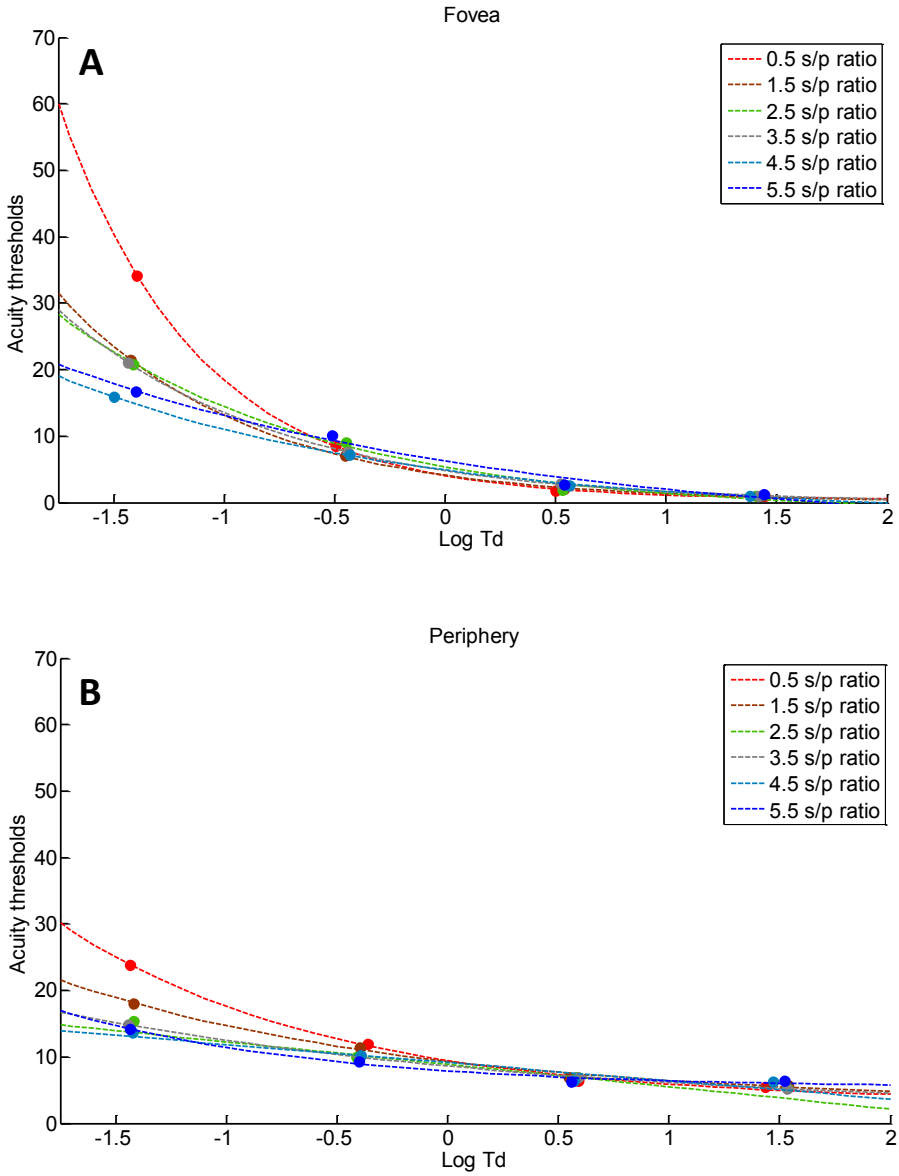

Figure 54. Acuity thresholds in arc min for each S/P ratio and light level at the fovea and peripheral averaged over all participants. Curves fitted to the points took the form: $T = a \times E^{-b} + c$, where T is the acuity threshold, E is retinal illuminance and a, b and c are free parameters

To examine the effect of S/P ratio in more detail, S/P ratios at particular retinal illuminances were plotted at the fovea and periphery together as shown in **Figure 55**. At the three highest retinal illuminances, a low S/P of 0.5 – 1.5 at the fovea results in the best acuity. It is possible that increasing the S/P ratio at these light levels activates rods which subsequently inhibit cone input, resulting in worsening acuity at this constant level of photopic luminance. At the lowest retinal illuminance considered, foveal results are similar to peripheral results, suggesting the conditions are effectively scotopic, as discussed in section 4.7.1. At the periphery, acuity is best at an S/P of 2.5 – 3.5, and there is little improvement with higher S/P ratios.

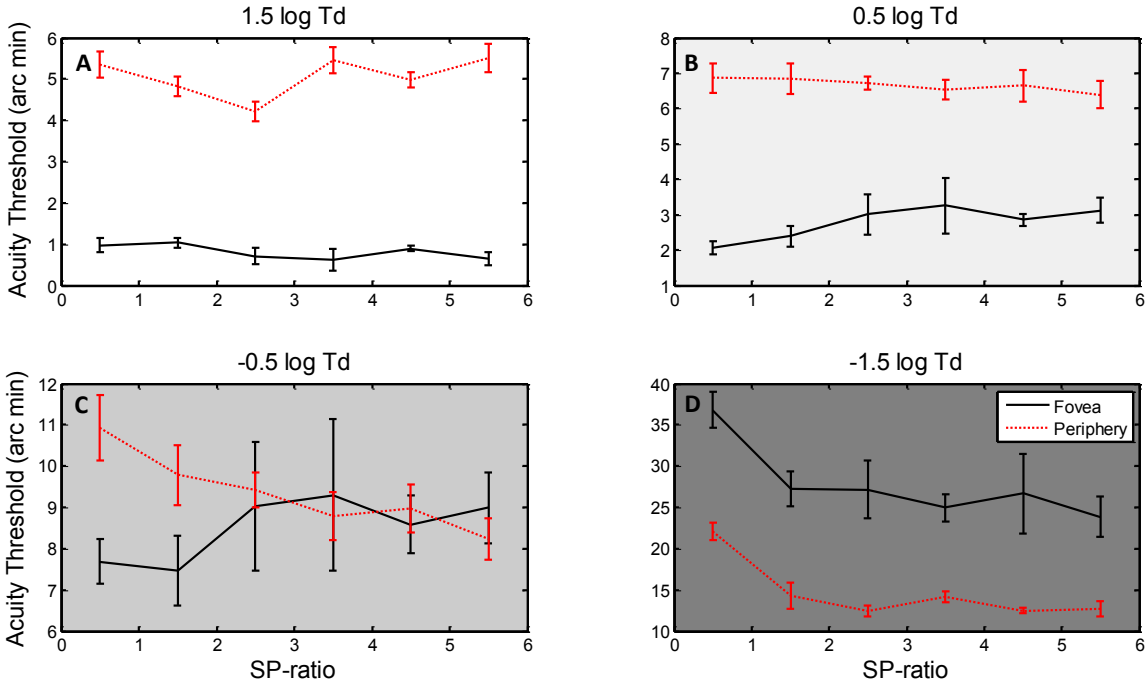

Figure 55. Effect of S/P ratio on acuity thresholds at specific retinal illuminances. Error bars show 1 SE.

In order to determine whether the improved performance at particular S/Ps was due to the S/P value or some other reason, such as particular cone excitation, these factors were investigated below.

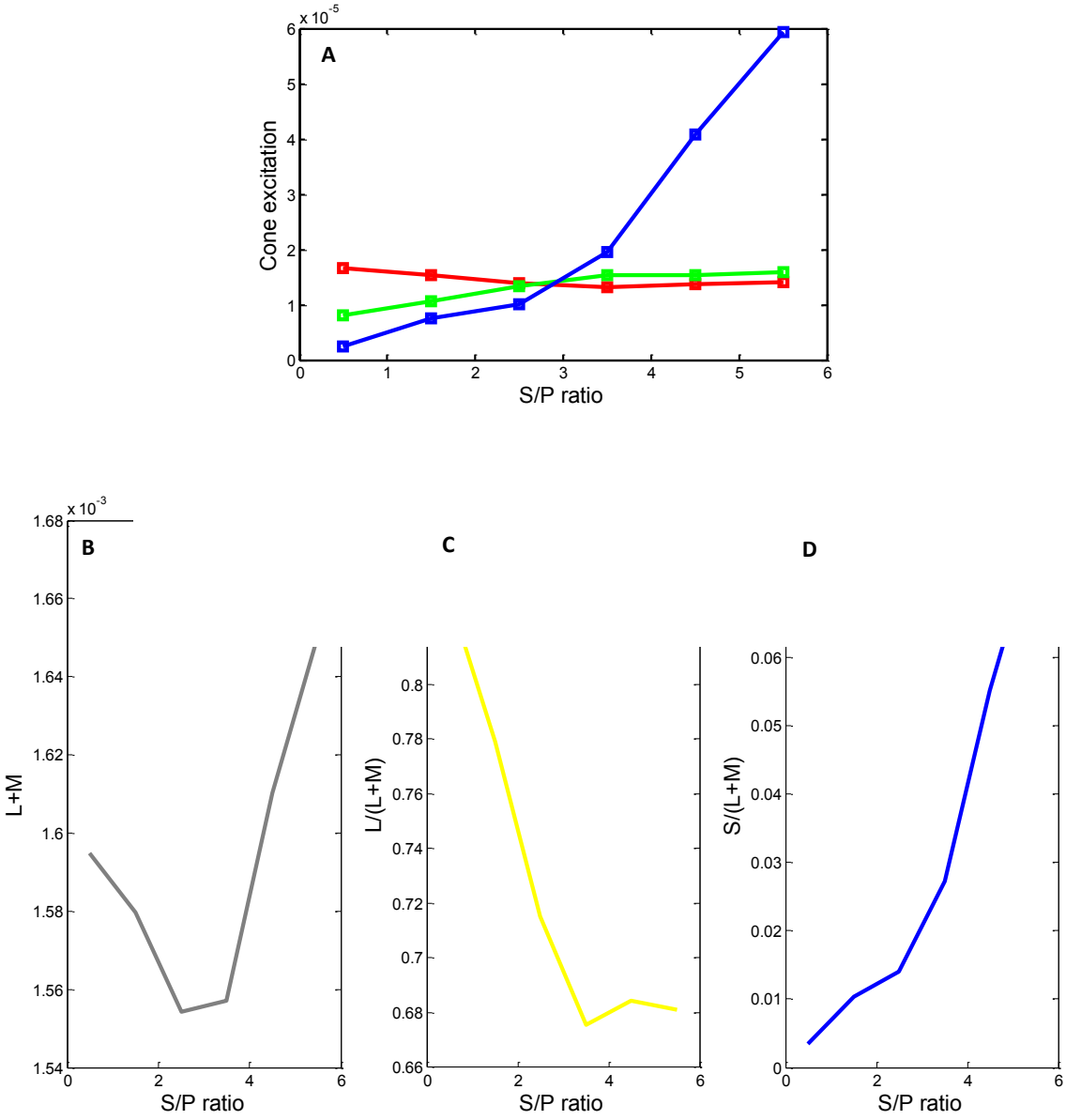

Figure 56. **A** Cone excitations at the S/P ratios used in the study. **B, C and D** Post-receptoral mechanisms at each S/P ratio selected. Note different scales for each graph showing that in **B**, luminance is effectively stable, in **C** L/(L+M) also changes little but in **D** S/(L+M) changes substantially with S/P ratio.

Figure 56 shows the cone excitations and sensitivity of post-receptoral mechanisms for the S/P ratios chosen in the study. **A**, **B** and **C** show that there is very little change in M or L cone sensitivity, and thus L+M or L/(L+M) over the S/P ratios, and therefore are unlikely to explain any changes in the results with S/P ratio. S cone activation and thus S/(L+M) changes substantially (see **A** and **D**), increasing with S/P ratio. As there are no S cones at the centre of the fovea, it is unlikely this would contribute to any changes in threshold at that eccentricity. If S cones were to contribute to acuity, this would be expected at the high S/P ratios, at the highest luminances and in the periphery only. However **Figure 55** A shows at in these conditions, there is very little effect of increasing S/P ratio at the three highest values, where S cone excitation increases the most. Therefore we suggest that the results observed are primarily due to changes in S/P ratio.

4.8. Discussion: Effect of S/P ratio in mesopic vision

4.8.1. The effect of S/P ratio in naturalistic viewing

Firstly, we considered the effect of a constant photopic illumination on both pupil size and acuity together, as if experiencing naturalistic viewing conditions, where both would vary if provided with specific lighting. If Berman et al. (1993, 1994) are correct, the S/P decreases pupil size and improves visual performance, and this extends to the mesopic range where rods are more actively involved in vision; therefore as S/P increases, pupils will decrease, as will acuity thresholds. However this was not found. Although we can confirm a small tendency for pupil size to decrease with increasing S/P ratio (**Figure 53**), this is often accompanied by an increase in acuity thresholds (**Figure 50**). Furthermore, when pupil size is maximum and stable at effectively scotopic luminances, the greatest effect of S/P ratio is found **Figure 50** and **Figure 51**)

4.8.2. The effect of S/P on visual acuity

Acuity thresholds at both the fovea and periphery are the result of rod and cone stimulation; the periphery contains both rods and cones and furthermore, peripheral rods can influence the responses of foveal cones. At the lowest light level tested, acuity could not be determined for cones because the conditions were effectively scotopic and the stimulus size exceeded the rod-free zone of the fovea. It is likely that at the three highest light levels, participants were utilising the fast pathways using rod-cone gap junctions between L- and M- cones, as some of the best acuity thresholds at the fovea were at low S/Ps and longer wavelength light (**Table 5**; Ahnelt et al., 1990; Cao et al., 2005; Sharpe & Stockman, 1999; Stockman & Sharpe, 2006). The lowest light level may have utilised the slow pathway using rods

only. Thresholds near the fovea at the lowest light level were substantially worse than peripheral thresholds, presumably due to the small number of rods at this eccentricity.

Table 5. Foveal acuity thresholds for S/P ratios 0.5 – 5.5 at retinal illuminances of 1.5 to -1.5 log trolands. The bold results show peak increases in the acuity thresholds. The highlighted values show the best acuity for that light level. Note that the poor acuity at the fovea at the lowest light level suggests that the stimulus size increases to stimulate rods outside the rod free zone.

Retinal illuminance (log td)	S/P ratio						Improvement (max-min)
	0.5	**1.5**	**2.5**	**3.5**	**4.5**	**5.5**	
1.5	0.97	1.03	0.71	0.62	0.89	0.65	0.41
0.5	2.07	2.40	**3.01**	**3.25**	2.85	3.13	1.18
-0.5	7.68	7.47	**9.02**	**9.30**	8.58	8.99	1.83
-1.5	36.83	27.29	27.15	24.96	26.65	23.83	13.00

Table 6. Peripheral acuity thresholds for S/P ratios 0.5 – 5.5 at retinal illuminances of 1.5 to -1.5 log trolands. The highlighted values show the best acuity for that retinal illuminance.

Retinal illuminance (log td)	S/P ratio						Improvement (max-min)
	0.5	**1.5**	**2.5**	**3.5**	**4.5**	**5.5**	
1.5	5.36	4.82	4.22	5.45	4.98	5.51	1.29
0.5	6.87	6.85	6.71	6.54	6.65	6.39	0.48
-0.5	10.92	9.78	9.41	8.79	8.98	8.22	2.70
-1.5	22.11	14.28	12.42	14.20	12.49	12.74	9.69

At the fovea at 0.5 and -0.5 log td, acuity was best at S/P values of 0.5 and 1.5. Increasing rod stimulation in the area surrounding the fovea reduced acuity and this finding is supported by many previous studies of the inhibiting influence of dark adapting rods, particularly for LW and MW light (Cao et al., 2006; Coletta & Adams, 1985; Coletta & Adams, 1984; Frumkes & Eysteinsson, 1988; Shapiro, 2002). The influence of rods was significant (as acuity declined from 7.5 to 9 arc min) possibly due to the small stimulus size (Alexander & Fishman, 1986).

A different pattern was evident for peripheral acuity at 0.5 and -0.5 log trolands, whereby increasing S/P improved acuity, probably due to the greater number of rods at this eccentricity. This pattern continued to the lowest retinal illuminance of -1.5 log trolands for both foveal and parafoveal stimuli which stimulated both rods and cones at each eccentricity. What is interesting is that when rods are stimulated by increasing S/Ps, the effect plateaus at around 2.5 – 3.5. One potential reason for this is that rods have a large summation area and attempting to stimulate them beyond a certain point does not increase their spatial sensitivity. This explanation also supports the previous argument of rod inhibition at the fovea, that beyond S/P ratios of 2.5 – 3.5, foveal acuity thresholds are not further inhibited. This assumes that rod signals that contribute to acuity and at the same time inhibit cones are the same and transmitted in the same way.

Despite using a large range of S/P ratios, we have found that increasing the S/P only improved cone-mediated acuity at high mesopic levels (**Table 5**), and the results do not generalise to lower mesopic levels. This result somewhat supports the findings of Berman et al. (1993, 1994) and Navvab (2001, 2002), of improved visual performance at photopic light levels, but the improvement is only marginal (approximately 0.4 arc min).

4.8.2. The effect of S/P on pupil size

In general, when considering pupil size alone, photopic luminance has the primary effect on pupil size, which increases with decreasing photopic luminance (**Figure 52**). Increasing S/P ratio at constant levels of photopic luminance only had a very marginal effect on decreasing pupil size at illuminances of 1 – 0.01 cd/m^2, but no effect at 0.001 cd/m^2, presumably because pupil size was already maximum at this light level (**Figure 53**).

We considered calculating "pupil luminance" ($L_P = P(S/P)^D$) for different values of 'D' to consider whether it would provide a better explanation for the variation in pupil size with illuminance, where D is 0.78 when the full field of view is illuminated by 10-300 cd/m^2 (Berman et al., 1992). However, given the marginal effect of S/P ratio, it was clear that photopic luminance was the best explanation of pupil size in the mesopic conditions tested.

We can therefore conclude that the effect of S/P on pupil size and its hypothesised improvements to visual performance do not generalise to mesopic conditions. There are two potential explanations for this. Firstly, as the spectral sensitivities of rods and S-cones are very similar, it could be that increasing the S/P ratio of the illuminant is simply increasing the excitation of the S-cones at photopic levels which can cause a constriction of pupil size, however these inputs tend to be weak compared to the influence of L + M cones (Verdon & Howarth, 1988). Another explanation is that S/P ratio really does have a significant effect on pupil sizes at high light levels, however the benefits of a smaller pupil size in photopic conditions (decreased aberrations) do not outweigh the disadvantages it causes in mesopic conditions (decreased retinal illuminance) in terms of visual performance. As can be seen from **Figure 54**, small changes in retinal illuminance when the retinal illuminance is already low can have a significant effect on visual acuity. Therefore, at mesopic levels the main effect that S/P has on acuity is more likely due to neural than optical factors.

4.8.4. Recommendations for street lighting

Any attempt to optimise spatial vision must balance the improvements to each area of the visual field. For lighting above 0.01 cd/m^2 it is suggested that an S/P ratio of 1.5 – 2.5 is optimal for the following reasons:

- The SPD is biased towards L- and M- cones which will contribute to good acuity at the fovea.
- It stimulates rods at the periphery, and further increases to S/P ratios do not result in greater improvements.
- Observers tend to prefer the appearance of lamps in the range of S/P 1.25 - 1.65 (Fotios & Cheal, 2011).

4.9. Conclusions

There is a small tendency for pupil size to decrease with higher S/P ratios in the mesopic range, but pupil size is primarily determined by photopic luminance. Furthermore, foveal visual acuity is better at higher S/P ratios. Increasing scotopic sensitivity will improve peripheral visual performance due to the higher numbers of rods at the periphery, however, no substantial improvements are obtained by increasing S/P ratio beyond 2.5, possibly due summation of rod signals. Therefore, to optimise lighting at mesopic levels for central and peripheral vision an S/P ratio of 1.5-2.5 should be chosen. Further work should investigate whether any additional improvements could be made to visual acuity by changing the chromaticity within areas of constant S/P, and whether varying S/P for a constant chromaticity has any effect.

5. General discussion

This thesis investigated the effects of aging and eccentricity on stimuli that varied in luminance either over space or time (Chapters 2-3). Furthermore, the effects of varying the light level (Chapters 2-4) and the spectral composition of the light (Chapter 4) were quantified, and these findings can be used to optimise lighting for performing tasks in photopic and mesopic conditions.

5.1. Aging of monocular spatial and temporal vision at photopic and mesopic light levels

This thesis has used the HR_{index} to quantify how aging affects spatial and temporal contrast vision at photopic and mesopic light levels in a single number. Measures were taken to ensure this metric represented age-related changes to the retina and higher visual pathways by the use of MW and LW light to avoid absorption of light by the lens, and we calculated retinal illuminance to account for pupil miosis in older participants. The aging of the retina causes a decline in performance for both spatial and temporal stimuli, consistent with other studies of aging (Casson et al., 1993; Elliott et al., 1990; Haegerstrom-Portnoy et al., 1999; Kim & Mayer, 1994; Mayer et al., 1988; Royer & Gilmore, 1985; Rubin et al., 1997; Tyler, 1989; Wright & Drasdo, 1985), but there are a number of important differences.

When considering thresholds at 900 td compared to 25 td in spatial and temporal contrast (**Figure 31** and **Figure 41**), the age related decline in thresholds is greater at the lower retinal illuminance. This implies that older people will experience more difficulty with both temporal and spatial vision in mesopic conditions when compared to younger people. The practical implications of this are

to either enhance the spatial or temporal contrast of signage or displays, or provide better lighting in order for reliable detection by older drivers, pedestrians or users. Best practice would be to do both, as there is an additional effect of reduced retinal illuminance for older people. One interesting point is that perhaps older people's thresholds do not increase with lower luminances *as a proportion* to those of younger people. However, in this case the absolute difference is more meaningful because the contrast of a stimulus remains the same at decreasing levels of luminance and does not scale in this way. Similarly, when plotted on a log scale, it appears that the decline in thresholds with age is less rapid at lower retinal illuminances. However, the contrast of a stimulus will remain the same as the surrounding illumination decreases and therefore to make our findings applicable to the real world, it is best to consider the findings on a linear scale.

The decline in the HR_{index} with age was linear for contrast vision (**Figure 28**). Previous studies have often found the change in contrast vision with age to be bilinear or exponential, however these studies did not account for retinal illuminance and thus these functions are the result of changes to both the retina and the optics of the eye with age (Hahn, et al., 2009; Schneck et al., 2004). However, temporal contrast vision was found to decline non-linearly with age **Figure 38**, despite taking similar measures to ensure thresholds were a result of age-related changes to the retina or other visual pathways. Previous findings of the HR_{index} for colour vision found very little decline in colour vision with age (Barbur & Konstantakopoulou, 2012). Furthermore, the normal limits of performance with age could follow the linear fit and do not expand with age (contrast and colour vision) or follow the non-linear fit and expand with age (temporal contrast vision). These findings suggest that each test taps into aging of different retinal mechanisms.

Contrast vision did not decline at a greater rate with age at the parafovea compared to the fovea which does not mirror the loss of rod receptors at the parafovea with age (Curcio & Drucker, 1993; Curcio et al., 1993). Similarly, the decline in temporal vision with age was non-linear, similar at the fovea and parafovea and unlikely to stimulate rods sufficiently due to the high-frequency employed (15 Hz). Therefore, the reduced flicker sensitivity may be due to well-documented changes in the loss of axons of retinal ganglion cells with age, retina-wide (Calkins, 2013; Curcio & Drucker, 1993; Gao & Hollyfield, 1992; Harman et al., 2000; Jonas et al., 1992; Mikelberg et al., 1989; Tyler, 1985). Furthermore, the HR_{index} for colour vision can be used to monitor changes to Yellow-Blue and Red-Green channels (Barbur & Konstantakopoulou, 2012)

Therefore, contrast and temporal thresholds each tap into different visual mechanisms due to the different trends of decline with age and may all be utilised in detecting age-related changes and departures away from the expected values could be the result of sub-clinical changes to the retina. The normal limits for each measure can be used to identify people with potentially abnormal changes, but further studies would have to be conducted to determine the sensitivity and specificity of the HR_{index}. However it is known that declines in spatial contrast vision precede the loss of acuity in older people (Schneck et al., 2004), and changes to temporal contrast sensitivity can predict the development from early to more severe forms of AMD (Luu et al., 2012). Furthermore, asymetric changes of the YB dimension can be indicative of retinal changes related to type II diabetes, or elevated levels on both dimensions could be a result of AMD related changes (O'Neill-Biba, Sivaprasad, Rodriguez-Carmona, Wolf, & Barbur, 2010). Fundus changes are not always the best predicter of risk of disease progression, and psychophysical methods may be more sensitive (Luu et al., 2013).

5.2. Aging of binocular spatial and temporal vision

BSR was calculated for spatial and temporal contrast thresholds, independent of retinal illuminance, as pupil size varies between monocular and binocular conditions (Boxer Wachler, 2003). The BSR was calculated for each participant at photopic to mesopic light levels and averaged to provide a single value. BSRs of spatial and temporal contrast vision were differentially affected by aging. This thesis found a decline in binocular summation for spatial contrast vision in normal aging, consistent with previous findings (Gagnon & Kline, 2003; Pardhan, 1996) and 18.3% of participants showing binocular inhibition (**Figure 32 A**). In contrast, BSRs for flicker detection were remarkably stable with age (**Figure 44 A**) with only 1.3% showing binocular inhibition. As far as we are aware, this is the first study that has documented binocular summation of flicker with age.

Interocular differences are correlated with contrast BSR (**Figure 32 B**), with higher interocular differences resulting in less binocular summation. Increasing interocular differences with age has been put forward as an explanation for the decline in BSR with age (Cagenello et al., 1993; Haegerstrom-Portnoy et al., 1999; Pardhan, 1997) but we defined interocular differences as a proportion of the best eye's threshold (equation (9) as with increasing thresholds, the difference between the eyes should increase as a proportion. Interocular differences defined in this way do not change with age in contrast vision (**Figure 32 C**) and thus cannot explain the decline in BSR with age. Interestingly, interocular differences do not change with age in flicker sensitivity (**Figure 44 B**) and therefore mirror the change in BSR with age. In conclusion, interocular differences are unlikely to explain either changes or stability of BSR with age because IPI and age do not consistently mirror the pattern of BSR changing with age. In support of a central, neural aetiology, BSR declines at the

same rate at the fovea and parafovea for spatial contrast signals and neither eccentricity shows any difference in BSR with age for temporal contrast signals.

There have not been extensive investigations into the possible cause of declines in BSR with age, but according to our findings it would have to be a factor that influenced spatial but not temporal neural factors. Proposed mechanisms include increases in cortical noise and/or delayed signal timing (Wang et al., 2005; Yang et al., 2008; Zhang et al., 2008). However, many studies have not found any changes in the speed of visual responses in terms of the IRF up to 80 years of age, but have found reduced amplitude of responses (Gerthet al., 2003; Kim & Mayer, 1994; Shinomori & Werner, 2003). Therefore one possibility to expain the different changes in BSR with age would be that as signals get noisier and their amplitude is reduced, peak timing of the signals can be maintained but reduced amplitude means that the spatial signal is selectively degraded. Future work would need to be conducted to determine if there is a mechanism which would account for selective degredation of spatial and not temporal binocular signals with age.

5.3. Scotopic/photopic ratios to optimise mesopic spatial vision

In the mesopic range, decreasing pupil size did not improve visual acuity thresholds, as would be predicted by Berman et al. (1993, 1994), perhaps because any benefits such as reduced optical aberrations are outweighed by the reduction in retinal illuminance. Photopic luminance was the primary determinant of pupil size, and increasing the S/P ratio with a constant photopic luminance may marginally reduce pupil size when it is below the maximum.

Increasing the S/P ratio to 2.5-3.5 at mesopic light levels seemed to increase acuity thresholds at the fovea, possibly due to the inhibition of surrounding rods. At these light levels foveal vision was optimal when the SPD of the light was a longer wavelength and rods were only marginally stimulated (S/P 0.5 – 1.5). However, due to the greater number of rods at the peripheral location (12°), increasing the S/P ratio improved acuity. However as can be seen from **Figure 55**, it did not substantially improve beyond an S/P of 1.5-2.5. We suggest that this occurs because of the large amount of spatial summation by rods; stimulating them beyond a certain S/P ratio does not result in improved spatial vision because they are optimised to be sensitive. This theory supports the previous assertion that rods are inhibiting the foveal thresholds because foveal acuity does not decline substantially below S/P ratios of 1.5 – 2.5 (**Figure 55**). It is therefore recommended that street lighting could provide mesopic illumination utilising an S/P ratio of 1.5 – 2.5, as it prevents rod inhibition of central fovea vision, stimulates rods sufficiently at the fovea and surround and is in the range of lamps that observers find acceptable (Fotios & Cheal, 2011).

5.5. Further work and limitations

Future work on the HR_{index} for contrast and flicker vision could determine the sensitivity and specificity of these tests, which are measures of the ability of a test to appropriately classify people into groups. Sensitivity is a measure of the true positives identified by the test, i.e. the number of people with AMD correctly identified by the HR_{index}. Specificity measures the true negatives identified by the test, i.e. the proportion of normal people who were correctly identified as falling within the normal limits of the HR_{index}. However there are problems with the use of specificity in particular if used with a group of participants for which the conditions

were determined but blind to the experimenter. The aim of these studies was to define normal aging. A person may appear to have a normal fundus, however, there may be sub-clinical changes that cannot be detected with current imaging techniques and can only be detected with psychophysical techniques. This has been found for early AMD, where psychophysical performance has predicted the development of later stages of AMD in flicker perception (Luu et al., 2012; Luu et al., 2013; Mayer et al., 1994). To truly determine specificity with great accuracy, a sample of people with normal fundus images should be followed for a number of years to see if they go on to develop AMD or other retinal disease, in which case this group could be excluded and the normal limits re-calculated. Another question would be how long participants should be followed up, as it is unknown how long it takes between subclinical retinal changes and further manifestation of the changes to be detected. Furthermore, a current limitation of the studies is that we did not have test-retest repeatability data for the same HR_{index} tests. This would be useful to establish the reliability of the HR_{index} values themselves.

There is much more work to be done into the effect of aging of the central visual system and its effect on BSR. For example, why is BSR stable with increasing age for flickering stimuli and not for spatial stimuli? Is there a mechanism by which increased neural noise with age will cause reduced BSR for spatial and not flickering stimuli?

The work presented in this thesis on the effects of S/P ratio on spatial acuity only represents a small fraction of what can be investigated with the equipment described, and there are many unanswered questions. For example, can spatial vision be improved by changing the chromaticity within areas of constant S/P ratios? I would predict that holding an S/P ratio at a low level of 1.5 would reduce

the inhibitory effects of rods on cones, and by biasing the chromaticity of the light to preferentially stimulate LW and MW cones could improve acuity by increased stimulation of the luminance channel. Furthermore, the question of whether varying S/P for a constant chromaticity has any effect could be investigated. Finally, as older people have fewer rods, it would be of interest to determine if they need a higher S/P ratio to obtain the benefits of increasing the S/P of light to enhance acuity at the periphery.

6. Conclusions

Spatial contrast vision declines linearly with age, whereas the ability to detect rapid flicker is reasonably stable until approximately 50 years of age and then declines rapidly with increasing age. These changes in vision are attributed to aging of the retina as the methods described bypass the some of the effects of aging on the optics of the eye such as increased absorption of SW light by the lens and pupil miosis in older observers. Furthermore, the variability of spatial contrast vision does not appear to change as age progresses, whereas after 50 years of age, the variability in rapid flicker detection increases immensely in observers. Tests of spatial and temporal contrast vision may tap into different retinal mechanisms such as the functioning of rods and cones and retinal ganglion cells respectively, and measuring visual function at photopic to mesopic light levels was critically important to distinguish between the aging of these different mechanisms. Tests of spatial contrast vision and rapid flicker have determined the limits of normal, age-related changes in visual performance in order to distinguish it from early stages of retinal disease. This information could be used to identify people who would benefit from potential treatments to prevent further disease progression. Further work is required to determine if these tests could be adapted for use in clinical practice, and to determine their sensitivity and specificity in a longitudinal study.

Additionally, when matched for retinal illuminance, older people experience substantially worse mesopic vision than photopic vision when compared to younger people in both the spatial and temporal domains. In naturalistic viewing conditions when pupil size is free to vary, older people are at a further disadvantage due to pupil miosis. To gain a true understanding of a person's vision, ideally vision should

be assessed in low light levels that are likely to be encountered by the individual, as well as the higher light levels in the eye clinic.

Aging also affects the more central visual system and can reduce binocular summation of spatial contrast signals, which in extreme cases can result in binocular inhibition, meaning that vision with two eyes is actually worse than monocular vision. However, the binocular summation of flicker signals were surprisingly stable with age. Binocular summation of spatial or temporal contrast vision may not change as a result of interocular differences because interocular differences do not always mirror changes in binocular summation and therefore the underlying change or stability has a foundation in the central visual system.

The SPD of light can be adjusted to improve foveal and peripheral visual acuity in mesopic light levels but these factors must be appropriately balanced due to the different distributions of rods and cones across the retina. Increasing the rod stimulation by changing the chromaticity of the light may improve acuity by increasing the stimulation of cones via rod-cone interactions, but large increases in rod stimulation may then inhibit cone vision.

The three studies reported in this thesis demonstrate that the vision of luminance-defined stimuli can be improved by optimising viewing conditions; by providing adequate levels of lighting, particularly for older participants and by optimising the SPD of light.

Appendix 1: Stability of accommodation at photopic and mesopic light levels

Accommodation can behave differently at lower levels of illumination; when visibility is degraded, people will adjust to an intermediate resting state, called dark focus, the degree of which varies significantly from person to person and can range from mild near myopic focus to optical infinity. To determine whether the luminances employed in Chapters 2 and 3 would result in suboptimal accommodation, the refractive power of the eye was measured in the right eye at 0.8, 1.2, 2.6, 7.6, 27 and 65 cd/m^2 while participants viewed a display at 2m, requiring 0.5 dioptres. The monitor displayed a fixation cross surrounded by guides at 80% negative contrast. Two subjects were measured. Crosses indicate results without optical correction and circles with optical correction. It is apparent that although the subjects vary in accommodation, there is no effect of luminance.

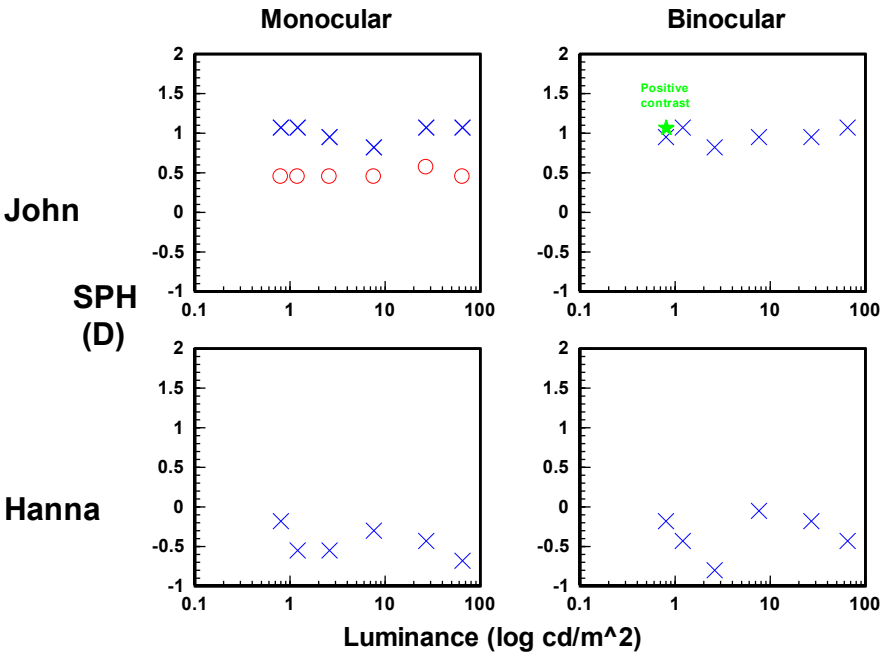

References

Access Economics Pty Limited. (2009). *Future sight loss UK (1): The economic impact of partial sight and blindness in the UK adult population: Prepared for the RNIB.* Retrieved from https://www.rnib.org.**uk**/sites/default/files/FSUK_Summary_**1**.pdf

Ahmad, A., & Spear, P. D. (1993). Effects of aging on the size, density, and number of rhesus monkey lateral geniculate neurons. *Journal of Comparative Neurology, 334*(4), 631-643.

Ahnelt, P., Keri, C., & Kolb, H. (1990). Identification of pedicles of putative blue-sensitive cones in the human retina. *Journal of Comparative Neurology, 293*(1), 39-53.

Ahnelt, P. K., Kolb, H., & Pflug, R. (1987). Identification of a subtype of cone photoreceptor, likely to be blue sensitive, in the human retina. *Journal of Comparative Neurology, 255*(1), 18-34.

Alexander, K. R., & Fishman, G. A. (1984). Rod-cone interaction in flicker perimetry. *British Journal of Ophthalmology, 68*(5), 303-309.

Alexander, K. R., & Fishman, G. A. (1986). Rod influence on cone flicker detection: variation with retinal eccentricity. *Vision Research, 26*(6), 827-834.

Alexandridis, E., Leendertz, J. A., & Barbur, J. L. (1991). Methods for studying the behaviour of the pupil. *Journal of Psychophysiology*, *5*(3), 223-239.

Allman, J. M., & Kaas, J. H. (1971). A representation of the visual field in the caudal third of the middle temporal gyrus of the owl monkey (Aotus trivirgatus). *Brain Research, 31*(1), 85-105.

Ambach, W., Blumthaler, M., Schöpf, T., Ambach, E., Katzgraber, F., Daxecker, F., & Daxer, A. (1994). Spectral transmission of the optical media of the human eye with respect to keratitis and cataract formation. *Documenta Ophthalmologica*, *88*(2), 165-173.

Anderson, P. A., & Movshon, J. A. (1989). Binocular combination of contrast signals. *Vision Research, 29*(9), 1115-1132.

Arden, G., Sidman, R., Arap, W., & Schlingemann, R. (2005). Spare the rod and spoil the eye. *British Journal of Ophthalmology, 89*(6), 764-769.

Armstrong, R. A. (2013). Statistical guidelines for the analysis of data obtained from one or both eyes. *Ophthalmic and Physiological Optics*, *33*(1), 7-14.

Artal, P., Ferro, M., Miranda, I., & Navarro, R. (1993). Effects of aging in retinal image quality. *Journal of the Optical Society of America A*, *10*(7), 1656-1662.

Artal, P., Guirao, A., Berrio, E., Piers, P., & Norrby, S. (2003). Optical aberrations and the aging eye. *International Ophthalmology Clinics, 43*(2), 63-77.

Arundale, K. (1978). An investigation into the variation of human contrast sensitivity with age and ocular pathology. *British Journal of Ophthalmology*, *62*(4), 213-215.

Azen, S. P., Varma, R., Preston-Martin, S., Ying-Lai, M., Globe, D., & Hahn, S. (2002). Binocular visual acuity summation and inhibition in an ocular epidemiological study: the Los Angeles Latino Eye Study. *Investigative Ophthalmology & Visual Science, 43*(6), 1742-1748.

Baker, D. H. (2008). *Interocular suppression and contrast gain control in human vision* (Doctoral dissertation, Aston University).

Barbur, J. L., & Connolly, D. M. (2011). Effects of hypoxia on color vision with emphasis on the mesopic range. *Expert Review of Ophthalmology, 6*(4), 409-420.

Barbur, J. L., & Konstantakopoulou, E. (2012). Changes in color vision with decreasing light level: separating the effects of normal aging from disease. *Journal of the Optical Society of America A*, *29*(2), A27-A35.

Barbur, J. L., Konstantakopoulou, E., Rodriguez-Carmona, M., Harlow, J. A., Robson, A. G., & Moreland, J. D. (2010). The Macular Assessment Profile test - a new VDU-based technique for measuring the spatial distribution of the macular pigment, lens density and rapid flicker sensitivity *Ophthalmic and Physiological Optics, 30*(5), 470-483.

Barbur, J. L., & Rodriguez-Carmona, M. (2015). Colour vision changes in normal aging. In A. J. Elliot & M. D. Fairchild (Eds.), *Handbook of Colour Psychology*: Cambridge University Press.

Barbur, J. L., & Stockman, A. (2010). Photopic, Mesopic, and Scotopic Vision and Changes in Visual Performance. In D. Dartt, J. Besharse & R. Dana (Eds.), *Encyclopedia of the Eye.* Oxford: Academic Press.

Barbur, J. L., & Thomson, W. D. (1987). Pupil response as an objective measure of visual acuity. *Ophthalmic and Physiological Optics, 7*(4), 425-429.

Berman, S. M. (1992). Energy efficiency consequences of scotopic sensitivity. *Journal of the Illuminating Engineering Society, 21*(1), 3-14.

Berman, S. M. (2000). The coming revolution in lighting practice. *Energy User News, 25*(10).

Berman, S. M., Fein, G., Jewett, D. L., Saika, G., & Ashford, F. (1992). Spectral determinants of steady-state pupil size with full field of view. *Journal of the Illuminating Engineering Society, 21*(2), 3-13.

Berman, S. M., Fein, G., Jewett, D., & Ashford, F. (1993). Luminance-controlled pupil size affects Landolt C task performance. *Journal of the Illuminating Engineering Society, 22*(2), 150-165.

Berman, S. M., Fein, G., Jewett, D., & Ashford, F. (1994). Landolt-C recognition in elderly subjects is affected by scotopic intensity of surround illuminants. *Journal of the Illuminating Engineering Society, 23*(2), 123-130.

Berman, S. M., Jewett, D. L., Bingham, L. R., Nahass, R. M., Perry, F., & Fein, G. (1987). Pupillary size differences under incandescent and high pressure sodium lamps. *Journal of the Illuminating Engineering Society, 16*(1), 3-20.

Bettelheim, F. A., & Ali, S. (1985). Light scattering of normal human lens III. Relationship between forward and back scatter of whole excised lenses. *Experimental Eye Research*, *41*(1), 1-9.

Betts, L. R., Taylor, C. P., Sekuler, A. B., & Bennett, P. J. (2005). Aging reduces center-surround antagonism in visual motion processing. *Neuron, 45*(3), 361-366.

Billino, J., Bremmer, F., & Gegenfurtner, K. R. (2008). Motion processing at low light levels: Differential effects on the perception of specific motion types. *Journal of Vision, 8*(3), 1-10.

Blake, R., & Fox, R. (1973). The psychophysical inquiry into binocular summation. *Perception & Psychophysics, 14*(1), 161-185.

Blakemore, C., & Rushton, W. (1965). The rod increment threshold during dark adaptation in normal and rod monochromat. *The Journal of Physiology, 181*(3), 629-640.

Bobak, P., Bodiswollner, I., Guillory, S., & Anderson, R. (1989). Aging differentially delays visual evoked-potentials to checks and gratings. *Clinical Vision Sciences, 4*(3), 269-274.

Boettner, E. A. (1967). *Spectral Transmission of the Eye*. Ann Arbor: Michigan University.

Boettner, E. A., & Wolter, J. R. (1962). Transmission of the ocular media. *Investigative Ophthalmology & Visual Science, 1*(6), 776-783.

Bogfjellmo, L. G., Bex, P. J., & Falkenberg, H. K. (2013). Reduction in direction discrimination with age and slow speed is due to both increased internal noise and reduced sampling efficiency. *Ophthalmology and Visual Science, 54*(8), 5204-5210.

Boxer Wachler, B. S. (2003). Effect of pupil size on visual function under monocular and binocular conditions in LASIK and non-LASIK patients. *Journal of Cataract & Refractive Surgery, 29*(2), 275-278.

Boyce, P. R., Akashi, Y., Hunter, C. M., & Bullough, J. D. (2003). The impact of spectral power distribution on the performance of an achromatic visual task. *Lighting Research and Technology, 35*(2), 141-161.

Brabyn, J., Schneck, M., Haegerstrom-Portnoy, G., & Lott, L. (2001). The Smith-Kettlewell Institute (SKI) longitudinal study of vision function and its impact among the elderly: an overview. *Optometry & Vision Science*, *78*(5), 264-269.

Branch, L. G., Horowitz, A., & Carr, C. (1989). The implications for everyday life of incident self-reported visual decline among people over age 65 living in the community. *The Gerontologist*, *29*(3), 359-365.

Brown, B., Adams, A. J., Coletta, N. J., & Haegerstrom-Portnoy, G. (1986). Dark adaptation in age-related maculopathy. *Ophthalmic and Physiological Optics, 6*(1), 81-84.

Brown, B., & Garner, L. F. (1983). Effects of luminance on contrast sensitivity in senile macular degeneration. *American Journal of Optometry and Physiological Optics*, *60*(9), 788-793.

Brown, B., & Lovie-Kitchin, J. (1987). Contrast sensitivity in central and paracentral retina in age related maculopathy. *Clinical and Experimental Optometry, 70*(5), 145-148.

Brown, J. L., & Woodward, L. K. (1957). Rod-cone interaction in the dark-adapted eye. *Journal of Modern Optics, 4*(3), 108-114.

Buck, S. L. (2004). Rod-cone interactions in human vision. In L. M. Chalupa & J. S. Werner (Eds.), *The Visual Neurosciences* (*Volume 1):* MIT Press.

Buck, S. L. (2014). The interaction of rod and cone signals: pathways and psychophysics. In J. S. Werner & L. M. Chalupa (Eds.), *The New Visual Neurosciences.* MIT Press.

Buck, S. L., & Knight, R. (1994). Partial additivity of rod signals with M-and L-cone signals in increment detection. *Vision Research, 34*(19), 2537-2545.

Buck, S. L., & Makous, W. (1981). Rod-cone interaction on large and small backgrounds. *Vision Research, 21*(7), 1181-1187.

Bühren, J., Terzi, E., Bach, M., Wesemann, W., & Kohnen, T. (2006). Measuring contrast sensitivity under different lighting conditions: comparison of three tests. *Optometry & Vision Science*, *83*(5), 290-298.

Burns, M. E., & Lamb, T. D. (2004). Visual Transduction by Rod and Cone Photoreceptors. In L. M. Chalupa & J. S. Werner (Eds.), *The Visual Neurosciences* (*Volume 1):* MIT Press.

Burton, K. B., Owsley, C., & Sloane, M. E. (1993). Aging and neural spatial contrast sensitivity: photopic vision. *Vision Research*, *33*(7), 939-946.

Cagenello, R., Arditi, A., & Halpern, D. L. (1993). Binocular enhancement of visual acuity. *Journal of the Optical Society of America A, 10*(8), 1841-1848.

Calver, R. I., Cox, M. J., & Elliott, D. B. (1999). Effect of aging on the monochromatic aberrations of the human eye. *Journal of the Optical Society of America A*, *16*(9), 2069-2078.

Calkins, D. J. (2013). Age-related changes in the visual pathways: blame it on the axon. *Investigative Ophthalmology & Visual Sciences, 54*(14), ORSF37-ORSF41.

Campbell, F. W, & Green, D. G. (1965a). Optical and retinal factors affecting visual resolution. *The Journal of Physiology, 181*(3), 576-593.

Campbell, F. W., & Green, D. G. (1965b). Monocular versus Binocular Visual Acuity. *Nature, 208*(5006), 191-192.

Cao, D., Pokorny, J., & Smith, V. C. (2005). Matching rod percepts with cone stimuli. *Vision Research, 45*(16), 2119-2128.

Cao, D., Zele, A. J., & Pokorny, J. (2006). Dark-adapted rod suppression of cone flicker detection: Evaluation of receptoral and postreceptoral interactions. *Visual Neuroscience, 23*(3-4), 531-537.

Carabellese, C., Appollonio, I., Rozzini, R., Bianchetti, A., Frisoni, G. B., Frattola, L., & Trabucchi, M. (1993). Sensory impairment and quality of life in a community elderly population. *Journal of the American Geriatrics Society*. *41*(4), 401-407.

Casson, E. J., Johnson, C. A., & Nelson-Quigg, J. M. (1993). Temporal modulation perimetry: the effects of aging and eccentricity on sensitivity in normals. *Investigative Ophthalmology & Visual Sciences, 34*(11), 3096-3102.

Cavonius, C. R. (1979). Binocular interactions in flicker. *The Quarterly Journal of Experimental Psychology*, *31*(2), 273-280.

Chisholm, C. M., Evans, A. D., Harlow, J. A., & Barbur, J. L. (2003a). New test to assess pilot's vision following refractive surgery. *Aviation, Space, and Environmental Medicine, 74*(5), 551-559.

CIE (1932). Commission Internationale de l'Eclairage Proceedings, 1931. Cambridge: University Press Cambridge.

CIE (1951). Commission Internationale de l'Eclairage Proceedings, Vol. 1, Sec 4; Vol 3, p. 37, Bureau Central de la CIE, Paris.

Coletta, N. (2002). Temporal factors in vision. In Norton, T. T., Corliss, D. A., & Bailey, J. E. (Eds.), *The Psychophysical Measurement of Visual Function* (pp. 180-214). Amsterdam, London, New York: Butterworth-Heineman.

Coletta, N. J., & Adams, A. J. (1984). Rod-cone interaction in flicker detection. *Vision Research, 24*(10), 1333-1340.

Coletta, N., & Adams, A. (1985). Loss of flicker sensitivity on dim backgrounds in normal and dichromatic observers. *Investigative Ophthalmology & Visual Science, 26*, S187.

Connolly, D. M., & Hosking, S. L. (2009). Oxygenation state and mesopic sensitivity to dynamic contrast stimuli. *Optometry & Vision Science, 86*(12), 1368-1375.

Connolly, D. M. (2010). Spatial contrast sensitivity at twilight: luminance, monocularity, and oxygenation. *Aviation, Space, and Environmental Medicine, 81*(5), 475-483.

Cooper, G. F., & Robson, J. G. (1969). The yellow colour of the lens of man and other primates. *The Journal of Physiology*, *203*(2), 411-417.

Coppens, J. E., Franssen, L., & van den Berg, T. J. (2006). Wavelength dependence of intraocular straylight. *Experimental Eye Research*, *82*(4), 688-692.

Culham, J. C., & Kline, D. W. (2002). The Age Deficit on Photopic Counterphase Flicker: Contrast, Spatial Frequency, and Luminance Effects. *Canadian Journal of Experimental Psychology, 56*(3), 177-186.

Curcio, C. A., Allen, K. A., Sloan, K. R., Lerea, C. L., Hurley, J. B., Klock, I. B., & Milam, A. H. (1991). Distribution and morphology of human cone photoreceptors stained with anti-blue opsin. *Journal of Comparative Neurology, 312*(4), 610-624.

Curcio, C. A., & Drucker, D. N. (1993). Retinal ganglion cells in Alzheimer's disease and aging. *Annals of Neurology, 33*(3), 248-257.

Curcio, C. A., Medeiros, N. E., & Millican, C. L. (1996). Photoreceptor loss in age-related macular degeneration. *Investigative Ophthalmology & Visual Science, 37*(7), 1236-1249.

Curcio, C. A., Millican, C. L., Allen, K. A., & Kalina, R. E. (1993). Aging of the human photoreceptor mosaic: evidence for selective vulnerability of rods in central retina. *Investigative Ophthalmology & Visual Science, 34*(12), 3278-3296.

Curcio, C. A., Owsley, C., & Jackson, G. R. (2000). Spare the rods, save the cones in aging and age-related maculopathy. *Investigative Ophthalmology & Visual Science, 41*(8), 2015-2018.

Curcio, C. A., Sloan, K. R., Kalina, R. E., & Hendrickson, A. E. (1990). Human photoreceptor topography. *Journal of Comparative Neurology, 292*(4), 497-523.

D'Zmura, M., & Lennie, P. (1986). Shared pathways for rod and cone vision. *Vision Research, 26*(8), 1273-1280.

Dacey, D. M., & Lee, B. B. (1994). The'blue-on'opponent pathway in primate retina originates from a distinct bistratified ganglion cell type. *Nature, 367*(6465), 731-735.

de Waard, P. W., IJspeert, J. K., van den berg, T. J., & de Jong, P. T. (1992). Intraocular light scattering in age-related cataracts. *Investigative Ophthalmology & Visual Science*, *33*(3), 618-625.

Derefeldt, G., Lennerstrand, G., & Lundh, B. (1979). Age variations in normal human contrast sensitivity. *Acta Ophthalmologica, 57*(4), 679-690.

Dimitrov, P. N., Robman, L. D., Varsamidis, M., Aung, K. Z., Makeyeva, G. A., Guymer, R. H., & Vingrys, A. J. (2011). Visual function tests as potential biomarkers in age-related macular degeneration. *Investigative Ophthalmology & Visual Science*, *52*(13), 9457-9469.

Dowse, E. (2012). *Loss of Rapid Flicker Sensitivity in Aging, Glaucoma & Ocular Hypertension*. Dissertation. City University London.

Duane, A. (1912). Normal values of the accommodation at all ages. *Journal of the American Medical Association*, *59*(12), 1010-1013.

Dubner, R., & Zeki, S. (1971). Response properties and receptive fields of cells in an anatomically defined region of the superior temporal sulcus in the monkey. *Brain Research, 35*(2), 528-532.

Eisner, A., Fleming, S. A., Klein, M. L., & Mauldin, W. M. (1987a). Sensitivities in older eyes with good acuity: cross-sectional norms. *Investigative Ophthalmology & Visual Science, 28*(11), 1824-1831.

Eisner, A., Fleming, S. A., Klein, M. L., & Mauldin, W. M. (1987b). Sensitivities in older eyes with good acuity: eyes whose fellow eye has exudative AMD. *Investigative Ophthalmology & Visual Science, 28*(11), 1832-1837.

Eisner, A., Klein, M. L., Zilis, J. D., & Watkins, M. D. (1992). Visual function and the subsequent development of exudative age-related macular degeneration. *Investigative Ophthalmology & Visual Science, 33*(11), 3091-3102.

Eisner, A., Stoumbos, V. D., Klein, M. L., & Fleming, S. A. (1991). Relations between fundus appearance and function. Eyes whose fellow eye has exudative age-related macular degeneration. *Investigative Ophthalmology & Visual Science, 32*(1), 8-20.

Elliott, D. B., Bullimore, M. A., Patla, A. E., & Whitaker, D. (1996). Effect of a cataract simulation on clinical and real world vision. *British Journal of Ophthalmology*, *80*(9), 799-804.

Elliott, S. L., Choi, S. S., Doble, N., Hardy, J. L., Evans, J. W., & Werner, J. S. (2009). Role of high-order aberrations in senescent changes in spatial vision. *Journal of Vision*, *9*(2), 24.

Elliott, D. B., & Whitaker, D. (1992). Clinical contrast sensitivity chart evaluation. *Ophthalmic and Physiological Optics*, *12*(3), 275-280.

Elliott, D., Whitaker, D., & MacVeigh, D. (1990). Neural contribution to spatiotemporal contrast sensitivity decline in healthy ageing eyes. *Vision Research*, *30*(4), 541-547.

Elliot, D. B., Yang, K. C., & Whitaker, D. (1995). Visual acuity changes throughout adulthood in normal, healthy eyes: seeing beyond 6/6. *Optometry & Vision Science*, *72*(3), 186-191.

Faubert, J. (2002). Visual perception and aging. *Canadian Journal of Experimental Psychology, 56*(3), 164-176.

Feigl, B., Brown, B., Lovie-Kitchin, J., & Swann, P. (2005). Monitoring retinal function in early age-related maculopathy: visual performance after 1 year. *Eye (London), 19*(11), 1169-1177.

Field, G. D., Greschner, M., Gauthier, J. L., Rangel, C., Shlens, J., Sher, A., Marshak, D. W., Litkem A. M., & Chichilnisky, E. J. (2009). High-sensitivity rod photoreceptor input to the blue-yellow color opponent pathway in macaque retina. *Nature neuroscience*, *12*(9), 1159-1164.

Fotios, S. (2014). Lighting Research Group. Retrieved 24/10/2014, from http://lightingresearch.group.shef.ac.uk/MERLIN.html

Fotios, S., Atli, D., Cheal, C., Houser, K., & Logadottir, A. (2013). Lamp spectrum and spatial brightness at photopic levels: A basis for developing a metric. *Lighting Research and Technology*.

Fotios, S., & Cheal, C. (2011). Predicting lamp spectrum effects at mesopic levels. Part 2: Preferred appearance and visual acuity. *Lighting Research and Technology, 43*(2), 159-172.

Frisén, L., & Frisén, M. (1979). Micropsia and visual acuity in macular edema. *Albrecht von Graefes Archiv für Klinische und Experimentelle Ophthalmologie, 210*(2), 69-77.

Frisén, L., & Frisén, M. (1981). How good is normal visual acuity? *Albrecht von Graefes Archiv für klinische und experimentelle Ophthalmologie*, *215*(3), 149-157.

Frisén, L., & Lindblom, B. (1988). Binocular summation in humans: evidence for a hierarchic model. *The Journal of Physiology*, *402*(1), 773-782.

Frumkes, T. E., & Eysteinsson, T. (1988). The cellular basis for suppressive rod–cone interaction. *Visual Neuroscience, 1*(03), 263-273.

Gaffney, A. J., Binns, A. M., & Margrain, T. H. (2011). Topography of cone dark adaptation deficits in age-related maculopathy. *Optometry & Vision Science, 88*(9), 1080-1087.

Gaffney, A. J., Binns, A. M., & Margrain, T. H. (2012). Aging and Cone Dark Adaptation. *Optometry & Vision Science, 89*(8), 1219-1224.

Gagnon, R. W. C., & Kline, D. W. (2003). Senescent effects on binocular summation for contrast sensitivity and spatial interval acuity. *Current Eye Research, 27*(5), 315-321.

Gao, H., & Hollyfield, J. G. (1992). Aging of the human retina. Differential loss of neurons and retinal pigment epithelial cells. *Investigative Ophthalmology & Visual Science, 33*(1), 1-17.

Gerth, C., Sutter, E. E., & Werner, J. S. (2003). mfERG response dynamics of the aging retina. *Investigative Ophthalmology & Visual Science*, *44*(10), 4443-4450.

Gilchrist, J., & Pardhan, S. (1987). Binocular contrast detection with unequal monocular illuminance. *Ophthalmic & Physiological Optics, 7*(4), 373-377.

Gillespie-Gallery, H., Konstantakopoulou, E., Harlow, J. A., & Barbur, J. L. (2013). Capturing age-related changes in functional contrast sensitivity with decreasing light levels in monocular and binocular vision. *Investigative Ophthalmology & Visual Science*, *54*(9), 6093-6103.

Ginis, H. S., Perez, G. M., Bueno, J. M., Pennos, A., & Artal, P. (2013). Wavelength dependence of the ocular straylight. *Investigative Ophthalmology & Visual Science*, *54*(5), 3702-3708.

Ginsburg, A. P. (2003). Contrast sensitivity and functional vision. *International Ophthalmology Clinics*, *43*(2), 5-15.

Glass, J. M. (2007). Visual function and cognitive aging: Differential role of contrast sensitivity in verbal versus spatial tasks. *Psychology and Aging*, *22*(2), 233-238.

Glasser, A., & Campbell, M. C. (1998). Presbyopia and the optical changes in the human crystalline lens with age. *Vision Research*, *38*(2), 209-229.

Goldstein, E. (2009). *Sensation and Perception* (8th ed.). Belmont, CA: Cengage Learning.

Grady, C. L., & Rapoport, S. I. (1992). Cerebral metabolism in aging and dementia. In J. E. Birren, R. B. Sloan and G. D. Cohen (Eds.), *Handbook of Mental Health and Aging*: Academic Press.

Green, D. G. (1970). Regional variations in the visual acuity for interference fringes on the retina. *The Journal of Physiology, 207*(2), 351-356.

Green, D. G., Powers, M. K., & Banks, M. S. (1980). Depth of focus, eye size and visual acuity. *Vision Research*, *20*(10), 827-835.

Grimson, J. M., Schallhorn, S. C., & Kaupp, S. E. (2002). Contrast sensitivity: establishing normative data for use in screening prospective naval pilots. *Aviation, Space, and Environmental Medicine, 73*(1), 28-35.

Guild, J. (1932). The colorimetric properties of the spectrum. *Philosophical Transactions of the Royal Society of London. Series A, Containing Papers of a Mathematical or Physical Character*, 149-187.

Guirao, A., Redondo, M., & Artal, P. (2000). Optical aberrations of the human cornea as a function of age. *Journal of the Optical Society of America A*, *17*(10), 1697-1702.

Habak, C., & Faubert, J. (2000). Larger effect of aging on the perception of higher-order stimuli. *Vision Research, 40*(8), 943-950.

Haegerstrom-Portnoy, G. (2005). The Glenn A. Fry Award Lecture 2003: vision in elders—summary of findings of the SKI study. *Optometry & Vision Science*, *82*(2), 87-93.

Haegerstrom-Portnoy, G., Schneck, M. E., & Brabyn, J. A. (1999). Seeing into old age: vision function beyond acuity. *Optometry and Vision Science, 76*(3), 141-158.

Hahn, G. A., Messias, A., MacKeben, M., Dietz, K., Horwath, K., Hyvärinen, L., Leinonen, M., & Trauzettel-Klosinski, S. (2009). Parafoveal letter recognition at reduced contrast in normal aging and in patients with risk factors for AMD. *Graefe's Archive for Clinical and Experimental Ophthalmology*, *247*(1), 43-51.

Harman, A., Abrahams, B., Moore, S., & Hoskins, R. (2000). Neuronal density in the human retinal ganglion cell layer from 16–77 years. *The Anatomical Record, 260*(2), 124-131.

Haughom, B., & Strand, T. E. (2013). Sine wave mesopic contrast sensitivity -- defining the normal range in a young population. *Acta Ophthalmologica, 91*(2), 176-182.

Hawken, M., & Parker, A. (1990). Detection and discrimination mechanisms in the striate cortex of the old-world monkey. In Blakemore, C. (Ed.), *Vision: Coding and efficiency*. Cambridge: Cambridge University Press.

He, Y., Bierman, A., & Rea, M. S. (1998). A system of mesopic photometry. *Lighting Research and Technology, 30*(4), 175-181.

Helmholtz, H. (1867*). Handbuch der Physiologischen Optik. Helmholtz's Treatise on Physiological Optics*. Leipzig: Leopold Voss.

Hemenger, R. P. (1988). Small-angle intraocular light scatter: a hypothesis concerning its source. *Journal of the Optical Society of America A*, *5*(4), 577-582.

Hendrickson, A. E., & Yuodelis, C. (1984). The morphological development of the human fovea. *Ophthalmology, 91*(6), 603-612.

Hendry, S., Hsiao, S., & Brown, C. (2008). Fundamentals of Sensory Systems. In L. Squire, D. Berg, F. Bloom, S. du Lac, A. Ghosh & N. Spitzer (Eds.), *Fundamental Neuroscience* (3rd ed.): Elsevier.

Hendry, S., & Yoshioka, T. (1994). A neurochemically distinct third channel in the macaque dorsal lateral geniculate nucleus. *Science, 264*(5158), 575-577.

Hennelly, M. L., Barbur, J. L., Edgar, D. F., & Woodward, E. G. (1998). The effect of age on the light scattering characteristics of the eye. *Ophthalmic and Physiological Optics, 18*(2), 197-203.

Hering, E. (1964). *Outlines of a theory of the light sense*. Cambridge MA: Harvard University Press.

Higgins, K. E., Jaffe, M. J., Caruso, R. C., & Demonasterio, F. M. (1988). Spatial contrast sensitivity: effects of age, test-retest, and psychophysical method. *Journal of the Optical Society of America A*, *5*(12), 2173-2180.

Hogg, R. E., & Chakravarthy, U. (2006). Visual function and dysfunction in early and late age-related maculopathy. *Progress in Retinal and Eye Research*,*25*(3), 249-276.

Hohberger, B., Laemmer, R., Adler, W., Juenemann, A. G., & Horn, F. K. (2007). Measuring contrast sensitivity in normal subjects with OPTEC® 6500: influence of age and glare. *Graefe's Archive for Clinical and Experimental Ophthalmology*, *245*(12), 1805-1814.

Home, R. (1978). Binocular summation: A study of contrast sensitivity, visual acuity and recognition. *Vision Research, 18*(5), 579-585.

Hornstein, E. P., Verweij, J., Li, P. H., & Schnapf, J. L. (2005). Gap-junctional coupling and absolute sensitivity of photoreceptors in macaque retina. *The Journal of Neuroscience, 25*(48), 11201-11209.

Hubel, D. H., & Wiesel, T. N. (1962). Receptive fields, binocular interaction and functional architecture in the cat's visual cortex. *Journal of Physiology, 160*(1), 106-154.

Hubel, D. H., & Wiesel, T. N. (1972). Laminar and columnar distribution of geniculo-cortical fibers in the macaque monkey. *Journal of Comparative Neurology, 146*(4), 421-450.

IJspeert, J. K., De Waard, P. W. T., Van den Berg, T. J. T. P., & De Jong, P. T. V. M. (1990). The intraocular straylight function in 129 healthy volunteers; dependence on angle, age and pigmentation. *Vision Research*, *30*(5), 699-707.

Ikeda, M., & Shimozono, H. (1981). Mesopic luminous-efficiency functions. *Journal of the Optical Society of America, 71*(3), 280-284.

Ivers, R., Cumming, R., & Mitchell, P. (2002). Poor vision and risk of falls and fractures in older Australians: the Blue Mountains Eye Study. *New South Wales Public Health Bulletin*, *13*(2), 8-10.

Ivers, R. Q., Mitchell, P., & Cumming, R. G. (1999). Sensory impairment and driving: the Blue Mountains Eye Study. *American Journal of Public Health, 89*(1), 85-87.

Jackson, G. R., McGwin, G., Phillips, J. M., Klein, R., & Owsley, C. (2006). Impact of aging and age-related maculopathy on inactivation of the a-wave of the rod-mediated electroretinogram. *Vision Research*, *46*(8), 1422-1431.

Jackson, G. R., & Owsley, C. (2000). Scotopic sensitivity during adulthood. *Vision Research, 40*(18), 2467-2473.

Jackson, G. R., Owsley, C., & Curcio, C. A. (2002). Photoreceptor degeneration and dysfunction in aging and age-related maculopathy. *Ageing Research Reviews*, *1*(3), 381-396.

Jackson, G. R., Owsley, C., & McGwin Jr, G. (1999). Aging and dark adaptation. *Vision Research, 39*(23), 3975-3982.

Jackson, G. R., Owsley, C., Cordle, E. P., & Finley, C. D. (1998). Aging and scotopic sensitivity. *Vision Research, 38*(22), 3655-3662.

Jennings, B., & Barbur, J. L. (2010). Colour detection thresholds as a function of chromatic adaptation and light level. *Ophthalmic and Physiological Optics, 30*(5), 560-567.

Johnson, P. T., Brown, M. N., Pulliam, B. C., Anderson, D. H., & Johnson, L. V. (2005). Synaptic pathology, altered gene expression, and degeneration in photoreceptors impacted by drusen. *Investigative Ophthalmology & Visual Science*, *46*(12), 4788-4795.

Johnson, P. T., Lewis, G. P., Talaga, K. C., Brown, M. N., Kappel, P. J., Fisher, S. K., Anderson, D. H., & Johnson, L. V. (2003). Drusen-associated degeneration in the retina. *Investigative Ophthalmology & Visual Science*, *44*(10), 4481-4488.

Jonas, J. B., Schmidt, A. M., Müller-Bergh, J., Schlötzer-Schrehardt, U., & Naumann, G. (1992). Human optic nerve fiber count and optic disc size. *Investigative Ophthalmology & Visual Science, 33*(6), 2012-2018.

Kalloniatis, M., & Luu, C. (1995). Visual acuity. In H. Kolb, E. Fernandez, and R. Nelson (Eds.), *Webvision: The Organization of the Retina and Visual System:* University of Utah Health Sciences Center. Retrieved from: http://webvision.med.utah.edu/

Kandel, E. R., Schwartz, J. H., & Jessell, T. M. (Eds.). (2000). *Principles of neural science*: New York: McGraw-Hill.

Keep, M., & Rutherford, T. (2013). *Reported Road Accident Statistics*: House of Commons Library. Retrieved from http://www.parliament.uk/business/publications/research/briefing-papers/SN02198.pdf

Kelly, D. (1961). Visual responses to time-dependent stimuli. I. Amplitude sensitivity measurements. *Journal of the Optical Society of America, 51*(4), 422-429.

Kim, C. B. Y., & Mayer, M. J. (1994). Foveal flicker sensitivity in healthy aging eyes. II. Cross-sectional aging trends from 18 through 77 years of age. *Journal of the Optical Society of America A, 11*(7), 1958-1969.

Kiryu, J., Asrani, S., Shahidi, M., Mori, M., & Zeimer, R. (1995). Local response of the primate retinal microcirculation to increased metabolic demand induced by flicker. *Investigative Ophthalmology & Visual Science, 36*(7), 1240-1246.

Kline, D. W., Schieber, F., Abusamra, L. C., & Coyne, A. C. (1983). Age, the eye, and the visual channels: contrast sensitivity and response speed. *Journal of Gerontology*, *38*(2), 211-216.

Kleiner, R. C., Enger, C., Alexander, M. F., & Fine, S. L. (1988). Contrast Sensitivity in Age-Related Macular Degeneration. *Archives of Ophthalmology, 106*(1), 55-57.

Koenker, R. (2001). Quantile Regresssion. In A. H. El-Shaarawi & W. W. Piegorsch, (Eds.). *Encyclopedia of Environmetrics*. John Wiley & Sons.

Kolb, H. (2005). *Gross anatomy of the eye.* Retrieved 2nd June, 2015, from http://www.ncbi.nlm.nih.gov/books/NBK11534/

Kolb, H., Fernandez, E., & Nelson, R. (2005). *Webvision: Simple anatomy of the retina.* Retrieved 2nd June, 2015, from http://webvision.med.utah.edu/book/part-i-foundations/simple-anatomy-of-the-retina/

Kolb, H., Linberg, K. A., & Fisher, S. K. (1992). Neurons of the human retina: a Golgi study. *Journal of Comparative Neurology, 318*(2), 147-187.

Kolesnikov, A. V., Fan, J., Crouch, R. K., & Kefalov, V. J. (2010). Age-related deterioration of rod vision in mice. *Journal of Neuroscience, 30*(33), 11222-11231.

Kuyk, T. K., & Wesson, M. D. (1991). Aging-related foveal flicker sensitivity losses in normal observers. *Optometry & Vision Science, 68*(10), 786-789.

Kvansakul, J. (2004). *The measurement of scattered light in the eye and its effects on visual performance.* (Doctoral dissertation, City University London).

Lachenmayr, B. J., Kojetinsky, S., Ostermaier, N., Angstwurm, K., Vivell, P. M., & Schaumberger, M. (1994). The different effects of aging on normal sensitivity in flicker and light-sense perimetry. *Investigative Ophthalmology & Visual Science, 35*(6), 2741-2748.

Legge, G. E. (1984a). Binocular contrast summation—I. Detection and discrimination. *Vision Research, 24*(4), 373-383.

Legge, G. E. (1984b). Binocular contrast summation-II. Quadratic summation. *Vision Research, 24*(4), 385-394.

Legge, G. E., Rubin, G. S., & Luebker, A. (1987). Psychophysics of reading-V. The role of contrast in normal vision. *Vision Research, 27*(7), 1165-1177.

Lerman, S. (1984). Biophysical aspects of corneal and lenticular transparency. *Current Eye Research*, *3*(1), 3-14.

Levi, D. M., Pass, A. F., & Manny, R. E. (1982). Binocular interactions in normal and anomalous binocular vision: effects of flicker. *British Journal of Ophthalmology, 66*(1), 57-63.

Levine, M. W., & Shefner, J. M. (1991). *Fundamentals of sensation and perception*: California: Brooks/Cole.

Livingstone, M. S., & Hubel, D. H. (1984). Anatomy and physiology of a color system in the primate visual cortex. *Journal of Neuroscience, 4*(1), 309-356.

Loewenfeld, I. E. (1979). Pupillary changes related to age. In H. S. Thompson (ed.), *Topics in Neuro-ophthalmology*: Williams and Wilkins.

Loewenfeld, I. E. (1999). *The Pupil: Anatomy, Physiology, and Clinical Applications*. Butterworth- Heinemann.

Ludwig, F. C., & Smoke, M. E. (1980). The measurement of biological age. *Experimental Aging Research*, *6*(6), 497-522.

Lund, J. S., Lund, R. D., Hendrickson, A. E., Bunt, A. H., & Fuchs, A. F. (1975). The origin of efferent pathways from the primary visual cortex, area 17, of the macaque monkey as shown by retrograde transport of horseradish peroxidase. *Journal of Comparative Neurology, 164*(3), 287-303.

Luu, C. D., Dimitrov, P. N., Robman, L., Varsamidis, M., Makeyeva, G., Aung, K. Z., Vingrys, A. J., & Guymer, R. H. (2012). Role of Flicker Perimetry in Predicting Onset of Late-Stage Age-Related Macular Degeneration Flicker Perimetry as a Predictor of Late-Stage AMD. *Archives of Ophthalmology, 130*(6), 690-699.

Luu, C. D., Dimitrov, P. N., Wu, Z., Ayton, L. N., Makeyeva, G., Aung, K. Z., Varsamidis, M., Robman, L., Vingrys, A. J., &. Guymer, R. H. (2013). Static and Flicker Perimetry in Age-Related Macular Degeneration. *Investigative Ophthalmology & Visual Science, 54*(5), 3560-3568.

MacLeod, D. I. (1972). Rods cancel cones in flicker. *Nature, 235*(5334), 173-174.

Maher, E. F. (1978). *Transmission and absorption coefficients for ocular media of the rhesus monkey*. School of Aerospace Medicine Brooks, AFB TX. Retrieved from: http://www.dtic.mil/cgi-bin/GetTRDoc?AD=ADA064868

Malania, M., Devinck, F., Knoblauch, K., Delahunt, P. B., Hardy, J. L., & Werner, J. S. (2011). Senescent changes in photopic spatial summation. *Journal of Vision, 11*(10), 1-15

Mathers, W. D., Lane, J. A., & Zimmerman, M. B. (1996). Tear film changes associated with normal aging. *Cornea*, *15*(3), 229-234.

Matin, L. (1962). Binocular summation at the absolute threshold of peripheral vision. *Journal of the Optical Society of America, 52*(11), 1276-1285.

Mayer, M. J., Kim, C. B. Y., Svingos, A., & Glucs, A. (1988). Foveal flicker sensitivity in healthy aging eyes. I. Compensating for pupil variation. *Journal of the Optical Society of America A, 5*(12), 2201-2209.

Mayer, M. J., Spiegler, S. J., Ward, B., Glucs, A., & Kim, C. B. (1992a). Foveal flicker sensitivity discriminates ARM-risk from healthy eyes. *Investigative Ophthalmology & Visual Science, 33*(11), 3143-3149.

Mayer, M. J., Spiegler, S. J., Ward, B., Glucs, A., & Kim, C. B. (1992b). Mid-frequency loss of foveal flicker sensitivity in early stages of age-related maculopathy. *Investigative Ophthalmology & Visual Science, 33*(11), 3136-3142.

Mayer, M. J., Ward, B., Klein, R., Talcott, J. B., Dougherty, R. F., & Glucs, A. (1994). Flicker sensitivity and fundus appearance in pre-exudative age-related maculopathy. *Investigative Ophthalmology & Visual Science, 35*(3), 1138-1149.

McLellan, J. S., Marcos, S., & Burns, S. A. (2001). Age-related changes in monochromatic wave aberrations of the human eye. *Investigative Ophthalmology & Visual Science*, *42*(6), 1390-1395.

Medeiros, N. E., & Curcio, C. A. (2001). Preservation of ganglion cell layer neurons in age-related macular degeneration. *Investigative Ophthalmology & Visual Science, 42*(3), 795-803.

Meese, T. S., Georgeson, M. A., & Baker, D. H. (2006). Binocular contrast vision at and above threshold. *Journal of Vision, 6*(11). 1-7.

Midena, E., Degli Angeli, C., Blarzino, M. C., Valenti, M., & Segato, T. (1997). Macular function impairment in eyes with early age-related macular degeneration. *Investigative Ophthalmology & Visual Science*, *38*(2), 469-477.

Mikelberg, F. S., Drance, S. M., Schulzer, M., Yidegiligne, H. M., & Weis, M. M. (1989). The normal human optic nerve: axon count and axon diameter distribution. *Ophthalmology, 96*(9), 1325-1328.

Naarendorp, F., Denny, N., & Frumkes, T. E. (1988). Rod light and dark adaptation influence cone-mediated spatial acuity. *Vision Research, 28*(1), 67-74.

Naarendorp, F., & Frumkes, T. E. (1991). The influence of short-term adaptation of human rods and cones on cone-mediated grating visibility. *The Journal of Physiology, 432*(1), 521-541.

Nameda, N., Kawara, T., & Ohzu, H. (1989). Human visual spatio-temporal frequency performance as a function of age. *Optometry & Vision Science*, *66*(11), 760-765.

Navvab, M. (2001). A Comparison of Visual Performance under High and Low Color Temperature Fluorescent Lamps. *Journal of the Illuminating Engineering Society, 30*(2), 170-175.

Navvab, M. (2002). Visual Acuity Depends on the Color Temperature of the Surround Lighting. *Journal of the Illuminating Engineering Society, 31*(1), 70-84.

Neelam, K., Nolan, J., Chakravarthy, U., & Beatty, S. (2009). Psychophysical function in age-related maculopathy. *Survey of Ophthalmology, 54*(2), 167-210.

Nesmith, B., Gupta, A., Strange, T., Schaal, Y., & Schaal, S. (2014). Mathematical Analysis of the Normal Anatomy of the Aging Fovea. *Investigative Ophthalmology & Visual Science, 55*(9), 5962-5966.

Norton, T. T., Corliss, D. A., & Bailey, J. E. (Eds.). (2002). *The psychophysical measurement of visual function.* Amsterdam, London, New York: Butterworth-Heineman.

O'Malley, P. (1976). The pattern of vitreous syneresis: a study of 800 autopsy eyes. In A. R. Irvine & C. O'Malley (Eds.), *Advances in vitreous surgery.* Springfield, IL: Charles C. Thomas.

O'Neill-Biba, M., Sivaprasad, S., Rodriguez-Carmona, M., Wolf, J. E., & Barbur, J. L. (2010). Loss of chromatic sensitivity in AMD and diabetes: a comparative study. *Ophthalmic & Physiological Optics, 30*(5), 705-716.

Office for National Statistics. (2009). *Mid-year population estimates for the UK; England & Wales*. London. Retrieved from http://www.statistics.gov.uk/statbase/Product.asp?vlnk=15106

Ohzawa, I., & Freeman, R. D. (1986). The binocular organization of simple cells in the cat's visual cortex. *Journal of Neurophysiology, 56*(1), 221-242.

Oksala, A. (1978). Ultrasonic findings in the vitreous body at various ages. *Albrecht von Graefes Archiv für klinische und experimentelle Ophthalmologie*, *207*(4), 275-280.

Osterberg, G. (1935). Topography of the layer of rods and cones in the human retina. *Acta Ophthalmologica (SuppI.), 13*(6), l-102.

Owens, D. A. (2003). Twilight vision and road safety: Seeing more than we notice but less than we think. In Andre, J., Owens, D. A., & Harvey, L. O. (Eds.), *Visual perception: The influence of H. W. Leibowitz.* Washington, DC, US: American Psychological Association.

Owens, D. A., & Tyrrell, R. A. (1999). Effects of luminance, blur, and age on night time visual guidance: A test of the selective degradation hypothesis. *Journal of Experimental Psychology: Applied, 5*(2), 115.

Owsley, C. (2011). Aging and vision. *Vision Research*, *51*(13), 1610-1622.

Owsley, C., Jackson, G. R., Cideciyan, A. V., Huang, Y., Fine, S. L., Ho, A. C., Maguire, M. G., Lolley, V., & Jacobson, S. G. (2000). Psychophysical Evidence for Rod Vulnerability in Age-Related Macular Degeneration. *Investigative Ophthalmology & Visual Science, 41*(1), 267-273.

Owsley, C., Jackson, G. R., White, M., Feist, R., & Edwards, D. (2001). Delays in rod-mediated dark adaptation in early age-related maculopathy. *Ophthalmology, 108*(7), 1196-1202.

Owsley, C., McGwin, G., Jr., Scilley, K., & Kallies, K. (2006). Development of a questionnaire to assess vision problems under low luminance in age-related maculopathy. *Investigative Ophthalmology & Visual Science, 47*(2), 528-535.

Owsley, C., McGwin, G., Jr., Jackson, G. R., Kallies, K., & Clark, M. (2007). Cone- and rod-mediated dark adaptation impairment in age-related maculopathy. *Ophthalmology, 114*(9), 1728-1735.

Owsley, C., Sekuler, R., & Boldt, C. (1981). Aging and low-contrast vision: face perception. *Investigative Ophthalmology & Visual Science, 21*(2), 362-365.

Owsley, C., Sekuler, R., & Siemsen, D. (1983). Contrast sensitivity throughout adulthood. *Vision Research*, *23*(7), 689-699.

Palmer, D. (1968). Standard observer for large-field photometry at any level. *Journal of the Optical Society of America, 58*(9), 1296-1298.

Paramei, G. V., & Oakley, B. (2014). Variation of color discrimination across the life span. *Journal of the Optical Society of America A, 31*(4), A375-A384.

Pardhan, S. (1996). A comparison of binocular summation in young and older patients. *Current Eye Research, 15*(3), 315-319.

Pardhan, S. (1997). A comparison of binocular summation in the peripheral visual field in young and older patients. *Current Eye Research, 16*(3), 252-255.

Pardhan, S., & Rose, D. (1999). Binocular and monocular detection of Gabor patches in binocular two-dimensional noise. *Perception, 28*, 203-216.

Perlman, I., Kolb, H., & Nelson, R. (2005). *S-Potentials and Horizontal Cells.* Retrieved 2nd June, 2015, from http://webvision.med.utah.edu/book/part-v-phototransduction-in-rods-and-cones/horizontal-cells/

Perry, V. H., & Cowey, A. (1985). The ganglion cell and cone distributions in the monkey's retina: implications for central magnification factors. *Vision Research, 25*(12), 1795-1810.

Peters, A. (2009). The effects of normal aging on myelinated nerve fibers in monkey central nervous system. *Frontiers in Neuroanatomy, 3*(11), 1-10.

Petzold, A., & Plant, G. T. (2006). Clinical disorders affecting mesopic vision. *Ophthalmic and Physiological Optics, 26*(3), 326-341.

Phipps, J. A., Dang, T. M., Vingrys, A. J., & Guymer, R. H. (2004). Flicker perimetry losses in age-related macular degeneration. *Investigative Ophthalmology & Visual Science, 45*(9), 3355-3360.

Pirenne, M. H. (1943). Binocular and uniocular threshold of vision. *Nature, 152*(3867), 698-699.

Pokorny, J., Smith, V. C., & Lutze, M. (1987). Aging of the human lens. *Applied Optics, 26*(8), 1437-1440.

Polyak, S. L. (1941). *The retina: the anatomy and the histology of the retina in man, ape, and monkey, including the consideration of visual functions, the history of physiological optics, and the histological laboratory technique.* Chicago: University of Chicago Press.

Poon, A., & Taylor, H. R. (1997). Photoastigmatic Refractive Keratectomy. In H. E. Kaufman, B. A. Barron & M. B. McDonald (Eds.), *The Cornea* (2nd ed.). Butterworth-Heinemann.

Puell, M. C., Palomo, C., Sanchez-Ramos, C., & Villena, C. (2004). Normal values for photopic and mesopic letter contrast sensitivity. *Journal of Refractive Surgery, 20*(5), 484-488.

Purves, D., Augustine, G. J., Fitzpatrick, D., Katz, L. C., LaMantia, A. S., McNamara, J. O., & Williams, S. M. (2001). Anatomical Distribution of Rods and Cones. In D. Purves, G. J. Augustine, D. Fitzpatrick, L. C. Katz, A. S. LaMantia, J. O. McNamara, & S. M. Williams, *Neuroscience* (2nd ed.). Sunderland, MA: Sinauer Associates.

Qiu, F., & Leat, S. J. (2009). Functional deficits in early stage age-related maculopathy. *Clinical & Experimental Optometry, 92*(2), 90-98.

Raman, C. V. (1978). *Scattering of light*. Bangalore, India: The Indian Academy of Sciences.

Ripamonti, C., Woo, W. L., Crowther, E., & Stockman, A. (2009). The S-cone contribution to luminance depends on the M-and L-cone adaptation levels: Silent surrounds? *Journal of Vision, 9*(3), 1-10.

Rodieck, R. W. (1998). *The first steps in seeing* (Vol. 15). Sunderland, MA: Sinauer Associates.

Rogers, K. (2010). *The eye: the physiology of human perception*. New York: The Rosen Publishing Group.

Ross, J. E., Clarke, D. D., & Bron, A. J. (1985). Effect of age on contrast sensitivity function: uniocular and binocular findings. *British Journal of Ophthalmology, 69*(1), 51-56.

Royer, F. L., & Gilmore, G. C. (1985). Spatiotemporal factors and developmental changes in visual processes. *Bulletin of the Psychonomic Society*.

Rubin, G. S., West, S. K., Munoz, B., Bandeen-Roche, K., Zeger, S., Schein, O., & Fried, L. P. (1997). A comprehensive assessment of visual impairment in a population of older Americans. The SEE Study. Salisbury Eye Evaluation Project. *Investigative Ophthalmology & Visual Science, 38*(3), 557-568.

Rushton, W. A. H. (1972). Review lecture. Pigments and signals in colour vision. *The Journal of Physiology*, *220*(3), 1-31.

Sample, P. A., Esterson, F. D., Weinreb, R. N., & Boynton, R. M. (1988). The aging lens: in vivo assessment of light absorption in 84 human eyes. *Investigative Ophthalmology & Visual Science, 29*(8), 1306-1311.

Schefrin, B. E., Bieber, M. L., McLean, R., & Werner, J. S. (1998). The area of complete scotopic spatial summation enlarges with age. *Journal of the Optical Society of America A, 15*(2), 340-348.

Schefrin, B. E., Tregear, S. J., Harvey, L. O., & Werner, J. S. (1999). Senescent changes in scotopic contrast sensitivity. *Vision Research*, *39*(22), 3728-3736.

Schneck, M. E., Haegerstrom-Portnoy, G., Lott, L. A., Brabyn, J. A., & Gildengorin, G. (2004). Low contrast vision function predicts subsequent acuity loss in an aged population: the SKI study. *Vision Research, 44*(20), 2317-2325.

Schneeweis, D. M., & Schnapf, J. L. (1995). Photovoltage of rods and cones in the macaque retina. *Science, 268*(5213), 1053-1056.

Scialfa, C. T., Tyrrell, R. A., Garvey, P. M., Deering, L. M., Leibowitz, H. W., & Goebel, C. C. (1988). Age differences in Vistech near contrast sensitivity. *American Journal of Optometry And Physiological Optics*, *65*(12), 951-956.

Sebag, J. (1987). Ageing of the vitreous. *Eye*, *1*(2), 254-262.

Sebag, J., & Balazs, E. A. (1985). Human vitreous fibres and vitreoretinal disease. *Transactions of the American Ophthalmological Society*, *104*(2), 123-128.

Sekuler, R., Hutman, L. P., & Owsley, C. (1980). Human aging and spatial vision. *Science*, *209*(4462), 1255-1256.

Shapiro, A. G. (2002). Cone-specific mediation of rod sensitivity in trichromatic observers. *Investigative Ophthalmology & Visual Science, 43*(3), 898-905.

Shapiro, A. G., Pokorny, J., & Smith, V. C. (1996). Cone–rod receptor spaces with illustrations that use CRT phosphor and light-emitting-diode spectra. *Journal of the Optical Society of America A, 13*(12), 2319-2328.

Sharpe, L. T., & Stockman, A. (1999). Rod pathways: the importance of seeing nothing. *Trends in Neurosciences, 22*(11), 497-504.

Sharpe, L. T., Stockman, A., Jägle, H., & Nathans, J. (1999). Opsin genes, cone photopigments, color vision, and color blindness. In K. R. Gegenfurtner & L. T. Sharpe (Eds.), *Color vision: From genes to perception*. Cambridge: Cambridge University Press.

Sharpe, L. T., Stockman, A., & MacLeod, D. I. (1989). Rod flicker perception: scotopic duality, phase lags and destructive interference. *Vision Research, 29*(11), 1539-1559.

Shaw, M. E., Lee, A., & Stollery, R. (2013). *Ophthalmic Nursing*. John Wiley & Sons.

Shinomori, K., & Werner, J. S. (2003). Senescence of the temporal impulse response to a luminous pulse. *Vision Research, 43*(6), 617-627.

Shinomori, K., & Werner, J. S. (2012). Aging of human short-wave cone pathways. *Proceedings of the National Academy of Sciences, 109*(33), 13422-13427.

Simpson, G. C. (1953). Ocular haloes and coronas. *The British Journal of Ophthalmology*, *37*(8), 450.

Sincich, L. C., & Horton, J. C. (2005). The circuitry of V1 and V2: integration of color, form, and motion. *Annual Review of Neuroscience, 28*, 303-326.

Sjöstrand, J. (1979). Contrast sensitivity in macular disease using a small-field and a large-field TV-system. *Acta Ophthalmologica, 57*(5), 832-846.

Sjöstrand, J., & Frisén, L. (1977). Contrast sensitivity in macular disease. *Acta Ophthalmologica, 55*(3), 507-514.

Smith, G. (1997). *The eye and visual optical instruments*. Cambridge: Cambridge University Press.

Smith, W., Assink, J., Klein, R., Mitchell, P., Klaver, C. C. W., Klein, B. E. K., Hofman, A., Jensen, S., Wang, J. J., & de Jong, P. T. V. M. (2001). Risk factors for age-related macular degeneration: Pooled findings from three continents. *Ophthalmology, 108*(4), 697-704.

Snellen, H., Landolt, E (1874) Ophthalmometrologie. Die Funktionsprtifung des Auges. I. Eidoptometrie (Bestimmung der Sehschfirfe) In: A. Graefe & T. Saemisch (eds.) Leipzig: Handbuch der Gesamten Augenheitkunde.

Spear, P. D. (1993). Neural bases of visual deficits during aging. *Vision Research, 33*(18), 2589-2609.

Spector, A., Li, S., & Sigelman, J. (1974). Age-dependent changes in the molecular size of human lens proteins and their relationship to light scatter. *Investigative Ophthalmology & Vision Science, 13*(10), 795-798

Spry, P. G. D., & Johnson, C. A. (2001). Senescent changes of the normal visual field: an age-old problem. *Optometry & Vision Science, 78*(6), 436-441.

Stiles, W. S., & Crawford, B. H. (1933). The luminous efficiency of rays entering the eye pupil at different points. *Proceedings of the Royal Society of London. Series B, Containing Papers of a Biological Character*, *115*(778), 428-450.

Steinmetz, R. L., Haimovici, R., Jubb, C., Fitzke, F. W., & Bird, A. C. (1993). Symptomatic abnormalities of dark adaptation in patients with age-related Bruch's membrane change. *British Journal of Ophthalmology, 77*(9), 549-554.

Stockman, A., & Sharpe, L. T. (2000). The spectral sensitivities of the middle-and long-wavelength-sensitive cones derived from measurements in observers of known genotype. *Vision Research, 40*(13), 1711-1737.

Stockman, A., & Sharpe, L. T. (2006). Into the twilight zone: the complexities of mesopic vision and luminous efficiency. *Ophthalmic and Physiological Optics, 26*(3), 225-239.

Stork, D. G., & Falk, D. S. (1987). Temporal impulse responses from flicker sensitivities. *Journal of the Optical Society of America A, 4*(6), 1130-1135.

Strauss, O. (2005). The retinal pigment epithelium in visual function. *Physiological Reviews, 85*(3), 845-881.

Sun, H., Pokorny, J., & Smith, V. C. (2001). Rod-cone interactions assessed in inferred magnocellular and parvocellular postreceptoral pathways. *Journal of Vision, 1*(1), 1-5.

Sunness, J. S., Rubin, G. S., Applegate, C. A., Bressler, N. M., Marsh, M. J., Hawkins, B. S., & Haselwood, D. (1997). Visual function abnormalities and prognosis in eyes with age-related geographic atrophy of the macula and good visual acuity. *Ophthalmology, 104*(10), 1677-1691.

Sunness, J. S., Rubin, G. S., Broman, A., Applegate, C. A., Bressler, N. M., & Hawkins, B. S. (2008). Low luminance visual dysfunction as a predictor of subsequent visual acuity loss from geographic atrophy in age-related macular degeneration. *Ophthalmology, 115*(9), 1480-1488.

Thomson, A. M. (2010). Neocortical layer 6, a review. *Frontiers in Neuroanatomy, 4*(13), 1-14.

Tyler, C. W. (1985). Analysis of visual modulation sensitivity. II. Peripheral retina and the role of photoreceptor dimensions. *Journal of the Optical Society of America A, 2*(3), 393-398.

Tyler, C. W. (1987). Analysis of visual modulation sensitivity. III. Meridional variations in peripheral flicker sensitivity. *Journal of the Optical Society of America A, 4*(8), 1612-1619.

Tyler, C. W. (1989). Two processes control variations in flicker sensitivity over the life span. *Journal of the Optical Society of America A, 6*(4), 481-490.

Tyler, C. W., & Hamer, R. D. (1993). Eccentricity and the Ferry-Porter law. *Journal of the Optical Society of America A, 10*(9), 2084-2087.

Ungerleider, L., & Mishkin, M. (1982). Two cortical visual systems. In D. Ingle, M. Goodale & R. Mansfield (Eds.), *Analysis of Visual Vehavior*. Cambridge, MA: MIT Press.

van den Berg, T. J., & Tan, K. E. (1994). Light transmittance of the human cornea from 320 to 700 nm for different ages. *Vision Research*, *34*(11), 1453-1456.

van den Berg, T. J. (1997). Light scattering by donor lenses as a function of depth and wavelength. *Investigative Ophthalmology & Visual Science*, *38*(7), 1321-1332.

VanNewkirk, M. R., Nanjan, M. B., Wang, J. J., Mitchell, P., Taylor, H. R., & McCarty, C. A. (2000). The prevalence of age-related maculopathy: The visual impairment project. *Ophthalmology, 107*(8), 1593-1600.

van de Kraats, J., & van Norren, D. (2007). Optical density of the aging human ocular media in the visible and the UV. *Journal of the Optical Society of America A*, *24*(7), 1842-1857.

Veitch, J. A., & McColl, S. L. (1995). Modulation of fluorescent light: Flicker rate and light source effects on visual performance and visual comfort. *Lighting Research and Technology, 27*(4), 243-256.

Verdon, W., & Howarth, P. A. (1988). The pupil's response to short wavelength cone stimulation. *Vision Research, 28*(10), 1119-1128.

Verstraten, P.F.J., Brinkmann, L.J.H., Stevens, N.L., & Schouten, J.S.A., (2005). Loneliness, adaptation to vision impairment, social support and depression among blind and partially sighted elderly. *International Congress Series, 1282,* 317-332.

Verweij, J., Dacey, D., Peterson, B., & Buck, S. (1999). Sensitivity and dynamics of rod signals in H1 horizontal cells of the macaque monkey retina. *Vision Research, 39*(22), 3662-3672.

Virsu, V., Lee, B. B., & Creutzfeldt, O. D. (1987). Mesopic spectral responses and the Purkinje shift of macaque lateral geniculate nucleus cells. *Vision Research, 27*(2), 191-200.

Virsu, V., & Lee, B. B. (1983). Light adaptation in cells of macaque lateral geniculate nucleus and its relation to human light adaptation. *Journal of Neurophysiology, 50*(864), 864-878.

Vos, J. J., & Bouman, M. A. (1964). Contribution of the retina to entoptic scatter. *Journal of the Optical Society of America*, *54*(1), 95-100.

Vos, J. J., & Boogaard, J. (1963). Contribution of the cornea to entoptic scatter. *Journal of the Optical Society of America, 53*(7), 869-873.

Vos, J. J. (2003). Reflections on glare. *Lighting Research and Technology*, *35*(2), 163-175.

Vrabel, P. L., Bernecker, C. A., & Mistrick, R. G. (1998). Visual Performance and Visual Clarity under Electric Light Sources: Part II—Visual Clarity. *Journal of the Illuminating Engineering Society, 27*(1), 29-41.

Walkey, H. C., Barbur, J. L., Harlow, J. A., Hurden, A., Moorhead, I. R., & Taylor, J. A. (2005). Effective contrast of colored stimuli in the mesopic range: a metric for

perceived contrast based on achromatic luminance contrast. *Journal of the Optical Society of America A, 22*(1), 17-28.

Wang, Y., Zhou, Y., Ma, Y., & Leventhal, A. G. (2005). Degradation of signal timing in cortical areas V1 and V2 of senescent monkeys. *Cerebral Cortex, 15*(4), 403-408.

Wässle, H., Grünert, U., Röhrenbeck, J., & Boycott, B. B. (1990). Retinal ganglion cell density and cortical magnification factor in the primate. *Vision Research, 30*(11), 1897-1911.

Weale, R. A. (1963). *The aging eye*: London: Lewis.

Weale, R. A. (1986). Real light scatter in the human crystalline lens. *Graefe's Archive for Clinical and Experimental Ophthalmology*, *224*(5), 463-466.

Weale, R. A. (1987). Senescent vision: is it all the fault of the lens? *Eye*, *1*(2), 217-221.

Westendorf, D., Blake, R. R., & Fox, R. (1972). Binocular summation of equal-energy flashes of unequal duration. *Perception & Psychophysics, 12*(5), 445-448.

Whitaker, D., & Elliott, D. B. (1992). Simulating age-related optical changes in the human eye. *Documenta Ophthalmologica, 82*(4), 307-316.

Whitaker, A., & Pardhan, S. (1997). Binocular summation in the peripheral visual field. *Ophthalmic and Physiological Optics, 17*(2), 173-173.

Whitaker, D., Steen, R., & Elliott, D. B. (1993). Light scatter in the normal young, elderly, and cataractous eye demonstrates little wavelength dependency. *Optometry & Vision Science*, *70*(11), 963-968.

Wiesel, T. N., & Hubel, D. H. (1966). Spatial and chromatic interactions in the lateral geniculate body of the rhesus monkey. Retrieved from: http://www.cns.nyu.edu/~tony/vns/readings/wiesel-hubel-1966.pdf

Winn, B., Whitaker, D., Elliott, D. B., & Phillips, N. J. (1994). Factors affecting light-adapted pupil size in normal human subjects. *Investigative Ophthalmology & Visual Science*, *35*(3), 1132-1137.

Wood, J. M., Collins, M. J., & Carkeet, A. (1992). Regional variations in binocular summation across the visual field. *Ophthalmic & Physiological Optics: the Journal of the British College of Ophthalmic Opticians (Optometrists), 12*(1), 46-51.

Wooten, B. R., & Geri, G. A. (1987). Psychophysical determination of intraocular light scatter as a function of wavelength. *Vision Research*, *27*(8), 1291-1298.

Wright, W. D. (1929). A re-determination of the trichromatic coefficients of the spectral colours. *Transactions of the Optical Society, 30*(4), 141.

Wright, C. E., & Drasdo, N. (1985). The influence of age on the spatial and temporal contrast sensitivity function. *Documenta Ophthalmologica, 59*(4), 385-395.

Yamada, E. (1969). Some structural features of the fovea centralis in the human retina. *Archives of Ophthalmology, 82*(2), 151-159.

Yang, Y., Liang, Z., Li, G., Wang, Y., Zhou, Y., & Leventhal, A. G. (2008). Aging affects contrast response functions and adaptation of middle temporal visual area neurons in rhesus monkeys. *Neuroscience, 156*(3), 748-757.

Yücel, Y. H., Zhang, Q., Weinreb, R. N., Kaufman, P. L., & Gupta, N. (2003). Effects of retinal ganglion cell loss on magno-, parvo-, koniocellular pathways in the lateral geniculate nucleus and visual cortex in glaucoma. *Progress in Retinal & Eye Research, 22*(4), 465-481.

Zayit-Soudry, S., Duncan, J. L., Syed, R., Menghini, M., & Roorda, A. J. (2013). Cone structure imaged with adaptive optics scanning laser ophthalmoscopy in eyes with nonneovascular age-related macular degeneration. *Investigative Ophthalmology & Visual Science*, *54*(12), 7498-7509.

Zele, A. J., Cao, D., & Pokorny, J. (2008). Rod-cone interactions and the temporal impulse response of the cone pathway. *Vision Research, 48*(26), 2593-2598.

Zele, A. J., Dang, T. M., O'Loughlin, R. K., Guymer, R. H., Harper, A., & Vingrys, A. J. (2008). Adaptation mechanisms, eccentricity profiles, and clinical implementation of red-on-white perimetry. *Optometry & Vision Science, 85*(5), 309-317.

Zele, A. J., Maynard, M. L., & Feigl, B. (2013). Rod and cone pathway signaling and interaction under mesopic illumination. *Journal of Vision, 13*(1).

Zele, A. J., Maynard, M. L., Joyce, D. S., & Cao, D. (2014). Effect of rod–cone interactions on mesopic visual performance mediated by chromatic and luminance pathways. *Journal of the Optical Society of America A, 31*(4), A7-A14.

Zhang, L., & Sturr, J. F. (1995). Aging, background luminance, and threshold-duration functions for detection of low spatial frequency sinusoidal gratings. *Optometry & Vision Science*, *72*(3), 198-204.

Zhang, J., Wang, X., Wang, Y., Fu, Y., Liang, Z., Ma, Y., & Leventhal, A. G. (2008). Spatial and temporal sensitivity degradation of primary visual cortical cells in senescent rhesus monkeys. *European Journal of Neuroscience, 28*(1), 201-207.